1
Introduction

1.1 Why Energy Conversion Electronics Circuits?

With the progress in using electrical energy in industrial, transportation, commercial and residential applications, there came the need to convert it to an appropriate electrical form; for example, from an AC form to a DC one, or from a high voltage to a low voltage, and so on. Electromagnetic-based transformers were soon developed. They present significant energy losses and require large space and maintenance costs. In addition, the use of transformers could not satisfy all the practical needs. What if the primary electrical energy source was a battery, whose voltage was decreasing in time, while the consumer needed a constant voltage? Or, what if the effective voltage of the supply generator was variable, but the DC needed by the consumer had to be constant? Thus, conversion of electrical energy had to be associated with a control mechanism.

The first solution was allowed by the invention of the mercury-arc rectifier at the beginning of the twentieth century. Solid-state switching mode devices of the gas tube type were developed in the period between the two world wars. Their use in the controlled conversion of the energy signified the start of power electronics. Saturable reactor magnetic amplifiers then followed, but the real breakthrough was the invention of the thyristor at Bell Laboratories in 1950s and its development in 1956 by General Electric. The modern use of power electronics came with the advent of new power solid-state switching elements like the high-frequency metal oxide semiconductor field-effect transistor (MOSFET), insulated gate bipolar transistor (IGBT), and later silicon carbide (SiC) devices. Almost no industrial electrical application or electronic consumer device can be envisioned today without a power electronics circuit. Power electronics circuits made their way from mW to GW applications; their use is still expanding into industry, utility and consumer electronics.

The term of "power electronics" in the twenty-first century has a much broader meaning that it did in the years 1970–1990. The power electronics circuit has become an intrinsic part of a system, be it an uninterruptible power supply, or a microprocessor server, or a consumer product. Apart from converting electrical energy and being a good citizen in the overall system, by not perturbing it, the power electronics circuit

Power Electronics and Energy Conversion Systems: Volume 1. Fundamentals and Hard-switching Converters, First Edition.
Adrian Ioinovici.

needs to add more value to the system. For example in a conversion from an AC voltage to a DC voltage, the converter should also provide good power quality, such as high input power factor and electromagnetic compatibility. More and more in the twenty-first century, underlining the more complex role the power electronics circuit has to play as well the more stringent requirements it has to meet, the term "power electronics" is replaced by that of "energy conversion electronic system."

Let us take a short look at different classical and modern applications. We will see that power electronics is widely used in our daily life. Going back to our childhood and bringing to memory the radio-controlled toy car, we will find the first power electronics circuit that we ever used. It had a remote controller that was guiding the speed of the car. In the car there was a power electronics circuit which was changing the car speed, depending on the received command. Let us look around now and see where we use power electronics.

1.1.1 Applications in the information and telecommunication industry

A typical server power supply is shown in Figure 1.1. The universal 90–264 V AC line is converted into a 380 V/400 V DC, which then is converted to the voltage necessary for supplying the consumer – here microprocessors. The backup time provided by uninterruptible power supplies (UPS) is far less than that a highly reliable server requires.

A consumer like a microprocessor cannot remain without a supply. To provide a longer reverse time, a −48 V power plant used by the telecommunications industry serves to supply the energy to the microprocessors when needed. As seen in Figure 1.1, this application requires a number of power electronics modules, each one having to answer other requirements: one module has to convert AC to DC by keeping a good input power factor; the second module has to increase the 48 V of the battery to the DC voltage bus of 380 V, raising many difficult design questions of how to realize such a large DC voltage ratio, without compromising the efficiency, the reliability, the cost, or the space; the third converter has to transform the DC bus of 380 V into the voltage required by servers. An important concern in such an application is electromagnetic interference (EMI), which has to be avoided or at least minimized.

Today, at the heart of communication systems and desktop PCs are advanced microprocessors and high-speed communication ASICs designed in deep submicron, low-voltage CMOS logic technologies. They operate at GHz clock frequencies and require large currents, at a sub −2 V DC supply voltage. A multiple tight regulation is also required, imposing difficult challenges on the DC/DC conversion circuit. Modern desktop PCs use a hybrid centralized–distributed power system. Their architecture is formed by a centralized multi-output AC/DC conversion circuit (called a silver box), and a distributed 12 V (or 48 V) intermediate bus which supplies the converter located near the microprocessor. As the converter has to supply a very tight regulated low voltage at a high current, it is known under the term of VRM (voltage regulation module).

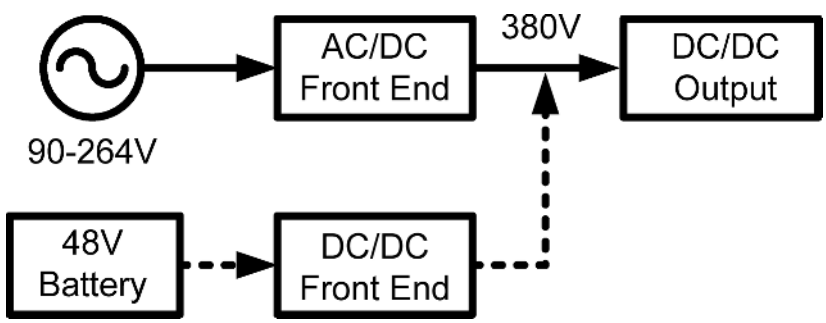

Figure 1.1 *Block diagram of a server power supply.*

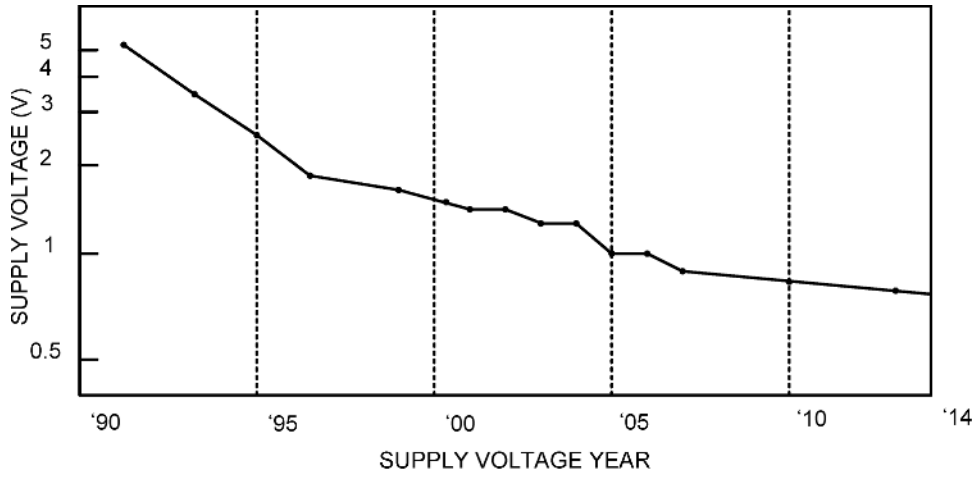

Figure 1.2 *Operating voltage roadmap for Intel's microprocessors. (Data taken, with permission, from A. Lidow and G. Sheridan, "Defining the future for microprocessor power delivery," in* Proc. Applied Power Electronics Conf. (APEC)*, 2003, Miami Beach, FL, vol. 1, pp. 3–9 and from Ed Stanford, Intel Corporation "Power technology roadmap for microprocessor voltage regulators," presentation at* Applied Power Electronics Conf. *(*APEC*), 2004.)*

In the first decades after their invention, the microprocessors required power of under 10 W; with the introduction of the Pentium model processor, power demand began to climb generation by generation, one chip at the beginning of the 2000s consuming 60–100 W. Following Moore's law, the power density of these chips will reach values that would attract unacceptable temperatures. Higher clock frequencies and more functions on a single chip will imply more load current. To reduce the power dissipation, and consequently the temperature of a chip, the solution is to reduce the supply voltage. According to Intel's roadmap, the supply voltage for microprocessors (Figure 1.2) will reach less than 0.65 V by 2014. To envisage a VRM able to supply a load of 200 A at 0.5–0.6 V, with a tight regulation of 5–10 mV slewing at 100 A/μs, means new challenges for the design of power electronics – and new efforts that future scientists in energy conversion will have to make to come up with inventive solutions. To decrease the size of the VRM, the switching frequency has to be increased beyond the present several hundred kilohertz well in the MHz range. To do so, new structures with lower switching losses will have to be developed. One solution is the use of multiple converters for load sharing. A digital signal processor (DSP) may be used in the control system. The control approach has been changed from using classical control design in frequency domain to intra-switching cycle control in the time domain. At the same time, the solid-state switching elements industry will be required to produce MOSFETs with still less parasitic capacitances, with improved gate driver efficiency, and even devices of zero reverse recovery time. Even the packaging will have to be re-thought in order to decrease the parasitic inductances between the MOSFET and its driver. The forecast for the power density and cost performance of converters are 400 W/in^3 and \$0.058/W, respectively, by 2013. A low-power (18 W) resonant boost converter operating at 110 MHz has already been demonstrated. The research for pushing the switching frequency toward 300 MHz is under way.

As we can see, the first half of the twenty-first century will require much research and innovative design in the energy conversion area to answer the ceaselessly more stringent requirements imposed by the information and telecommunication industry.

1.1.2 Applications in renewable energy conversion

For centuries, the world economy has been running on fossil fuels. Aside from the scarcity of such traditional sources of energy, and all the geo-politic attached problems, their negative effects on the environment became visible in the last decades. Nowadays, in order to diversify the energy sources, people look to "harvest" energy from the surrounding environment (solar or wind energy, temperature gradients, vibrations, ocean tidal energy, bio-mass, etc.). Renewable energy sources not only help in reducing the greenhouse effects but also feature much flexibility and portability: they are easily installed, are modular, and can be situated close to the user, thus saving in the energy transmission cost. The environmentally clean renewable sources are heavily dependent on power electronics.

One of most available sources of energy in nature is solar energy. A photovoltaic system converts sunlight into electricity. Photovoltaic cells can be grouped to form panels and arrays. Panels are composed of cells in series for obtaining larger output voltages. By increasing the surface area or by connecting cells in parallel, a larger output current can be achieved. Series and/or parallel connection of the panels form an array. A photovoltaic cell is essentially a semiconductor diode whose *p-n* junction is exposed to light. The incidence of the light on a cell generates charge carriers that give an electric current if the cell is short-circuited; that is, the absorption of solar radiation leads to generation of carriers which are collected at the cell's terminals. The rate of generation of electric carriers depends on the flux of incident light. As, during the daytime, the flux of light varies, the generated energy has variable parameters. Partial shading also changes the cell output. Consequently, the output power varies from day to day depending on the weather. A large number of photovoltaic arrays can be connected to the grid of power utilities. Each photovoltaic farm forms a microgrid.

Power output variations of individual arrays would cause problems in the electrical power system, such as serious voltage or frequency deviations from the nominal values. In order to smooth the power variation and achieve the maximum possible power in any insolation condition, so-called maximum power point tracking power electronics circuits are used. These circuits have to extract the maximum power from the photovoltaic cell. They operate in the following way. At any level of solar radiation and temperature, there is an operating point on the array's power-voltage curve (called maximum power point MPP) where the power generation is maximum. To extract maximum power from a solar cell, the input resistance of the power electronics converter has to be equal to the solar cell output resistance at the MPP. A special control technique has to be developed for the converter to satisfy such a condition. Advanced control methods like fuzzy controllers are implemented nowadays for tackling the frequency deviations due to variance in insolation ("insolation" refers to solar radiation energy). DC energy conversion electronic circuits are used in the power conditioning system, whose grid is based on the connection of individual photovoltaic arrays, to increase the overall efficiency. Power electronics circuits are also needed to store the excess energy from solar power to a temporary storage, such as a battery bank. Power electronics circuits also serve to convert the DC power into AC power back to the grid, with high power quality. Some processing techniques, like islanding, have to be integrated: if there is a breakout or outage of the main grid, the microgrid of the alternative energy sources should continue to supply power with regulated voltage to consumers. These applications require purposely-designed power electronics circuits.

Integrating the power electronics circuit with the photovoltaic cell brings advantages in cost and efficiency. However, for this to be realized is not simple. Practical problems arise: the high temperature and high ambient humidity in which the converter has to operate, as well as the relative inaccessibility in case repair is needed. The integrated converter-photovoltaic cell has to be designed for high reliability (by using very reliable components) and long life, while also permanently bearing in mind the modern $/watt mentality, which requires a low cost.

The alternative environmentally friendly sources of energy supply low voltages and currents. Even for very low power consumers, like smart sensors or smart security cards, the power provided in such a way is

insufficient. For example, consider a thermopile (which is an electronic device that converts thermal energy into electrical energy). It is composed of thermocouples, usually connected in series. The thermopile generates an output voltage proportional to a local temperature difference. When exposed to low temperature gradients, it can deliver energy, but at a too low voltage to be useful as such (200 mV in a thermopile formed by 127 miniaturized Peltier cells under a temperature gradient of 5 °C). To become useful for a range of practical applications, from supplying the voltage to small consumers to serving as a front-end for a power utility grid, the variable low voltage produced by the alternative energy cells has to be stabilized and increased several times. Purposely-oriented power electronics have to be developed and designed for achieving such a goal. To convert a 200 mV input voltage to a practical output such as 1.2 V needs a special architecture of the converter. It is especially challenging to realize such a power electronics circuit in a small size by using integrated technology, as is required for portable electronic devices. For example, low threshold voltage NMOS transistors have to be used, by compromising between constraints like low parasitics, low threshold voltage and low channel resistivity. Or the capacitors have to be chosen based on a trade-off between the area consumption and maximum voltage step-up increment.

A great potential of renewable energy exists in ocean waves. However, to make this cost effective, the maximum possible power has to be absorbed. An electronic converter, with its control function, can realize "a maximum power point tracking" operation. Such a function is also necessary when solar energy is absorbed by the solar cells. However, in the case of ocean waves, the power is delivered in time-varying sinusoids of long duration steady-state cycles. For maximizing the power extraction, the system has to be tuned for the slowly changing sea state.

The world has enormous resources of wind energy. It is estimated that if we are able to tape only 10% of it, this would supply all the electricity needs of the world. It is expected that the wind energy share in the USA will increase from the current 1% of the total consumed energy to about 20% by 2030. But the introduction of large wind turbines (more than 5 MW) requires new power converters based on modular technology. This imposes the study of new techniques in power electronics, like the interleaved and multilevel ones. For large offshore wind parks, a system for DC transmission of the energy to mainland consumers can be beneficial. With state-of-the art DC transmission lines, the skin effects losses of AC energy cables are eliminated. For the same level of energy to be transported, the physical space taken by the DC system is smaller than that needed by an AC transmission system. The power carrying capability is increased, without affecting the stability. The new power electronics based DC transmission systems offer full control of reactive power on both the producer and consumer sides and minimization of the included filters. The maximum wind energy is transferred if the turbine is run at variable speed. A special converter is used for this purpose. The nature of wind adds more variability to the system: "grid-friendly" wind plants are needed.

Ideally, the wind and solar energy-derived electricity has to be complementary: use of solar energy during the day and wind energy during the night, when the winds are usually stronger.

With the exception of those alternative energy sources that supply local, isolated consumers, most of the renewable energy sources must be connected to the available national electric grids. New ideas are currently proposed to create "smart" grids; for example, to create energy hubs to manage multiple energy carriers (electricity, gas, etc.). In each hub, energy converters will transform part of the energy flow from one form of energy to another form. The management of the energy flow will include energy control and information flow, enabling a flexible interconnection between the producers (traditional or renewable sources of energy), energy storage elements and loads. All parties will have responsibilities in the security of the grid. Different operational modes will be possible, from the stand-alone case, when the energy producer is disconnected from the grid and supplies a single load, to the "microgrid" scenario, involving a few players, and finishing with the "cluster" model. In the last one, distributed producers form a virtual high cumulative power producer, directed by supervisory signals from the utility operator. Integrating the new sources of energy in this grid, as well as the operation of the smart grid, requires specific power electronics systems.

1.1.3 Future energy conversion – fuel cells

Maybe the most widespread sources of alternative energy are now fuel cells. A fuel cell is based on an electrochemical process: hydrogen and oxygen react, generating electrical energy. This process has zero pollution emission, as the only byproduct is water vapor, which can be used for heating. The power density of fuel cells is higher than that of other alternative energy cells. The fuel cells are used as the front end in a power supply grid, or in vehicles, or in portable applications. In 2008, Boeing flew for 20 minutes a small manned airplane powered by hydrogen fuel cells, opening the way for hydrogen or solid oxide fuel cells to become the power supply for small manned or unmanned air vehicles.

As the output voltage of fuel cells is very low and load variable (it can range between 0.4 V at full load to 0.8 V at no load), many cells have to be stacked in series to realize a useful power supply. For example, 250 cells have to be connected in series to realize 100 V at full load. The voltage produced by each cell is affected by the membrane humidity, by the pressure of the basic elements or of the air, and by the state of the catalyst. The membrane humidity may vary from cell to cell depending on the heat distribution within the cell. Cells with a more moisturized membrane will produce a larger voltage. This results in an uneven voltage distribution among the cells in a stack and a variable voltage will occur. Therefore, a fuel cell stack provides a variable low output voltage; in addition, its current ripple should be small to ensure an optimal operation. This is why a power electronics circuit able to step-up and stabilize the DC cell voltage must follow a fuel cell stack. The difficulty in conceiving such a power electronics DC-DC converter is aggravated by the need to feature a low-input current ripple. An additional LC filter for eliminating the current ripple is unconceivable, as it would reduce the energy conversion efficiency. A special structure for this type of converter, purposely for use in conjunction with fuel cells, must be researched. The usual structure of a fuel cell stack followed by an electronic converter is shown in Figure 1.3a. In such an implementation, which is equivalent to a connection of voltage sources in series, a malfunctioning cell can take out the whole system of service. A modular stack (Figure 1.3b) which electrically divides the fuel cells stack into several sections has the property of fault tolerance: if a section is faulty, it can be disabled, while the rest of the system can continue to operate by supplying a lower power. If the end application is in the automotive industry, in the case of a fault the driver would be able to steer the vehicle at reduced power until the garage. However, such a solution imposes a new challenge for the designer of the power electronics circuit: the need of a modular DC-DC converter able to enhance the system reliability.

Fuel cells cannot respond to quick load fluctuations. A series converter between the fuel cell and the load is not sufficient, because a fluctuation in the load current becomes immediately a fluctuation in the current of the cell, decreasing its lifetime. One possible solution is to use two converters between the fuel cell and the load: a converter connected in series and a converter connected in parallel to the cell. When the load is constant, to realize the regulation of the output voltage only the series converter operates, assuring a high energy efficiency, as the output power is directly provided by the fuel cell. When the output power changes, the parallel converter with a battery will compensate for the quick variation in the load current.

1.1.4 Electric vehicles

Hybrid electric vehicles have gained much popularity as they use less fuel and pollute the environmental with less carbon dioxide emission than classic gas (petrol) driven vehicles. They necessitate batteries or ultracapacitors that provide energy to the electrical drive system of a car or train during acceleration. Nickel metal hydride or lithium ion batteries are mostly used, with the later showing higher power, higher energy density, and lower self-discharge rate. A battery can be formed by many cells. The rated voltage of the commercially available batteries at the end of the first decade of the twenty-first century is in the range of

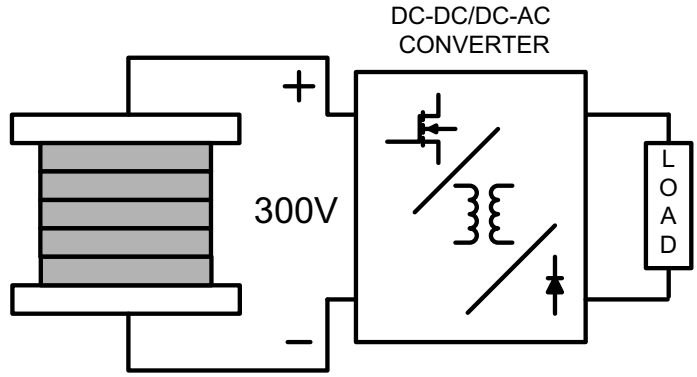

(a)

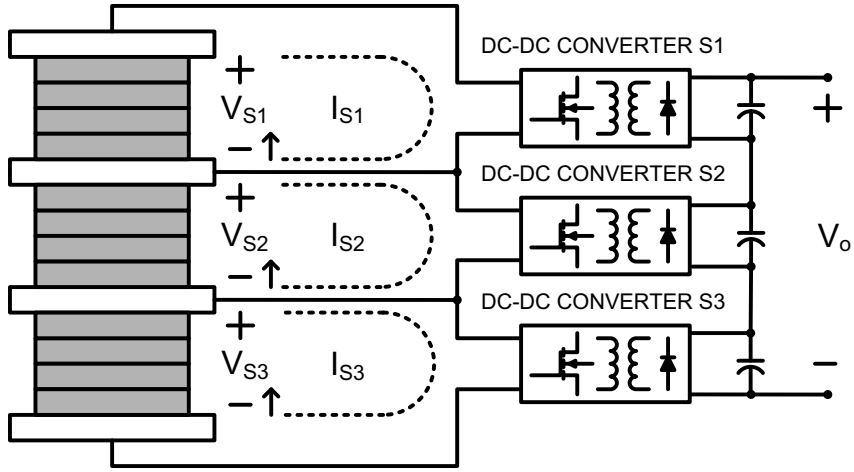

(b)

Figure 1.3 *Fuel cell stack followed by a power electronics converter. (a) Compact implementation. (b) Modular implementation. (Reproduced with permission from L. Palma and P. N. Enjeti, "A modular fuel cell, modular DC-DC converter concept for high performance and enhanced reliability,"* IEEE Trans. Power Electronics, *June 2009.)*

250 V; however, their operating voltage is in the range 150–270 V, depending on the state of the charge. Large battery installations require sophisticated battery charging systems to obtain the best possible performance from the batteries, to lengthen the life expectancy of the batteries, to provide consumers with efficient charging, and to protect large financial investments. Such battery charging systems are power electronics circuits that can adaptively adjust the charging current and cell equalization throughout the charging process.

For train drives of up to 100 kW power, the nominal DC-link voltage is 400 V. Therefore, during acceleration periods, the DC voltage of the battery has to be stepped up to the inverter DC-link bus. In addition, the

conversion electronic circuit has to assure a constant DC-link voltage at the consumer side despite variations in the output voltage of the battery. As the load also has a variable characteristic (depending, for example, on the ground slope), even the DC-link voltage becomes variable without a control circuit. Thus, the conversion circuit has to assure regulation for both changes in the battery voltage and load.

A hybrid electric vehicle has an additional advantage: regenerative braking. When braking or descending a slope, the energy from the wheels is not lost but is conveyed back to the battery. This demands that the conversion electronic circuit between the battery and the DC-link acts in this phase as a voltage step-down circuit. A new type of constraint is thus imposed on the power electronics circuit: it has to allow a bidirectional power flow, with time intervals when it steps-up and time intervals when it steps-down the input voltage. In addition, for use in automotive applications, the power electronics circuit needs to meet more features: low cost, minimization of the component size and count to get a low weight, good conversion efficiency over a wide load power range, a compact design, and low electromagnetic interference (EMI) emission. Reliability and safety are first to be ensured. The battery must be maintained within the range of allowed voltage and current limits for preventing explosions or fire in the vehicle. If a high voltage for driving the motor is needed, a series-connected battery string is used. To avoid charge imbalance among the cells during their repetitive charging and discharging operation, which would affect both the whole capacity and lifetime of the battery, a charge-type cell equalization converter is used. Therefore, to conceive a converter for an automotive purpose means a new research and design challenge in power electronics: create bidirectional and bipolar circuits that can give a smooth acceleration and deceleration of the entire vehicle.

1.1.5 Applications in electronic display devices

Electronic display devices with a large size, high resolution and high information capacity are in increasing demand in the information and multimedia industry. The conventional inefficient cathode ray tube has been replaced with various flat panel displays using electroluminescence, gas discharge or a liquid crystal technology. Plasma display panels (PDPs), which uses a gas discharge, and liquid crystal displays (LCDs) are sharing the flat panel display market for the high-definition television at the end of the first decade of the twenty-first century. (LCDs are optoelectronic devices. Electrical current passed through specific portions of the liquid crystal solution causes the crystals to align, blocking the passage of light.)

The PDPs have a large screen size, wide view angle, high-contrast ratio, thinness and lightness, and long lifetime. However, they are still expensive. A PDP contains three types of electrodes: the sustaining electrodes X and the scanning electrodes Y on the front glass substrate, and the addressing electrodes A on the rear glass substrate. The space between the opposing substrates is filled with a gas under pressure. An alternative current high-voltage pulse applied between the electrodes X and Y will ionize the gas and create plasma. A sustaining power electronics circuit is needed to invert a DC voltage to the required AC high voltage, high frequency square waveform. The power electronics design for this specific application has to meet other challenges, too: as the electrodes are covered by dielectric and magnesium oxide (MgO) layers, a parasitic capacitance appears between the X and Y electrodes. In each switching cycle, an energy loss proportional to this capacitance and the square of the amplitude of the pulses will appear, this energy being dissipated in the inherent parasitic resistances of the switches. A special energy recovery circuit has to be added to avoid such an energy loss. Such circuits contain additional switches, diodes and inductors. It is a challenging problem for researchers in power electronics to find the best structure for the recovery circuit to concomitantly accomplish a low cost, a reduced number of additional elements (to reduce the size), zero switching losses in the switching devices, and a reduction in the gas discharge current flowing through the inverter switches (to reduce the conduction losses and thus improving the luminous efficiency of the panel). As the voltage pulses create excessive surge charging and discharging currents, EMI noises and heating will become annoying. The design of the power electronics inverter with the energy recovery circuit will have to

tackle this problem too. Simple ideas like that of using a current source built-in inductor in the power circuit can increase the brightness of the display by reducing the transition time of the panel polarity. Approximately half of the cost of a PDP goes into the driving circuit. New solutions to reduce the cost and size of the driver, and reduce the power consumption, have to be looked after by power electronics scientists.

Many of the information displays today are based on liquid crystal technology. Since LCD devices are non-emissive, a backlighting source to give brightness is necessary. Cold cathode fluorescent lamps and mercury-free flat fluorescent lamps are widely used for this purpose. To drive the lamps, a purposely designed power electronics inverter for generating high-voltage pulses is used. The lamp uses a mixed gas to generate a dielectric barrier discharge between a pair of electrodes. The inverter has not only to generate the pulses which maintain the glow discharge but must also offer an energy recovery function. Since the lamp requires narrow voltage pulses, additional coupled-inductor elements have to be used, giving the specificity of the power electronics circuit for this application.

However, both the cold cathode fluorescent lamps and mercury-free flat fluorescent lamps have their problems. A new trend that began in the last years of the first decade of the twenty-first century was the use of light-emitting diodes (LEDs) to give the necessary backlighting to the LCD panel. The new solution offers some advantages: it is energy efficient, has a longer lifetime, is mercury free, and consumes less power. Television sets containing this technology are known as LED televisions. A little later (Section 1.1.9), some more details about LED technology and its requirements on the power electronics are given.

The beginning of the second decade of our century saw the development of OLED (Organic Light Emmiting Diode) displays for TVs : Thin films of organic (carbon based) materials are placed between two conductors. When electrical current is applied, a bright light is emitted. The OLED materials emit light and do not require a backlight. OLED televisions are thinner, brighter, draw less power, offer better contrast than previous displays.

1.1.6 Audio amplifiers

Conventional digital audio playback systems involve two main processes: the conversion of digital audio data to low level analog audio signal using a high-precision digital-to-analog converter, and the amplification of the analog signal using an analog power amplifier. Starting from the early 1980s, much research has been devoted to developing different types of digital amplifiers that perform power amplification directly from the digital audio data. This kind of amplifier is called a digital power amplifier and it has two main features: elimination of the digital to low level analog signal conversion and improvement of the amplification efficiency using a special type of power electronics circuit.

1.1.7 Applications in portable electronic devices

Portable electronic devices, such as digital cameras, cellular phones, smart cards, PDAs (personal digital assistants), MP3s, i-phones, hand-held communication instruments, and so on, today represent a consumer electronics industry in full flourish. Every day new devices are invented for a larger mass of customers. The energy source is often a battery. The operation depends on a power supply circuit aimed at regulating the supply voltage. For example, a 2.9–5.5 V lithium battery can be used, the power electronics converter having to provide a constant 5 V voltage at a 48 mA load current to a LED module in the portable device. The main concerns in manufacturing these devices are miniaturization and low fabrication cost. The power converter can be manufactured as a single chip or integrated into a system-on-chip (SoC). The reduction of the area on silicon and printed circuit boards means a tinier size. A CMOS implementation of the electronic circuit is favored. The size and height of the external components, like capacitors and inductors, will limit the layout on the printed circuit board (PCB), and thus will affect the size covered by the electronic

converter. Most of the power electronics circuits use inductors and transformers. However, the size of an inductor is large and it is difficult to shrink its height. As, for portable devices, a DC isolation is not required, transformers can be avoided. And, for eliminating inductors, a special type of power electronics can be used: switched-capacitor (SC) converters.

Essentially, an SC power supply contains in its power stage only switches and capacitors. The lack of inductors assures that the SC converter has a small size, low weight and high power density. The SC converter is, consequently, the ideal power supply for mobile electronic devices. The theory of regulating the converted energy by means of an SC circuit represents a special chapter in power electronics, which was developed in the 1990s. Difficult questions, like the need for a non-pulsating input current and soft changes in the capacitor charging current, for avoiding EMI noise, or finding structures and designs able to provide an acceptable efficiency had to be answered. Regulating the output voltage for a broad range of variation of the input voltage and/or load was a challenging task.

A recent application of the SC converter was in a nanosatellite (a satellite whose weight is under 10 kg), where it was used to boost the energy provided by a photovoltaic solar array. Miniaturization of the electromechanical systems on board, new MEMS propulsion systems, and small sensors made the realization of such low weight space craft possible. They are highly cost effective in both terms of launch and building costs. Little ground support is required for their operation. The photovoltaic array is the only source of energy. The panel temperature varies between $-80\,^{\circ}\mathrm{C}$ in the lack of insolation to $+70\,^{\circ}\mathrm{C}$ in sunlit condition. During sunlight, the array has to provide the necessary energy on board and charges a battery that will be used at eclipse. Several solar cells have to be connected in series to provide the required voltage at board, thus increasing the weight of the energy system. By using a voltage step-up SC circuit, the number of solar cells necessary can be significantly reduced. In the quoted application for an 8 kg remote sensing nanosatellite, the power system had an overall weight of 750 g, with the solar cells array weighing 300 g, the battery 100 g, and the SC converter 350 g.

Switched-capacitor converters have also been proposed for use as the maximum power point tracker of photovoltaic sources for portable electronic equipment. For example, in order to extend the battery backup time of a personal computer, a photovoltaic array of 75 g with a 1 mm thick Mylar sheet for protection of 70 g and 10 g of adhesives can be configured on the cover of the laptop. A high-power density SC MPP tracker, weighting less than 50 g, may be housed in the laptop. Such an array can generate about 20 W in direct sunlight and about 4 W in the shade.

1.1.8 Applications in high voltage physics experiments and atomic accelerators

The SC converters are based on previous charge pump circuits. J.D. Cockcroft and E.T.S. Walton (based on an older idea of H. Greinacher from 1919) built the first SC charge pump circuit in 1932 and used it to get a 200 kV voltage needed in the first particle accelerator. From here, the first artificial nuclear disintegration in history was performed. (Infamously, the Cockcroft–Walton voltage multiplier, built in 1937 at Philips, Eindhoven, in The Netherlands was part of one of the early particle accelerators used in the later development of the atomic bomb.) Essentially, the first voltage multipliers were realized as a ladder network of capacitors and diodes, stepping low voltages to high voltages. Unlike in transformers, the need for a heavy core or bulk of insulation was eliminated in SC charge pumps, resulting in cheap and lighter circuits. However, they suffered from many problems, including the lack of regulation for changes in the input voltage and large voltage ripple in the output voltage, which restricted their use to light load applications only. Except for high energy physics experiments, where voltages of millions of volts have been obtained in such a way, the voltage multipliers have been used in lightning safety testing, X-ray systems, ion pumps, laser systems, copying machines, oscilloscopes, and so on. However, to reach the modern SC converters of our times, much research was needed, to solve the drawbacks of the SC charge pump circuits.

Power electronics circuits used in particle accelerators operate in a highly hostile environment: high radiation fluxes and stationary magnetic fields. For example, at CERN (The European Organization for Nuclear Research, Geneva, Switzerland), where the world's largest particle physics laboratory is situated, the converters, placed at the very heart of the set-up in order to reduce power consumption, face a very high background magnetic field that can reach 4 Tesla. This excludes the use of magnetic materials in the inductor cores. Only inductor-less or high frequency (MHz) converters employing an air core can be considered.

1.1.9 Lighting technology

Lighting consumes around 16–20% of the total energy a commercial building uses. To align the lighting levels with human needs, and thus save energy, a dimming technology is used. For a linear fluorescent lamp, the cathode voltage must be maintained while the lamp arc current is reduced. A dimmable ballast consists essentially of a cascade of power electronics circuits: an EMI filter, an AC–DC conversion circuit (called rectifier) that should also assure a high power factor, and an inverter which supplies the lamp. It will generate a high voltage to ignite the lamp and then stabilize the current flowing through the lamp. To maintain a sufficiently high filament temperature ($>850\,^{\circ}$C) over the dimming range, the ballast has to maintain the filament voltage. To increase the efficacy, that is the luminance with respect to the input power, the ballast, and thus the lamp, has to be operated at a frequency higher than 20 kHz. Moreover, the energy efficiency of electronic ballasts has to be high, as they generate heat that is a burden on the air-conditioning system.

The recent advancement of light-emitting diodes (LEDs) opens a new era of lighting. The LED is an electronic light source. Even if it was invented in the 1920s in Russia, it became a practical electronic component only in 1960s. LEDs are used today in a large variety of applications, from street displays, traffic lights, and lighting to remote controls, optoisolators, sensors, scanners, and so on. The LED is based on the semiconductor diode: when the diode is forward-biased, electrons are able to recombine with holes, emitting energy in the form of light. The effect is called electroluminescence. The color of the light is determined by the energy gap of the semiconductor. The first devices emitted only low-intensity red light but nowadays a wide spectrum of colors is available, from green and blue to ultraviolet and infrared. Compared with traditional light sources, LEDs have longer lifetime, lower power consumption, faster switching, improved robustness, smaller size, are more resistant to external shocks, can focus their light, and produce more light per watt, that is, are more efficient. It is estimated that the new LED lamps consume 50% less energy than compact fluorescent lamps and have five times longer life. However, they require a more precise and a better heat management, as high ambient temperature can lead to overheating and failure. (Some LEDs have also some disadvantages, such as the emission of more blue light, which is a hazard for eye safety.) Similar to other diodes, the LED current is dependent exponentially on the voltage, implying that a small change in voltage would give a large change in current. So, even if the voltage increases only slightly over its nominal value, the current could increase seriously, thus deteriorating the device. Consequently, a constant current electronic power supply has to be used. Since the power system of a building or a battery cannot provide a constant current, any LED has to be accompanied by a power electronics converter, which, for this application, has to withstand a high operating temperature.

1.1.10 Aerospace applications

In aircraft, the variable frequency (360–800 Hz) energy supplied from the engine alternator has to be converted to a fixed 400 Hz power supply in a variable-speed constant frequency system. In hot-strip-mill drives rated at more than 5 MW, frequencies of around 40 Hz are needed. Power electronics circuits, called cycloconverters, have to convert the input (line) frequency AC waveform of 50/60 Hz supplied by the utility grid to the higher/lower requested frequency.

1.1.11 Power system conditioning

Active power filters based on solid-state switching elements are used for power conditioning: harmonics filtering and VAr compensation in utilities lines. For example, high-speed trains, with powers in the 12 MW range, draw unbalanced varying active and reactive powers from the transformer, whose primary is connected to the 154 kV utility grid. This causes imbalance at the terminals of the high-voltage utility system, and serious deterioration in the power quality offered to other consumers connected to the same grid. Active filters consisting of inverters using GTO (gate-turn-off) thyristors of a total ranking in the range of 48 MVA compensate for the voltage impact drop and sustain the power quality of the grid.

Power electronics technology has lots of applications in power systems. A unified power flow controller is a device for controlling the active and reactive power flow on high-voltage transmission networks, so that the system security, stability, voltage and frequency can be maintained.

Voltage sags are unavoidable brief reductions in the voltage due to momentary disturbances, such as lightning strikes or rambunctious animals, on the power system. Nowadays, they are the major cause of disruption in power supply systems and can lead to severe production process disruption and substantial economic losses. Utility customers generally experience about five to ten voltage sag events a year. The average magnitude of the sags is 70% of the nominal voltage. This is why cost-effective solutions like power electronics-based dynamic voltage restorers that can help voltage-sensitive loads ride through momentary disturbances have attracted much attention.

1.1.12 Energy recycling in manufacturing industry

Climate change is prompting a worldwide economic and industrial restructuring to confront global warming. Eco-friendly electronic products can help the environment and save consumers money by using less electricity. The importance of energy efficiency in the whole chain of energy-related activities and energy consumption in production cannot be disregarded. When a product is initially manufactured, it has to go through a "burn-in" process to weed out components or systems with early failures, before customer delivery. In this process, the new product is operated at a full load for a few hours. This is an effective and important procedure to improve the product reliability. However, traditional burn-in processes could consume huge amounts of energy, particularly in energy-intensive manufacturing industries. A typical example is in the power supply industry: manufacturers will burn-in every new power supply for four to twenty-four hours before shipment. The conventional burn-in method was to connect resistors at the output of the power supply to simulate the load condition, thus converting, and therefore wasting, all the electrical energy into heat. The concept of using an energy recycling technique in conducting the burn-in process has become increasingly popular in the power supply industry nowadays. The idea is to use an energy recycling device (ERD) to recycle the output energy of the tested power supply by means of a grid-interactive inverter technology: instead of using resistors as a load, an ERD is connected to the output of the power supply under test, and the output of the ERD is connected to the grid. Commercially available ERDs can recycle up to 87% of the electricity provided by the power supply. This can effectively reduce the electricity consumption in the burn-in process, and thus indirectly reduce carbon dioxide emission. The ERD is implemented by a power electronics inverter, which has to satisfy challenging requirements: its output waveform has to include a very low content of harmonics so as not to disturb the main grid to which the energy is recycled.

1.1.13 Applications in space exploration

The conquest of the universe puts its tough and very diverse demands on research in power electronics circuits: long life, high reliability, low mass/volume, high energy density, radiation tolerance, and wide temperature operation. Future NASA objectives will include missions to Venus, Titan and Lunar quest. An

electronic converter in a battery system in a Titan mission will have to be capable of operating at temperature extremes from −100 to 400 °C, in a Venus mission up to 500 °C, the span for a Lunar quest being from −230 to 120 °C. Rechargeable electrochemical battery systems will have to offer more than 50 000 charge/discharge cycles (equivalent to 10 years operating life) for low-earth-orbiting spacecraft and up to 20 years operating life for geosynchronous spacecraft. Advanced electronic packaging for thermal control and electromagnetic shielding will be necessary for the power electronics devices to enable and enhance the capabilities of future space missions. The current state of the art cannot answer all these requirements, making the field of power electronics specifically designed for space missions a hot research field.

The mobile Mars Science Laboratory rover launched in 2009 contains radiation-hardened power electronics to withstand exposure to radiation as strong as 100 kilorads for a long-endurance mission (the "rad" is the unit of absorbed radiation, equal to 10 milligrays – the new SI unit for radiation): one Mars year, which is equivalent to two Earth years, after landing.

To create the test backgrounds for simulating flight conditions from Mach 4.7 to 8 (a Mach unit is the speed of the spacecraft divided by the speed of the sound), a NASA Scramjet test facility requires a 20 MW DC power supply able to power a plasma arc to heat the incoming air.

The power system of the International Space Station (ISS) contains much power electronics circuitry. The energy supply is assured by photovoltaic arrays and batteries. The batteries store energy during "insolation" periods and supply it to loads during orbital eclipses. The voltage output of the photovoltaic array is regulated by a special unit. The 120 V American and 28 V Russian networks exchange bidirectional power flow via converter units. Converters step-down the 160 V power to the secondary distribution system of 120 V; remote power controller modules distribute power to the load converters. A similar power distribution structure is used for satellites: the primary side of the system is formed by the photovoltaic arrays, battery and power control unit; the secondary side is formed by the battery charge and discharge converters, and a low voltage converter module of redundant DC-DC converters which feed the spacecraft loads as part of the power distribution unit. The modularity makes it possible to vary the battery voltage and output power levels, by adding or subtracting converter modules. Redundancy allows for re-configuration for different missions. The need for bidirectional converters for battery charge/discharge functions and the requirement of multiple loads asks for the development of bidirectional converters with multi-output voltage levels.

Power electronics are constituent parts of the power processing unit of spacecraft electric propulsion. This unit provides power for the spacecraft "thruster" (which is a small propulsive device used in spacecraft or watercraft for (a) station keeping, that is, for keeping a spacecraft in the assigned orbit, (b) attitude control, that is, for manipulating the orientation of a spacecraft with respect to a defined frame of reference, and (c) long duration low " thrust" acceleration. Thrust is a reaction force described quantitatively by Newton's second and third laws. When a system expels or accelerates mass in one direction, the accelerated mass will cause a proportional but opposite force on that system). The power electronics converters used in this unit have to meet tough requirements; in particular they have to rapidly supply a constant current to offset thruster voltage variations, typical of a start-up period. These units have to generate a high voltage start pulse to ignite up to four arc-jet thrusters for "north-south station" keeping orbit maneuvers, thus reducing the propulsion system mass and reducing launch vehicle requirements (The "north-south station" is used to correct the inclination of a satellite to keep it in a "geosynchronous orbit" – the meaning for an observer at a fixed location on Earth is that a satellite in a geosynchronous orbit returns to exactly the same place in the sky at exactly the same time each day).

Power electronics circuits at the board of a space/aircraft are also used to solve the incompatibility between variable-frequency drives and the fixed 400 Hz craft equipment, like the motors of the fuel or hydraulic pumps. Variable frequency drives are superior to constant frequency drives, because they can reduce the transient inrush current at motor start, or, in the case of fuel pumps, the variable-frequency drive can assure that only the required amount of fuel is provided.

1.1.14 Defense applications

The use of power electronics in the defense industry is becoming more and more extensive. Hybrid electric combat vehicles are the army preferred vehicles for the twenty-first century. The converters at the board of such a vehicle must have minimum volume, versatility, and high power quality. Substantial space can be saved if the filter section commonly found in standard converters is eliminated. A new type of converter (the "matrix converter") was developed to satisfy this demand. These converters, which utilize the same components as other power electronics circuits but with a different control sequence, can perform different functions, thus reducing the logistic burden at the board of the vehicle. As the military vehicles face a harsh environment, with a broader range of ambient temperature, thermal management of the electronic converters becomes more stringent.

Other harsh environmental conditions, particularly in defense applications, include moisture, dust, and vibration. The resistivity of the materials involved in the devices of a power electronic system depends on variable environmental conditions. High humidity may lead to corrosion. The behavior of the power electronics converter is dependent on its board layout. In highly sensitive systems, special design alternatives are considered for diminishing the effect of unavoidable harsh conditions: the placement of the elements on the printed circuit board may be changed, or the routing of exposed conductive layers may be modified.

In hazardous environment we shall never use non-isolated converters: metal contacts between the converter and the voltage supply can create dangerous electrical arcs. Contact-less converters containing transformers with a large air gap will be the preferred solution.

One of the critical problems facing soldiers on the battlefields of the twenty-first century will be the availability of electric power. They will need voice, data and image transmissions over extended distances and for long periods when detached from any supporting base. Multiperforming power electronics will have to accompany the dismounted soldier. The USA Land Warrior Program considers two time frames – up to 2015 ("Force XXI") and 2015–2025 ("The Army After Next") – for equipping the necessary advanced low-power circuitry. It is envisaged that the use of fuel cells instead of primary batteries for missions requiring energy greater than 1 kWh could reduce the total mass of the energy sources by an order of magnitude. Of course, the fuel cells have to be accompanied by suitable electronic converters to render them useful, as we have seen previously. If the soldier uses a portable solar tent, containing photovoltaic panels, he has to carry it to remote locations to run electronic devices. Often, these tents are placed near trees or fences and, as a result, the solar cell becomes illuminated non-uniformly. The shading can cause performance loss that has to be dealt with by the power electronics circuitry.

All-electric defense aircraft carriers are envisaged, with electric power used for everything, from propellers, to aircraft launching catapults, to deck guns. Two types of power electronics will be required for two specific applications: variable-speed motors in fuel pumps and vehicle drives, and precision-control "actuators" for gun turrets and flight control (an actuator is a mechanical device that takes electrical energy for moving or controlling a device). Both low power loads and high-power devices like radars, traveling wave tubes, or electronic countermeasures will have to be supplied by the power distribution system.

The US Navy has its special requests. For example, for detecting sea turtle activities near naval bases, such that the turtles would not be endangered by ships, the navy uses "hydrophones." These are electronic devices anchored to the bottom of the sea. Originally they were powered by batteries, which had to be replaced frequently by divers, a costly and dangerous process. A new way for powering the hydrophones is to use microbial fuel cells, which can "harvest" energy in the water by using the largely abundant bacteria there, with certain electrochemical reactions generating electricity. These bacteria-based cells remain in activity as long as there are living bacteria, with little maintenance. However, these alternative sources of energy produce a very low power: the voltage output is less than 700 mV, the current output is just less than 2 mA. The supply voltage requested by a hydrophone is 3.3 V, at a load of at least 5 mA. In open sea, it is not

possible to stack several microbial cells in series, like batteries. Neither is possible to increase the current capacity of the cell by increasing the surface areas of the anode and cathode of the cell, as this would result in a hard-to-deploy cell. The solution belongs to power electronics: a circuit able to boost the cell's voltage to the load's voltage level and accumulate energy from the cell to burst power to the load. Available power electronics circuits draw high current at low voltage; such a current would exceed that supplied by a cell. Therefore, at the low voltage supplied by the cell, the power converter could not even start up. A new type of converter had to be developed for this application, one that can draw very low current from its input source and use the energy received from the cell to charge a "supercapacitor." Then, the supercapacitor voltage is stepped up and stabilized by another DC-DC converter.

The specific demands and standards of the defense industry lead to the need for designing customized power electronics.

1.1.15 Drives and high-power industrial applications

In the quest for modern applications of power electronics, particularly in consumer electronics, automotive industry or spacecraft, do not forget that, initially, power electronics technologies were used in drives of DC and AC motors in industry and traction. The role of the power electronics circuit was not only that of a power supply. It was also used in controlling the induction motors speed. The high-power inverters used for this purpose could assure a broad range of speed control, with excellent speed-control accuracy, and a constant torque operation over a very large speed range. Many old industrial applications of power electronics include heating, melting, and heat treatment of metals based on an induction heating method which requires the use of inverters, electrochemical processes such as metal refining, electroplating, production of chemical gases, or electronic welding. Medium power range driving applications include machine tools, paper mills, textile mills, and pumps. In the high end of the power range, that of multimegawatts, applications like gas line compressors, feed pumps, ship propulsion, or cement mills can be found. For example, adjustable-speed pumped-storage systems in the range of 400 MW have been used in hydroelectric power plants; the motor is supplied by three-phase low-frequency AC currents produced by a cycloconverter connected to a 500 kV, 50/60 Hz utility grid through a step-up transformer. Or, the use of power electronics-based variable frequency drive in diesel–electric ship propulsion can save a considerable amount of fuel. It is estimated that around 60–65% of the grid-generated energy in the USA is spent by electrical machine drives, around 75% of them being fan, pump and compressor type drives. Running the induction motors coupled to pumps or fans at constant speed in traditional control of fluid speed, causes a lot of energy wastage, because it creates fluid vortex. Replacing the system with a variable-frequency motor speed control can save much energy. Variable-speed air conditioning can reduce the consumption of electricity. Specific power electronics are used to get load-proportional speed control of the air-conditioner pump. The glamorous applications discussed at the beginning of this chapter do not mean that the old uses of power electronics are less important today than they were in the past.

The different applications discussed above are visualized in Figure 1.4.

1.1.16 Classification of power electronic circuits

As we can see, basically the energy conversion electronic circuits can be classified in four groups according to the type of the input and output (load) power: *DC-DC converters*, where the controlled conversion is from DC input to DC output, serving, in most of the cases, as switching mode DC power supplies; *AC-DC rectifiers*, where the AC (single- or three-phase) input energy is converted to a DC waveform (in most of the cases, besides the regulation function, a power factor correction function has also to be fulfilled); *DC-AC inverters*, for the controlled conversion of DC electric power to single- or three-phase AC output of a certain

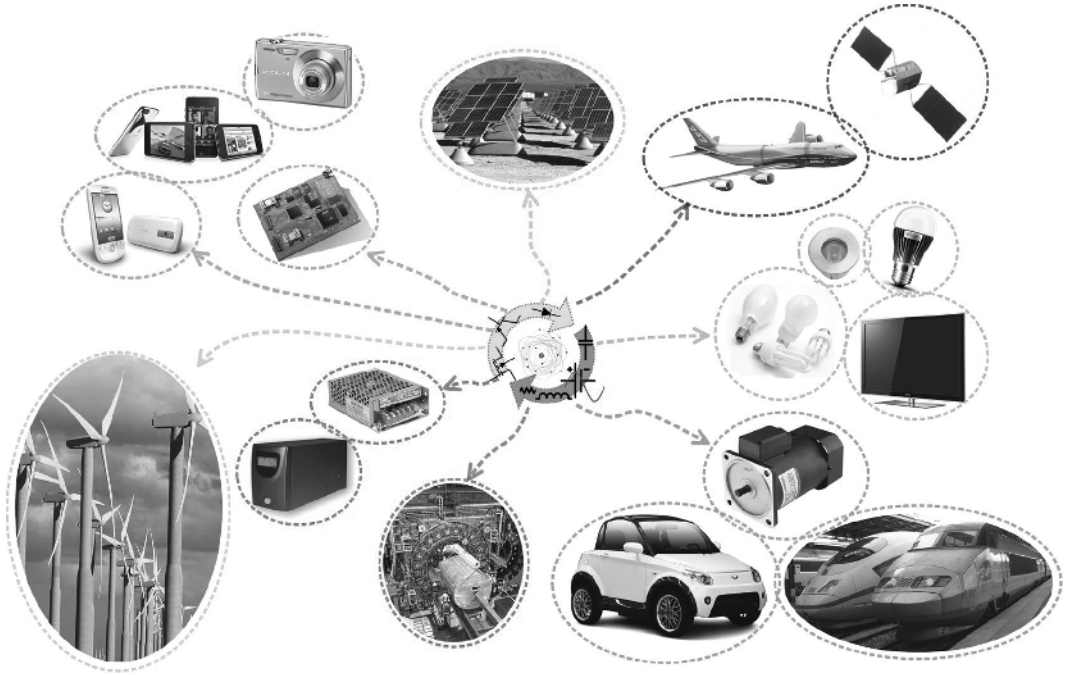

Figure 1.4 *A tree of power electronics applications.*

frequency; and *cycloconverters*, where an AC electric power of a given frequency (most often, the line frequency of 50/60 Hz) is converted to an AC electric power of another frequency (or variable frequency, in the case that the cycloconverter is used to control the speed of AC motors). Recently, with the advent of the switching and modular techniques, the classical cycloconverters have lost ground to efficient AC-DC-AC converters. Converters with more outputs are also available; for example, DC power supplies with different load voltages.

A modern system contains a large number of power electronics circuits. For example, Figure 1.5 shows the electrical network on a train of the Hong Kong railway. The electric power is transmitted to the trains through the 1500 V DC overhead lines, and is inverted into a three-phase 440 V, 60 Hz AC voltage, to supply the AC loads. For supplying the DC loads, the 440 V AC voltage is further transformed down and is rectified into a DC voltage of 110 V. This voltage is used for charging up the backup batteries and powering various

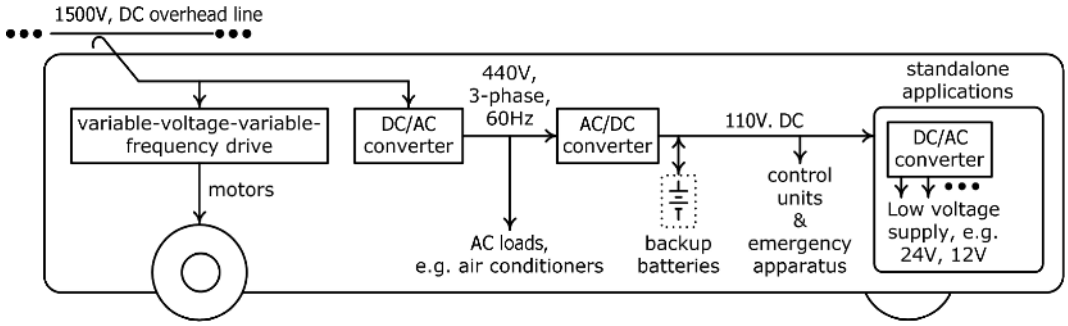

Figure 1.5 *The architecture of the electrical system on trains in the Hong Kong MTR (mass transit railway).*

control units. However, it is energy inefficient to go through so many conversion steps in order to step-down the 1500 V DC to 110 V DC. Present research looks for a way of realizing this conversion in a single stage. The 110 V DC is further converted to 24 V DC and 12 V DC for stand-alone applications (like information boards in carriages). Again, a direct conversion from 1500 V to 12 V/24 V is a serious challenge for power electronics researchers.

From the applications described in this section, it can be seen that power electronics circuits penetrate all the aspects of our life. These applications span from under 1 W power hand-held gadgets to hundreds of megawatt industrial processes, from under 1 V voltage for supplying IC electronic circuits to hundreds of kilovolt utilizations in experimental physics. In addition, it was also seen that each type of application imposes certain specific requirements on the features of the power electronic circuit.

A modern design concept looks not only to the best circuit topology but also to the spatial design: components that fit together as closely as possible, minimum empty space within the converter structure, and liquid cooled thermal management based on short heat paths in the case of high-power applications. For example, a bidirectional DC-DC converter used on a train can reach a power density of 40 kW/l at a power of 60 kW.

This is why an extremely large variety of energy conversion electronic circuits have been developed. In the quest for better circuits – first of all with a better efficiency in processing the electrical energy in the energy-saving conscious world of today and also pushed by new, more demanding applications – more challenges are facing the people working in the power electronics industry, from researchers, designers, and manufacturers, to those making use of these circuits. New and better power electronics systems are to be expected.

1.2 Basic Principles of Operation of a Power Electronics Circuit

When discussing different applications, it was noted that the purpose of a power electronics circuit is to ensure a controllable output characteristic; for example, a constant output voltage which is supplied to a variable DC load, or a controlled AC voltage for managing the speed of an AC motor. Therefore, regardless of the type of application, the power electronics circuit is placed between the non-regulated input (whose parameters, a DC or an effective AC voltage for example, can arbitrarily vary) and the load. This means that all the energy is channeled through the circuit, that is, a power electronics circuit can be viewed as a *power processing* system (unlike electronic circuits, used for example in communications, that serve for signal processing). As the power electronics circuit is just an intermediate stage before the load, it is unconceivable to lose much electrical energy in the processing stage, that is, even before the energy in the desired form was supplied to the load. This is why the first requirement from this circuit is *to process the energy efficiently.* It firstly means that dissipative resistors will never be used in its structure; this is easily said but more difficult to be implemented: even if resistors are not inserted, all the other elements feature a parasitic resistance. Taking into account that the current can reach a few thousand amperes in some power applications, it means that even a small resistance will lead to a non-negligible loss of energy. For example, a current sensor of 1 mΩ resistance would dissipate 10 W power in measuring a 100 A current. Apart from the efficiency problem, as the energy dissipated in the resistors is in the form of heat, complex thermal management is required, resulting in higher production cost and larger physical size. Sometimes, resistors are unavoidable, such as in current sensors for control purposes (today, new solutions of current sensing, which do not make use of resistors, are being implemented more and more), or in some auxiliary circuits, called snubbers, used for dissipating parasitic energy, which would otherwise destroy the switching devices (today, non-resistive snubbers are being implemented more and more). All the power losses are converted in the end into heat. This causes the devices within the converter to operate at high temperature, reducing their lifetime and reliability. For converters of higher power, a rather large cooling system is necessary, any increase in the efficiency having beneficial effects.

To illustrate the principle of operation of a power electronics circuit, DC-DC converters will be considered. The input of these converters is often a battery or a rectified AC line voltage. They have to process a variable DC (line/supply) voltage, V_{in}, in order to provide a constant output (load) voltage, V_{out}, despite variations in the load value, R. How can such a goal be achieved? We know from basic electronics that, by using a transistor operating in its linear region, we can regulate the output. However, in such a case, the transistor is equivalent to a resistor (operating as a potentiometer). In power electronics such a technique would lead to a loss of energy. In addition, it does not allow a step up of the line voltage, as is needed in many applications. This is why we had to find another regulation approach in power electronics.

The solution we came up with is based on a switching operation. The simplest DC-DC converter's structure contains one inductor, L, one capacitor, C, and a single pole, double throw switch (which is a simple changeover switch having two positions) (Figure 1.6a). When the switch is in position (1), the energy is transferred from the line to inductor L, by charging it (Stage 1; Figure 1.6b). The energy is stored in its magnetic field. When the switch is moved to position (2), the inductor energy is transferred to the load (Stage 2; Figure 1.6c), that is, the inductor is discharged. The switch position is varied periodically, all the time, in a cyclical operation. The two topologies the circuit goes through cyclically are called *switching stages*. We can notice immediately *the role of the capacitor: it has to maintain the output voltage* during the first stage. As we want a constant V_{out}, it means that C must have a large value (output capacitors of hundreds of μF are usual in power electronics), and the duration of the stage has to be very small in order to prevent C discharging significantly. This implies that the switch operates with a high frequency. We shall see that even the most classical converters were operating with frequencies up in tens of kHz. In the second stage, the inductor energy also recharges C. As a basic law in Circuit Theory says that at the transition moment the inductor current (i_L) cannot change direction, it means that i_L charges C at a voltage polarity opposite to that of V_{in}. Thus, the polarity of V_{out} will also be opposite to that of V_{in} in the converter shown in Figure 1.6.

How can we assure a constant V_{out} if V_{in} has variations? Consider that for a certain (nominal) value of the input voltage and for a certain (nominal) duration of the inductor's charging stage, we get the desired output voltage. Let us say that then V_{in} has a drop from the previous value. If we increase the duration of Stage 1, the value of the transferred energy to L would be the same as in the previous case; therefore, in Stage 2, V_{out} will remain the same. Similarly, if there is an increase in V_{in}, the duration of Stage 1 can be reduced, so as to give less time to charging L (from a larger V_{in} now), the effect being again that the energy accumulated in the magnetic field of L (and therefore V_{out}) is the same, regardless of the value of V_{in}. A similar operation occurs if there is a change in the load value: by controlling the duration of the charging time of the inductor, more or less energy is transferred to L (in order to cope with a variable load and thus assure a constant V_{out}). Therefore, *the switching action is essential*, because by controlling the duration of the stages, the supply of a constant voltage can be assured, despite variations in the line and/or load. These converters are also known under the name of *switching mode power supplies. The role of the inductor becomes clear: to assure a controllable transfer of the energy from line to load.* When V_{in} and R have nominal values, we say that the converter operates in *steady state*.

To electronically implement the switch, we can use an externally controlled element, that is, a transistor, T, and a diode D (Figure 1.6d). The driving signal of the transistor is denoted as $d(t)$ (or v_{GS} in case of transistors of the MOSFET type). When the driving signal (Figure 1.6e) has the logical value (1), the transistor is on, the inductor is being charged, and the diode will be blocked by an inverse polarity. When the driving signal has the logical value (0), the transistor is off, the inductor current needs to find a path for continuing to flow, thus turning on the diode. Therefore, the diode acts as an automatically synchronous switch with the transistor (Later we will see that in some modern applications with a low load voltage and high output current, it is preferable to use transistor-based self-driven synchronous rectifiers instead of diodes, as they have less voltage drop when conducting). The converter obtained in Figure 1.6d is called **buck-boost**.

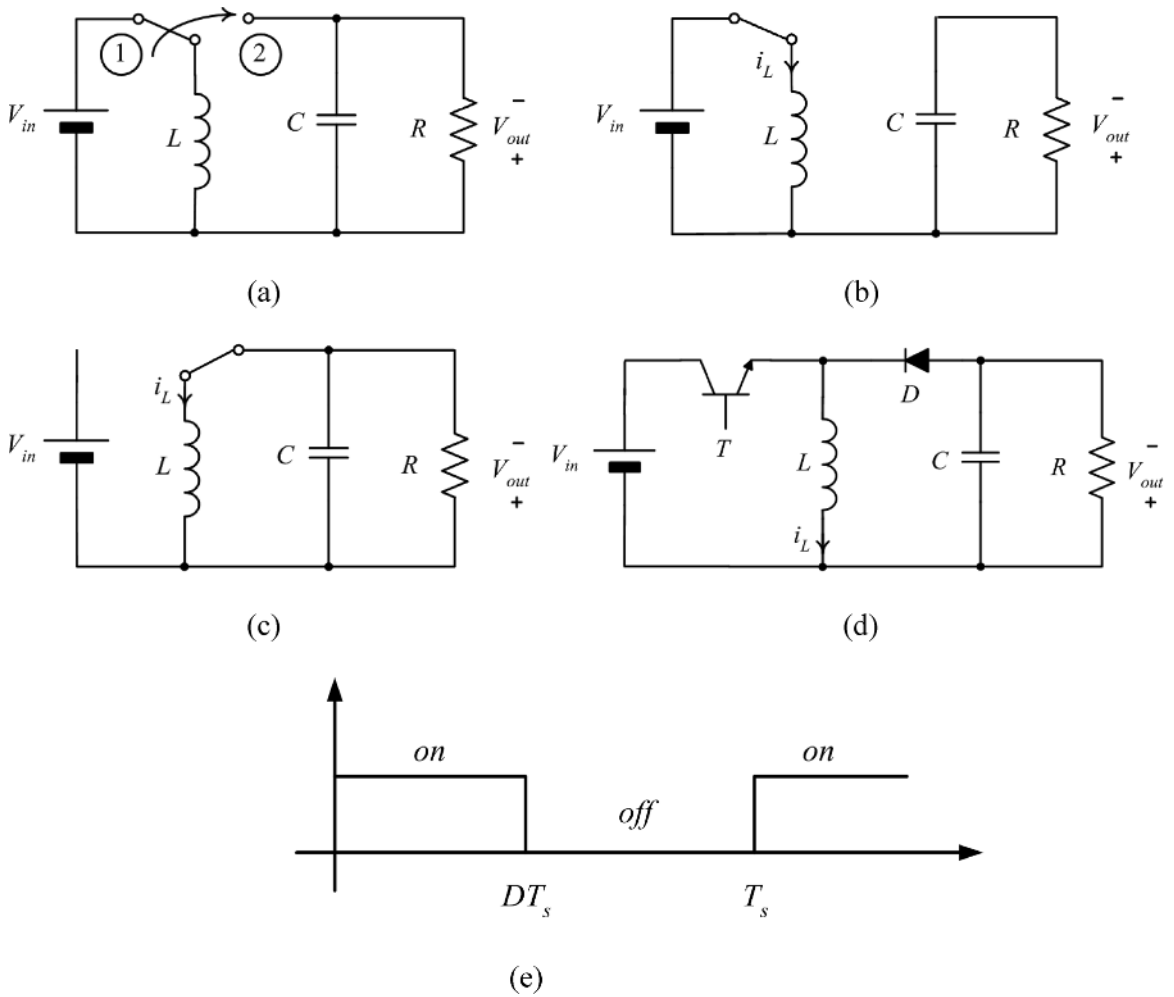

Figure 1.6 *The simplest structure of a DC-DC converter and its switching operation: (a) basic circuit; (b) switching stage 1; (c) switching stage 2; (d) electronic implementation; (e) driving signal.*

The driving signal repeats itself with the periodicity T_s. T_s is called the switching period and its inverse, $\boldsymbol{f_s}$ ($f_s = 1/T_s$), is called the *switching frequency*. The fraction of T_s for which the transistor is on is called the *duty ratio* (or *duty cycle*), D:

$$D = T_{on}/T_s$$

implying:

$$T_{on} = D\,T_s, \quad T_{off} = T_s - D\,T_s = (1 - D)T_s$$

T_{on} and T_{off} are the respective durations of the switching stages 1 and 2 that form the switching cycle, T_s.

Clearly, D is a number that takes values between 0 and 1:

$$0 < D < 1$$

Therefore, for keeping V_{out} constant despite variations in line and load, we can vary the duty ratio, by keeping constant T_s. Obviously, when V_{in} and R are at nominal values, D is also at its nominal value. This type of control, with constant switching frequency, is called duty-cycle-control. We will see that there is also another possibility for control, by varying the switching frequency.

Other two types of basic DC-DC structures are given in Figures 1.7 and 1.8. The converter in Figure 1.7 is called **boost**. The operating principle is, of course, the same as for the buck-boost converter: when the switch is in position (1) (Figure 1.7a), that is, when the transistor in Figure 1.7d is turned on, compelling the diode to be turned off, the inductor is charged by the line voltage, V_{in}. This is the first switching stage (Figure 1.7b). When the switch is in position (2), that is, the transistor is turned off, the inductor current must continue to flow in the same direction, turning on the diode. This is the second switching topology (Figure 1.7c), in which the energy from the line, together with the energy provided by the inductor in a discharging operation, is transferred to the load. It is natural to expect that V_{out} would be larger than V_{in}.

In Figure 1.8, a **buck** converter is shown. With the switch in position (1), that is, when the transistor is turned on, the diode is reversed biased, and the input energy is transferred concomitantly to the inductor, by charging it, and to the load. It is natural to expect in this case that V_{out} is lower than V_{in}. In the second switching topology, when the switch moves to position (2), that is, the transistor is turned off, the inductor current continues to flow, turning on the diode. From this description of the switching operation, we can notice that for buck and boost converters also it is possible to keep the output voltage constant under variations of the line and load by playing with the duration of charging the inductor, that is, by adjusting the duty ratio.

The three structures considered above are the basic DC-DC converters. The inductor in the boost converter is connected to the line in both switching stages; this prevents large variations in the input current during a switching cycle, as the input current is identical with the inductor current. In a first-order approximation, the input voltage source with the series inductor can be seen as a current source, giving a so-called "current-driven" characteristic of the boost converter. (The approximation is more accurate at high frequencies. For an ideal current source, one should be able to control its terminal voltage to an arbitrary value. By imposing a voltage v different from V_{in} at the terminals of the cell formed by the line and L, a voltage difference would be applied across the inductor, resulting in an increasing or decreasing inductor current). As the capacitor serves to maintain the output voltage during a cycle, the parallel combination of capacitor and load R can be seen, in a first-order approximation, as a voltage sink (Figure 1.9). On the other hand, the output current of the boost converter would be given by the current through the diode in the absence of capacitor C. Only an AC current flows through the output capacitor C. The output current of a boost converter has a highly pulsating character during a switching cycle. In the case of the buck converter, the input

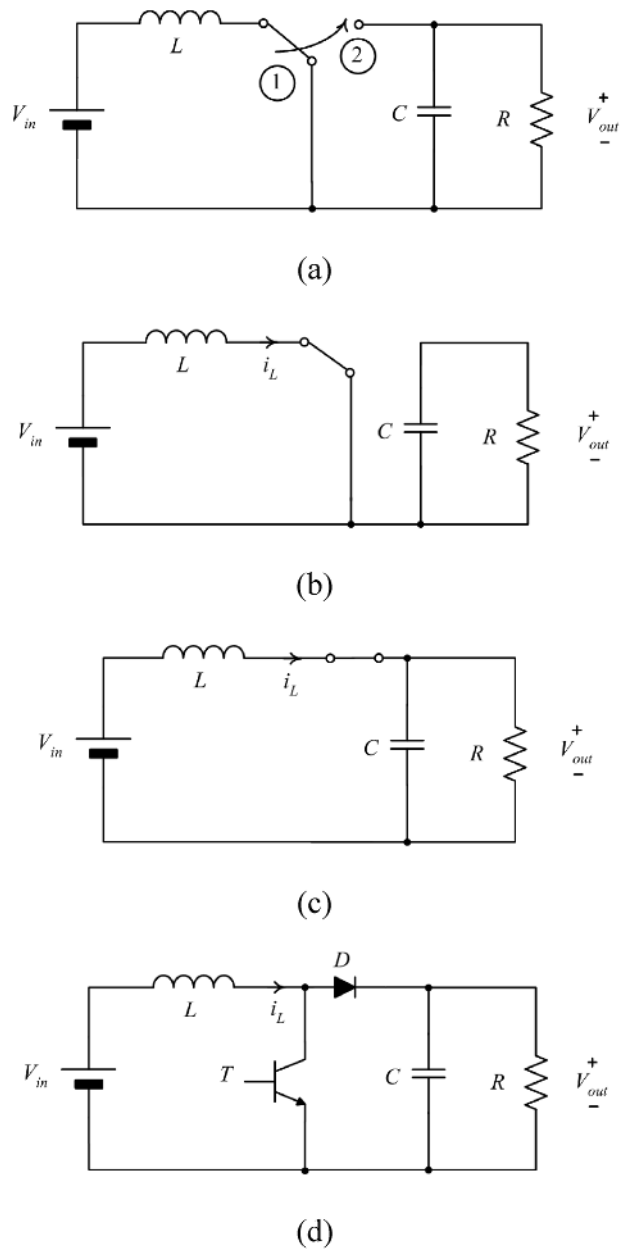

Figure 1.7 *Boost converter: (a) basic structure; (b) switching stage 1; (c) switching stage 2; (d) electronic implementation.*

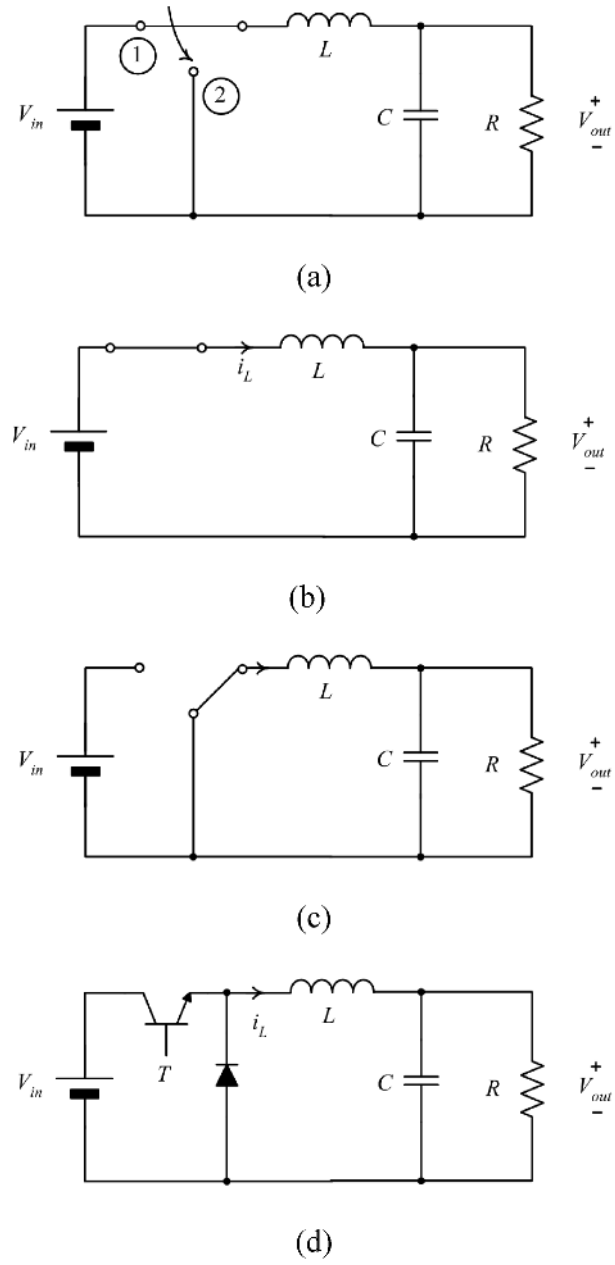

Figure 1.8 *Buck converter: (a) basic structure; (b) switching stage 1; (c) switching stage 2; (d) electronic implementation.*

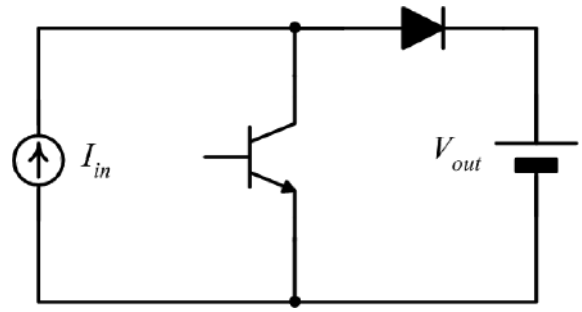

Figure 1.9 *First-order approximation equivalent switching scheme of a boost converter (current-driven converter).*

current drawn from the line is given by the current through the transistor, therefore it has a very pulsating character during a switching cycle (it is zero when the transistor is off). However, the output current, in a first-order approximation, is given by the inductor current, as L, C, and R can be seen as a current sink (Figure 1.10). The buck converter has a "voltage-driven" character. It is wrong to see the buck-boost converter as a combination of a buck and a boost converter. In the case of a buck-boost converter, the inductor switches from a connection to the line to a connection to the load in each switching cycle, giving a very pulsating character to both the input and output currents. In addition, the output voltages of the buck and boost converters have the same polarity as V_{in}, but V_{out} of the buck-boost has an opposite polarity to V_{in}, giving the specificity of this converter.

Let us try to get, in a very approximate way, the relation between the output and input voltages of the buck converter. Despite all the assumptions we make, later, when finding the exact equation, we will be amazed how close to the correct result we arrive at in this section. Assuming 100% efficiency, we can write that the output energy (or power) is equal to the input energy (or power), that is:

$$V_{out}\, I_{out} = V_{in}\, I_{in}$$

As we have seen, in the first switching topology of a buck converter, of duration DT_s, $I_{out} \approx I_{in}$, and, in the second stage, $I_{in} = 0$, but I_{out} continues to flow, that is, I_{in} flows only for a DT_s time duration and I_{out} flows during all the cycle T_s. Therefore, we can say that approximately I_{in} is only the "D" part of I_{out}: $I_{in} = D\, I_{out}$, which substituted in the previous equation gives:

$$V_{out}\, I_{out} = V_{in}\, D\, I_{out}$$

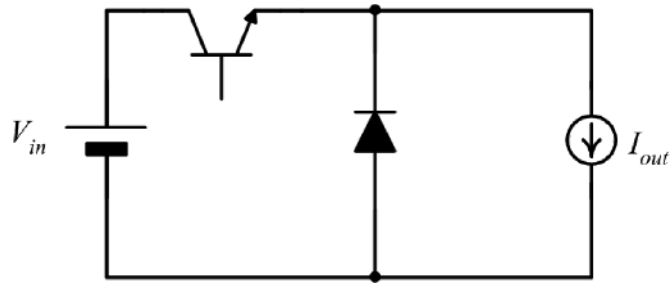

Figure 1.10 *First-order approximation equivalent switching scheme of a buck converter (voltage-driven converter).*

implying:

$$V_{out} = D\,V_{in}$$

For a better understanding of the process taking place in a converter, take as an example the buck converter (Figure 1.11). Use an oscilloscope to visualize the voltage in a few parts of the converter. The voltage waveform between nodes 1 and 2 is, of course, the input voltage, V_{in}. Between nodes 3 and 4, we see a square pulse waveform with a height of V_{in}, and a width of each pulse of $D\,T_s$ (because, when the transistor is on and diode off, $v_{34} = V_{in}$, and, when the transistor is off and diode on, $v_{34} = 0$, this repeating itself in each switching cycle), that is, the DC waveform was transformed into a periodical one. At the load, we see the voltage $v_{56} = D\,V_{in}$, according with the previous equation, that is, the periodical waveform was rectified back to a DC one (this is why the output diode is also called *rectifier diode*). We can note that if V_{in} changes, by changing the width of the pulse, that is, of D, we can assure the desired constant, V_{out}. Due to the approximations considered here, we cannot yet see how V_{out} is kept constant for load changes; this will become clear only when deriving the exact formula in the next chapter. From Figure 1.11, we see that the input waveform of the block LC is a square pulse wave and the output is a constant voltage (as the converter performs the role of a DC power supply, its output has to be a "clean" DC wave). We know that if we perform a Fourier analysis of the square wave, we will find that it contains a DC component of value DV_{in}, a harmonic of the fundamental frequency, f_s, and odd high-frequency harmonics. As, at the output, we must get only the DC component, it means that the inductor and capacitor have to also fulfill the role of a low-pass filter. In order to eliminate all the harmonics, including the fundamental frequency one, the corner frequency of this filter has to meet the condition:

$$f_c = \frac{1}{2\pi\sqrt{LC}} \ll f_s$$

If we imagine the Bode plot of the low-pass LC filter (Figure 1.12), the above condition would ensure that the magnitude reaches minus many tens of db at the frequency f_s, that is, even the fundamental frequency harmonic is almost completely rejected from the output waveform (and so the higher frequencies harmonics for which the magnitude is even more negative). The output results in an almost clean DC, as required from a DC power supply.

However, the above formula, as simple as it is, creates the most difficult challenges in power electronics: to meet it one has either (a) to design an inductor and a capacitor of large values, implying an undesirable large size for the electronic supply and energy loss in the larger parasitic resistances of these reactive elements, or (b) to operate the converter at a very high switching frequency, implying a high frequency of turning the switches on and off, each operation taking place with loss of energy, as will be explained in the following section. How to fulfill the above formula was a permanent objective in the development of power electronics in the last decades; in the following chapters we shall see the appropriate solutions that have been found.

A general structure for a switched-mode power converter is shown in Figure 1.13. It consists of four main parts: an input filter, a power processing circuit, an output filter and a controller. Let us see their roles.

A switching operation always creates harmonics that could pollute the supply system. For example, since the input current of a buck converter is highly pulsating, its frequency spectrum is widely spread. As a result, the converter would generate electromagnetic interference (EMI). In Figure 1.14 we can see the conducted EMI (this is the EMI reaching the supply source through the connecting wires, with the frequency range from 9 kHz to 30 MHz) of a 50 W buck converter switching at 115 kHz. For the same converter, Figure 1.15 shows the radiated EMI (this is the EMI radiated from the converter to the surrounding air, with the frequency range 30–300 MHz).

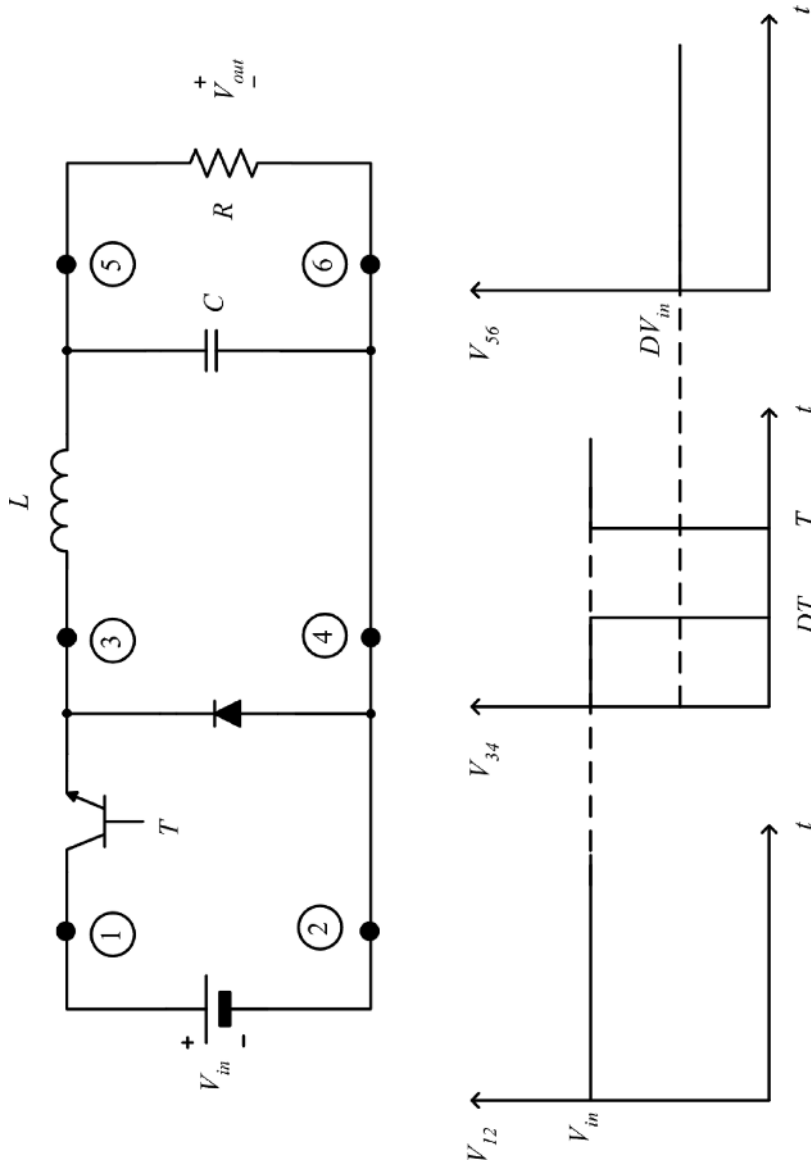

Figure 1.11 *Interpretation of the operating principle of a buck converter.*

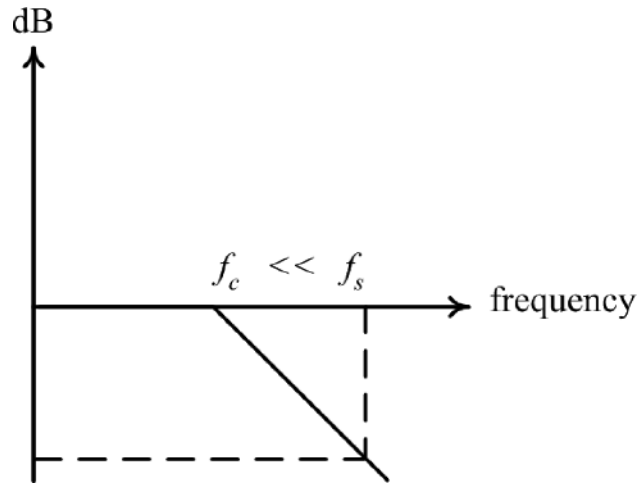

Figure 1.12 *Bode magnitude characteristic of a* LC *low-pass filter.*

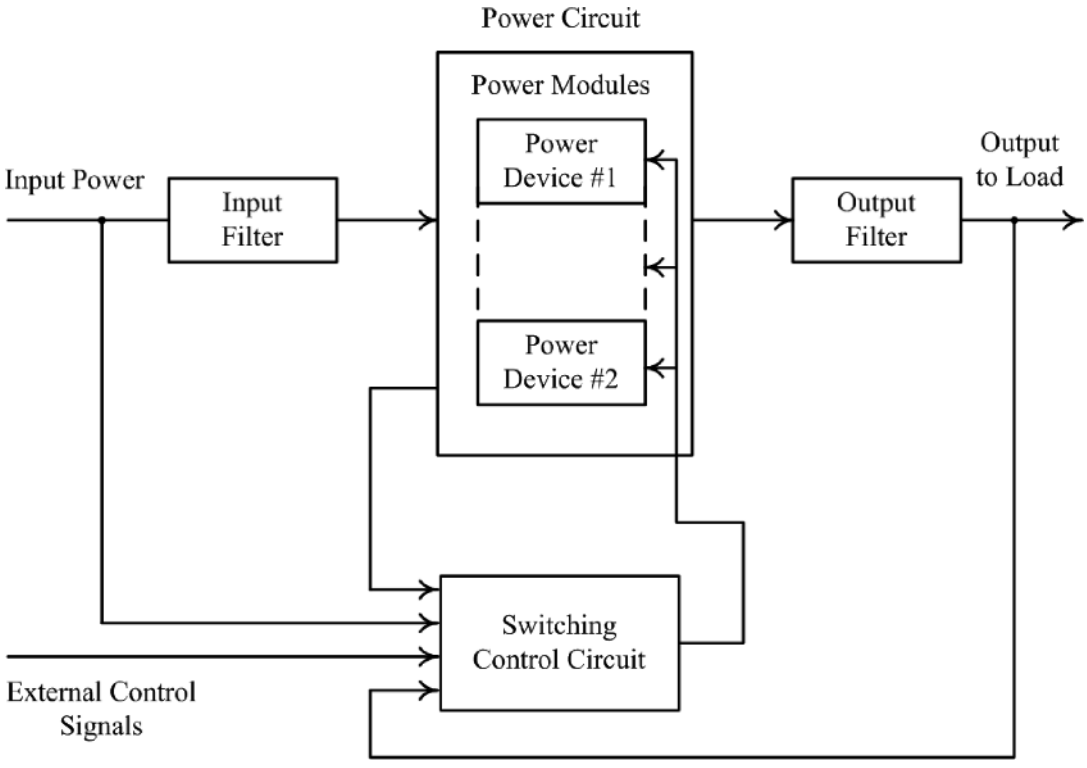

Figure 1.13 *General structure of a switched-mode power converter.*

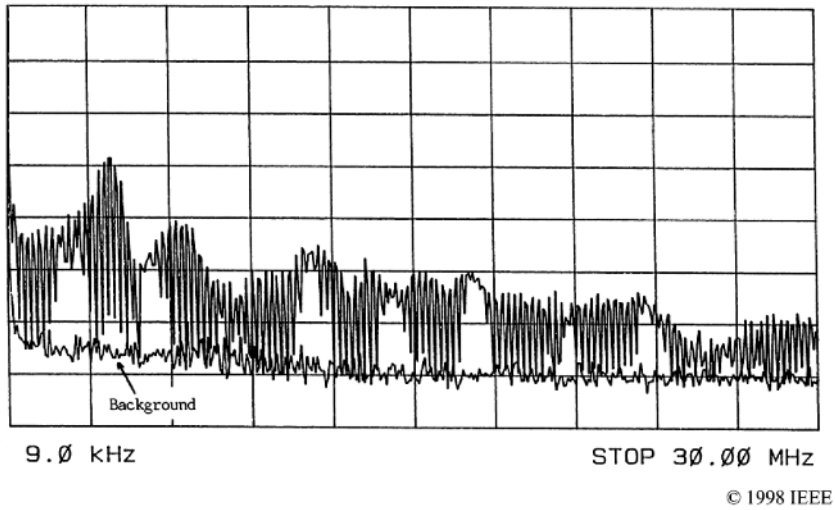

Figure 1.14 *Experimental spectrum of the conducted EMI from a 50 W buck converter switching at 115 kHz. (y-axis: 10 dB/div). (Reproduced, with permission, from: H. Chung, S.Y.R. Hui, and K.K. Tse, "Reduction of Power Converter EMI Emission Using Soft-Switching Technique,"* IEEE Transactions on Electromagnetic Compatibility*, August 1998.)*

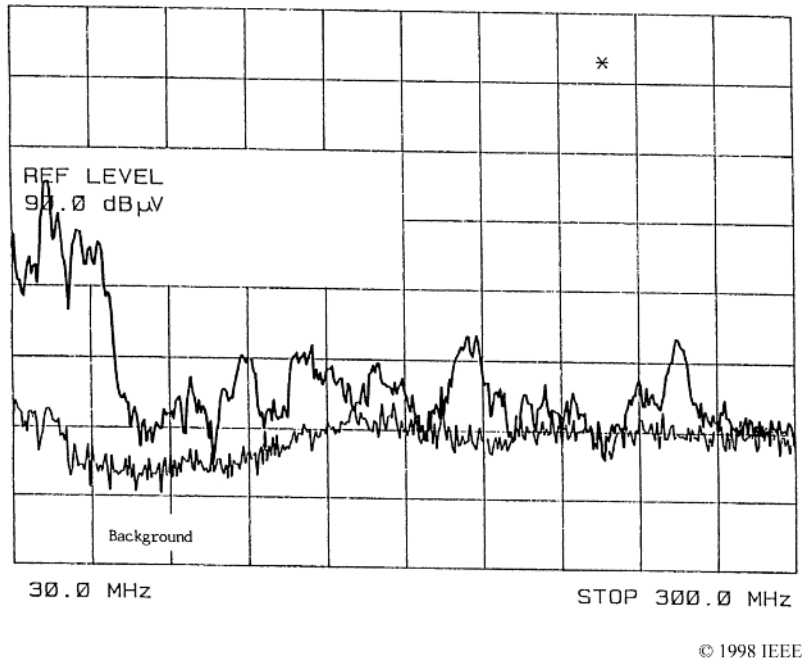

Figure 1.15 *Experimental spectrum of the radiated EMI from a 50 W buck converter switching at 115 kHz (y-axis: 10 dB/div) (Reproduced, with permission, from: H. Chung, S.Y.R. Hui, and K.K. Tse, "Reduction of Power Converter EMI Emission Using Soft-Switching Technique,"* IEEE Transactions on Electromagnetic Compatibility*, August 1998.)*

The statutory standards impose tough limits on the harmonic interference created by electrical equipment into the power system. In order to prevent the switching harmonics from interfering with the supply source, an input filter is used.

The switching circuit is the power processing stage, which consists of power semiconductor switches and passive reactive elements, such as capacitors and inductors. For the buck-boost converter shown in Figure 1.6d, the switching circuit consists of the switch, *T*, inductor, *L*, and diode, *D*.

The output filter is used to smooth out any switching harmonics at the output to get the desired output waveform. As mentioned previously, in the buck converter the section *LC* plays the role of an output filter. In other converters, sometimes we need to add one or more cascaded filter sections to enhance the quality of the output waveform.

As discussed, it is not desirable to use resistors in the power processing stage. However, there are practical applications that require using small resistors in the input and output filters to attenuate the natural oscillations of the filters. For example, a small resistor would be connected in series with the capacitor of the *L-C-L* output filter used in a grid-connected inverter.

Finally, the controller is used to generate gate signals to all active switching devices in the switching circuit. In the past, all controllers were implemented with analog circuits. Nowadays, following advances in microelectronics, hybrid controllers containing both analog and digital circuitry are becoming popular. The analog part is characterized by fast response. This is why it is used for functions like short-circuit protection, or in the ultra-fast transient control loop. The digital part is comparatively slower but it can be programmed flexibly for different functions like housekeeping (start-up sequence, alarms) and control of slow feedback loops.

1.3 Basic Components of the Power Circuit: Power Semiconductor Switches and Passive Reactive Elements

As seen in the preceding section, any power processing stage contains switches. As, in power electronic circuits, some critical features of the switches play a particular role, they are discussed in this section. We can classify power semiconductor switches into three main categories. The first type is the *uncontrollable switch*. Such a switch conducts automatically when it is forward-biased. The biasing condition is determined by the circuit comprising the switch. A typical example is the diode. It will automatically be in the on-state when it is forward-biased. The second group is represented by *semicontrollable switches*. Such a switch conducts when it is triggered by an external gate signal. It will automatically block when the current flowing through the switch is zero. An example is the thyristor. The third group is formed by *controllable switches*. The switch is turned on and off by an external gate signal. Examples include bipolar transistor, metal oxide semiconductor field-effect transistor (MOSFET), insulated gate bipolar transistor (IGBT). New field-effect transistors are fabricated by using semiconductors such as gallium arsenide (GaAs), gallium nitride (GaN) or silicon carbide (SiC).

1.3.1 Uncontrollable switches – power diodes

A diode is a two-terminal device allowing unidirectional current flow. There are two main kinds of semiconductor diodes. These are the p-n junction diode and Schottky barrier diode.

The *p-n junction diode* is formed by joining two different types of semiconductor materials, one of p-type and one of n-type (Figure 1.16a). The majority of carriers in p-type material are holes, while the majority of carriers in the n-type material are electrons. The holes and electrons, in movement, combine near the junction of the two materials, resulting in a depletion layer at the junction (i.e., a region in which

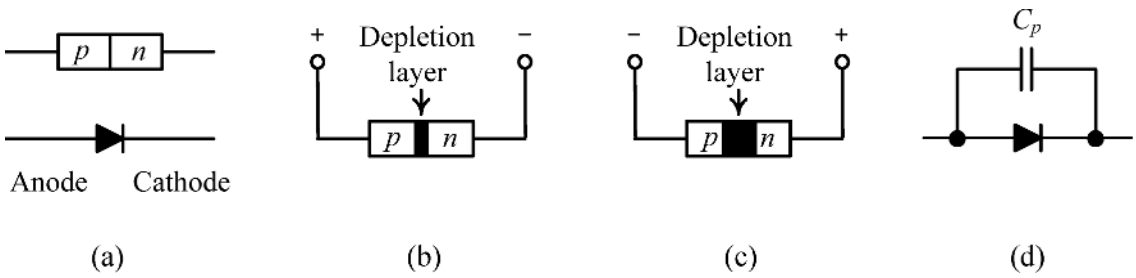

Figure 1.16 *Symbol and biasing conditions of a p-n junction diode: (a) symbol; (b) forward-biased; (c) reverse-biased; (d) equivalent circuit in reverse-biased condition.*

all the mobile charge carriers have been removed, leaving none for carrying a current). A small barrier potential across the diode is created. If a forward bias potential is applied to the diode, as in Figure 1.16b, the depletion region will become narrow, reducing the resistance to the current flow. There is a voltage drop across a conducting, *forward-biased diode*, which is called *forward voltage*. Typically, for silicon p-n diodes used in electronic circuits of small current, this forward voltage is 0.7 V. However, for power diodes, the forward voltage can reach 1.4 V. A reverse bias potential (Figure 1.16c) causes the depletion layer to widen, increasing the resistance to the current flow. Actually, a very small amount of current can go through a *reverse-biased* diode. It is called the (***reverse***) *leakage current*.

The *Schottky* barrier *diode* uses a metal–semiconductor junction, resulting in a low forward voltage drop and high switching speed. Its forward voltage drop is around 0.15–0.45 V. However, the Schottky diodes feature a relatively high reverse leakage current, which increases with temperature. A new type of Schottky diode is the *silicon carbide* (SiC) Schottky barrier diode, which uses a wide band gap semiconductor material, SiC, instead of a silicon semiconductor. It has a lower reverse leakage current and a very fast operating speed (the rate of change of the diode current for SiC diodes can be up to 1000 A/μs, that is, five to ten times faster than that for p-n junction diodes or silicon-based Schottky diodes). However, the leakage current of SiC Schottky diodes is still larger than that of p-n silicon diodes. The electrical characteristics of SiC are less sensitive to temperature variation.

The state of a diode is determined by the voltages and currents of the circuit in which the diode is connected. When the diode is on, a current flows from anode to cathode through the p-n junction. When it is off, its anode–cathode voltage is negative. The actual voltage on a diode in the off-state depends on the circuit to which the diode belongs (e.g., in a buck converter operating in the first switching stage, the voltage across the diode in off-state is equal to the input voltage of the circuit). When the diode is in conduction, the average conduction power loss equals the product of the forward voltage and average anode current.

In high-power applications, when choosing a suitable diode, apart from considering the voltage and current ratings, it is crucial to consider the turn-off characteristics. These characteristics are significantly different for a p-n junction diode and a Schottky diode. The transition of a diode from a conduction state (on-state) to a blocking one (off-state) is not instantaneous; rather, it comprises a complicated process. During the forward conduction, there is an excess of minority carriers in each diode region (i.e., holes in the n-region and electrons in the p-region). These carriers must be removed at turn-off. And the depletion layer must be re-established for a diode to regain the blocking state. In power electronics, we need diodes with a high switching speed. If the switching characteristics of the diodes are far away from an ideal on/off operation, they may create energy losses and heat in other circuit components. This is why, in power electronics, the transition from the "on" to the "off" state of a diode, known as *reverse recovery*, has to be studied in detail and measures taken to avoid negative effects either on the diode itself or on other elements of the converter. In an ideal situation, at the on–off transition the current through the diode, I_D, will decrease

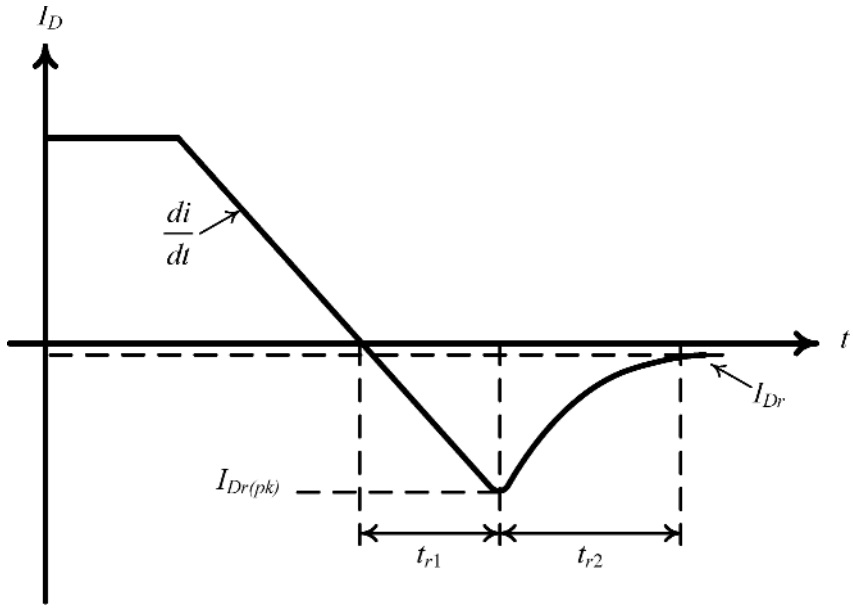

Figure 1.17 *Reverse recovery process of a diode.*

linearly to zero and the diode will reach the blocking state. However, the current does not stop when reaching zero but continues flowing in a reverse direction due to the minority carriers discussed above (Figure 1.17). After a time, t_{r1}, the reverse diode current will reach its peak, $I_{Dr(pk)}$. During the period t_{r1}, the diode does not behave as being in the blocking state, that is, no high blocking voltage appears across it. This causes other elements in the converter to have to support an additional voltage, leading to energy losses and thus heat in other parts of the power circuit. Particularly if I_D presents a large di/dt during this time, the other elements have to absorb a larger switching energy, which hinders the power electronics converter from being operated at very high switching frequencies. The duration t_{r1} depends on the time needed for the minority carriers to be removed (swept out). It is, therefore, dictated by the design of the semiconductor diode. When the depletion layer is re-established, the diode begins supporting the reverse blocking voltage. Immediately after t_{r1}, the reverse voltage reaches its overshoot peak ($V_{r(pk)}$). During the period t_{r2}, the reverse current drops to near zero, that is, reaches its value characteristic for the blocking state, and the reverse voltage reaches its blocking value. The overshoot peak and the duration t_{r2} depend on both the design of the semiconductor junction and the interaction with the inductance in the circuit to which the diode belongs. As, during t_{r2}, the diode is supporting the reverse voltage, V_r, and the current I_D is only slowly decreasing to its reverse value, I_{Dr}, their product produces a significant switching loss, which is dissipated by the diode in the form of heat. Sometimes, an auxiliary circuit (snubber) may be needed to dissipate this energy. At high switching frequencies, the heating process taking place in the rectifier diodes has to be taken into account. The total recovery time, t_{rr}, is given by $t_{r1} + t_{r2}$. Diodes presenting a reverse recovery time of less than 500 ns are considered to be "fast" and those with t_{rr} of less than 100 ns as "ultrafast." Ultrafast diodes are available for voltages in the range 100–1500 volt. The recovery charge, Q_{rr}, may be approximated by considering the area covered by the negative diode current as a triangle:

$$Q_{rr} = \frac{I_{Dr(pk)}}{2} t_{rr}$$

It also gives an indication regarding the energy spent in the reverse recovery of the diode.

Schottky diodes can cease conduction faster than the p-n junction diodes, because there is nothing for them to recover from (In Schottky diodes there are no minority carriers and no slow recombination of p- and n-type carriers. There are only majority carriers in the semiconductor region that are quickly injected into the conduction band of the metal contact in the recovery process.) The switching time for power Schottky diodes is up to tens of nanoseconds.

For SiC Schottky diodes, the reverse recovery charge is zero, so the problem associated with the reverse recovery characteristic does not exist. However, the cost of SiC Schottky diodes is a few times higher than that of p-n silicon diodes.

During the reverse recovery process, the depletion layer is established. It is equivalent to a capacitance that is charged by the reverse recovery current. This is why the equivalent circuit of a diode during the reverse recovery time and blocking state contains a capacitance in parallel with an ideal diode (Figure 1.16d). The value of the capacitance is a nonlinear function of the voltage across the diode. This capacitance creates many practical problems in power electronics. When the diode turns off, due to the reverse recovery current, this capacitance will resonate with the parasitic inductances in the circuit, creating oscillations (called *ringing*). As a result, voltage stress on the diode appears.

When a power electronics circuit is designed, for choosing a diode we shall follow the procedure:

a. Calculate the required blocking voltage (i.e., the voltage at which the diode is submitted in the off-state, as determined by the circuit in which the diode is embedded; for example, the input voltage for a buck converter) and maximum current flowing through the diode.
b. Choose a suitable type for the diode (e.g., SiC Schottky diodes for high voltage applications where the switching loss can be reduced significantly).
c. Choose a diode of voltage and current ratings that can sustain at least twice the required values as calculated at point (a). Of course, the breakdown voltage of the chosen diode is higher than its voltage rating.

For example, an often used diode is the ultrafast power diode having the part number MUR460. It has the following characteristics: current rating of 4 A, voltage rating of 600 V, reverse current (I_{Dr}) of 250 μA at the junction temperature of 150 °C, forward voltage of 1.05 V at the anode current of 3 A, and reverse recovery time (t_{rr}) of 75 ns.

An example of SiC Schottky diode is CSD10060. It has the current rating of 10 A, voltage rating of 600 V, reverse current (I_{Dr}) of 1000 μA (maximum) at the junction temperature of 150 °C, forward voltage of 2.4 V (maximum) at the junction temperature of 175 °C and anode current of 10 A. The distinct feature of this diode is its zero reverse recovery charge.

A string of diodes is commonly used in high-voltage applications. As practically the diodes are never completely identical, the steady-state voltage distribution along the string will be uneven. To balance the voltages across each diode, we can connect a very large resistor in parallel to each diode. For ensuring equal transient voltage distribution among diodes, we can connect a resistor–capacitor network in parallel to each diode.

A normal diode permits a current flow only in one (forward) direction. If the breakdown voltage is exceeded, the diode will fail and pass a large current in the reverse direction. The diode will be permanently damaged. (The *breakdown voltage* is the maximum potential that can be applied across a semiconductor before it collapses and starts conducting. The breakdown voltage of a diode is the minimum reverse voltage that makes the diode conduct in reverse.)

A particular type of diode is the *Zener diode*. Its symbol is given in Figure 1.18. In a normal operation, this diode permits current flow not only in the forward direction like a normal diode but also in the reverse direction if the voltage is larger than the breakdown voltage. A Zener diode contains a heavily doped p-n

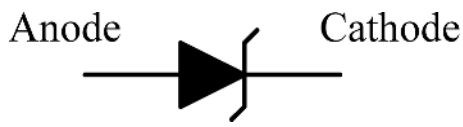

Figure 1.18 *Symbol of Zener diode.*

junction. It is specially designed so as to have a greatly reduced breakdown voltage, the so-called Zener voltage. If, in the reverse-biased region, a voltage larger than the breakdown value is applied, the Zener diode will not break down like a normal p-n diode but will allow a current in the reverse direction. No matter how high the reverse bias voltage is above the Zener voltage, the voltage drop across a Zener diode conducting a reverse current is always equal to the Zener voltage value. This is why, Zener diodes are used to regulate the voltage in electronic circuits.

In power electronics, the Zener diode is used either to generate a reference for the output voltage in the control circuit of converters, or as a part in a protection circuit for shielding the gate of the switch or the switch by itself from overvoltage, or as a voltage clamping device in a snubber for reducing the voltage stress on the switching device. Except for the above applications, the Zener diode is seldom used in power electronics, due to the considerable power dissipation when it conducts. The large conduction losses make the use of the Zener diodes impractical as a voltage regulator in the power flow. Practical Zener diodes have different breakdown voltages; for example, part 1N746A has a Zener voltage of 3.3 V and its maximum power dissipation is 0.5 W. In the switch gate's protection, we often use part 1N4744A with a Zener voltage of 15 V and maximum power dissipation of 1 W. In the overvoltage protection circuit for switches, part 1N5278 is used; it has a Zener voltage of 170 V and power rating of 0.5 W.

1.3.2 Semicontrollable switches (thyristors)

Thyristor is a family name for bipolar devices which comprise four semiconductor layers. The most used devices belonging to this category are the silicon-controlled rectifier (SCR), the triode for alternating current (TRIAC), which is a bidirectional thyristor with five layers that can be also seen as a combination of two thyristor structures, the reverse-conducting thyristor (RCT) and the gate-turn-off (GTO) thyristor. The SCR is turned on by applying a gate signal to it. Except for the GTO, any other thyristor cannot be turned off from the gate terminal. They can be turned off only by making the anode current zero.

A typical structure and symbol of an SCR are shown in Figure 1.19. The SCR was proposed in 1950 and first manufactured in 1956.

When the anode voltage, V_{AK}, is positive, the junctions J_1 and J_3 are forward-biased, but junction J_2 is reverse-biased, and a leakage current flows from A to K. The SCR is then said to be in a forward blocking or off-state condition, and the leakage current is known as the off-state current, I_D. If V_{AK} is increased to a sufficiently large value – larger than V_{FB} (forward breakdown voltage) – an avalanche breakdown occurs in the reverse-biased junction, J_2. Since the other junctions J_1 and J_3 are already forward-biased, there will be a free movement of carriers across all three junctions, resulting in a large forward anode current. The device will then be in a conducting state (on-state). The on-state voltage drop across the four layers is equivalent to that of two diodes connected in series. In the absence of a gate current, the SCR is turned on only by increasing the anode voltage V_{AK} over V_{FB}. By applying a positive gate current, I_G, the value of the minimum anode voltage for turning on the SCR can be reduced (Figure 1.20). With the anode voltage already positive, to turn on any thyristor we have to apply a gate current, I_G, by using either gate triggering, or irradiation in a light-activated SCR.

In the on-state, I_A is dependent on the external circuit, such as the external impedance. However, to maintain the required amount of carrier flow across the junction, the anode current I_A must be larger than

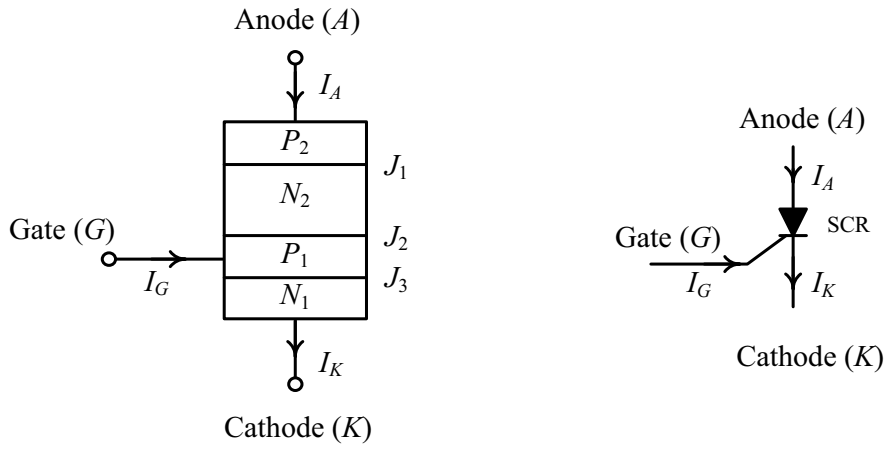

Figure 1.19 *Silicon-controlled rectifier (SCR) and its symbol.*

a value known as "latching current" (I_L), otherwise the device will revert to the blocking condition if V_{AK} is reduced. This means that once the device is switched on, it remains latched in the on-state providing that I_A exceeds I_L. Once a SCR is conducting, it behaves like a conducting diode and there is no control over the device. The device will continue to conduct because there is no depletion layer at the junction J_2 due to a free movement of carriers. With a gate current $I_G > 0$, as long as the anode remains positively biased the device cannot be switched off if I_A exceeds the holding current value, I_H. Only if the forward anode current is reduced below the level known as the "holding current" (I_H), would a depletion region develop around junction J_2 due to the reduced number of carriers, and the SCR would move to the blocking state. The turn-on characteristic of the SCR is given in Figure 1.20. After the SCR is turned on,

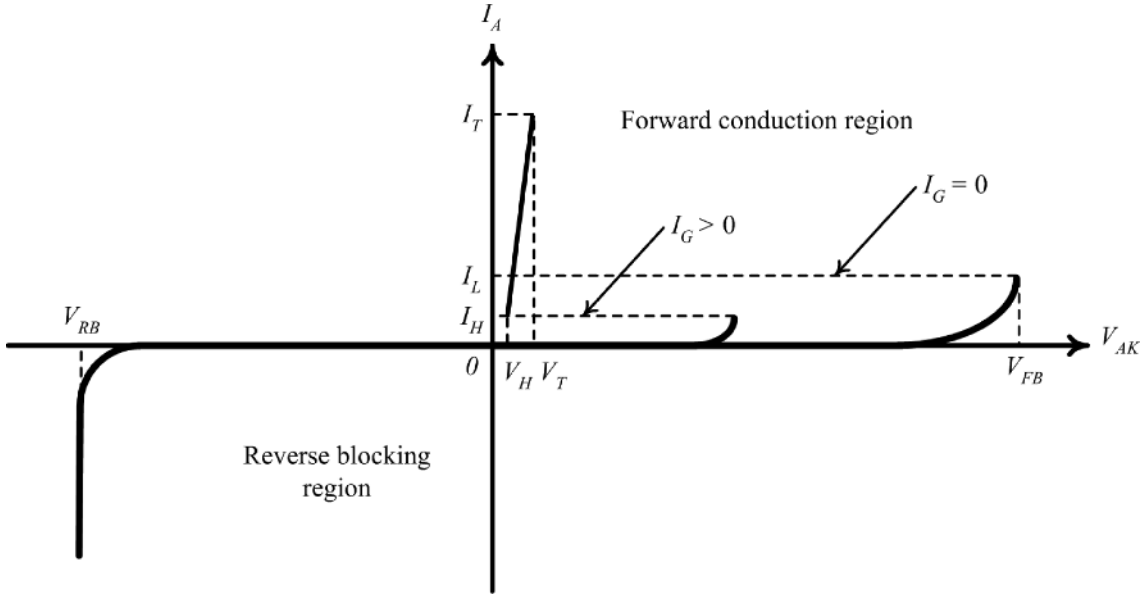

Figure 1.20 *Turn-on characteristics of a SCR.*

depending on the circuit, the anode current varies between the values I_H and I_T, and the forward voltage takes values between V_H and V_T.

Applying a negative (reverse) voltage on the SCR larger than V_{RB} (the reverse breakdown voltage) can cause the SCR to fail by punch-through of the reverse-biased junction J_1. In a high-voltage SCR, such a failure is prevented by using a thick N_2 layer.

As discussed, reducing the anode current below the holding current (I_H) is the way to turn off a thyristor. There are two basic methods of achieving it, both making use of an auxiliary switch. The first one is to connect an impedance in series with the thyristor, such that the current will drop to zero. The second one consists of superimposing a negative current on the thyristor current, bringing it to zero; this can be realized either by applying a reverse voltage across the switch or by creating a resonant path through the switch. After a thyristor has been switched off by force commutation, a certain time must elapse before the anode can be again positively biased. During this time, the remaining carriers recombine, re-establishing the depletion layer. Such a long transition time makes the thyristor suitable only for applications with low frequencies (50 or 60 Hz). For higher frequency applications, fast thyristors are necessary. They are obtained by diffusing into the silicon heavy metals ions which act as charge combination centers, or by neutron irradiation of the silicon semiconductor.

At turn-on, the charge carriers start to spread across the junction. If there is a very steep rise in the current (large di/dt) before enough horizontal migration of the carriers has been produced, the large current will pass through a small area in the junction, raising the temperature very quickly and destroying the device. To limit di/dt, we have to connect an inductor in series with the switch. In high-power applications, we need a very large gate signal for triggering the switch. To create it, we use an auxiliary low-power thyristor, which is driven by a small gate signal.

When the thyristor is off, it is not allowed to have a fast changing voltage waveform across it; otherwise, if an even small amplitude voltage with large dv/dt is applied, it will result in a gate-cathode current ($C\frac{dv}{dt}$ effect), triggering the switch involuntarily. To avoid such an action, either we insert an auxiliary circuit between the gate and cathode to suppress the undesired gate signal, or we insert in parallel with the switch (between anode and cathode) a capacitor or a resistor–capacitor circuit which will reduce dv/dt.

The main disadvantage of thyristors is their low-frequency operation (less than 1 kHz). This led to their replacement by controllable switches in the range of powers and frequencies in which controllable switches are available on the market. Today, thyristors are seldom used in low-power applications, where they have been replaced by transistors. They are still used in protection circuits. For example, if an overcurrent or an overvoltage appears in the converter, a thyristor in an auxiliary protection circuit will be triggered, to lock up (latch up) the converter. The thyristor will remain in the conduction state until the system is re-set. Thyristors are also used in low-cost low-power applications, such as AC-DC controlled rectifiers in battery chargers for golf carts, or low-cost solar-powered inverters for lighting. The area where thyristors are heavily used is the megawatt scale AC-DC rectification in high-voltage-DC transmission (HVDC).

Recently, SiC thyristors have been developed. They have applications in high temperature environments, being capable of operating at temperatures up to 350 °C. Inverters based on SiC thyristors have been proposed; they could reduce the conversion losses by more than 50% compared to silicon-based inverters. Such inverters can be used in heat pumps or in systems transferring power from windmills or solar sources to the utility grid. There are available GTO thyristors made with SiC, that can offer 20–50 times lower switching losses compared to silicon-based thyristors and lower on-state voltage drops for voltage ratings of more than 6 kV. They have found use in pulse power systems or in utilities. The SiC features a higher breakdown electrical field, allowing for the fabrication of thyristors suitable for higher voltage applications than those allowed by silicon-based thyristors.

1.3.3 Controllable switches

There are three popular types of controllable switch for power electronics systems. These are the bipolar junction transistor (BJT), the metal oxide semiconductor field-effect transistor (MOSFET), and insulated gate bipolar transistor (IGBT).

1.3.3.1 Bipolar Junction Transistor (BJT)

A bipolar junction transistor (BJT) is a three-terminal current-operated device constructed of doped semiconductor materials. The three terminals are called base, collector and emitter (Figure 1.21). There are two types of BJT: NPN and PNP transistors. Both of them have three layers. For the NPN transistors, as shown in Figure 1.21, the three layers are arranged in the order: n-type, p-type and n-type semiconductors. For the PNP transistors, the order of the three layers is: p-type, n-type and p-type semiconductors (Figure 1.22). The difference between them is in the way of biasing/turning on the transistor. In the case of the NPN transistor, it is necessary to provide a positive current injected into the base. To turn on the switch, a positive voltage has to be applied across the base–emitter junction. Conversely, for the PNP transistors, it is necessary to draw a current out of the base. To turn on the switch, a negative voltage has to be applied across the base–emitter junction. Similar to a diode having a depletion layer at the junction between the p-type and n-type layers, the transistor has depletion layers at the two junctions n-p and p-n, or p-n and n-p. Thus, similar to Figure 1.16d, there are capacitances formed across the junctions, C_{be} and C_{bc}.

The BJT has three operating regions: cutoff, linear (or active), and saturation. The operating region is determined by the magnitude of the base current. If the base current, I_B, is zero, the collector current, I_C, is zero. Thus, the transistor is in the off-state. If the base current is increased and the collector current is proportional to the base current, the transistor is operating in the linear region:

$$I_C = \beta I_B$$

where β is the DC current gain. There is a considerable power loss in the transistor when it conducts in the linear region. (The base–emitter junction is forward-biased, but the collector–base junction is still

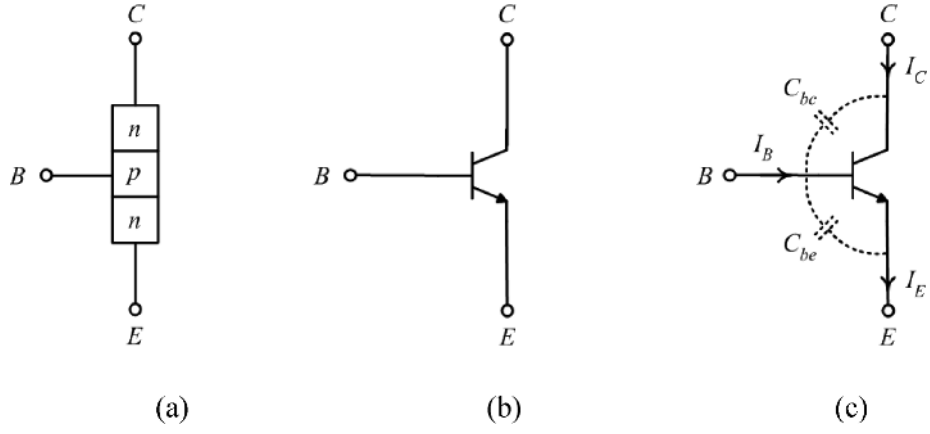

Figure 1.21 *The NPN bipolar junction transistor (BJT): (a) structure; (b) symbol; (c) associated junction capacitances.*

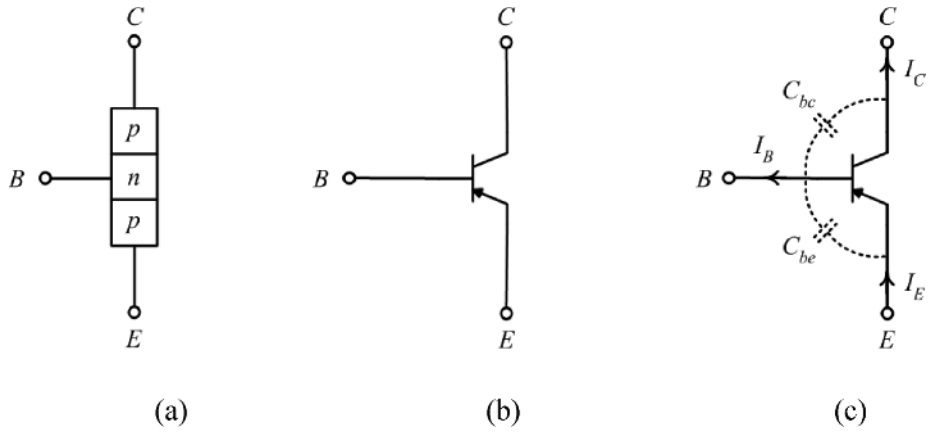

Figure 1.22 *The PNP bipolar junction transistor (BJT): (a) structure; (b) symbol; (c) associated junction capacitances.*

reverse-biased. So the collector–emitter voltage is not small, it is determined by the value of the collector current and the external circuit.) If the base current is increased to a value at which the linear relationship between the base and collector currents does not hold any more, the transistor is said to be in the saturation region. Then, the collector current is determined by the circuit and the base current has to be maintained higher than I_C/β. (In practice, we will maintain the base current at around 1.5–2.0 times the minimum required value, but not too high. Otherwise, there will be too much stored charge in the base and this will lengthen the turn-off time, because at turn-off the charge has to be extracted completely from the base.) Since the collector–emitter voltage is low as both semiconductor junctions are forward-biased, the power loss in the transistor operating in the saturation region is small. This is why, in power electronics circuits, a transistor is usually operated in either the cutoff or saturation regions.

BJTs are current-driven devices. The gate drive circuit has to deliver sufficient base current to maintain the on-state of the transistor. Nowadays, voltage-driven switches, like the MOSFETs discussed in the next section, have replaced BJTs in most cases because they do not require a continuous current drive. However, in some applications, like the electronic ballast circuit using a self-oscillating gate drive circuit, a BJT is preferable because the resonant inductor in the circuit can provide a current driving signal.

The collector current is determined by the load current, which is considerably large in power electronics. The base current is proportional to the collector current in the linear region, implying that power bipolar transistors consume considerable gate power. An intermediate low-power driving transistor must be used to boost the base current of the power transistor. In high current applications, the following Darlington structures are used for driving the main NPN power switch T (Figure 1.23). Depending on the type of the driving transistor, T_d, the equivalent structure of the complementary connection of transistors T and T_d can be of NPN type (Figure 1.23a) or PNP type (Figure 1.23b). The antiparallel diode shown in Figure 1.23 is used for providing a path for the load current when the transistor is off. It is named the feedback diode or protection diode. The resistors in the structures shown in Figure 1.23 have two functions. One is to stabilize the collector current when the temperature of the switch increases, by diverting a part of the base current. Otherwise, the base and collector currents will continue increasing, causing a further rise in the temperature, which would attract a further rise in the current. In the end, the transistor

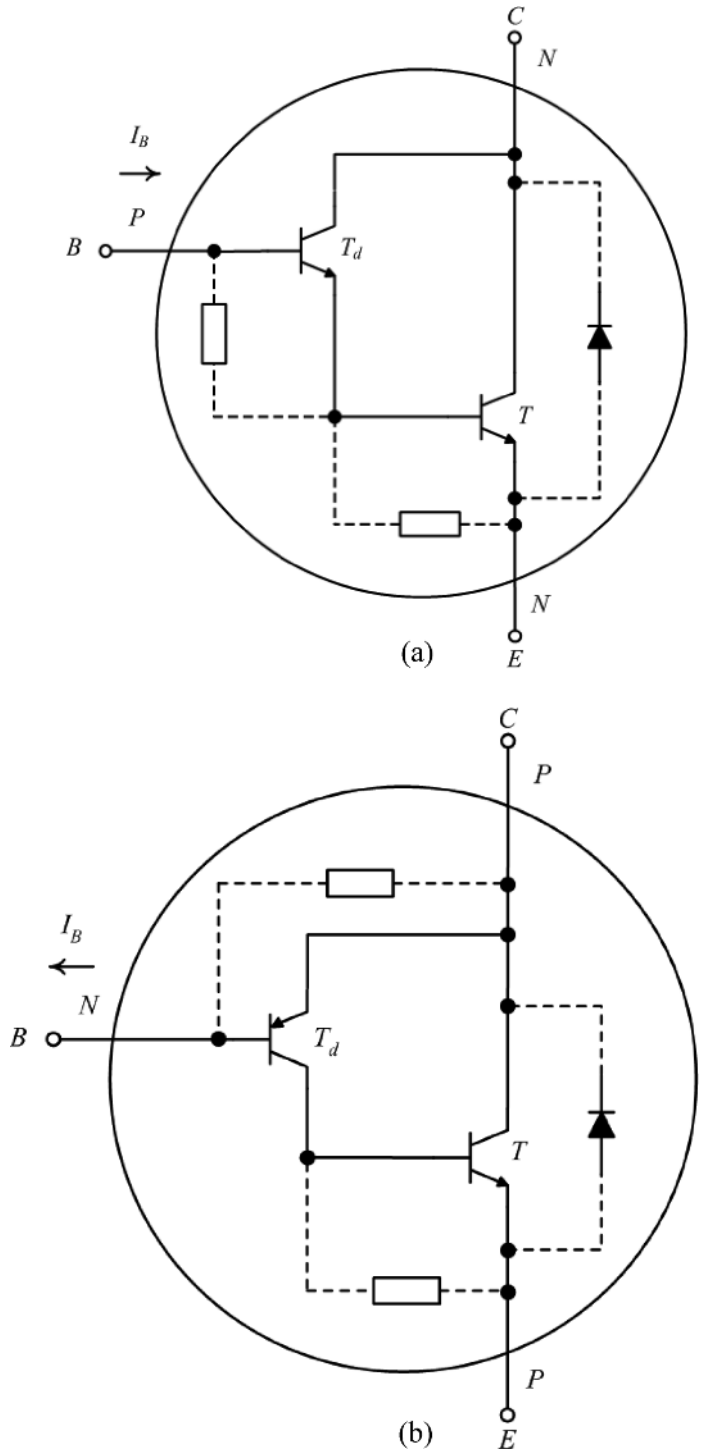

Figure 1.23 *Darlington structures for driving power bipolar junction transistors: (a) NPN equivalent; (b) PNP equivalent.*

will be broken down. This phenomenon is called "thermal runaway" ("secondary breakdown"). The second function is to provide a discharging path for the B–E junction when the switch is turned off, thus accelerating the turn-off speed.

When the base current is applied to turn on the switch, the B–E junction capacitance is charged firstly. During this time, called the *delay time*, the collector current is still zero. After the voltage between base and emitter has reached its threshold value (typically 0.7 V), the collector current starts increasing until it reaches the load current, while the voltage between collector and emitter starts decreasing towards its saturation value. This time interval is called the *rise time*, during which the transistor operates in the active region. The turn-on time, given by the delay and rise times, can be significantly reduced by increasing the rate and magnitude of the base current. After the turn-on process has been finished, the transistor operates in the saturation region.

The turn-off process of a transistor consists of a *storage time* and a fall time. The storage time is the time required to remove the charges from the base before entering the active region. During the storage time, the collector current keeps its value. Then, in the active region operation, the collector current starts decreasing towards zero, while the collector–emitter voltage starts increasing until reaching the cutoff value. This time is called the *fall time*. For example, for the bipolar transistor BUL381D, for a resistive load of 2 A and off-state collector–emitter voltage of 250 V, the storage time is 2.5 μs and the fall time is 0.8 μs. Such a very long transient turn-off time makes the BJT suitable only for low-frequency applications.

1.3.3.2 Power Metal Oxide Semiconductor Field-Effect Transistor (MOSFET)

A MOSFET is a three-terminal voltage-operated device. The three terminals are called the gate, drain and source. A MOSFET performs the same function as a BJT, with the basic difference being that the *MOSFET is a voltage-controlled device*. The structure of a power MOSFET is different from that of the one used in low-power electronics circuits. The former has a vertical structure, while the latter has a planar structure. By using a vertical structure, it is possible for the transistor to sustain both a high blocking voltage and high current. As shown in Figure 1.24, a MOSFET is formed by several layers, n^+, p, n^- and n^+. The low-resistance heavily doped n^+ layer is connected to the drain terminal through a metal connection. A lightly doped n^- layer is placed on the n^+ layer. Then, a p layer is placed on the n^- layer. Finally, another heavily doped n^+ layer is placed on the p layer. The source terminal is electrically connected to the top n^+ layer through a metal connection. The superscript "$^+$" signifies the fact that the regions are "heavily" doped. An insulator layer made of silicon oxide is placed on the substrate on the top of the entire structure, its other side forming the gate terminal through a metal connection.

If a positive voltage is applied between the gate and source, the gate will attract the n-type carriers into the p-type layer. The n-type carriers will accumulate at the surface beneath the silicon oxide layer. Thus, through the p layer, an n-channel between the drain and source is formed. The higher the gate voltage, the wider the channel will be. The mechanism is similar to the function of the valve in the water pipe. The valve is used to control the water flow, which is similar to the current flow. Moving the valve is similar to changing the gate voltage. For the MOSFET to start conducting, the channel has to reach a certain width. The value, V_{GS}, for which this width is reached is called "*threshold voltage,*" V_T. The current rating of the power MOSFET is a function of the area of the horizontal cross-section, giving a full utilization of the silicon layers, unlike in the planar structure where the current rating is dependent only on the width of the channel. Similarly, the voltage rating and breakdown voltage of the power MOSFETs are functions of the doping and thickness of all silicon layers, unlike in the planar structure where the voltage rating is

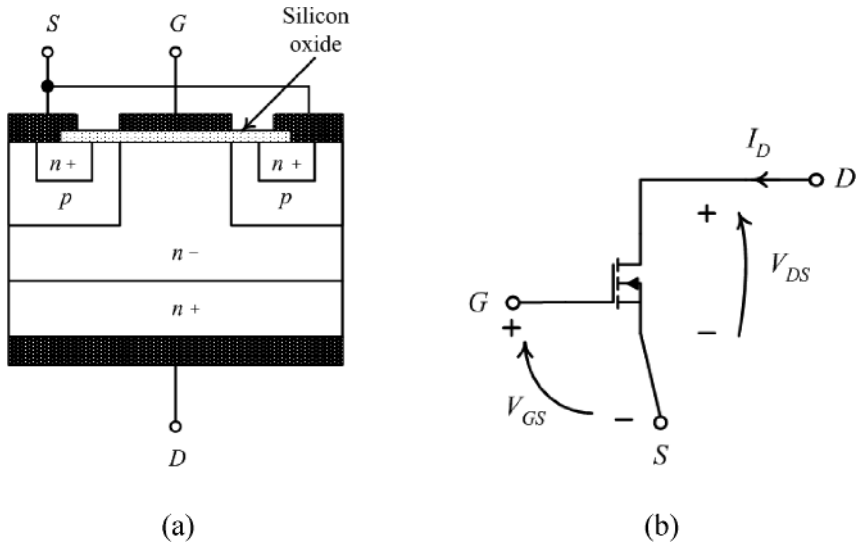

Figure 1.24 *Power MOSFET structure: (a) vertical cross-section of an n-channel MOSFET; (b) symbol of n-channel MOSFET.*

dependent only on the width and length of the channel. This is why the vertical-type MOSFET is used in power applications.

Similar to the enhancement-type low-power MOSFET, the state of the power MOSFET is normally off. When there is a gate voltage applied to the MOSFET, its state will change into the on-state.

The MOSFET has three operating regions: cutoff mode, active (saturation) mode and ohmic (triode or linear) mode. The resistance of the MOSFET operating in the cutoff region is very large, that is, the switch is off. In the saturation region, the drain current is given by:

$$I_D = K(v_{GS} - V_T)^2$$

where K is a factor depending on the physical parameters of the MOSFET and drain-source voltage, and V_T is the threshold voltage. In the ohmic mode, the drain-source resistance is given by:

$$r_{DS(on)} = \frac{1}{G\left[(v_{GS} - V_T) - \dfrac{v_{DS}}{2}\right]}$$

where G is a factor depending on the physical parameters of the MOSFET and v_{DS} is the drain-source voltage.

The value of $r_{DS(on)}$ of a p-type MOSFET is three times higher than that of an n-type MOSFET with the same dimensions, due to the low mobility of the p-type carriers.

In power electronics, MOSFETs are operated in either the cutoff mode or ohmic mode, equivalent to a switch operated in an off-state and on-state, respectively.

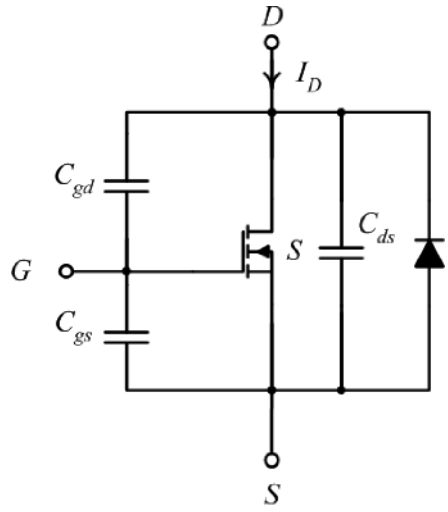

Figure 1.25 *Parasitic capacitances and body diode in a power MOSFET.*

Due to the presence of the oxide layer, there is a capacitance between the gate and source, C_{gs}, and a capacitance between the gate and drain, C_{gd} (also called the "Miller capacitance") (Figure 1.25). The n^+–p–n^-–n^+ arrangement between the drain and source forms a diode structure. *This diode is called the "body diode" and C_{ds} is the capacitance of the junction.* This diode allows a current flowing in the opposite direction to the drain current. This is why it is also called *antiparallel diode*.

The switching speed of this body diode is typically very slow. In many applications, a path is needed for a negative current (i.e., a current flowing in opposite direction to the drain current). How can we prevent such a current from flowing through the slow body diode? We can insert a series diode with the MOSFET that will stop any negative current and a fast diode in parallel with the MOSFET to create the new path. So, to circumvent the body diode, we use the circuit shown in Figure 1.26: connect a Schottky diode in series with the MOSFET and a fast recovery diode across the switch. The Schottky diode has a low forward voltage drop, thus it will give low power dissipation when the MOSFET drain current flows through it. A negative current will go through the fast recovery diode, which has good turn-off characteristics.

Instead of switching between the cutoff mode and ohmic mode instantaneously, a MOSFET will go through the saturation mode. The duration of the transition is dependent on the junction capacitances associated with the MOSFET (Figure 1.25). To explain the turn-on and turn-off processes of a MOSFET, consider, as an example, that the transistor is the main switch in a buck converter. In Figure 1.10, we saw that the current flowing through the switch in the on-state is a constant, I_{out}, due to the presence of the output inductor. Figure 1.27a describes graphically the turn-on process. When the switch is off, the capacitances C_{gd} and C_{ds} are charged, the voltage across them being the off-state voltage, V_{DS} (which is the input voltage for a buck converter or the output voltage for a boost converter), and C_{gs} is discharged. When the switch is turned on, by applying the gate-source voltage, C_{gs} starts being charged and C_{gd} discharged by the gate current. The drain current remains zero until V_{GS} reaches the threshold voltage, V_T. The duration of this interval is given by the delay time, t_{r1}. With a further increase in V_{GS}, the MOSFET starts conducting. The drain current starts increasing. The transistor is in the saturation mode. During this interval of duration t_{r2}, the drain-source voltage remains unchanged at its off-state value, $V_{off\text{-}state}$, due to

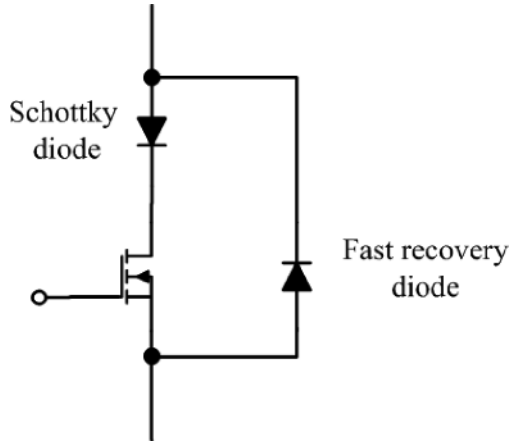

Figure 1.26 *Circuit for circumventing the body diode of MOSFETs.*

the presence of the conducting freewheeling diode in the buck converter which still carries a part of the load current ($I_{out} - I_D$). The process of charging C_{gs} and discharging C_{gd} continues. The duration t_{r2} depends on the values of C_{gs}, C_{gd}, and gate current. When the drain current reaches the on-state current (which is the output current in the case of a buck converter or the input current for a boost converter), V_{DS} starts decreasing until reaching the on-state voltage. During the interval of duration t_{r3}, V_{GS} is kept constant at its "plateau" voltage. C_{ds} is discharged and C_{gd} starts being charged in a polarity opposite to that in the off-state. The duration of t_{r3} depends on the value of the drain current. At the end of t_{r3}, the MOSFET is in the on-state (linear mode) and is equivalent to a resistance $r_{DS(on)}$ determined by the physical parameters of the MOSFET, V_{DS}, and V_{GS}. The nominal value of this resistance is nonlinearly dependent on the *voltage rating* V_{BV} (the maximum voltage the MOSFET can withstand in the off- state). It is given by:

$$r_{DS(on\_\text{nominal})} = kV_{BV}^{2.5-2.7}$$

where k is a constant depending on the switch geometry.

After t_{r3}, the freewheeling diode starts the turn-off process, entering firstly into the reverse recovery process. It will introduce a large oscillatory drain current. The magnitude of such an additional current (current stress) depends on the converter structure (buck structure or boost structure, etc.), parasitic (*stray*) inductances and capacitances of the converter, and the reverse recovery characteristics of the freewheeling diode. This oscillation will settle into the final on-state current. In a buck converter supplied from a low input voltage, the reverse recovery current of the freewheeling diode is relatively small. In boost converters providing a high voltage, as in AC-DC rectifiers, such a reverse recovery current can take a very large value because the freewheeling diode is submitted to the output voltage. With the recent advancement in SiC diode technology, for which we saw that the reverse-recovery charge is close to zero, this problem becomes less important. What still hinders today the wide usage of SiC diodes in industrial power electronics is their high cost.

When the switch is on, C_{gs} and C_{gd} are charged at V_{GS}, and the charge stored in C_{ds} is very small. When the switch is turned off, by bringing the gate-source voltage to zero, C_{gs} and C_{gd} start being discharged. For turning off the transistor in converters with a single switch (like buck, boost, buck-boost converters), we

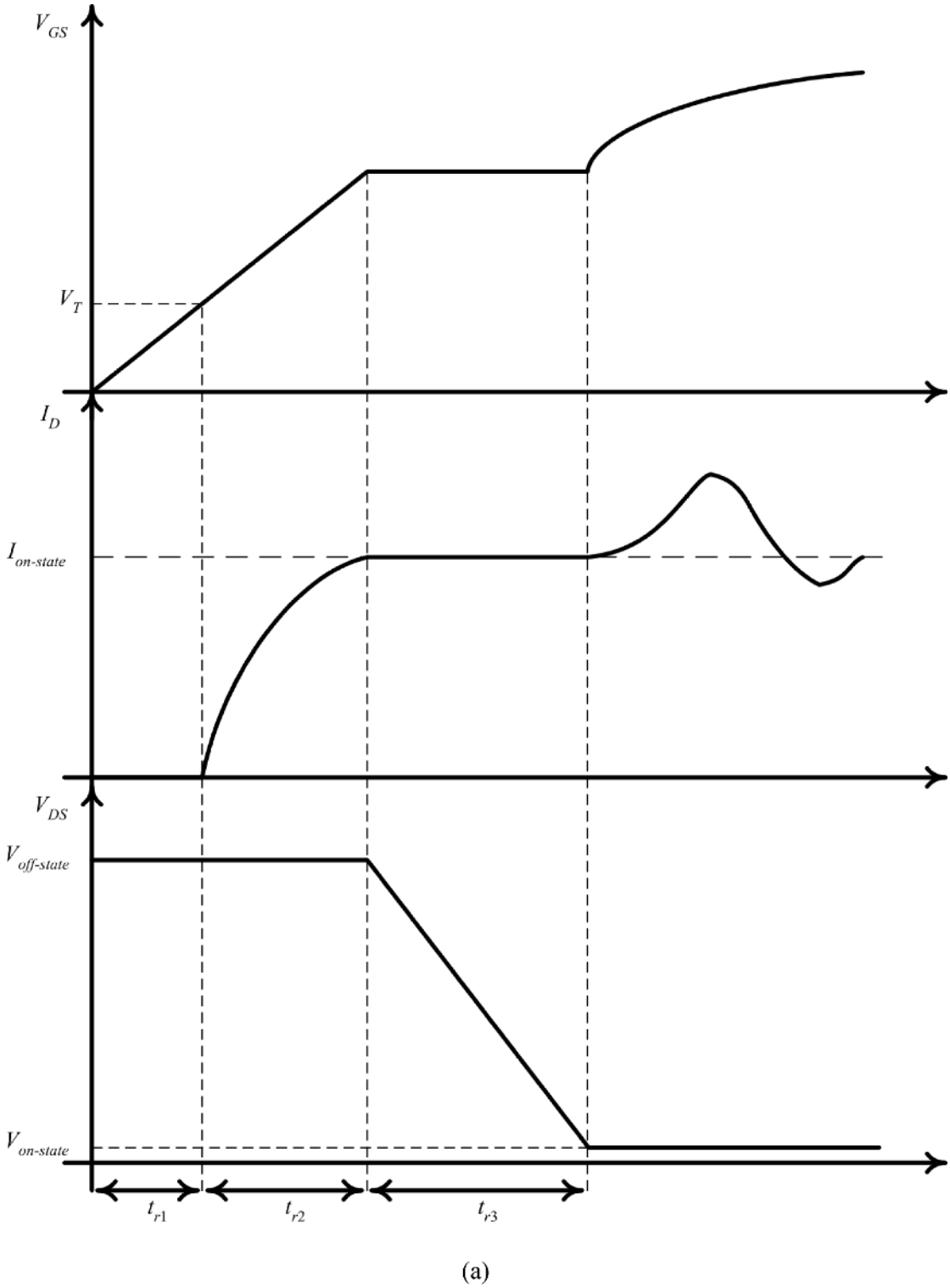

Figure 1.27 *Switching processes of a MOSFET in converters with inductors: (a) turn-on; (b) turn-off.*

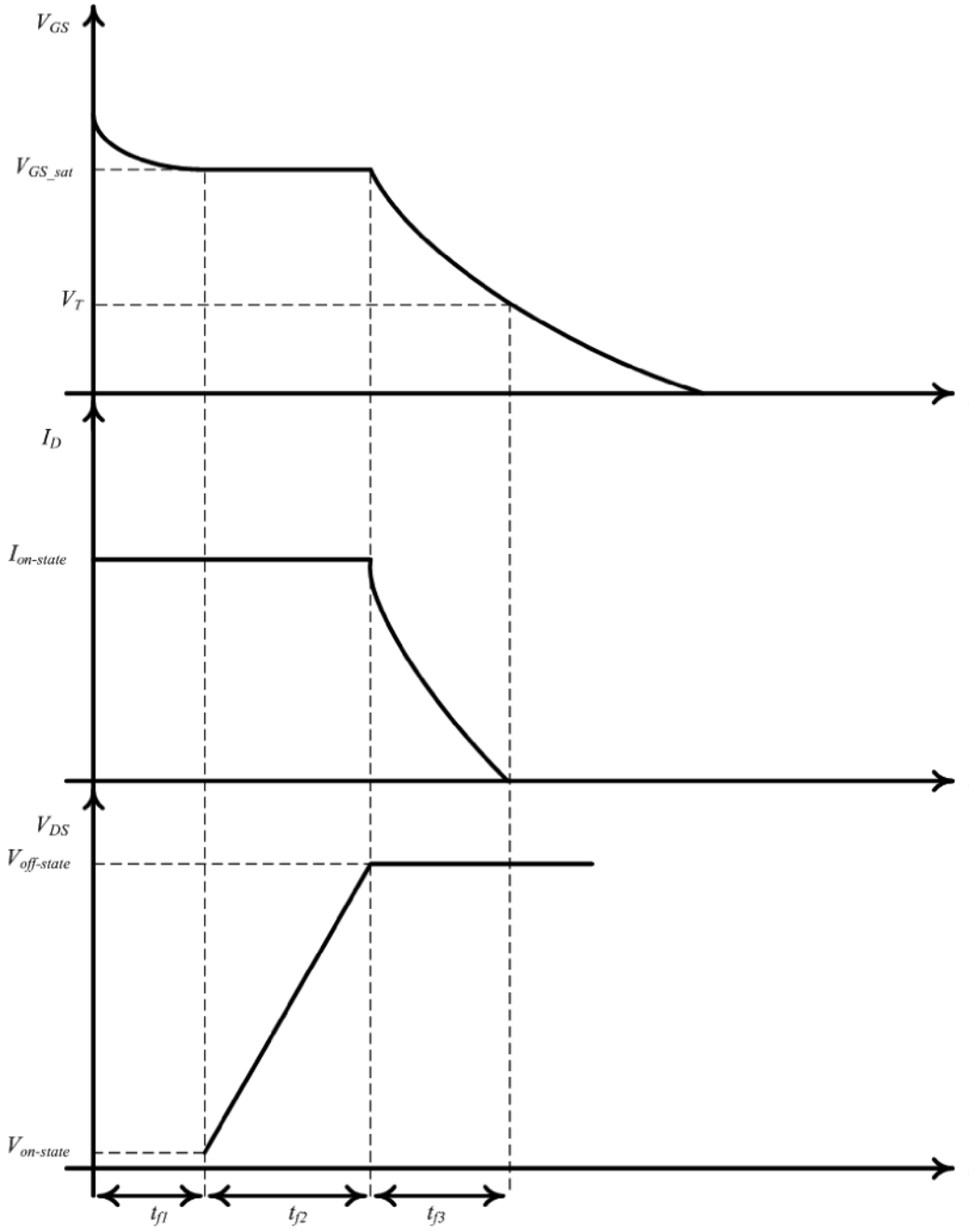

(b)

Figure 1.27 (*Continued*)

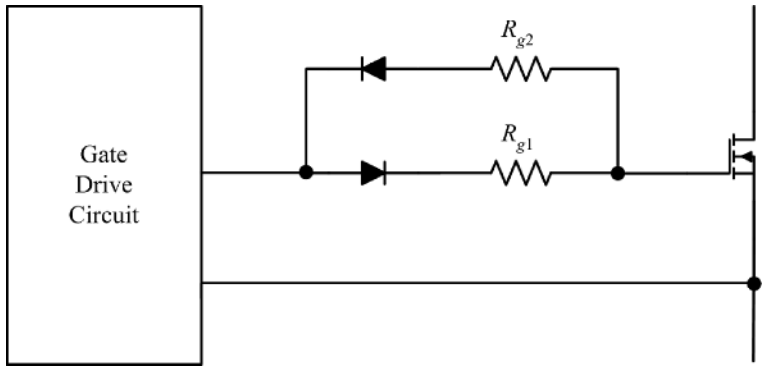

Figure 1.28 *Gate drive circuit for controlling the turn-on/off speed.*

apply a negative gate drive voltage to increase the gate discharging current, and thus accelerate the decrease of the gate-source voltage to zero. In the first time interval of the turn-off process (Figure 1.27b), V_{DS} is constant. V_{GS} is decreasing until reaching the value:

$$V_{GS\_sat} = V_T + \sqrt{\frac{I_D}{K}}$$

from where the drain current fulfills the equation characterizing the saturation mode. The duration of the first interval is given by the delay time t_{f1}. The delay time depends on the values of the gate current, C_{gs} and C_{gd}. After t_{f1}, the MOSFET is operating in the saturation mode, where the voltage on C_{gs}, that is, V_{GS_sat}, remains unchanged, C_{gd} is discharged and then charged in the reverse polarity, causing V_{DS} to increase. During this interval, the drain current remains unchanged. The interval of duration t_{f2} ends when V_{DS} reaches the off-state voltage. The duration of t_{f2} depends on the gate current and C_{gd}. At this moment, V_{GS} starts decreasing and the drain current follows it until V_{GS} is equal to V_T, when the drain current reaches zero, meaning the end of saturation mode. The duration of this period is t_{f3} and depends on the values of the gate current, C_{gs} and C_{gd}. Then, V_{GS} is further reduced to zero and the switch is operated in the cutoff mode.

To control the speed of the turn-on and turn-off processes, that is, the duration of these processes, two sets of gate resistors are usually used (Figure 1.28). When the switch is turned on, the gate current will flow through R_{g1}. When the switch is turned off, the gate current will flow through R_{g2}.

MOSFETs have a positive temperature-resistance coefficient (the channel resistance will increase with temperature). At a higher temperature, the drain current will reduce. This is why MOSFETs do not suffer from secondary breakdown, as BJTs do.

To enhance the switching speed, the MOSFET has to be driven by a current source followed by a voltage source. As shown in Figure 1.29, the totem pair formed by two bipolar transistors, T_1 and T_2, is used to deliver the gate current to the MOSFET. When a gate signal is applied to the totem pair, T_1 is turned on, T_2 is turned off, and the gate voltage, V_g, is effectively connected to the gate. Since C_{gs} is uncharged (as the MOSFET was in the off-state), V_g will generate a large current through T_1 and R_{g1}. When C_{gs} is charged up (i.e., the MOSFET is in the on-state), the gate current is zero and the gate drive will maintain a constant gate-source voltage. When the gate signal is brought to a negative value in order to switch off the MOSFET, T_1 is turned off and T_2 is turned on. A negative voltage ($-V_g$) will be connected to the output of the drive. C_{gs} will be discharged through T_2 and R_{g2} until it is fully discharged.

To protect the gate from damaging overvoltage, a Zener diode protection is necessary. The Zener diode is chosen such that its breakdown voltage is equal to a voltage level which starts to be dangerous for the

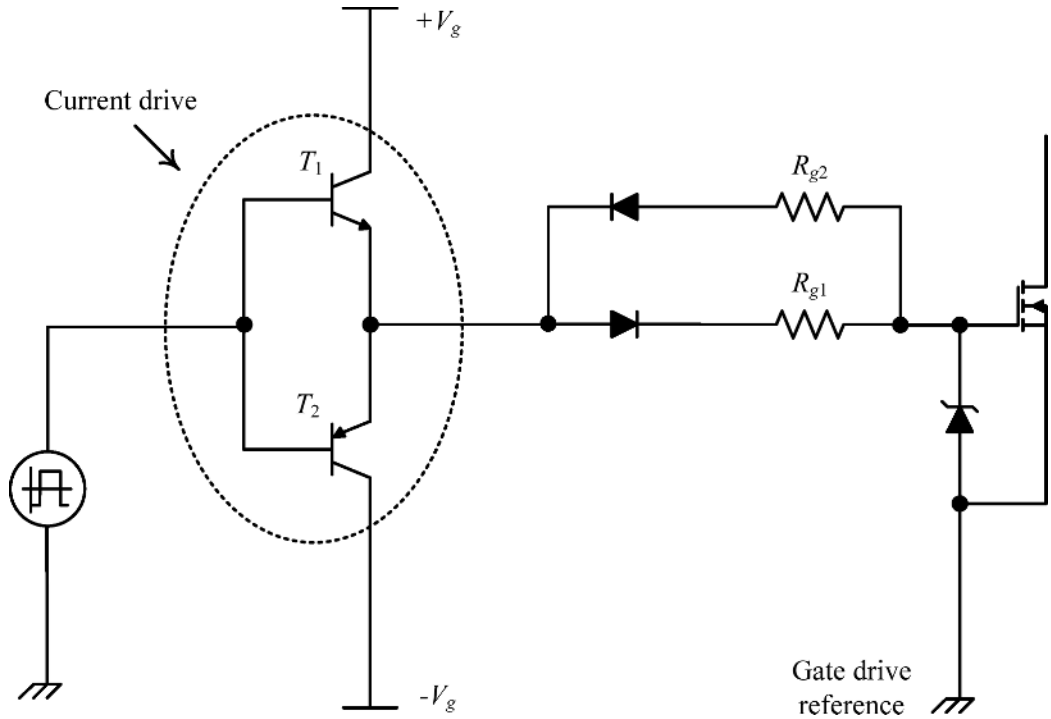

Figure 1.29 *Gate drive circuit of a MOSFET using a totem-pair.*

MOSFET's gate. When the voltage V_{GS} reaches a value larger than the breakdown voltage of the Zener diode, the Zener diode in Figure 1.29 starts conducting, keeping ("*clamping*") V_{GS} at the Zener voltage.

As said before, we have to apply a voltage between the gate and source larger than the plateau voltage to maintain the switch in the on-state. If the gate is referenced to the source and the source voltage is not fixed (i.e., is "floating"), then the gate voltage, v_G, has to be at least the source voltage plus the plateau voltage. This cannot be accomplished if the source voltage reaches a high value. In such a case, a solution called bootstrap circuit is used.

Figure 1.30 shows a circuit that produces a switching output voltage waveform. It contains two MOSFETs. As we can see immediately, we can turn on the low-side switch, S_2, with no problem but we need an additional circuit to turn on the high-side switch, S_1. The power circuit is supplied by a DC source, V_{dc}, with respect to the reference GND. The output voltage, V_{out}, is controlled by two MOSFETs, S_1 and S_2, which are operated complementarily. When S_1 is on and S_2 is off, V_{out} is equal to V_{dc}. When S_1 is off and S_2 is on, V_{out} is equal to zero. The gate drive circuit generates the gate signals H_o and L_o for S_1 and S_2, respectively. The gate drive circuit is supplied by the source V_{cc} with respect to the reference V_{ss}. The reference V_{ss} is connected to the source of the low-side MOSFET S_2. However, the source of the high-side MOSFET S_1 is connected to V_{out}. The node V_{out} is floating because its voltage level is varying. Consequently, S_2 will be turned on if L_o is V_{cc}, and will be turned off if L_o is zero. It is easy to maintain S_2 in the on-state, as its source is connected to the ground, so its V_{GS} becomes equal to V_{cc}. To turn off S_1, it is also easy: the lower MOSFET S_B in the gate driver is turned on and the upper MOSFET S_A is turned off. Thus, the gate-source voltage of S_1 is zero. More difficult is to turn-on and maintain so is the upper MOSFET S_1. If S_1 is on, the voltage level of V_{out} is V_{dc}. In order to maintain the on-state of S_1, the gate-source voltage has to be higher than its plateau voltage. Then, how can the gate drive circuit maintain such a gate-source voltage? If H_o is

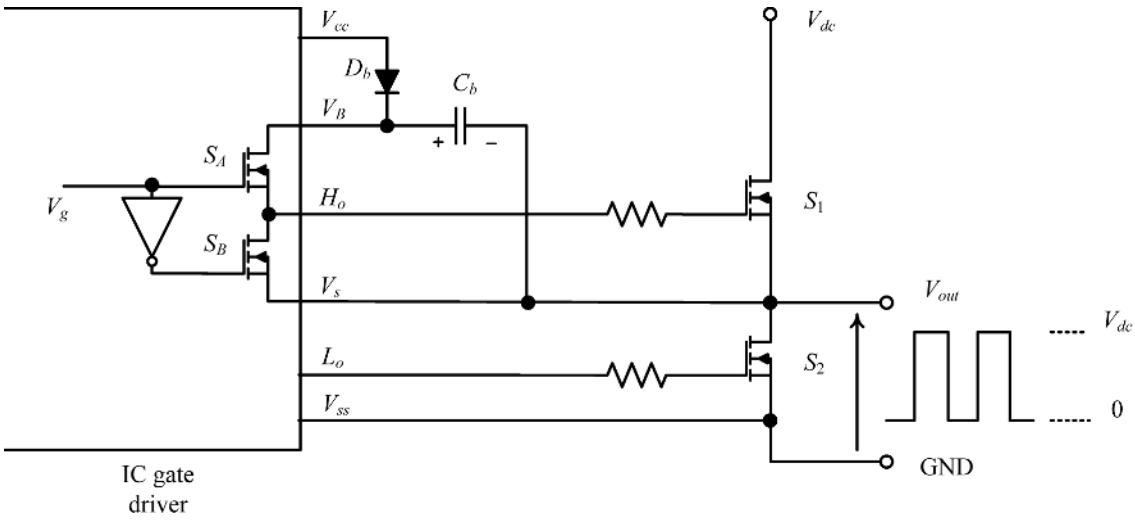

Figure 1.30 *Circuit for producing a switching waveform which uses a bootstrap circuit for driving the high-side MOSFET.*

V_{cc}, with respect to the reference GND (as it was the case of L_o when turning on S_2), it is not enough to turn on S_1, as V_{cc} would have to be larger than the plateau voltage plus the potential V_{dc} with reference to GND of the source of S_1. An additional circuit is needed to create the desired voltage. A bootstrap circuit composed of a diode, D_b, and a capacitor, C_b, can achieve such a function. One plate of the capacitor is connected to the source of S_1.When S_2 is on, through the path of diode D_b, C_b and S_2, the boostrap capacitor is charged to V_{cc} with the polarity illustrated in the figure. To command S_1 to turn on, S_A in the gate drive is turned on by V_g, and S_B is turned off. Through S_A, C_b appears in parallel with the gate-source of S_1 in series with the gate resistance. As C_b has been fully charged, a sufficient voltage will be applied between the gate and source of S_1. Thus, the on-state of S_1 can be maintained. Consequently, no matter the value of V_{out}, the gate driver can supply the necessary gate-source voltage to the high-side MOSFET with the bootstrap circuit. Therefore, without the bootstrap circuit, V_{cc} (H_o) was being applied between the gate of S_1 and GND, which was requiring a high V_{cc}. With the bootstrap circuit, V_{cc} (the voltage on C_b now) is applied directly across the gate-source of S_1 in series with the gate resistance, which necessitates a lower V_{cc}.

The gate drivers are available in the form of integrated circuits. For example, for driving the switch in a buck, boost or buck-boost converter, we can choose the driver MC34152, which has a maximum driving current of 1.5 A. If we need a bootstrap driver, we can use the chip IR2110.

A particular application of a MOSFET is as a *Synchronous Rectifier* (*Diode*). All the diodes in conduction, including Schottky diodes, have a relatively large voltage drop. In low-output voltage applications, such a forward voltage drop would be significant, causing a large power loss relative to the output power, being thus an important factor in the worsening of the efficiency. In such a case, it is preferable to replace the diode by a MOSFET (which features a low $r_{DS(on)}$) operated like a diode (Figure 1.31). Unlike the usual way of operating a MOSFET, here the synchronous rectifier driver continuously senses the drain-source voltage V_{DS}. If V_{DS} is positive, the body diode is reverse-biased, the driver will not generate any gate signal, meaning that the MOSFET is in the off-state. When V_{DS} becomes negative, the body diode is forward-biased and the drain current starts flowing through it. If V_{DS} is more negative than the "knee voltage" (which is the forward voltage of the body diode, for example, -1 V), the driver is designed to generate a turn-on gate signal, and a channel inside the MOSFET will be created. Therefore, the driver is operated in a

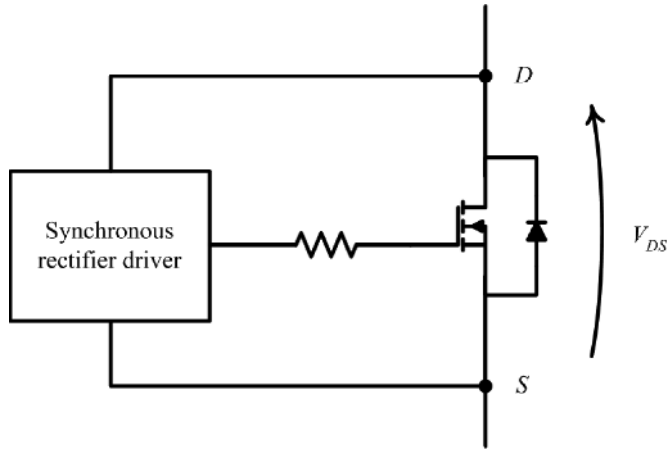

Figure 1.31 *MOSFET as a synchronous rectifier.*

synchronized way with the body diode. Since $r_{DS(on)}$ is smaller than the forward equivalent resistance of the body diode, the drain current will flow through the channel of the MOSFET. Thus, the power loss of a synchronous rectifier is much lower than that of ordinary diodes. A typical application is the switching mode power supply for the microprocessors in computers (the so-called voltage regulator module (VRM) which is discussed in a later chapter).

Vertical MOSFETs suffer from high gate charge and gate capacitance due to the vertical trench gate structure. When operated at very high switching frequencies, the gate drive loss becomes overwhelming, mitigating the low conduction loss in the on-state resistance. MOSFETs serving as synchronous rectifiers in applications like power supplies for microprocessors operate at switching frequencies well above 1 MHz, at voltages under 10 V. In such cases, *flip-chip lateral MOSFETs* present superior performances. As the lateral transistor has a small overlap area between its polysilicon gate electrode and $n+$ drain, its Miller capacitance is smaller than in a vertical transistor. However, traditional lateral MOSFETs suffer from a relatively high on-resistance due to a worse silicon utilization (the current flows horizontally along the silicon surface). And this parasitic resistance increases with the device die size due to the resistance of the metal interconnects. In 2006, the company Great Wall Semiconductor, USA, modified the metal interconnect structure of the lateral transistor for attenuating the above deficiency. Its *n*-channel power MOSFET, type GWS24N07CS, rated at 7 and 24 A, presents a total parasitic on-resistance of 1.25 mΩ and a total gate capacitance of 22nC at a gate voltage of 4.5 V. Its breakdown voltage is 11.5 V. It can be used in converters operated at switching frequencies of several MHz.

1.3.3.3 Insulated Gate Bipolar Transistor (IGBT)

The structure of an IGBT is quite similar to that of a vertical MOSFET. The difference is in that that the lowest layer (connected to the drain terminal) in a MOSFET is a heavily doped n^+ type region, but the lowest layer (connected to the collector terminal) in an IGBT is a p^+ type region. The function of the p^+ layer is to inject minority charges into the *n* layer while the IGBT operates in the on-state. This reduces the on-resistance of the *n* layer, thus improving the conductivity. Consequently, high-voltage IGBTs with low forward voltage drop can be constructed. The price paid for this advantage is the increased switching times compared to those of a MOSFET, especially the turn-off time when the stored minority charges have to be removed. As there is no way to actively remove them, they are slowly removed via recombination. So, the

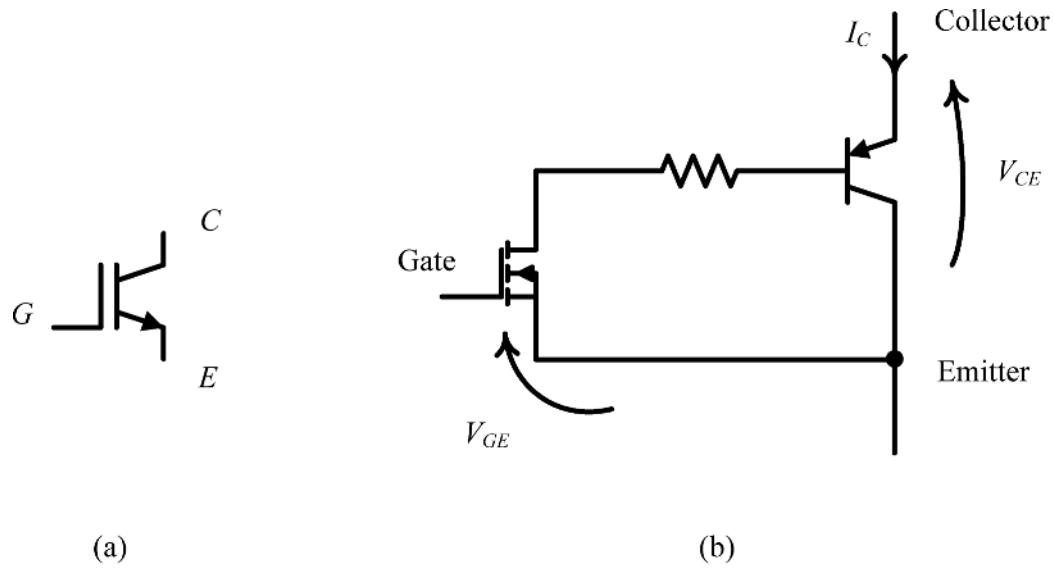

Figure 1.32 *IGBT: (a) symbol; (b) equivalent circuit model.*

current at turn-off decays slower than is the case in a MOSFET. As a result, the switching frequencies of the converters using IGBTs are much lower than if MOSFETs were used. The turn-off current tail can be reduced by adding a n^+ buffer layer between the p^+ substrate and the n^- region (obtaining the so-called PT-IGBT), improving the rate of recombination.

An insulated gate bipolar transistor can be seen as the equivalent of a bipolar transistor driven by a MOSFET. The base of the equivalent BJT is actually the *n* layer of the IGBT. *The IGBT combines the characteristics of the BJT and MOSFET. As with BJTs, its voltage and current ratings are higher than those of the MOSFETs. Instead of being a current-driven gate circuit like a BJT, the IGBT is a voltage-controlled device, similar to a MOSFET. For large currents, the power dissipation of an IGBT in the on-state is lower than that of a MOSFET. On the other hand, the turn-on and turn-off transients of the IGBT, like those of a BJT, are slower than those of a MOSFET. Another disadvantage of the IGBT (a tail current at turn-off)* is discussed below.

Figure 1.32 shows the symbol and circuit model of the IGBT, in which the IGBT is modeled as a PNP transistor driven by a MOSFET. In this model, the base of the BJT is connected to the drain of the MOSFET. These two layers (base of equivalent BJT and drain of equivalent MOSFET) have different doping levels. This is why there appears an equivalent resistance between them. The IGBT terminals are denoted as Gate, Collector and Emitter.

As when we explained the switching processes for the MOSFET, let us also consider the case of a buck converter (shown in Figure 1.10) for studying the turn-on and turn-off of an IGBT.

The turn-on characteristic of IGBTs shown in Figure 1.33a is a combination of the turn-on characteristics of the equivalent driving MOSFET and BJT. When the switch is turned on by applying the gate-emitter voltage, V_{GE}, C_{gs} and C_{gd} of the driving MOSFET start being charged, respectively discharged by the gate current. The drain current of the MOSFET remains zero until V_{GE} reaches the threshold voltage, V_T. So, the collector current of the IGBT also remains zero. The duration of this interval is given by the delay time t_{r1}. With further increase in V_{GE}, the MOSFET and BJT start conducting. The collector current starts increasing. During this interval, of duration t_{r2}, the collector–emitter voltage of the IGBT remains unchanged at its off-state value, $V_{off\text{-}state}$. The process of charging C_{gs} and discharging C_{gd} continues. The duration t_{r2} depends

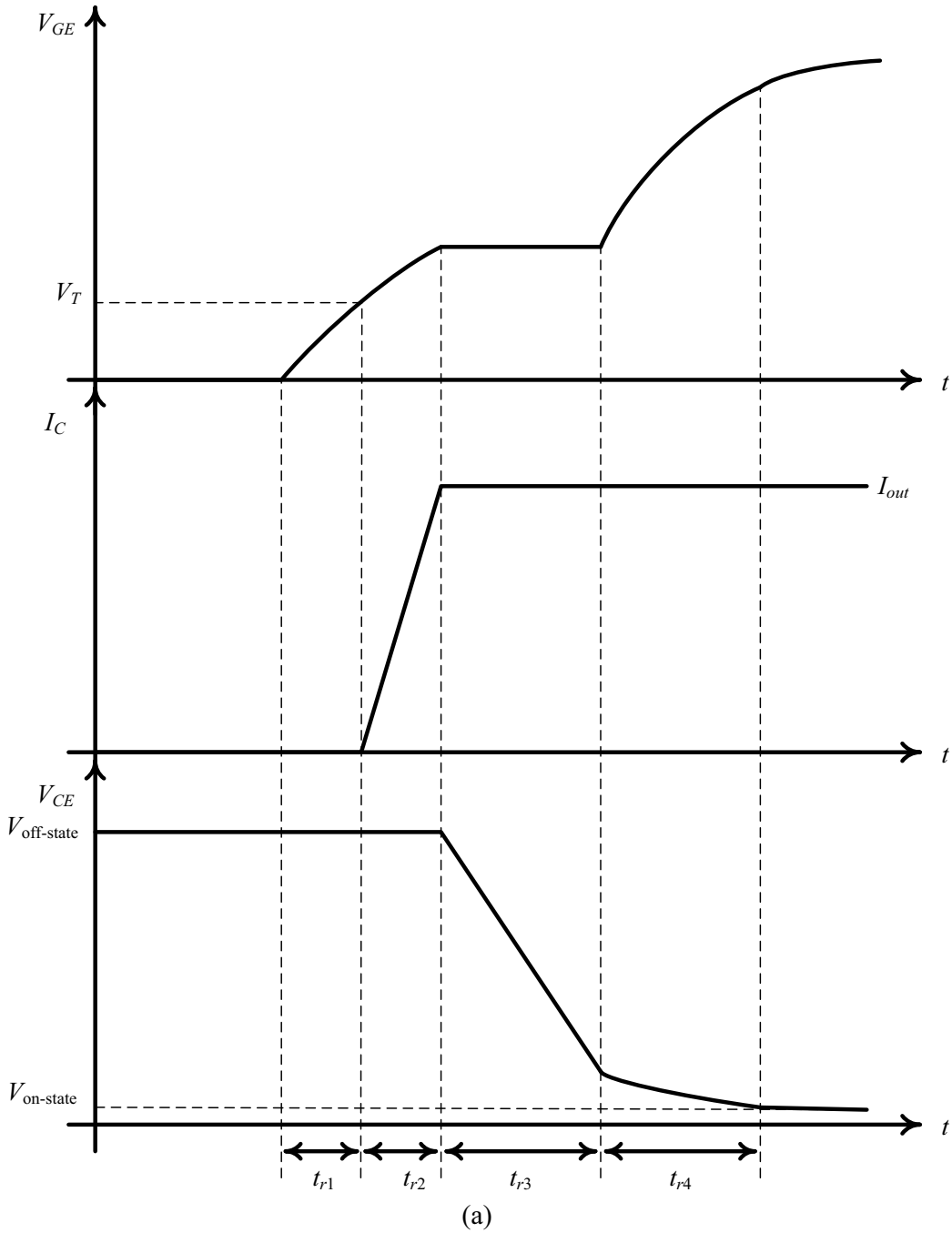

Figure 1.33 *Switching processes of an IGBT: (a) turn-on; (b) turn-off.*

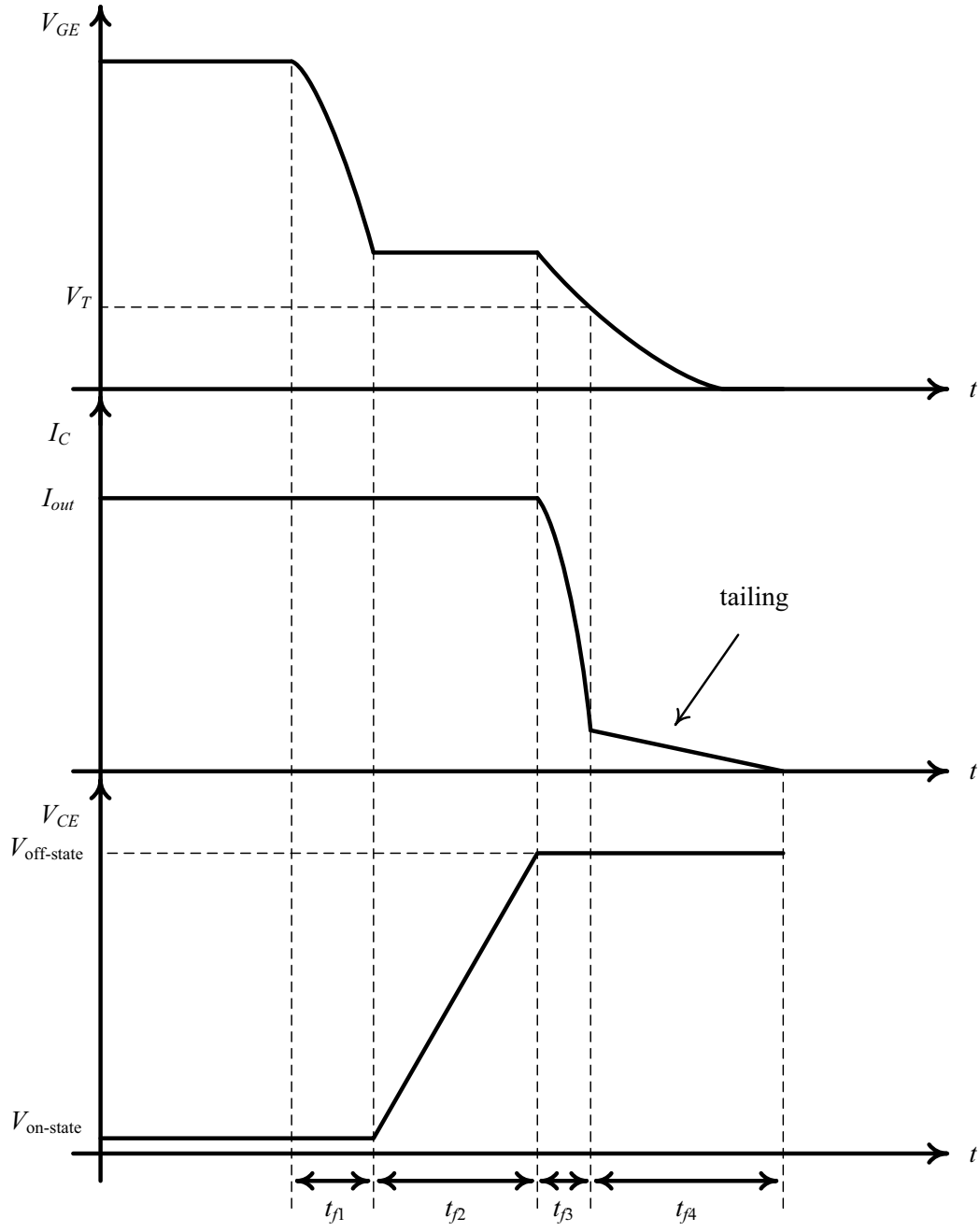

(b)

Figure 1.33 *(Continued)*

on the values of C_{gs}, C_{gd}, and gate current. When the collector current of the IGBT reaches the on-state current, I_{out}, V_{CE} starts decreasing. During the duration t_{r3}, C_{ds} is discharged and C_{gd} starts being charged in the polarity opposite to that in the off-state. The duration of t_{r3} depends on the value of the drain current of the MOSFET. At the end of t_{r3}, the MOSFET is in the on-state (linear mode), its drain-source voltage having reached the on-state value, but the BJT is still in the active region because of its slow switching speed. The rate of reduction of the collector–emitter voltage of the IGBT, V_{CE}, is reduced. It takes a further duration t_{r4} to fully turn on the BJT, and thus the entire IGBT. At the end of t_{r4}, the collector–emitter voltage of the IGBT reaches $V_{on-state}$.

To turn off the switch, the gate-source voltage is brought to zero. C_{gs} and C_{gd} of the driving MOSFET start being discharged. In the first time interval of this process, V_{CE} of the IGBT is constant. V_{GE} is decreased until the value at which the MOSFET enters the saturation mode. The duration of the first interval is given by the delay time t_{f1}. The delay time depends on the values of the gate current, and of C_{gs} and C_{gd} of the MOSFET. After t_{f1}, the MOSFET is operating in the saturation mode when the voltage on C_{gs}, that is, V_{GE_sat}, remains unchanged, C_{gd} is discharged and then charged in the reverse polarity, causing V_{DS} of the driving MOSFET to increase, and so V_{CE} of the IGBT. During this interval, the collector current remains unchanged. This interval, of duration t_{f2}, ends when V_{CE} of the IGBT reaches the off-state value. The duration t_{f2} depends on the gate current and C_{gd}. The voltage across the freewheeling diode of the buck converter (Figure 1.10) is given by $V_{in} - V_{CE}$, that is, up to now, this diode was reversed-biased. At the end of the t_{f2} interval, this diode becomes forward-biased, starting to take a part of the load current ($I_{out} - I_C$). The collector current and the drain current of the MOSFET start decreasing, and the voltage V_{GE} follows it until V_{GE} is equal to V_T, when the drain current of the MOSFET reaches zero, meaning the end of the saturation mode. The duration of this period is t_{f3} and depends on the values of the gate current, and of C_{gs} and C_{gd}. However, the collector current, I_C, of the IGBT has not yet reached zero, because there is still some charge in the base of the BJT. Then, V_{GE} is further reduced to zero and the MOSFET is operated in the cutoff mode. Since the equivalent MOSFET has completely turned off, the charge stored in the base of the BJT cannot be completely removed. Thus, there appears a *"tailing"* of the collector current after t_{f3}. The tailing period, t_{f4}, lasts until all charges at the base of the equivalent BJT are completely recombined in the base layer (the actual n layer of the IGBT).

1.3.4 Gallium nitride (GaN) switch technology

As already seen, the transistor is the main switch in power electronics. In its evolution during the second half of the twentieth century, the fabrication technology has continuously been improved, moving from using silicon to gallium arsenide (GaAs) semiconductors. The silicon power transistor has approached maturity, where small improvements involve large manufacturing costs. The first decade of the twenty-first century saw the appearance in the semiconductor-based switching devices world of a new material, gallium nitride (GaN). Gallium nitride is able to be operated at high frequency and high power. It has a wide band gap of 3.4 electron volts (eV), compared to that of 1.11 for silicon and 1.43 for GaAs. (The band gap represents the amount of energy required to free an electron from an outer orbit around a nucleus to become a mobile charge carrier. The eV is a unit of energy, $1\,\text{eV} = 1.6 \times 10^{-19}$ J). A large band gap means that it is not easy to release free electrons, even at a higher temperature. In consequence, the performance of a GaN transistor is maintained up to a higher temperature than that of a silicon transistor (the band gap reduces with the temperature, so a large band gap provides more stability margin). Therefore, GaN transistors can operate at higher temperatures and higher voltages compared to silicon transistors. High conduction electron density, high electron mobility and wide band gap make GaN transistors exhibit a very low on-state resistance for a given reverse voltage capability. Gallium nitride-based power devices are starting a new era of high density, high efficient and cost effective power conversion circuits. They can operate in hot, harsh,

radiation field, and high-power environments, extending the use of the switching devices to areas previously prohibited by the limitations imposed by less tolerant silicon transistors.

A metal oxide field-effect transistor based on a single crystal GaN was fabricated in 1993. The GaN layer was deposited over a sapphire substrate. Its gate (channel) length was 4 μm. One of the problems of GaN technology is the self-heating effect due to the extremely high power density involved and a large thermal resistance of the device structure. Self-heating can result in abrupt increase of the local temperature leading to a thermal breakdown at lower bias voltages. Another technological problem was the interface between the insulating layer (oxide) and the substrate body. In 2008, a new GaN MOSFET prototype was fabricated with a good interface. In 2009, a high-electron-mobility-transistor (HEMT) using a three-layer structure – n-GaN, AIN (aluminum nitride), n-GaN – was developed. It allowed the switch to be completely off when a voltage of less than 2 V was applied to the gate. These GaN HEMT were claimed to have less than one-fifth of the conduction losses in the on-state of those of the silicon transistors, as well as excellent high-speed characteristics, implying switching losses of 1% of those of silicon transistors (Figure 1.34a). Also in 2009, a gallium nitride-on-silicon 30 V rated power MOSFET (GaNpowIR) with a very low on-resistance for a given reverse voltage capability was introduced. It is claimed that it allows the switching frequency of converters to be raised to 5 MHz while holding efficiency constant. A roadmap for a 200 V GaN-on-Si based HEMT forecasts a $r_{DS(on)}$ of 5 mΩ. A comparison of the $r_{DS(on)}$ of silicon-, SiC- and GaN-based transistors is given in Figure 1.34b. Gallium nitride-based diodes feature the same low reverse recovery charge as SiC diodes, due to the absence of minority carriers. Gallium nitride technology is envisaged to be used in making hybrid ICs out of both silicon and gallium nitride for distributing power on chips.

We can expect that the second decade of the twenty-first century will see more advances in GaN technology. As we can see in Figure 1.34b, GaN-based transistors have the potential of much higher breakdown voltages, making them useful in very high-voltage applications where the use of SiC-based transistors is penalized by their large on-state resistances. It seems that the actual implementations of GaN transistors in the first decade of the twenty-first century are a long way away from the limits of this technology.

1.3.5 Energy losses associated with power switches

An ideal switch has zero resistance in the on-state and zero leakage current in the off- state. Its turn-on and turn-off times are zero. Thus, it has zero power loss. However, in practice, the non-ideal characteristics of the switch cause power loss. The power losses can be classified into four types.

1.3.5.1 Switching Losses

We saw in Section 1.3.3.2 that when a switch is changed from the off-state to on-state (Figure 1.27a), or from the on-state to off-state (Figure 1.27b), there is a transition time until it is fully turned on or off, respectively. During the transition periods of duration $t_{r2} + t_{r3}$ and $t_{f2} + t_{f3}$, respectively, both the switch voltage and current are non-zero. For converters with inductors, as considered in Section 1.3.3.2, assuming that the trajectories of the switch voltage and current are straight lines and neglecting the reverse recovery current of the freewheeling diode, the turn-on switching power loss, $P_{sw(ON)}$, and turn-off switching loss, $P_{sw(OFF)}$, can be calculated as:

$$P_{sw(ON)} = \frac{V_{off\_state}\, I_{on\_state}}{2}(t_{r2} + t_{r3})f_S$$

$$P_{sw(OFF)} = \frac{V_{off\_state}\, I_{on\_state}}{2}(t_{f2} + t_{f3})f_S$$

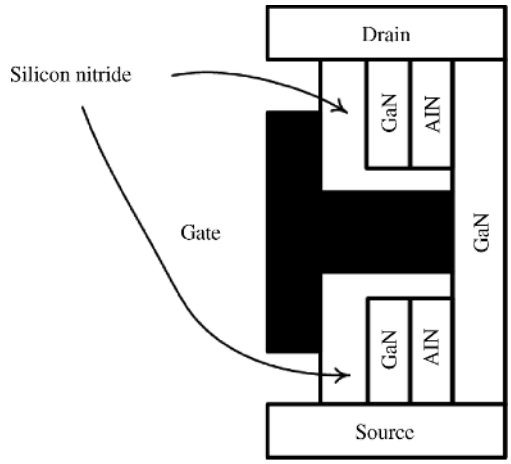

(a)

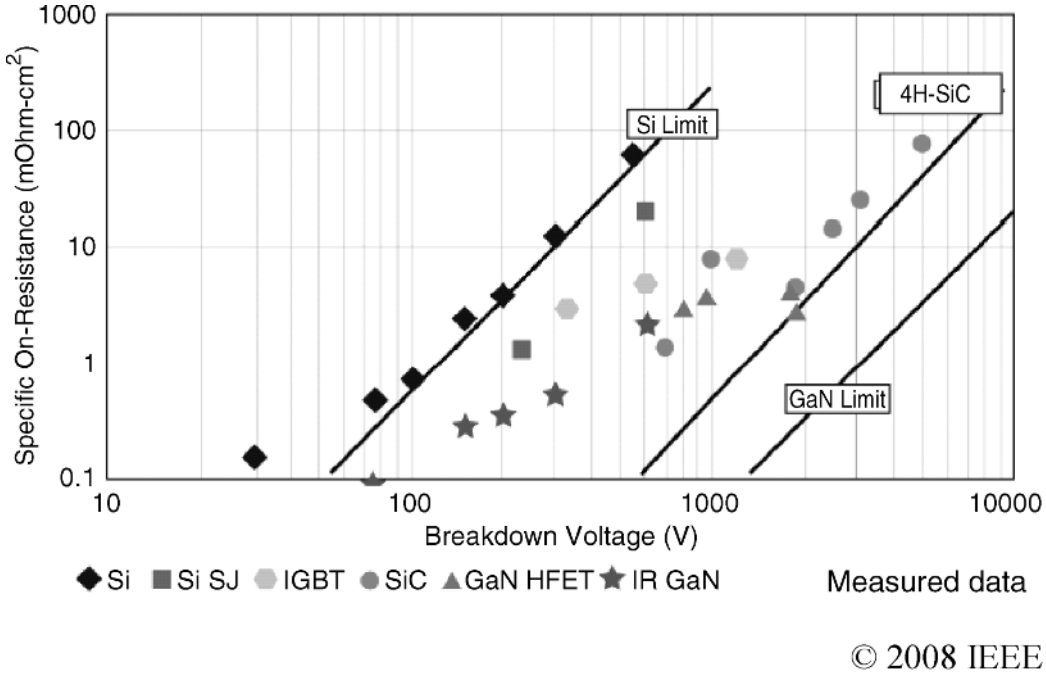

(b)

Figure 1.34 *(a) HEM-MOSFET with three-layer structure. (b) Comparison of* $r_{DS(on)}$ *for silicon-, SiC-, and GaN-based transistors. (Reproduced with permission from N. Ikeda* et al., *"High power AlGaN/GaN HFET with a high breakdown voltage of over 1.8 kV on 4 inch Si substrates and the suppression of current collapse,"* Proc. of the 20th Int. Symp. on Power Semiconductor Devices & ICs, *2008 Orlando, FL, pp. 287–290.)*

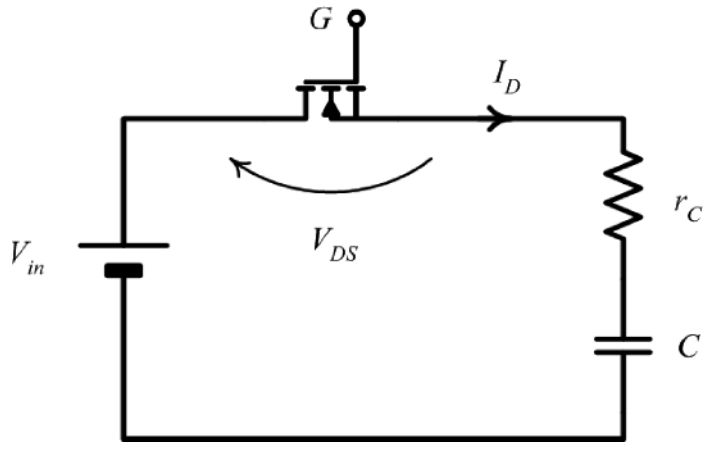

Figure 1.35 *Equivalent scheme of a switching circuit without inductors.*

We shall see later in this chapter that there are converters without inductors. In such a converter, each switch is connected only between two capacitors, or a voltage source and a capacitor. The equivalent circuit is shown in Figure 1.35. The transient process is a little different from that explained in Figure 1.27 for converters with inductors. In the turn-on process, at the end of the delay interval, t_{r1}, when V_{GS} reaches V_T, the drain current starts increasing. However, now there is no freewheeling diode in conduction to keep V_{DS} constant. As we can see in Figure 1.35, when I_D starts increasing, V_{DS}, which is given by $V_{in} - r_C I_D - V_C$ starts decreasing. The operation in this region finishes when V_{DS} drops to V_{on_state}, which marks the end of the turn-on process (Figure 1.36).

In the turn-off process, at the end of the delay interval, t_{f1}, when V_{GS} reaches V_{GS_sat}, unlike converters with an inductor where the switch current is maintained by the inductor connected to it, now the drain current starts decreasing. V_{DS} starts increasing as V_{DS} equals $V_{in} - r_C I_D - V_C$. The turn-on power loss, $P_{sw(ON)}$, and turn-off power loss, $P_{sw(OFF)}$, are:

$$P_{sw(ON)} = \frac{V_{off\_state}\, I_{on\_state1}}{6} t_{r2} f_S$$

$$P_{sw(OFF)} = \frac{V_{off\_state}\, I_{on\_state2}}{6} t_{f2} f_S$$

where V_{off_state} is the off-state voltage, I_{on_state1} is the switch current when the switch becomes fully turned on, and I_{on_state2} is the switch current prior to the turn-off of the switch. (We leave the reader to prove the above formulas.)

The switching power loss will be dissipated as heat in the switch. It is very important to reduce it.

1.3.5.2 Off-State Leakage Power Loss

When a switch is off, its equivalent resistance is large but not infinite. There is a small leakage current flowing through the switch that is generally neglected. However, there are a few cases when we have to take

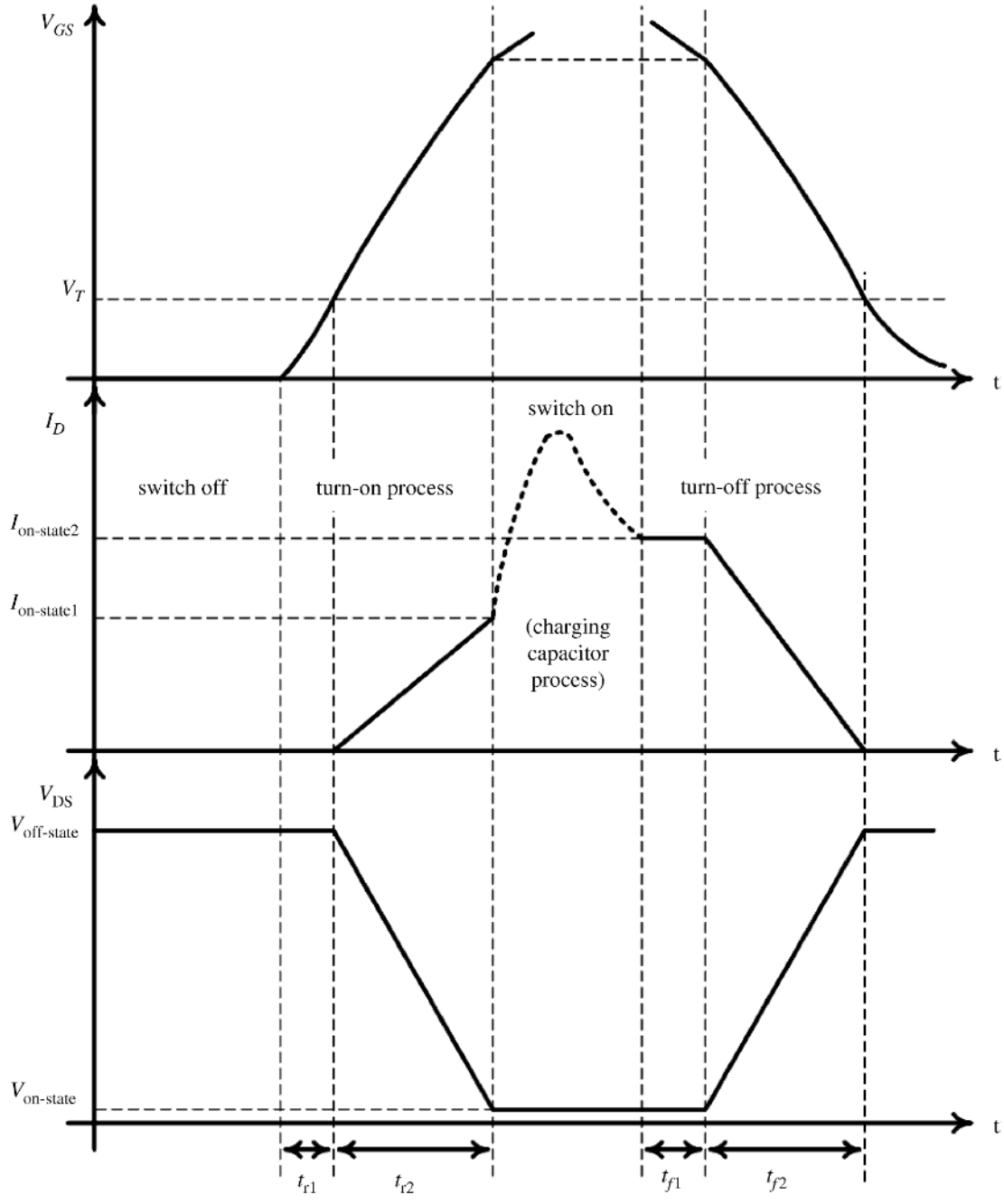

Figure 1.36 *Transient processes of a MOSFET in a converter without inductors.*

it into account; for example, in Schottky diodes, or in converters operating at a very high switching frequency. At high frequencies, the effect of the junction capacitance of the switch becomes dominant, causing resonance with the stray inductances in the circuit and, thus, high-frequency oscillations (leading to *ringing* or *spikes*). For example, the junction capacitance of the main switch in a converter with transformer (of the types we will see in the next chapter) will resonate with the self-inductance of the primary side of the transformer. Therefore, in such a situation the leakage current through the junction capacitance causes leakage power losses.

1.3.5.3 Conduction Power Loss

When a switch is in the on-state, there is a finite voltage drop across it, causing energy loss as heat. The power loss, P_{ON}, is:

$$P_{ON} = \frac{1}{T_S}\int_0^{T_{sw}} i_{sw\_on}(t)v_{sw\_on}(t)dt$$

where T_{sw} is the time when the switch is in conduction (this time is called *duty time*), i_{sw_on} is the current through the switch, and v_{sw_on} is the voltage across the switch in conduction.

The manufacturers of switching devices have continued to reduce the on-state resistance of MOSFETs and on-state voltage drop of IGBTs, in order to reduce the conduction loss. For example, for a 30 V rated MOSFET, the value of $r_{DS(on)}$ for the 7th generation in the year 2000 was 5 mΩ, dropping to 3 mΩ for the 9th generation in 2005, and 1.7 mΩ for the 11th generation in 2010.

1.3.5.4 Gate Drive Power Loss

It requires power to drive semicontrollable and controllable switches. For example, when driving a MOSFET, we charge C_{gs} at the gate voltage, V_{GS}, when turning it on, and then dissipate this energy ($C_{gs}\,V_{GS}^2/2$) as heat when turning it off. To reuse this energy, we have started to introduce advanced gate driving technologies. We shall discuss them in Volume III in the chapter about resonant converters.

1.3.5.5 Heat Sinks

To dissipate the heat produced by the energy losses in the switches, devices called "heat sinks" are included in converters. By calculating the total dissipated power, and taking into account some thermal coefficients given in the datasheet of the switch (called thermal resistances, specified in °C/W) and the temperature of the ambient space, we can calculate the necessary heat sink. By using heat sinks, we have to make sure that the surface temperature of the device is maintained within the manufacturer's specified range, for example less than 120 °C, to ensure the reliability and life expectancy of the power switches. After the prototype is realized, the temperature of each switch is measured by using thermocouples or a thermal camera. If the temperature range is surpassed, the heat sink has to be re-designed. The actual mounting of the heat sink (e.g., a large one for all switches, or individual ones for each device, etc.) depends also on the switches' location. Both the effectiveness of the heat dissipation and the size of the converter depend on how well the thermal design is realized. In high power applications, a cooling fan can be used to realize an effective transfer of heat to the ambient space. In Volume V, a special section is dedicated to packaging and thermal design.

1.3.5.6 Outline for Choosing a Transistor

When a power electronics circuit is designed, for choosing a transistor, the following procedure will be followed:

a. Calculate the required blocking voltage (the maximum designed value of V_{off_state} plus a 20% margin) and maximum current (the maximum designed value of the switch current plus a 20% margin).
b. Choose a switch (MOSFET or IGBT) of voltage and current ratings 1.5–2 times the required values as calculated. MOSFETs are used in high-frequency and low-voltage applications, while IGBTs are used in low-frequency and high-voltage applications (as can be seen in Tables 1.1 and 1.2).
c. Based on the available options from item (b), choose the one with the lowest on-state resistance $r_{DS(on)}$ (for a MOSFET) or the lowest on-state voltage drop V_{on_state} across the switch (for an IGBT).
d. Check the turn-on and turn-off times of the chosen switch to make sure that the total switching time is much shorter than the switching period, T_s.

In applications where the switch current is high, we prefer to use several MOSFETs connected in parallel to reduce the total equivalent on-state resistance. Of course, this is at the expense of needing more drivers and, consequently, a higher current driving capability. Each MOSFET is chosen to carry only one part of the switch current calculated at stage (b). An application known by all of us is the radio-controlled toy car where the speed controller makes use of up to eight, or even more, MOSFETs in its converter.

We can conclude the discussion about the switching elements with a figure showing the power and switching frequency range of availability of different types of switches: thyristors, GTOs, IGBTs, MOSFETs, when different technologies are used (Figure 1.37). The SiC-based switches have still further potential for improvement.

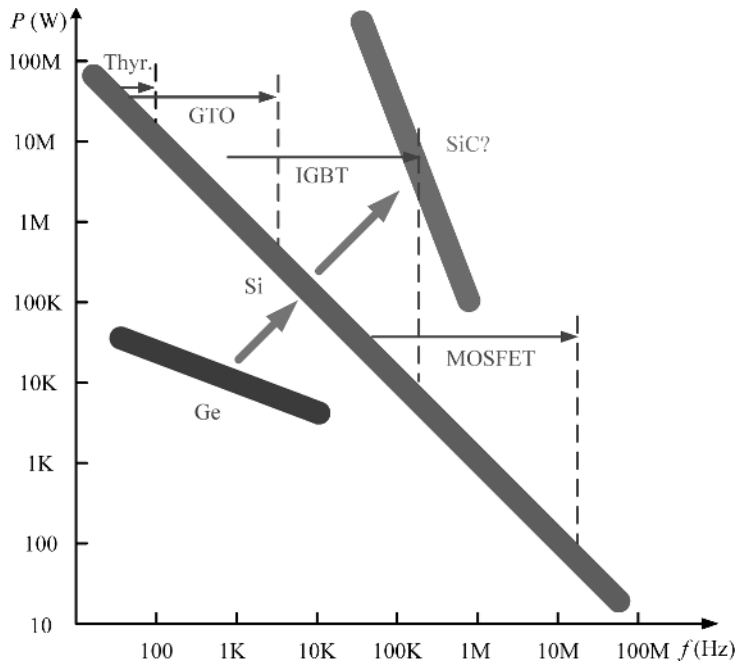

Figure 1.37 *Present power and switching frequency range of available switches.*

Table 1.1 *Examples of MOSFETs and their characteristics.**

VBV	Manufacturer	Part No.	ID, max at 25 °C (A)	Rds (on) (Ω)	t_{on} (ns)	t_r (ns)	t_{off} (ns)	t_f (ns)	P_d (W)	C_{gs} (pF)	C_{ds} (pF)	C_{gd} (pF)	f_s (duty cycle: 0.15–0.85) (MHz)
30	**On Semi**	NTD4805N	88	0.005	10.8	20.5	30.8	4.4	66	2527	272	338	2.26
		MTP50P03HDL	50	0.025	22	340	90	218	125	2950	1000	550	0.22
		NTD4815N	35	0.015	6.3	17.6	18.4	2.3	32.6	662	73	108	3.36
		NTR4003N	0.56	1	16.7	47.9	65.1	64.2	0.83	12.9	11.6	8.1	0.77
		MTD20P03HDL	20	0.099	18	178	21	72	75	640	230	130	0.52
	Fairchild	FDP6030BL	40	0.018	9	11	23	8	60	1060	150	100	2.94
		FDMS7692	14	0.0075	8	2.7	17	2.3	27	970	280	45	5.00
		FDB8870	160	0.0039	10	98	75	47	160	4630	400	570	0.65
		FDB8832	80	0.0021	24	73	54	38	300	10140	880	1260	0.79
		FDB8880	54	0.0116	8	107	47	51	55	1093	108	147	0.70
	IRF	IRFR3708	61	0.0125	7.2	50	17.6	3.7	87	2365	655	52	1.91
		IRLI3803	76	0.006	14	230	29	35	63	4120	920	880	0.49
		IRF6722M	56	0.0047	11	7.8	9.5	6.1	42	1150	340	150	4.36
		IRF6638	25	0.0022	19	45	28	6.2	89	3360	400	410	1.53
		IRLR7843	161	0.0033	25	42	34	19	140	3950	510	430	1.25
	Infineon	BSB053N03LP G	71	0.0053	4.2	4	19	3.4	42	1909	609	91	4.90
		BSB012N03LX3 G	180	0.0012	7.9	8.6	47	8.4	89	12500	3100	200	2.09
		BSB017N03LX3 G	147	0.0017	5.8	6.4	35	6	57	5780	2180	120	2.82
		IPP070N08N3 G	80	0.0067	16	66	31	8	136	2860	750	30	1.24
		BSF024N03LT3 G	106	0.0024	5.7	5.6	29	4.8	42	4016	1646	84	3.33
60	**Microsemi**	MSAEH50A06A	50	0.022	70	70	75	75	210	1900	1100	200	1.03
		MSAER45N06A	45	0.022	215	215	200	200	300	4260	1660	340	0.36
		MASEZ58N06A	58	0.018	290	290	900	900	300	NA	NA	NA	0.13
		FSE3506	35	0.03	NA	NA	NA	NA	125	NA	NA	NA	NA
		FSF2606	26	0.03	NA	NA	NA	NA	125	NA	NA	NA	NA
	IXYS	IXTQ150N06P	150	0.01	27	53	66	45	480	2150	1250	850	0.79
		IXTU12N06T	12	0.085	12	29	29	18	33	245.6	35.6	10.4	1.70
		IXTY12N06T	12	0.085	12	29	29	18	33	245.5	35.5	10.5	1.70
		IXTQ 200N06P	200	0.006	35	60	90	40	714	4040	2190	1360	0.67
	IRF	IRFIZ24E	14	0.071	4.9	34	19	27	29	305	75	65	1.77
		IRFS3006	293	0.0015	14	61	118	69	375	8325	482	525	0.57
		IRFZ44	55	0.0165	13	97	40	57	115	1707	290	103	0.72
		IRF1018	79	0.0071	13	35	55	46	110	2160	140	130	1.01
		IRF7749L2TR	200	0.0011	17	43	78	39	125	11470	960	850	0.85
	Infineon	IPP048N06L G	100	0.0044	18	25	98	24	300	5350	1150	350	0.91
		IPB019N06L3 G	120	0.0019	35	79	131	38	250	20860	3160	140	0.53
		IPB120N06N G	75	0.0117	14	27	34	26	158	1480	340	120	1.49
		IPB037N06N3 G	90	0.0037	30	70	40	5	188	7942	1642	58	1.03
		IPB065N06L G	80	0.0065	11	21	60	20	250	3580	670	220	1.34

100	**Microsemi**	MSAER57N10A	57	0.025	14	59	58	48	215	2800	850	300	0.84
		APT10M19BVRG	75	0.019	16	40	50	20	370	4300	1100	800	1.19
		APT10M25BVRG	75	0.025	13	22	40	10	300	3650	950	650	1.76
		APT10M07JVFR	225	0.007	25	60	80	20	700	15 200	4000	2800	0.81
		MSAFR38N10A	38	0.055	35	190	170	130	300	3500	900	200	0.29
	IXYS	DE150-101N09A	9	0.16	4	4	4	4	200	670	170	30	9.38
		IXFC110N10P	60	0.017	21	25	65	25	120	3110	930	440	1.10
		IXTA75N10P	75	0.025	27	53	66	45	360	1975	615	275	0.79
		IXTP60N10TM	33	0.019	27	40	43	37	60	2590	275	60	1.02
		IXFX420N10T	420	0.0026	47	155	115	255	1670	46 470	3860	530	0.26
	IRF	IRFB4410	96	0.008	24	80	55	50	250	4960	170	190	0.72
		IRF540N	33	0.044	11	35	39	35	130	1920	210	40	1.25
		IRF530N	17	0.09	9.2	22	35	25	70	901	111	19	1.64
		IRF6644	60	0.0103	17	26	34	16	89	2110	320	100	1.61
		IRF3710	57	0.023	12	58	45	47	200	3058	338	72	0.93
	Infineon	IPD49CN10N G	20	0.049	10	4	14	3	44	812	110	10	4.84
		IPI08CN10N G	95	0.0082	15	24	26	6	167	4967	714	43	2.11
		IPB05CN10N G	100	0.0051	28	42	64	21	300	8975	1295	75	0.97
		IPB042N10N3 G	100	0.0042	27	59	48	14	214	6279	1169	41	1.01
		IPB79CN10N G	13	0.078	9	4	13	3	31	530	68	8	5.17
200	**Microsemi**	APT20M11JLL	176	0.011	24	65	55	9	694	10 230	4130	90	0.98
		APT20M11JVR	175	0.011	20	40	75	10	700	16 650	2750	1350	1.03
		MSAER30N20A	30	0.085	35	190	170	130	300	3390	590	110	0.29
		MSAEZ30N20A	33	0.07	40	110	450	160	300	2370	270	230	0.20
		MSAFX50N20A	50	0.045	20	15	75	20	300	4115	515	285	1.15
	IXYS	IXFT60N20F	60	0.038	15	14	42	7	315	2610	620	320	1.92
		IXTP50N20PM	20	0.06	26	35	70	30	90	2615	385	105	0.93
		IXTA32N20T	32	0.078	14	18	55	31	200	1729	181	31	1.27
		IXTP32N20T	32	0.078	14	18	55	31	200	1729	181	31	1.27
		IXFN230N20T	230	0.0075	41	35	104	29	1090	27 690	2230	310	0.72
	IRF	IRFR15N20	17	0.165	9.7	32	17	8.9	140	879	139	31	2.22
		IRFB4103	17	0.139	9.6	40	16	5.4	140	878	98	22	2.11
		IRF630N	9.3	0.3	7.9	14	27	15	82	550	64	25	2.35
		IRFI4227	26	0.021	17	19	11	29	46	4509	369	91	1.97
		IRFS38N20D	43	0.054	16	95	29	47	300	2827	377	73	0.80
	Infineon	IPD320N20N3 G	34	0.032	11	9	21	4	136	1766	131	4	3.33
		IPP110N20N3 G	88	0.0107	18	26	41	11	300	5335	396	5	1.56
		IPP320N20N3G	34	0.032	11	9	21	4	136	1766	131	4	3.33
		IPB107N20N3 G	88	0.0107	18	26	41	11	300	5335	396	5	1.56
		IPI110N20N3 G	88	0.0107	18	26	41	11	300	5335	396	5	1.56
500	**Microsemi**	MSAEX8P50A	8	1.2	33	27	35	35	300	3225	275	175	1.15
		MSAFX11P50A	11	0.75	33	27	35	35	300	4565	295	135	1.15
		MSAFR12N50A	12	0.4	35	190	170	130	300	2460	360	240	0.29
	IXYS	IXZ318N50	19	0.34	4	4	5	6	880	1933	158	17	7.89
		IXFP3N50PM	2.7	2	25	28	63	29	36	402.9	41.9	6.1	1.03

(Continued)

Table 1.1 (*Continued*)

VBV	Manufacturer	Part No.	ID, max at 25 °C (A)	Rds (on) (Ω)	t_{on} (ns)	t_r (ns)	t_{off} (ns)	t_f (ns)	P_d (W)	C_{gs} (pF)	C_{ds} (pF)	C_{gd} (pF)	f_s (duty cycle: 0.15–0.85) (MHz)
		IXTP1R6N50P	1.6	6.5	20	26	45	23	43	137.4	17.4	2.6	1.32
		IXTH20N50D	20	0.33	35	85	110	75	400	6218	303	82	0.49
		IXTY02N50D	0.2	30	9	4	28	45	25	115	20	5	1.74
	Fairchild	FDA16N50	16.5	0.38	40	150	65	80	205	1475	215	20	0.45
		FDH15N50	15	0.38	9	5.4	26	5	300	1834	214	16	3.30
		FDH44N50	44	0.12	16	84	45	79	750	5295	605	40	0.67
		FDP18N50	18	0.265	55	165	95	90	235	2175	305	25	0.37
		FDP20N50	20	0.23	95	375	100	105	250	2373	328	27	0.22
	Infineon	IPB50R299CP	12	0.299	35	14	80	12	104	1187.5	50.5	2.5	1.06
		SPB12N50C3	11.6	0.38	10	8	45	8	125	1170	370	30	2.11
		IPB50R140CP	23	0.14	35	14	80	8	192	2537	107	3	1.09
		IPB50R250CP	13	0.25	35	14	80	11	114	1417.5	60.5	2.5	1.07
		IPB50R199CP	17	0.199	35	14	80	10	139	1797	77	3	1.08
800	**Microsemi**	MSAER07N80A	7.1	1.2	100	NA	105	NA	300	2600	200	200	0.73
		MSAFX11N80A	11	0.95	100	NA	150	NA	310	4100	260	100	0.60
		APT11N80BC3G	11	0.45	25	15	70	7	156	1567	752	18	1.28
		APT12M80B	13	0.8	14	20	60	18	335	2428	203	42	1.34
		APT24M80B	25	0.39	26	38	115	33	625	4515	375	80	0.71
	IXYS	IXFP7N80PM	3.5	1.44	28	32	55	24	50	1877	120	13	1.08
		IXFA7N80P	7	1.44	28	32	55	24	200	1790.5	118.5	9.5	1.08
		IXFC12N80P	7	0.00093	21	22	62	22	120	2781	191	19	1.18
		IXFI7N80P	7	1.44	28	32	55	24	200	1877	120	13	1.08
		IXFC20N80P	10	0.5	22	24	70	25	166	4652	332	28	1.06
	Fairchild	FQP7N80C	6.6	1.9	35	100	50	60	167	1280	110	10	0.61
		FQP3N80C	3	4.8	15	43.5	22.5	32	107	537.5	48.5	5.5	1.33
		FQP8N80C	8	1.55	40	110	65	70	178	1567	122	13	0.53
		FQP5N80	4.8	2.6	22	60	55	40	140	939	84	11	0.85
		FQPF6N80CT	5.5	2.5	26	65	47	44	158	1002	82	8	0.82
	Infineon	SPD06N80C3	6	0.9	25	15	72	8	83	765	13	20	1.25
		SPP17N80C3	17	0.29	25	15	72	12	227	2240	34	60	1.21
		SPP11N80C3	11	0.45	25	15	72	10	156	1560	25	40	1.23
		SPA02N80C3	2	2.7	25	15	72	18	30.5	284	7	6	1.15
		SPP04N80C3	4	1.3	25	15	72	12	63	558	13	12	1.21
1000	**Microsemi**	MSAER05N100A	5.6	2	75	NA	270	NA	300	2320	160	80	0.43
		MSAFA1N100D	1	12.5	6.3	5.9	315	2600	NA	275	21	15	0.05
		MSAFX10N100A	10	1	100	NA	150	NA	310	3930	240	70	0.60
		MSAFX13N110A	13	0.92	60	NA	150	NA	310	5550	250	150	0.71
		MSAFX14N100A	14	0.82	60	NA	150	NA	310	5550	250	150	0.71
	IXYS	IXFX24N100F	24	0.39	22	18	52	11	560	6370	530	230	1.46
		IXFP05N100M	0.7	17	11	19	40	28	25	252	14	8	1.53

		IXTU01N100	0.1	80	12	12	28	28	25	52	4.9	2	1.88
		IXTH10N100D	10	1.4	35	85	110	75	400	2400	200	100	0.49
		IXTY01N100D	0.4	80	7	10	34	64	25	98	10	2	1.30
	Infineon	IPI90R500C3	11	0.5	70	20	400	25	156	NA	NA	NA	0.29
		IPA90R340C3	15	0.34	70	20	400	25	35	NA	NA	NA	0.29
		IPW90R120C3	36	0.12	70	20	400	25	417	NA	NA	NA	0.29
		IPA90R1K2C3	5.1	1.2	70	20	400	40	31	NA	NA	NA	0.28
		IPI90R800C3	6.9	0.8	70	20	400	32	104	NA	NA	NA	0.29
	TOSHIBA	2SK1119	4	3	30	18	70	12	100	645	45	55	1.15
		2SK1120	8	1.5	40	25	100	20	150	1200	80	100	0.81
		2SK1489	12	0.8	140	100	500	150	200	1780	140	220	0.17
1200	**Microsemi**	APT12057B2LLG	22	0.57	11	20	36	21	690	5025	640	130	1.70
		APT14M120B	14	0.87	26	15	85	24	625	4710	295	55	1.00
		APT19M120J	19	0.53	50	31	170	48	545	9555	600	115	0.50
		APT22F120B2	23	0.7	45	27	145	42	1040	8270	515	100	0.58
		APT26F120B2	27	0.58	50	31	170	48	1135	9555	600	115	0.50
	IXYS	IXZR08N120B	8	1.5	4	5	4	6	250	1889	75	11	7.89
		IXFA3N120	3	4.5	17	15	32	18	200	1025	75	25	1.83
		IXTP02N120P	0.2	75	6	10	21	39	33	102.1	6.7	1.9	1.97
		IXFN32N120P	32	0.31	70	62	88	58	1000	20923	1023	77	0.54
		IXFB30N120P	30	0.35	57	60	95	56	1250	22472	922	28	0.56

*With VBV as breakdown voltage, $R_{ds(on)}$ for its maximum value at an operating temperature of 25 °C, t_{on} as turn-on delay time (t_{r1} in the text), t_r as rise time (t_{r2} in the text), t_{off} as turn-off delay time ($t_{f1} + t_{f2}$ in the text), t_f as fall time (t_{f3} in the text), P_d as the maximum rating of the total power dissipation of the switch, f_s as the switching frequency (the values of f_s in the table are only informative. They have been calculated with the formula

$$f_s = \frac{0.15}{t_{on} + t_r + t_{off} + t_f}$$

and can differ from the actual value that can be provided by the manufacturer. Depending on the specific application and actual thermal limitations, the same MOSFET can have a different allowed switching frequency range. As, in the manufacturers catalogues, the parasitic capacitances are not expressed in terms of our definitions C_{gs}, C_{ds}, C_{gd}; the values for these capacitances for MOSFET and IGBT have been calculated from the other data in catalogues referring to the parasitic capacitances.

With thanks for the help and permission for compiling the data from their catalogue to the companies: SCILLC dba ON Semiconductor, Fairchild, International Rectifier, Infineon, Microsemi. The table contains data available at the time of writing. These tables have an informative character. No accuracy is guaranteed. For use in practical applications, it is suggested that readers check for updated, accurate data in the companies' catalogues.

Used with permission from SCILLC dba ON Semiconductor.

Compiled with permission from Fairchild products catalogue, Infineon products catalogue and Microsemi products catalogue.

Reproduced by permission of International Rectifier, IXYS and Toshiba.

Table 1.2 *Examples of IGBT and their characteristics (with f_s from manufacturer' datasheets).**

VBV	Manufacturer	Part No	I_{ce}, max at 25 °C (A)	V_{ce}, sat (V)	t_{on} (ns)	t_r (ns)	t_{off} (ns)	t_f (ns)	P_d (W)	C_{gs} (pF)	C_{ds} (pF)	C_{gd} (pF)	f_s (MHz)
300	**IXYS**	IXGH120N30C3	75	2.10	28.00	37.00	109.00	86.00	540.00	8505.00	520.00	195.00	0.1500
		IXGH100N30B3	75	1.70	27.00	51.00	110.00	33.00	460.00	4917.00	277.00	93.00	0.0400
		IXGK400N30A3	400	1.15	45.00	45.00	210.00	107.00	1000.00	18810.00	1160.00	190.00	0.0100
		IXGA42N30C3	42	1.85	21.00	23.00	113.00	65.00	223.00	2080.00	158.00	60.00	0.1500
		IXGH85N30C3	75	1.90	25.00	34.00	100.00	70.00	333.00	5020.00	230.00	80.00	0.1500
	IRF	IRG6I320U	24	1.45	24.00	20.00	89.00	70.00	39.00	1122.00	23.00	38.00	NA
		IRGI4086	25	1.29	36.00	31.00	112.00	65.00	43.00	2192.00	52.00	58.00	NA
		IRGI4090	21	1.20	20.00	14.00	99.00	68.00	34.00	1126.00	32.00	27.00	NA
		IRGB4086	70	1.90	36.00	31.00	112.00	65.00	160.00	2192.00	52.00	58.00	NA
		IRGP4072D	70	1.46	18.00	36.00	144.00	95.00	180.00	2207.00	132.00	58.00	NA
	FAIRCHILD	FGA120N30D	25	1.10	30.00	270.00	100.00	130.00	290.00	2210.00	260.00	100.00	NA
		FGA180N30D	40	1.10	30.00	210.00	100.00	140.00	480.00	3270.00	370.00	150.00	NA
		FGA90N30D	20	1.10	30.00	200.00	110.00	140.00	219.00	1620.00	210.00	80.00	NA
		FGH50N3	75	1.40	20.00	15.00	135.00	12.00	463.00	NA	NA	NA	NA
600	**IXYS**	IXSA10N60B2D1	20	2.50	30.00	30.00	180.00	165.00	100.00	389.00	39.00	11.00	0.0200
		IXSH10N60B2D1	20	2.50	30.00	30.00	180.00	165.00	100.00	389.00	39.00	11.00	0.0200
		IXSP10N60B2D1	20	2.50	30.00	30.00	180.00	165.00	100.00	389.00	39.00	11.00	0.0200
		IXSP24N60B	48	2.50	50.00	50.00	150.00	170.00	150.00	1413.00	93.00	37.00	0.0200
		IXSH30N60B2D1	48	2.50	30.00	30.00	130.00	140.00	250.00	1178.00	68.00	42.00	0.0200
	IRF	IRG4PC30S	34	1.40	22.00	18.00	540.00	390.00	100.00	1087.00	59.00	13.00	0.0010
		IRGP4063	96	1.65	60.00	40.00	145.00	35.00	330.00	2935.00	155.00	90.00	NA
		IRG4PC40KD	42	2.10	53.00	33.00	110.00	100.00	160.00	1545.00	75.00	55.00	0.0250
		IRG4PSC71KD	85	1.83	82.00	107.00	282.00	97.00	350.00	6710.00	540.00	190.00	0.0250
		IRGP4068D	96	1.65	NA	NA	145.00	35.00	330.00	2935.00	155.00	90.00	NA
	Microsemi	APT50GN60B	107	1.45	20.00	25.00	230.00	100.00	366.00	3100.00	25.00	100.00	NA
		APT20GN60K	40	1.50	9.00	10.00	140.00	95.00	136.00	1065.00	15.00	35.00	NA
		MSAHX75L60C	75	1.80	50.00	210.00	600.00	500.00	300.00	3900.00	240.00	100.00	NA
		APT28GA60BD15	50	2.00	11.00	8.00	101.00	27.00	222.00	2083.00	188.00	26.00	NA
		APT50GS60BRG	93	2.80	16.00	33.00	225.00	37.00	415.00	2490.00	95.00	145.00	NA
	Infineon	SGP30N60HS	41	2.80	20.00	21.00	250.00	25.00	250.00	1408.00	58.00	92.00	0.1000
		SGP02N60	6	1.90	20.00	13.00	259.00	52.00	30.00	132.00	8.00	10.00	0.0400
		SGP20N60HS	36	2.80	18.00	15.00	207.00	13.00	178.00	1036.00	41.00	64.00	0.1000
		SGP15N60	31	2.00	32.00	23.00	234.00	46.00	139.00	748.00	32.00	52.00	0.0400
		IGP50N60T	100	1.50	26.00	29.00	299.00	29.00	333.00	3047.00	107.00	93.00	0.0200
900	**IXYS**	IXGT50N90B2	75	2.70	20.00	28.00	350.00	200.00	400.00	2425.00	105.00	75.00	0.0400
		IXGH50N90B2	75	2.70	20.00	28.00	350.00	200.00	400.00	2425.00	105.00	75.00	0.0400
		IXGH50N90B2D1	75	2.70	20.00	28.00	350.00	200.00	400.00	2425.00	130.00	75.00	0.0400
		IXGK50N90B2D1	75	2.70	20.00	28.00	350.00	200.00	400.00	2425.00	130.00	75.00	0.0400
		IXGT32N90B2	64	2.70	20.00	22.00	260.00	150.00	300.00	1741.00	72.00	49.00	0.0400
	IRF	IRG4PF50W	51	2.25	29.00	26.00	110.00	150.00	200.00	3255.00	155.00	45.00	0.1000
		IRG4PF50WD	51	2.25	71.00	50.00	150.00	110.00	200.00	3255.00	155.00	45.00	NA

	Microsemi	APT35GA90B	63	2.50	12.00	15.00	104.00	86.00	290.00	1906.00	145.00	28.00	NA
		APT43GA90BD30	78	2.50	12.00	16.00	82.00	57.00	337.00	2431.00	193.00	34.00	NA
		APT46GA90JD40	87	2.50	18.00	26.00	153.00	45.00	284.00	4107.00	375.00	63.00	NA
		APT27GA90BD15	48	2.50	9.00	8.00	98.00	84.00	223.00	1360.00	115.00	30.00	NA
		APT64GA90B	117	2.50	18.00	26.00	131.00	104.00	500.00	3472.00	265.00	53.00	NA
	Infineon	IGW30N100T	60	1.55	33.00	21.00	535.00	34.00	412.00	3499.00	22.00	76.00	0.0200
		IHW30N90R	60	1.50	NA	NA	511.00	24.00	454.00	2810.00	4.00	79.00	0.0600
		IHW30N90T	60	1.50	45.00	26.00	556.00	29.00	428.00	2579.00	58.00	38.00	0.0200
1200	IXYS	IXSA15N120B	30	3.40	30.00	25.00	148.00	160.00	150.00	1363.00	61.00	37.00	0.0200
		IXST45N120B	75	3.00	36.00	27.00	360.00	380.00	300.00	3235.00	175.00	65.00	0.0200
		IXGX82N120A3	260	2.05	34.00	75.00	265.00	780.00	1250.00	7510.00	330.00	190.00	0.0400
		IXGX120N120A3	240	2.20	40.00	67.00	490.00	325.00	830.00	9660.00	415.00	240.00	0.0400
		IXGN82N120C3H1	130	3.90	30.00	77.00	194.00	100.00	595.00	7703.00	488.00	197.00	0.1500
	IRF	IRG4PH20KD	11	3.17	50.00	30.00	100.00	250.00	60.00	426.70	35.70	8.30	0.0200
		IRG7PH42U	90	1.70	25.00	32.00	229.00	63.00	385.00	3263.00	49.00	75.00	0.0400
		IRG7PH30K10	33	2.05	14.00	24.00	110.00	38.00	210.00	1044.00	37.00	26.00	0.0200
		IRG4PSH71UD	99	2.52	46.00	77.00	250.00	220.00	350.00	6580.00	360.00	60.00	0.0400
		IRGPS60B120KD	105	2.50	72.00	32.00	366.00	45.00	595.00	4140.00	235.00	160.00	NA
	Microsemi	APT15GN120BDQ1	45	1.70	10.00	9.00	150.00	110.00	195.00	1150.00	15.00	50.00	NA
		APT30GP60B2DL	100	2.20	13.00	18.00	55.00	46.00	463.00	3180.00	275.00	20.00	NA
		MSAGZ52F120A	52	2.70	75.00	65.00	420.00	45.00	300.00	1540.00	140.00	110.00	NA
		PPNGZ52F120A	52	2.70	75.00	65.00	420.00	45.00	300.00	1540.00	140.00	110.00	NA
		APT100GT120JRDL	123	3.20	50.00	100.00	630.00	36.00	570.00	2320.00	2150.00	4380.00	NA
	Infineon	IGW08T120	16	1.70	40.00	23.00	450.00	70.00	70.00	572.00	8.00	28.00	0.0200
		IGW15T120	30	1.70	50.00	30.00	520.00	60.00	110.00	1050.00	50.00	50.00	0.0200
		SGP02N120	6.2	3.10	23.00	16.00	260.00	61.00	62.00	193.00	8.00	12.00	0.0400
		IGB01N120H2	3.2	2.20	13.00	6.30	370.00	28.00	28.00	88.20	6.40	3.40	0.1000
		IGP03N120H2	9.6	2.20	9.20	5.20	281.00	29.00	62.50	198.00	17.00	7.00	0.1000
1700	IXYS	IXGX100N170	170	3.00	35.00	192.00	285.00	395.00	830.00	9050.00	305.00	150.00	NA
		IXGX32N170H1	75	3.30	45.00	38.00	270.00	250.00	350.00	3460.00	210.00	40.00	NA
		IXGT32N170	75	3.30	45.00	38.00	270.00	250.00	350.00	3460.00	125.00	40.00	NA
		IXGT16N170	32	3.50	45.00	48.00	400.00	770.00	190.00	1624.00	49.00	26.00	NA
		IXGT24N170AH1	24	6.00	21.00	36.00	336.00	40.00	250.00	2802.00	140.00	58.00	NA
	Infineon	SIGC42T170R2C	17	2.70	100.00	100.00	900.00	30.00	NA	NA	NA	NA	NA
		SIGC185T170R2C	100	2.70	100.00	100.00	900.00	30.00	NA	6700.00	NA	300.00	NA
		SIGC101T170R3	75	2.00	400.00	50.00	800.00	300.00	NA	6418.00	57.00	220.00	NA
		SIGC158T170R3	125	2.00	400.00	50.00	800.00	300.00	NA	10636.00	95.00	365.00	NA
		SIGC186T170R3	150	2.00	300.00	66.00	1000.00	300.00	NA	12758.00	111.00	438.00	NA
2200	IXYS	IXBH2N250	5	3.50	30.00	180.00	70.00	182.00	32.00	141.80	5.50	3.20	NA
		IXBT2N250	5	3.50	30.00	180.00	70.00	182.00	32.00	141.80	5.50	3.20	NA
		IXGH2N250	5.5	3.10	22.00	74.00	70.00	100.00	32.00	140.80	5.50	3.20	NA
		IXGF20N250	23	3.10	57.00	160.00	136.00	930.00	100.00	1172.00	35.00	18.00	NA
		IXGX75N250	180	2.30	50.00	255.00	245.00	175.00	735.00	9190.00	215.00	110.00	NA

(Continued)

Table 1.2 (*Continued*)

VBV	Manufacturer	Part No	I_{ce}, max at 25 °C (A)	V_{ce}, sat (V)	t_{on} (ns)	t_r (ns)	t_{off} (ns)	t_f (ns)	P_d (W)	C_{gs} (pF)	C_{ds} (pF)	C_{gd} (pF)	f_s (MHz)
4500	**IXYS**	T2400GA45E	2198	3.50	2100.00	3300.00	1400.00	1600.00	19000.00	NA	NA	NA	NA
		T1800GA45A	1808	3.60	2000.00	2000.00	2500.00	2200.00	20000.00	NA	NA	NA	NA
		T1200EB45E	1200	2.80	1800.00	3000.00	1600.00	2200.00	12500.00	NA	NA	NA	NA
		T0800TA45E	1267	3.60	1400.00	1900.00	1100.00	2900.00	8300.00	NA	NA	NA	NA
		T0600TA45A	776	3.50	1600.00	2100.00	1200.00	1200.00	6200.00	NA	NA	NA	NA
6500	**Infineon**	FZ750R65KE3	750	3.00	700.00	220.00	7300.00	400.00	14500	201800.00	NA	3200.00	NA
		FZ600R65KE2	600	4.3	750	370	5500	400	11500	NA	NA	NA	NA
		FZ400R65KF2	400	4.3	750	370	5500	400	7350	NA	NA	NA	NA
		FZ200R65KF2	200	4.3	750	370	5500	400	3800	NA	NA	NA	NA

*With thanks for the help and permission for compiling the data from their catalogue to the companies: SCILLC dba ON Semiconductor, Fairchild, International Rectifier, Infineon, Microsemi. The table contains data available at the time of writing. These tables have an informative character. No accuracy is guaranteed. For use in practical applications, it is suggested that readers check for updated, accurate data in the companies' catalogues.
ABB AG Semiconductors also produces high-power IGBTs for high voltages of 1.7 kV (with a collector current from 800 to 2400 A) 2.5 kV, 3.3 kV, 4.5 kV and 6.5 kV (with a collector current from 400 to 750 A).
Compiled with permission from Fairchild products catalogue, Infineon products catalogue and Microsemi products catalogue.
Reproduced by permission of International Rectifier, IXYS and Toshiba.

1.3.6 Passive reactive elements

1.3.6.1 Capacitors

A capacitor is formed by two conductive plates with a dielectric between them. The dielectric is an insulator. The capacitor is a circuit element that stores energy in its electrical field. Its capacitance, C, depends on the permittivity of the dielectric, ε (permittivity is a property associated with how much electrical charge a material can store in a given volume), cross-sectional area of the plates, A, and distance between the two plates, d:

$$C = \frac{\varepsilon A}{d}$$

Each practical capacitor presents a loss. One of the models of a practical capacitor is an ideal capacitor in series with a resistor, r_C, called *equivalent series resistance* (ESR), shown in Figure 1.38a.

The quality factor, Q, of a capacitor is a dimensionless number defined as the ratio between the capacitance reactance and its ESR:

$$Q = \frac{1}{\omega C r_C}$$

Usually, we use an alternative term: loss angle, loss tangent, or dissipation factor, to render evident the ESR of a capacitor (the loss tangent is defined as ESR over reactance, that is, is $1/Q$).

In power electronics circuits we use several types of capacitors. They differ in the dielectric medium and physical form. When we chose a capacitor in the design of a converter, we had to take into account the voltage rating of the capacitor, its calculated capacitance value, the operating frequency, physical dimensions, and life expectancy. It is important to make sure that the root-mean-square value of the current ripple flowing through the capacitor is within the specifications, to avoid overheating of the device due to the dielectric and equivalent series resistance losses. Related to capacitors, we shall use the following terms:

- "Dielectric strength" is the maximum electric field strength that the capacitor can withstand without breaking down (i.e., without experiencing failure of its dielectric properties).
- "Leakage current" refers to a gradual loss of energy from a charged capacitor. Due to the imperfection of the dielectric materials, which are not perfect insulators but have some non-zero conductivity, the dielectric allows a small amount of current to flow, slowly discharging the capacitor. However, the leakage current is very small, so in most applications in power electronics it can be neglected.
- "Temperature coefficient" is the change of the capacitance with temperature.
- "Equivalent series inductance (ESL)" is mainly caused by the leads used to connect the plates to the outside circuit and the interconnects used to join the plates together. Any capacitor operating at a very high frequency ceases to behave like a pure capacitance. Its equivalent model is shown in Figure 1.38b. For example, for a 220 μF aluminum electrolytic capacitor, the measured ESR and ESL are 0.185 Ω and 15 nH, respectively. The impedance characteristics of this capacitor are given in Figure 1.38c. We can see that the capacitor behaves like a resonant circuit, and starting from the frequency of 98 kHz (called the resonant frequency) the ESL can no longer be neglected. For modern converters operating at a high switching frequency, the parasitic effects of the capacitors (ESR and ESL) can slow down the transient response. Recently, a method of canceling the ESR and ESL effects has been proposed. The method is based on connecting an AC voltage source in series with the capacitor to counteract the total voltage drop across the ESR and ESL.

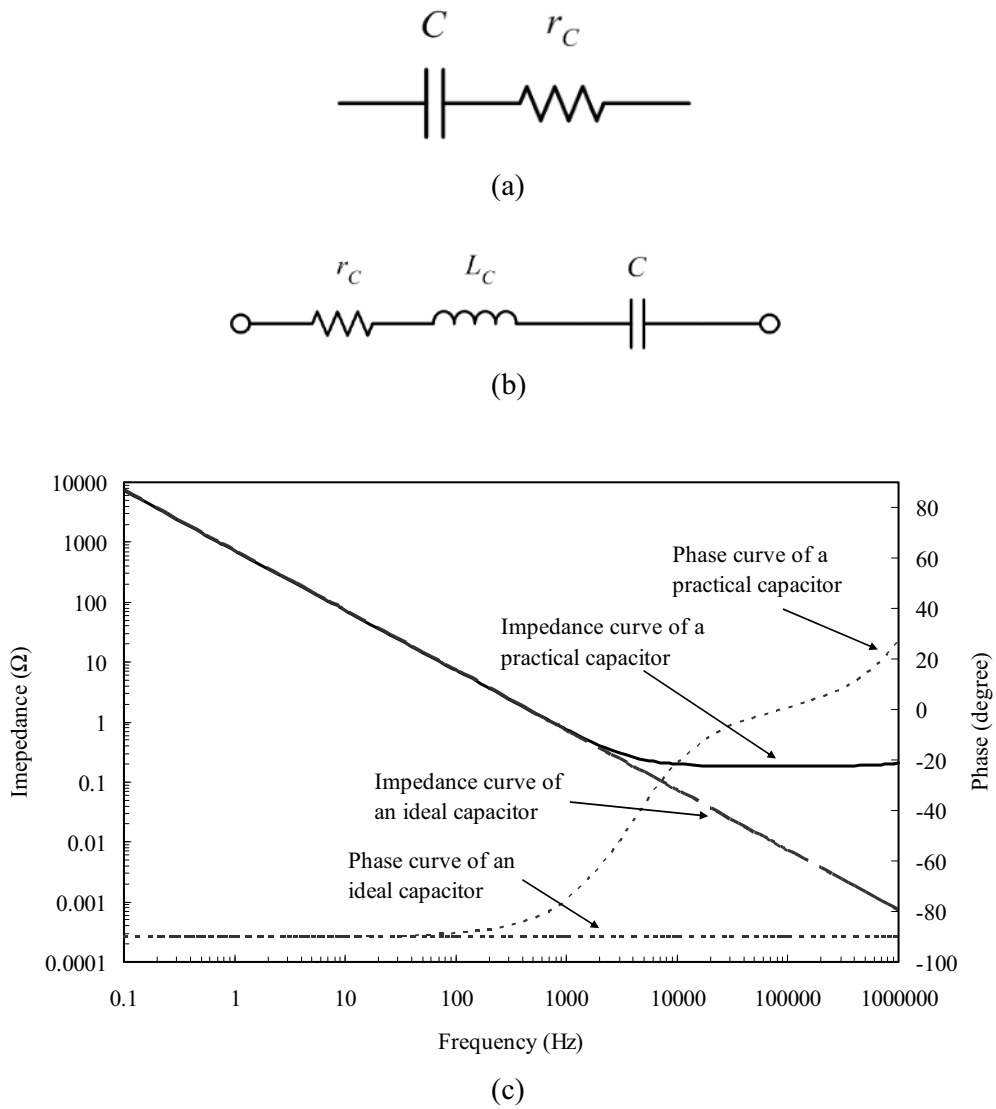

Figure 1.38 *(a) Capacitor model. (b) High-frequency model of a capacitor. (c) Impedance characteristics of a 220 μF electrolytic capacitor.*

- "Ripple current rating." Capacitors have a rating for maximum ripple current. A larger ripple current can cause damaging heat to be generated within the capacitor due to the current flow through its ESR. The ripple current rating depends on the thermal limitation of a certain capacitor: it is given by the allowed power dissipation

$$I_r = \sqrt{\frac{P_d}{r_C}}$$

where P_d is the maximum power dissipation. The ripple current rating is given by the manufacturer in the datasheet of the product.

A few capacitors used very often in power electronics are described in the following sections.

Electrolytic capacitors An electrolytic capacitor is a type of capacitor in which one of the plates is an electrolyte. Electrolytic capacitors offer very high capacitance for high-voltage, high-current and low-frequency applications. Among different types of capacitors, the electrolytic capacitors have the largest capacitance per unit volume. Thus, they have high energy density. The major drawbacks of the electrolytic capacitors are their large equivalent series inductance and equivalent series resistance, and short lifetime. The electrolytic capacitors are mostly used in the output filter of the converters, or as an intermediate capacitor in the AC-DC rectifier. Usually, the electrolytic capacitors used in power converters have an ESR of around 0.1–0.3 Ω for an operating frequency of tens to hundreds of kilohertz.

Low impedance aluminum electrolytic capacitors are cheap and have large capacitance values, but also their ESR is high. Organic semiconductor electrolytic capacitors (containing, for example, a conductive polymer) offer high capacitances with a much lower ESR, so they can be used as output capacitor in the structure of converters.

Tantalum capacitors Tantalum capacitors are electrolytic capacitors in which the dielectric is a tantalum-based material. They are compact in size, offer high capacitance values, and are suitable for low-voltage, high-frequency and miniature applications. They feature a low ESR and high ripple current capability. Compared with electrolytic capacitors, tantalum capacitors have a stable capacitance for large variation in temperature and a low leakage current. They are used in applications with lower voltages (up to a few tens of volts) compared with the electrolytic capacitors, which are used in applications with voltages of hundreds of volts.

Film capacitors Film capacitors are usually used in applications requiring large currents but relatively low capacitance, such as in resonant tanks and snubbers. They generally have a high voltage rating and a high ripple current rating. The film capacitors have a lower ESR than that of the electrolytic capacitors and also a lower capacitance density, that is, they are more voluminous for the same capacitance value. And, the film capacitors are rather more expensive. Film capacitors are also available at high voltage ratings where no electrolytic capacitors exist. The two plates of film capacitors are separated by a thin insulating film. The material of the film can be polyester, polypropylene, polycarbonate, polystyrene, or other dielectric material. The film capacitors contain no acid inside and pose no storage problems. Polyester film capacitors provide a high dielectric constant and high dielectric strength in terms of their physical volume. Metalized polyester films can withstand high-pulsed voltages without breaking the dielectric. Polypropylene film capacitors provide high dielectric strength and very low losses. They also offer a very low leakage current and negative temperature coefficient (the capacitance decreases with temperature). Thus, they are most commonly used in power electronics circuits. Polycarbonate film capacitors offer very low temperature dependency, wide operating temperature range, good long-term stability, and low losses. They are the second choice for power electronics circuits. Polystyrene film capacitors provide extremely low losses, low dielectric absorption, good long-term stability, low leakage current, and a small negative temperature coefficient. For example, the AVX polypropylene film capacitor, series 160–390 μF, has an ESR of 3.5–6.1 mΩ, and an ESL of 60–85 nH. A few examples of applications of medium power film capacitors are: in filtering the high frequency ripple coming from the converter in a speed power converter of a mass-transit system; as the intermediate capacitor between the battery and converter in an electrical vehicle; in a cardiac defibrillator for storing the energy necessary to generate electrical pulses; or as a DC link filter in a motor drive system.

Ceramic capacitors A ceramic capacitor is a capacitor constructed with one layer of ceramic dielectric. A multilayer ceramic capacitor contains alternating layers of metal and ceramic, with the ceramic material acting as the dielectric. As a result, higher capacitance values can be obtained. Recent advancements in the dielectric materials allowed the production of multilayer ceramic capacitors of higher voltage ratings. For the same physical size, the capacitance values of the multilayer ceramic capacitors lie between the values of film capacitors and those of electrolytic capacitors. Their ESR is comparable with that of film capacitors.

Mica capacitors (silver mica capacitors) The silver mica capacitors use silver electrodes, which are plated directly onto the mica dielectric.

The silver mica capacitors have a very low DC resistance and a very high accuracy, offer a very high quality factor, Q, and their value is almost independent of the frequency. They are suitable in resonant applications, but their cost is very high and their size is large.

Tables 1.3 and 1.4 show a few types of capacitors and their characteristics.

Table 1.3 *Datasheet for electrolytic, ceramic and tantalum capacitors.**

Electrolytic capacitors

Manufacturer	Voltage (V)	Capacitor (μF)	ESR (ohm)		Maximum temperature (°C)	Frequency range (Hz)	Ripple current (Arms)
			@120 Hz	@20 kHz			@120 Hz
PANASONIC	200	270–2200	0.553–0.068	0.249–0.033	105	0–120	1.42–4.12
	250	220–1500	0.678–0.099	0.305–0.05	105	0–120	1.28–3.56
	400	82–560	1.617–2.35	0.728–0.107	105	0–120	0.8–2.35
	420	68–470	1.95–0.282	0.878–0.127	105	0–120	1.08–3.18
	450	56–470	2.368–0.282	1.066–0.127	105	0–120	0.67–2.47
TDK- EPC/EPCOS	200	220–2200	0.58–0.065	0.7–0.08	105	0–200	1.7–9.1
	250	220–1800	0.58–0.08	0.7–0.1	105	0–200	1.8–8.4
	400	47–680	1.86–0.13	2.31–0.16	105	0–200	0.79–5.16
	420	82–560	1.65–0.24	1.95–0.29	105	0–200	1.12–4.52
	450	68–470	1.99–0.29	2.35–0.34	105	0–200	1.01–4.24

Ceramic capacitors

Manufacturer	Voltage (V_{DC}/V_{AC})	Capacitor (pF)	Temperature range (°C)
AVX	100	390–4700	−30–125
	500	390–4700	−30–125
	1000	100–3900	−30–125
	2000	100–3900	−30–125
	3000	330–15 000	−30–125
PANASONIC	4000	100–2200	−25–85
	6000	100–2200	−25–85
	8000	100–1500	−25–85
	10 000	100–1000	−25–85
	15 000	100–1000	−25–85

Tantalum capacitors

Manufacturer	Voltage (V_{DC}/V_{AC})	Capacitor (μF)	Temperature range (°C)
NICHICON	6.3	2.2–100	−55–125
	16	1.0–47	−55–125
	20	0.68–22	−55–125
	25	0.47–15	−55–125
	35	0.33–10	−55–125
Kemet	6	2.2–470	−55–125
	16	1.0–150	−55–125
	20	0.68–100	−55–125
	25	0.33–47	−55–125
	50	0.1–68	−55–125

*With thanks for the help and permission for compiling the data from their catalogue to the companies: Nichikon, Cornell Dubilier, TDK-EPC/EPCOS, AVX Corporation, Murata Manufacturing Co. Ltd. The table contains data available at the time of writing. These tables have an informative character. No accuracy is guaranteed. For use in practical applications, it is suggested that readers check for accurate, updated data in the companies' catalogues.
Reproduced from Panasonic, Kemet, Nippon Chemi-Con and Ashcroft Capacitor Ltd.

Table 1.4 *Datasheet for multilayer ceramic, silver mica, and film capacitors.**

Multilayer ceramic capacitors

Manufacturer	Voltage (V_{DC}/V_{AC})	Capacitor (nF)	Temperature range (°C)
AVX	50	0.68–1	−55–125
	250	0.0001–0.1	−55–125
	500	0.0001–0.1	−55–125
	1500	0.1–1	−55–125
	2000	0.027–1	−55–125
TDK-EPC/EPCOS	16	22–47	−55–125
	50	0.22–56	−55–125
	100	0.1–2.2	−55–125
	50	68–470	−55–125
	100	22–150	−55–125
NIPPON CHEMI-CON	25–250	0.033–470	−55–125

Series	Rated voltage (V)	Capacitance (μF)	Dimensions (L × W × H) (mm)	ESR (Ω)			
				Capacitance	100 kHz	1 MHz	2 MHz
NTS (Chip type)	25	1–33 (1.0, 1.5, 2.2, 3.3, 4.7, 6.8, 10, 15, 22, 33)	From 3.2 × 1.6 × 1.8 (1 μF) to 5.7 × 5.0 × 3.0 (33 μF)	@ 33 μF	0.0035	0.005	0.012
	50	0.33–15 (0.33, 0.47, 0.68 1.0, 1.5, 2.2, 3.3 4.7, 6.8, 10, 15)	From 3.2 × 1.6 × 1.8 (0.33 μF) to 5.7 × 5.0 × 2.8 (15 μF)	@ 15 μF	0.0045	0.005	0.012
	100	0.1–6.8 (0.1, 0.15, 0.22, 0.33, 0.47, 0.68, 1.0, 1.5, 2.2, 1.5, 2.2, 3.3, 4.7, 6.8)	From 3.2 × 1.6 × 1.8 (0.1 μF) to 5.7 × 5.0 × 2.8 (6.8 μF)	@ 6.8 μF	0.012	0.012	0.035
	250	0.033–1.5 (0.033, 0.047, 0.068, 0.1, 0.15, 0.22, 0.33, 0.47, 0.68, 1.0, 1.5)	From 3.2 × 1.6 × 1.8 (0.033 μF) to 5.7 × 5.0 × 2.8 (1.5 μF)	@ 1.0 μF	0.035	0.02	0.03
THC (Chip type)	25	0.33–47 (0.33, 0.47, 0.68, 1.0, 1.5, 2.2, 3.3, 4.7, 6.8, 10, 15, 22, 33, 47)	From 2.0 × 1.25 × 1.25 (0.33 μF) to 7.5 × 6.3 × 3.0 (47 μF)	@ 10 μF	0.002	0.02	0.03
	50	0.1–22 (0.1, 0.15, 0.22, 0.33, 0.47, 0.68, 1.0, 1.5, 2.2, 3.3, 4.7, 6.8, 10, 15, 22)	From 2.0 × 1.25 × 1.25 (0.1 μF) to 7.5 × 6.3 × 2.5 (22 μF)	@ 10 μF	0.011	0.01	0.025
	100	0.047–6.8 (0.047, 0.068, 0.1, 0.15, 0.22, 0.33, 0.47, 0.68, 1.0, 1.5, 2.2, 3.3, 4.7, 6.8)	From 2.0 × 1.25 × 1.25 (0.047 μF) to 7.5 × 6.3 × 3.0 (6.8 μF)	@ 2.2 μF	0.03	0.02	0.03
	200	0.047–2.2 (0.047, 0.068, 0.1, 0.15, 0.22, 0.33, 0.47, 0.68, 1.0, 1.5, 2.2)	From 3.2 × 1.6 × 1.6 (0.047 μF) to 7.5 × 6.3 × 3.0 (2.2 μF)	@ 1.5 μF	0.035	0.02	0.03

Series	Rated voltage (V)	Capacitance (μF)	Dimensions (L × W × H) (mm)
NTJ (Metal cap type)	25	33, 47	6.0 × 5.3 × 5.5
	50	15, 22	6.0 × 5.3 × 5.5
	100	6.8, 10	6.0 × 5.3 × 5.5
	250	1.5, 2.2	6.0 × 5.3 × 5.5
NTD (Dipped radial lead type)	25	3.3–33 (3.3, 4.7, 6.8, 10, 15, 22, 33)	From 5.0 × 6.0 × 3.5 (3.3 μF) to 7.5 × 9.0 × 4.5 (33 μF)
	50	1.0–15 (1.0, 1.5, 2.2, 3.3, 4.7, 6.8, 10, 15)	From 5.0 × 6.0 × 3.5 (1 μF) to 7.5 × 9.0 × 4.5 (15 μF)
	100	0.33–6.8 (0.33,0.47, 0.68, 1.0,1.5, 2.2, 3.3, 4.7, 6.8)	From 5.0 × 6.0 × 3.5 (0.33 μF) to 7.5 × 9.0 × 4.5 (6.8 μF)
	250	0.1–1.5 (0.1,0.15, 0.22, 0.33, 0.47, 0.68, 1.0, 1.5)	From 5.0 × 6.0 × 3.5 (0.1 μF) to 7.5 × 9.0 × 4.5 (1.5 μF)

(*continued*)

Table 1.4 *(Continued)*

THP (Metal cap type)	25	15–100 (15, 20, 33, 47, 68, 100)	From 4.8 × 3.5 × 5.5 (15 μF) to 7.8 × 6.6 × 6.5 (100 μF)
	50	4.5–47 (4.5, 6.8, 10, 15, 22, 33, 47)	From 4.8 × 3.5 × 5.5 (4.5 μF) to 7.8 × 6.6 × 6.5 (47 μF)
	100	1.5–15 (1.5, 2.0, 3.0, 4.7, 6.8, 10, 15)	From 4.8 × 3.5 × 5.5 (1.5 μF) to 7.8 × 6.6 × 6.5 (15 μF)
	200	0.45–4.7 (0.45, 0.68, 1.0, 1.5, 2.2, 3.3, 4.7)	From 4.8 × 3.5 × 5.5 (0.45 μF) to 7.8 × 6.6 × 6.5 (4.7 μF)
THD (Dipped radial lead type)	25	3.3–470 (3.3, 4.7, 6.8, 10, 15, 22, 33, 47, 68, 100, 150, 220, 330, 470)	From 5.0 × 6.5 × 3.0 (3.3 μF) to 28.5 × 20.0 × 7.5 (470 μF)
	50	1.0–220 (1.0, 1.5, 2.2, 3.3, 4.7, 6.8, 10, 15, 22, 33, 47, 68, 100, 150, 220)	From 5.0 × 6.5 × 3.0 (1 μF) to 28.5 × 20.0 × 7.5 (220 μF)
	100	0.33–100 (0.33, 0.47, 0.68, 1.0,1.5, 2.2, 3.3, 4.7, 6.8, 10, 15, 22, 33, 47, 68, 100)	From 5.0 × 6.5 × 3.0 (0.33 μF) to 28.5 × 20.0 × 7.5 (100 μF)
	250	0.1–15 (0.1,0.15, 0.22, 0.33, 0.47, 0.68, 1.0, 1.5, 2.2, 3.3, 4.7, 6.8, 10, 15)	From 6.5 × 7.0 × 3.5 (0.1 μF) to 28.5 × 20.0 × 7.5 (15 μF)

Silver mica capacitors

Manufacturer	Voltage (V)	Capacitor (pF)	Temperature range (°C)
Cornell-Dubilier	100	330–91 000	−55–125
	500	1–51 000	−55–125
	1000	5–13 000	−55–125
	2000	24–4300	−55–125
	2500	24–3000	−55–125
Ashcroft Capacitor Ltd (A.C.L.)	100	1–100 000	−40–85
	500	1–220 000	−40–85
	1000	5–130 000	−40–85
	1500	5–62 000	−40–85
	2000	5–22 000	−40–85

Film capacitors

Manufacturer	Voltage (V_{DC}/V_{AC})	Capacitor (μF)	Temperature range (°C)
TDK-EPC/EPCOS	63/40	0.22–1.0	−55–125
	250/160	0.022–0.15	−55–125
	4000/450	0.001–0.01	−40–85
	8000/450	0.001–0.01	−40–85
	12 500/450	0.00068–0.0025	−40–85
Nichicon	100	0.001–0.47	−40–85
	250/125	0.047–3.3	−40–105
	400/160	0.022–1.5	−40–105
	630/200	0.01–0.68	−40–105
	800/250	0.01–0.47	−40–105

Series	Rated voltage (V_{DC})	Capacitance (μF)	Dimensions (H × L × W) (mm)	ESR (mΩ)	Temperature range (°C)
AVX (FILFIM, dielectric: polypropylene)	6500	188–612 (188, 275, 362, 450, 537, 612)	From 315 × 350 × 185 (188 μF) to 770 × 350 × 185 (770 μF)	3.4, 3.3, 3.2, 3.2, 3.1, 3.1	−55–85
	14 500	37.5–121 (37.5, 55, 72, 89 106, 121)	From 315 × 350 × 185 (37.5 μF) to 770 × 350 × 185 (121 μF)	5.6, 4.9, 4.6, 4.4, 4.3, 4.2	−55–85
	28 000	5.8–21.5 (5.8, 9, 12, 15.5, 18.3, 21.5)	From 315 × 350 × 185 (5.8 μF) to 770 × 350 × 185 (21.5 μF)	6.8, 5.9, 5.5, 5.2, 5.1, 5.1	−55–85
	56 000	2.6–10.3 (2.6, 4.2, 5.7, 7.3, 8.8, 10.3)	From 315 × 695 × 185 (2.6 μF) to 770 × 695 × 185 (10.3 μF)	11.6, 9.2, 8.3, 7.8, 7.5, 7.4	−55–85
AVX (FFVS, dielectric: polypropylene)	600	22–195 (22, 90, 140, 195)	From 34 × 101 × 71.7 (22 μF) to 64 × 101 × 71.7 (195 μF)	0.74, 0.60, 0.83, 1.04	−40–105
	800	58–128 (58, 92, 128)	From 40 × 101 × 71.7 (58 μF) to 60 × 101 × 71.7 (128 μF)	0.72, 0.99, 1.25	−40–105
	1000	53–135 (53, 95, 135)	From 40 × 101 × 71.7 (53 μF) to 64 × 101 × 71.7 (135 μF)	1.56, 1.98, 2.42)	−40–105
	1900	14–32 (14, 22, 32)	From 40 × 101 × 71.7 (14 μF) to 64 × 101 × 71.7 (32 μF)	(1.05, 1.26, 1.58	−40–105

Table 1.4 *(Continued)*

Series	Rated voltage (V_{DC}/V_{AC})	Capacitance (μF)	Dimensions (D × L) (mm)	Temperature range (°C)
EPCOS (MKT-S, dielectric: polyester)	50/20	0.47–10 (0.47, 0.68, 1.0, 1.5, 2.2, 3.3, 4.7, 6.8, 10)	From 7.4 × 18.5 (0.47 μF) to 12.7 × 21.0 (10 μF)	−55–125
	100/35	0.10–100 (0.10, 0.15, 0.22, 0.33, 0.47, 0.68, 1.0, 1.5, 2.2, 3.3, 4.7, 6.8, 10, 22, 47, 100)	From 7.4 ×18.5 (0.1 μF) to 29.7 × 34.0 (100 μF)	−55–125
	160/60	0.10–10 (0.10, 0.15, 0.22, 0.33, 0.47, 0.68, 1.0, 1.5, 2.2, 3.3, 4.7, 6.8, 10)	From 7.4 ×18.5 (0.10 μF) to 15.7 × 34.0 (10 μF)	−55–125
	250/90	0.10–10 (0.10, 0.15, 0.22, 0.33, 0.47, 0.68, 1.0, 1.5, 2.2, 3.3, 4.7, 6.8, 10)	From 7.4 ×18.5 (0.10 μF) to 20.7 × 34.0 (10 μF)	−55–125

Series	Rated voltage (V)	Capacitance (μF)	Dimensions (H × L × W) (mm)	Temperature range (°C)
Nichicon (EC, dielectric: polypropylene)	200 V (AC)	2.0–50 (2.0, 2.5, 3.0, 3.5, 4.0, 4.5, 5.0, 6.0, 7.0, 8.0, 10.0, 12.0, 14.0, 15.0, 16.0, 18.0, 20.0, 22.0, 25.0, 30.0, 40.0, 50.0)	From 25.0 × 37.0 × 11.5 (2.0 μF) to 49.0 × 58.0 × 34.0 (50 μF)	−25–85
	250 V (AC)	2.0–50 (2.0, 2.5, 3.0, 3.5, 4.0, 4.5, 5.0, 6.0, 7.0, 8.0, 10.0, 12.0, 14.0, 15.0, 16.0, 18.0, 20.0, 22.0, 25.0, 30.0, 40.0, 50.0)	From 25.0 × 37.0 × 11.5 (2.0 μF) to 49.0 × 58.0 × 34.0 (50 μF)	−25–85
	400 V (AC)	1.0–20 (1.0, 1.5, 2.0, 2.5, 3.0, 3.5, 4.0, 4.5, 5.0, 6.0, 7.0, 8.0, 10.0, 12.0, 14.0, 15.0, 16.0, 18.0, 20.0)	From 25.0 × 37.0 × 11.5 (1.0 μF) to 49.0 × 58.0 × 34.0(20 μF)	−25–85

Series	Rated voltage (V)	Capacitance (nF)	Dimensions (H × L × W) (mm)	Temperature range (°C)
Kemet (PFR, dielectric: polypropylene)	63 V (DC)/ 40 V (AC)	0.1–22 (0.1, 0.15, 0.22, 0.33, 0.47, 0.68, 1.0, 1.5, 2.2, 3.3, 4.7, 6.8, 10, 15, 20, 22)	From 6.0 × 7.2 × 4.5 (0.1 nF) to 8.0 × 7.2 × 6.5 (22 nF)	−55–100
	100 V (DC)/ 63 V (AC)	0.1–10 (0.1, 0.15, 0.22, 0.33, 0.47, 0.68, 1.0, 1.5, 2.2, 3.3, 4.7, 6.8, 10)	From 6.0 × 7.2 × 4.5 (0.1 nF) to 8.0 × 7.2 × 6.5 (10 nF)	−55–100
	250 V (DC)/ 160 V (AC)	0.1–6.8 (0.1, 0.15, 0.22, 0.33, 0.47, 0.68, 1.0, 1.5, 2.2, 3.3, 4.7, 6.8)	From 6.0 × 7.2 × 4.5 (0.1 nF) to 8.0 × 7.2 × 6.5 (6.8 nF)	−55–100
	400 V (DC)/ 220 V (AC)	0.1–6.8 (0.1, 0.15, 0.22, 0.33, 0.47, 0.68, 1.0, 1.5, 2.2, 3.3, 4.7, 6.8)	From 6.0 × 7.2 × 4.5 (0.1 nF) to 8.0 × 7.2 × 6.5 (6.8 nF)	−55–100
	630 V (DC)/ 250 V (AC)	0.1–4.7 (0.1, 0.15, 0.22, 0.33, 0.47, 0.68, 1.0, 1.5, 2.2, 3.3, 4.7)	From 6.0 × 7.2 × 4.5 (0.1 nF) to 8.0 × 7.2 × 6.5 (4.7 nF)	−55–100
	1000 V (DC)/ 250 V (AC)	0.1–1.0 (0.1, 0.15, 0.22, 0.33, 0.47, 0.68, 1.0)	From 6.0 × 7.2 × 4.5 (0.1 nF) to 8.0 × 7.2 × 6.5 (1.0 nF)	−55–100

Series	Rated voltage (V)	Capacitance (μF)	Dimensions (H × L × W) (mm)	Temperature range (°C)
Panasonic (ECWF(L), dielectric: polypropylene)	400 V (DC)	0.022–2.4 (0.022, 0.024, 0.027, 0.030, 0.033, 0.036, 0.039, 0.043, 0.047, 0.051, 0.056, 0.062, 0.068, 0.075, 0.082, 0.091, 0.10, 0.11, 0.12, 0.13, 0.15, 0.16, 0.18, 0.20, 0.22, 0.24, 0.27, 0.30, 0.33, 0.36, 0.39, 0.43, 0.47, 0.51, 0.56, 0.62, 0.68, 0.75, 0.82, 0.91, 1.0, 1.1, 1.2, 1.3, 1.5, 1.6, 1.8, 2.0, 2.2, 2.4)	From 8.6 × 12.5 × 5.7 (0.022 μF) to 24.8 × 28.0 × 17.5 (2.4 μF)	−40–105
	450 V (DC)	0.022–2.4 (0.022, 0.024, 0.027, 0.030, 0.033, 0.036, 0.039, 0.043, 0.047, 0.051, 0.056, 0.062, 0.068, 0.075, 0.082, 0.091, 0.10, 0.11, 0.12, 0.13, 0.15, 0.16, 0.18, 0.20, 0.22, 0.24, 0.27, 0.30, 0.33, 0.36, 0.39, 0.43, 0.47, 0.51, 0.56, 0.62, 0.68, 0.75, 0.82, 0.91, 1.0, 1.1, 1.2, 1.3, 1.5, 1.6, 1.8, 2.0, 2.2, 2.4)	From 8.6 × 12.5 × 5.7 (0.022 μF) to 24.8 × 28.0 × 17.5 (2.4 μF)	−40–105

(*continued*)

Table 1.4 (*Continued*)

Series	Rated voltage (V)	Capacitance (μF)	Dimensions (H × L × W) (mm)	Temperature range (°C)
	630 V (DC)	0.010–1.3 (0.010, 0.011, 0.012, 0.013, 0.015, 0.016, 0.018, 0.020, 0.022, 0.024, 0.027, 0.030, 0.033, 0.036, 0.039, 0.043, 0.047, 0.051, 0.056, 0.062, 0.068, 0.075, 0.082, 0.091, 0.10, 0.11, 0.12, 0.13, 0.15, 0.16, 0.18, 0.20, 0.22, 0.24, 0.27, 0.30, 0.33, 0.36, 0.39, 0.43, 0.47,0.51, 0.56, 0.62, 0.68, 0.75, 0.82, 0.91, 1.0, 1.1, 1.2, 1.3)	From 8.0 × 12.5 × 5.2 (0.010 μF) to 24.4 × 28.0 × 17.6 (1.3 μF)	−40–105

*With thanks for the help and permission for compiling the data from their catalogue to the companies: Nichikon, Cornell Dubilier, TDK-EPC/EPCOS, AVX Corporation, Murata Manufacturing Co. Ltd. The table contains data available at the time of writing. These tables have an informative character. No accuracy is guaranteed. For use in practical applications, it is suggested that readers check for accurate, updated data in the companies' catalogues.
Reproduced from Panasonic, Kemet, Nippon Chemi-Con and Ashcroft Capacitor Ltd.

Figure 1.39a shows a comparison of the properties of three types of capacitor – electrolytic, polyester film, and ceramic – with regard to their lifetime versus the ambient temperature. Figure 1.39b gives a few examples of general use of different capacitors.

Among the three types of capacitors, the electrolytic capacitors provide the highest capacitance value available in a single package. Thus, they are widely used as energy reservoirs in power electronics systems. However, the advantage is offset by their short lifetime and fast lifetime decay against the operating temperature. The expected operating lifetime, L_{op}, of electrolytic capacitors is:

$$L_{op} = L_b \, M_v \, 2^{\frac{T_m - T_a}{10}}$$

where L_b is the expected operating life in hours at the rated voltage and temperature, M_v is the voltage multiplier for voltage de-rating (de-rating is the operation of the capacitor at less than its rated maximum voltage; usually, we choose M_v as 0.8 and, thus, we assure a safety margin), T_m is the maximum permitted internal operating temperature in °C given in the datasheet, and T_a is the actual capacitor internal operating temperature in °C. The value of L_b is provided by the manufacturer for the chosen capacitor.

The lifetime of electrolytic capacitors will be shortened by half if the operating temperature is increased by 10 °C. Thus, for applications operating at a high ambient temperature, such as LED drivers, the lifetime of the electrolytic capacitor becomes the critical factor that determines the lifetime of the entire application.

In terms of lifetime expectancy, a polyester film capacitor is the best choice, although its maximum available capacitance value is not as high as that of electrolytic capacitors. The popular polyester capacitors are metalized polyester film capacitors. They are particularly suited for AC applications, as they have a low dissipation factor, allow high AC currents and are available in a moderate range of values.

1.3.6.2 Inductors, Transformers, Coupled Inductors

An inductor is a passive electrical component that can store energy in a magnetic field created by the electric current passing through it. Typically an inductor is a conducting wire shaped as a coil around a core, the loops helping to create a strong magnetic field inside the coil. The core is either air or is made from ferromagnetic or ferrimagnetic materials. Different magnetic materials have different frequency responses. Knowing the switching frequency of the converter, we shall choose that material that has the best performance at the designed frequency. Best performance means the highest value of the product of the frequency and the maximum of the magnetic flux density, B_m. A magnetic core can generally increase the inductance due its high magnetic permeability but it will cause a nonlinear characteristic of the inductor (permeability

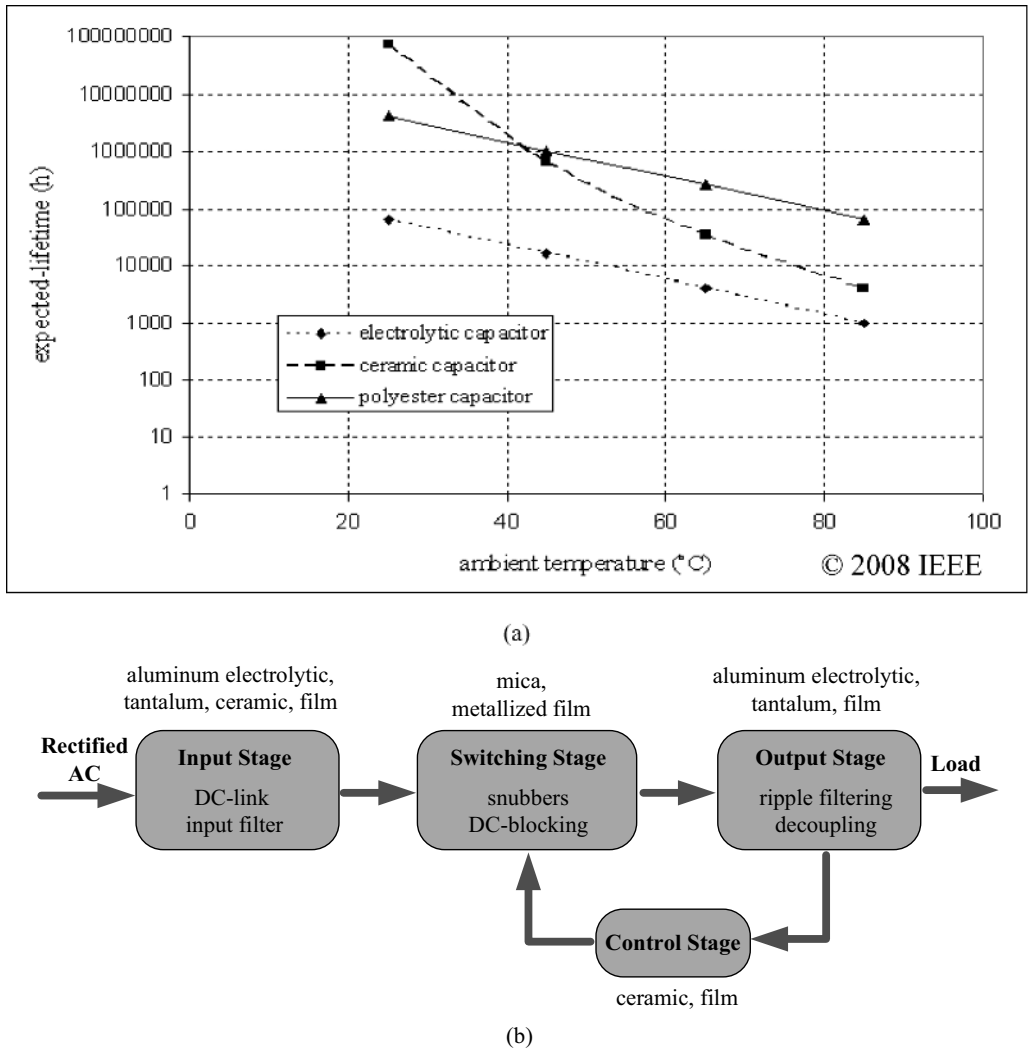

Figure 1.39 *(a) Comparison among several types of capacitors with regard to their expected lifetime versus ambient temperature (b) Examples of applications of different types of capacitors in different sections of a power electronics circuit. (Reproduced, with permission from Y.X. Qin, H. Chung, D.Y. Lin, and S.Y.R. Hui, "Current source ballast for high power lighting emitting diodes without electrolytic capacitor," in* Proc. 34th IEEE Annual Conf. Industrial Electronics, *November 2008, pp. 1968–1973.)*

is the degree of magnetization of a material in response to an applied magnetic field). Moreover, due to the hysteresis characteristic, a time-varying current passing through an inductor with magnetic core can cause energy loss in the core's material.

An ideal inductor has zero power loss. However, the presence of the winding resistance causes heat dissipation. The quality factor, Q, is used to measure the efficiency of the inductor. It is defined as:

$$Q = \frac{\omega L}{r_L}$$

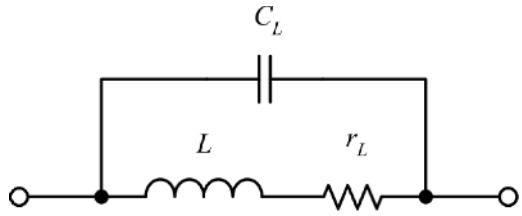

Figure 1.40 *High-frequency model of an inductor.*

where r_L is the winding resistance. The higher the value of Q, the better the quality of the inductor is. The model of a practical inductor is usually an ideal inductor in series with r_L. At very high frequencies, we have to take into account the inner winding capacitance (Figure 1.40). For example, the series resistance, r_L, of the inductor in EPCOS SMT-Power-Inductor Series 100 μH is 0.28 Ω measured at 20 °C.

A new solution today for building inductors is a three-dimensional design. Each inductor is built on a separate chip, which is bonded to the converter main chip. By using three-dimensional inductors on chip, the total size of a converter is reduced. The price we pay for this is the need to use this additional chip for implementing the inductor.

In the last few years, new monolithic (chip) inductors have been produced. They have a low DC resistance and a high Q-factor at high frequencies. For example, the power inductors produced by MURATA are of either the magnetically shielded multilayer type or the wire-wound type, their thickness being between 0.5 and 1.85 mm, with the tendency to decrease it to 0.4 mm. In the first group, there are elements with part numbers like LQM21P, with a value range of 0.47–2.2 μH, for a rated current of 600–1300 mA, dimensions 2 × 1.25 (or 1.5) mm, and DC resistance of 0.12–0.34 Ω; LQM2MP: with values in the range 0.47–4.7 μH, rated current 1100–1600 mA, dimensions 2 × 1.6 mm, and DC resistance of 0.06–0.14 Ω; LQM2HP_J0: 1–3.3 μH, 1100–1500 mA, 2.5 × 2 mm, 0.09–0.12 Ω; LQM2HP_G0: 0.47–4.7 μH, 1100–1800 mA, 2.5 × 2 mm, 0.04 −0.11 Ω; LQM2HP_E0: 0.56 μH, 1500 mA, 2.5 × 2 mm,0.06 Ω, LQM31P_00: 0.47–4.7 μH, 700–1400 mA, 3.2 × 1.6 mm, 0.07–0.3 Ω; and LQM31P_C0: 0.47–2.2 μH, 900–1300 mA, 3.2 × 1.6 mm, 0.085–0.25 Ω. All of these have a magnetic shield of ferrite. In the above given range of values, usual inductors are found for the values 0.47, 1, 1.5, 2.2, 3.3, 4.7 μH. They are used in DC-DC converters for mobile equipment. In the wire-wound group, without a magnetic shield, there are inductors with part numbers: LQH2MC-02, with a range of 1–82 μH, at a rated current of 90–485 mA, of dimensions 2 × 1.6 mm, and DC resistance in the range 0.3–7.5 Ω, their discrete values being 1, 1.5, 2.2, 3.3, 4.7, 5.6, 6.8, 8.2, 10, 12, 15, 18, 22, 27, 33, 39, 47, 56, 68, 82 μH, the DC resistance increasing, of course, with the inductance value, and the allowable DC current (rated current) decreasing with the inductance value; and LQH2MC_52, 1–22 μH, 130–595 A, 2 × 1.6 mm, 0.25–5.5 Ω. In the same group, but with a magnetic shield of magnetic powder of resin, are: LQH3NP_M0, 1–100 μH, 200–1400 mA, 3 × 3 mm, 0.044–3.5 Ω; LQH3NP_J0, 1–47 μH, 200–1620 mA, 3 × 3 mm, 0.04–1.3 Ω; LQH3NP_G0, 1–250 μH, 80–1525 mA rated current, 3 × 3 mm, 0.08–15 Ω, the largest inductances being 150, 200, and 250 μH; LQH32P, 0.47–22 μH, 450–2550 mA, 3.2 × 2.5 mm, 0.03–0.081 Ω; LQH44P_P0, 1–22 μH, 790–2450 mA, 4 × 4 mm, 0.03–0.37 Ω; LQH44P_J0, 1– 47 μH, 300–1530 mA, 4 × 4 mm, 0.048–1.014 Ω; LQH55P, 1.2–22 μH, 670–2600 mA, 5.8 × 5.2 mm, 0.021–0.26 Ω; LQH6PP, 1–100 μH, 800–4300 mA, 6 × 6 mm, 0.009–0.436 Ω; and LQH88P, 1–100 μH, 1000–8000 mA, 8 × 8 mm, 0006–0.265 Ω.

TDK's inductors for DC-DC converters come in two types: the multilayer and wire-wound types. Ferrite material technology and formulation including reduced grain size (smaller diameter raw ferrite powder provides a tighter ferrite structure after firing) combined with low loss conductor materials

Table 1.5 *Examples of smaller sized multilayer and wire-wound power inductor types (TDK-EPC)*

Construction type	Series	Inductance range (μH)	Rated current (mA)	Mechanical dimensions (L × W × T range) [T = thickness (height)] (mm)	Weight (mg)	DC resistance (Ω)
Multilayer	MLP2012	0.47–4.7	700–1200	2.0 × 1.25 × (0.5–0.85)	7–10	0.12–0.34
	MLP2520	1.0–4.7	700–1500	2.0 × 2.5 × (1.0–1.2)	15–25	0.085–0.18
Wire-wound	VLS2010E	0.56–22	330–2000	2.0 × 2.0 × 1.0	16 (typ.)	0.06–2.04
	VLS2012E	0.47–22	330–2050	2.0 × 20 × 1.2	17 (typ.)	0.059–1.764
	VLS201610E	0.47–10	400–1850	2.0 × 1.6 × 0.95	12 (typ.)	0.065–1.38
	VLS201612E	0.47–10	470–1900	2.0 × 1.6 × 1.2	14 (typ.)	0.063–1.026
	VLS252010E	0.47–10	560–2500	2.5 × 2.0 × 1.0	17 (typ.)	0.046–0.854
	VLS252012E	0.47–10	730–2750	2.5 × 2.0 × 1.2	24 (typ.)	0.056–0.756
	VLS252015E	1.0–10	720–1950	2.5 × 2.0 × 1.5	28 (typ.)	0.082–0.588
	VLS3010E	1.0–22	350–1600	3.0 × 30 × 1.0	36 (typ.)	0.072–0.9
	VLS3012E	1.0–47	310–1900	3.0 × 30 × 1.2	40(typ.)	0.068–1.5
	VLS3015E	1.0–47	320–2000	3.0 × 3.0 × 1.5	52 (typ.)	0.058–1.5
	VLS4012E	1.0–47	410–2500	4.0 × 4.0 × 1.2	67 (typ.)	0.06–1.02

facilitate favorable performance at MHz switching frequencies. A wire-wound type provides low DC resistance and a high-efficiency closed magnetic circuit design, using high μ ferrite particle resin material outside the winding wire, achieving low power consumption. (Magnetic shielding adhesive applied over the winding wire contains actual ferrite powder material. Since this mixture is applied directly to the winding wire, no gap is present between the shielding material and the core on which the wire is wound. The benefit is that the magnetic flux energy remains within the component.) Wire-wound types generally provide higher rated currents due to the increased core volume of ferrite material. This improved current performance characteristic, however, most often results in a larger overall physical package size of the inductor.

Examples of smaller sized multilayer and wire-wound power inductor types (TDK-EPC) are shown in Table 1.5.

An older series of surface-mounted device wire-wound power inductors from TDK is the VLF series, which includes larger inductance values, for example: VLF5014A comprised inductances from 1.5 to 100 μH, at a rated current of 260–1700 mA, and dimensions of 4.7 × 4.5 × 1.4 mm, with DC resistance of 0.059–2.7 Ω; or VLF12060, for inductors of 1.8–330 μH, with a rated current of 1000–12 000 mA, dimensions of 12 × 11.7 × 6 mm, and 4.4–464 mΩ DC resistance (the 464 mΩ is for the 330 μH inductance). The VLC series contains inductors in the range 0.47–150 μH; the series VLCF comprises the range 1.2–470 μH, for example VLCF5028-2 is for inductances in the range 1.3–470 μH, at a rated current 140–2560 mA, with dimensions of 5.0 × 5.3 × 2.8 mm, and 0.022–3.12 Ω being the respective DC resistances. The series SLF, CLF, VLP, RLF, SPM, VLM, and VLB are particularly suited for very high rated currents. For example, RLF12560 contains inductors in the range 1.0–10 μH, for a rated current of 7.5–14.4 A, their dimensions being 12.5 × 12.8 × 6.0 mm, and DC resistances being in the range 2.8–12.4 mΩ. The VLB series contains only low value inductances (up to a few hundred nH). Depending on the series, we can usually find inductors of the values 0.47, 1.0, 1.3, 1.5, 1.8, 2.2, 2.7, 3.3, 4.7, 6.8, 10, 15, 22, 33, 47, 56, 68, 100, 220, and 470nH. The DC resistance increases with the inductance, and the rated current decreases with the value of the inductance.

For power supply line applications, larger values of inductances can also be found in the radial lead through hole series SL or TSL. For example, SL1923 offers inductors in the range 470–15 000 μH, for a rated current in the range 260–1500 mA, or TSL 1112 offers a range of 1.0–15 000 μH, for a rated

current of 120–7700 mA. Of course, for such values, the inductors are physically very large, 11.2 mm diameter × 12.2 mm height, weight 3.3 g, and their DC resistance is considerable: the 15 mH inductor, suitable for a rated current of 0.13 A, has a maximum DC resistance of 24 Ω.[1]

In DC-DC converters, we can utilize TDK inductors, which are either magnetically-shielded or non-shielded, and within construction technology types including multilayer; wire-wound; smd; or through hole construction. The target switching frequencies for the lower inductance values and small case-sized power inductors are in the MHz range.

In power electronics, the inductors are used in input and output filters or as energy storage elements. Some small inductors, like the ferrite bead, are used to attenuate high-frequency currents, such as the reverse recovery current of diodes.

By winding two or more inductors on the same core, energy can be transferred from one inductor to the other(s) through the core, creating *a transformer* or *a coupled inductor*. There are some differences between a transformer and a coupled inductor. Firstly, the coupled inductor has an air gap in the core while the transformer does not. This causes differences in the flux levels in the two devices. Secondly, the primary function of a transformer is power transfer. An ideal transformer does not store energy. However, due to the presence of the leakage inductance of each winding of the transformer, this device stores energy. Ideally, at any point in time, the power entering the transformer is equal to the power exiting the transformer. The primary function of a coupled inductor is to store energy during some intervals and release it during other intervals. Thus, at a given time, the power entering the coupled inductor does not equal the power exiting it. Thirdly, transformers are used to obtain different input-to-output voltage and current ratios, for DC isolation, and to realize converters with multiple outputs. Coupled inductors are used in more complex DC-DC converters (Chapter 3).

For an ideal transformer, the core permeability is considered to be infinite. The equivalent circuit of an ideal transformer is given in Figure 1.41, where n is the turns ratio, implying that, for the voltage and current references as shown in the figure:

$$v_1 = n\, v_2$$

$$i_2 = n\, i_1$$

The dot notation shown in Figure 1.41 is used to show the polarity between the primary and secondary windings. In the figures, i_2 indicates the direction of the actual current in the secondary winding.

The equivalent circuit of a transformer with two windings consists of a mutual inductance, L_{12}, and two leakage inductances, L_{l1} and L_{l2} (Figure 1.42). The flux created by the current in each winding divides itself into two parts. One part goes into the core and cuts the other winding, giving the mutual inductance, L_{12}, of the two windings. The mutual inductance is

$$L_{12} = \frac{L_m}{n}.$$

The value of the magnetizing inductance, L_m, depends on the permeability and physical dimensions of the core. If the permeability of the core is infinite, L_m is infinite, meaning that there is no magnetizing current, i_m (ideal core). (An ideal core is different from an ideal transformer. An ideal core has zero reluctance but the transformer still has leakage inductance. An ideal transformer has, in addition, zero leakage inductance.) The other part of the flux goes into the air surrounding the winding, giving the leakage inductance of that winding. L_{l1} denotes the leakage inductance of the primary winding and L_{l2} denotes the leakage inductance

[1] With thanks for the help and permission for compiling the data from their catalogue to the companies: Murata Manufacturing Co Ltd. (not for military applications) and TDK Corporation of America. The above data (including Table 1.5) were available at the time of writing. They have an informative character. No accuracy is guaranteed. For use in practical applications, it is suggested that readers check for update, accurate data in the companies' catalogues.

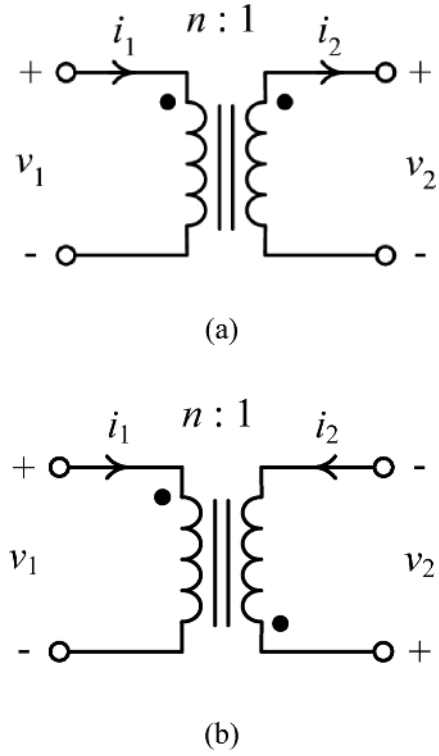

Figure 1.41 *Models of an ideal transformer.*

of the secondary winding. r_{L1} and r_{L2} represent the winding resistances of the primary and secondary windings, respectively. To show the proportion of the leakage flux with respect to the total flux, the *coupling coefficient*, k, can be defined in the form:

$$k = \frac{\frac{1}{n}L_m}{\sqrt{(L_m + L_{l1})\left(\frac{1}{n^2}L_m + L_{l2}\right)}}$$

If all the flux created in one winding cuts the other winding, that is, if the leakage inductance is zero, the coupling coefficient takes its maximum value, 1.

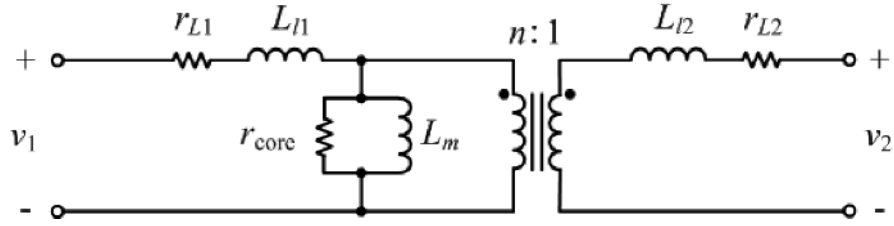

Figure 1.42 *Equivalent circuit of a transformer.*

If the reflected-to-primary secondary winding leakage inductance is equal to the primary winding leakage inductance, that is, $n^2 L_{l2} = L_{l1} = L_l$, k equals:

$$k = \frac{L_m}{L_m + L_l}$$

The model of a coupled inductor has some differences. Firstly, due to the presence of the air gap, which has finite permeability, the mutual inductance can never be neglected. Its value is primarily determined by the air permeability and the physical dimensions of the gap. The air gap increases the magnetic reluctance,[2] thus the coupled inductor can store more magnetic energy before the core reaches saturation. In some converters that are discussed in the next chapters (like the so-called flyback converter), we shall use this property. Secondly, in the case of a transformer, an input current, i_1, causes an output current, i_2, in the direction shown in Figure 1.41. However, in the case of a coupled inductor, when i_1 flows in the primary winding, there is no current in the secondary winding. And when there is no current flowing in the primary winding, i_2 flows in an opposite direction to that shown in Figure 1.41.

In practice, in order to reduce the voltage drop in a transformer, we prefer that the leakage inductance is small. Moreover, in a switching power converter, the transformer is sometimes connected to a semiconductor switch. If a current was flowing through the transformer before turning off the switch, at the instant the switch commutates a very high voltage spike will appear across the leakage inductance, $L_l \frac{di}{dt}$, resulting in a high voltage stress on the switch. Thus, a small leakage inductance is beneficial. One of the methods for reducing the leakage inductance is to use a bifilar winding (such a winding consists of two insulated wires, side by side, with currents flowing through them in opposite directions). However, if there is a large difference between the primary and secondary voltages, other methods are more effective, as we will see in Chapter 3 when speaking about converters with transformers or coupled inductors.

The power losses in transformers or coupled inductors are determined by the conduction losses in the winding resistances and the core loss. The core loss is due to the hysteresis characteristics of the core material. The hysteresis loss P_m is expressed as:

$$P_m = k f_s^a (B_m)^d$$

where k, a, and d are constants depending on the core material, f_s is the switching frequency, and B_m is the maximum flux density in the core. In usual calculations, B_m is given in kGauss, f_s in kHz, and the power loss, P_m, is obtained in mW. To model the hysteresis loss, a resistor, r_{core}, is included into the transformer equivalent circuit (Figure 1.42).

The hysteresis (core) loss can be calculated by using the datasheet of the manufacturer. In Table 1.6a, we can see a typical datasheet for a core of certain dimensions (a 34.3 mm outer diameter is taken here as an example). If we choose from this datasheet, for example, the MPP core with part number 55585, its permeability, μ, is 125. Say, again for exemplification, that the switching frequency is 100 kHz and the AC magnetic flux is 0.4 kGauss. The manufacturer gave the values of the constants for the considered example of core: $k = 1.199$, $a = 1.40$, $d = 2.31$ (Table 1.6b). With these values, the power loss per unit of volume (cm^3) can be calculated:

$$P_{core/vol}\left(\mathrm{mW/cm^3}\right) = 1.199 \times 0.4^{2.31} \times 100^{1.4} = 91.1\ \mathrm{mW/cm^3}$$

[2] Magnetic reluctance (or magnetic resistance) is a concept used in magnetic circuits. It is analogue to a resistance in the electrical field: an electrical field causes a current to follow the path of least resistance. A magnetic field causes magnetic flux to follow the path of least magnetic reluctance. The inverse of magnetic reluctance is called permeance. The reluctance is inversely proportional to permeability.

Table 1.6a *Core data of toroid with 34.3 mm outer diameter*

Core Data

34.3 mm O.D.

23.4 mm I.D. x 8.89 mm HT.

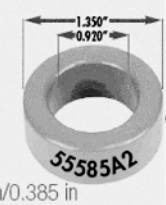

Core Dimensions (after finish)

O.D. (max.) 35.2 mm/1.385 in I.D. (min.) 22.6 mm/0.888 in HT. (max.) 9.78 mm/0.385 in

Permeability (μ)	$A_L \pm 8\%$	Part Number				Nominal DC Resistance Ohms/mH*	B/NI Gauss per Amp. Turn*
		MPP	High Flux	Kool Mμ	XFLUX		
14	9	55588	58588	-	-	0.366	1.96 (<1500 gauss)
26	16	55587	58587	77587	-	0.206	3.64 (<1500 gauss)
40	25	-	-	77591	-	-	-
60	38	55586	58586	77586	78586	0.0866	8.40 (<1500 gauss)
75	47	-	-	77590	-	-	-
90	57	-	-	77589	-	-	-
125	79	55585	58585	77585	-	0.0417	17.5 (<1500 gauss)
147	93	55584	58584	-	-	0.0354	20.6 (<1500 gauss)
160	101	55583	58583	-	-	0.0326	22.4 (<1500 gauss)
173	109	55579	-	-	-	0.0302	24.2 (<1500 gauss)
200	126	55582	-	-	-	0.0261	28 (<600 gauss)
300	190	55580	-	-	-	0.0173	42 (<300 gauss)
550	348	55581	-	-	-	0.0094	77 (<50 gauss)

* These values are only applicable for MPP Cores

Physical Characteristics

Window Area	401 mm²	788,500 c.mils
Cross Section	45.4 mm²	0.0704 in²
Path Length	89.5 mm	3.53 in
Volume	4,060 mm³	0.249 in³
Weight- MPP	34.9 gm	0.081 lb
Weight- High Flux	32.9 gm	0.076 lb
Weight- Kool Mμ	25.0 gm	0.055 lb
Weight - XFLUX	30.4 gm	0.067 lb
Area Product	1.821 cm⁴	0.0436 in⁴

Winding Turn Length

WINDING FACTOR	LENGTH/TURN	
100% (Unity)	5.87 cm	0.1923 ft
60%	4.84 cm	0.1586 ft
40%	3.84 cm	0.1258 ft
20%	3.39 cm	0.1113 ft
0%	3.23 cm	0.1059 ft

* Reference General Winding Data pages

Wound Coil Dimensions

Max. O.D. (u.w.f.)	50.1 mm	1.974 in
Max. HT. (u.w.f.)	29.0 mm	1.142 in

Surface Area

Unwound Core	29.3 cm²	4.537 in²
40% Winding Factor	51.3 cm²	7.95 in²

We could arrive at the same result by using the manufacturer graphics from Table 1.6b: we see that for a flux density of 0.4 kGauss and a frequency of 100 KHz, the core loss per unit of volume is, approximately, 90 mW/cm^3.

According to the physical characteristics given in Table 1.6a, the volume of this core is 4060 mm^3, so the total core loss will be:

$$P_{core} = 90 \times \frac{4060}{1000} = 365.4 \text{ mW}$$

(or 370 mW by following the exact calculation of the core loss: 91.1 mW/cm^3).

Recently, nanocrystalline magnetic materials such as FT-3M have been used for transformers in high-power applications, where large, bulky cores are commonly required, as well as in transformers to be imbedded in printed circuit boards. Thanks to the high saturation level, high operating temperature and

Table 1.6b *Graphic for calculating the power loss of the core (part number MPP55585)*

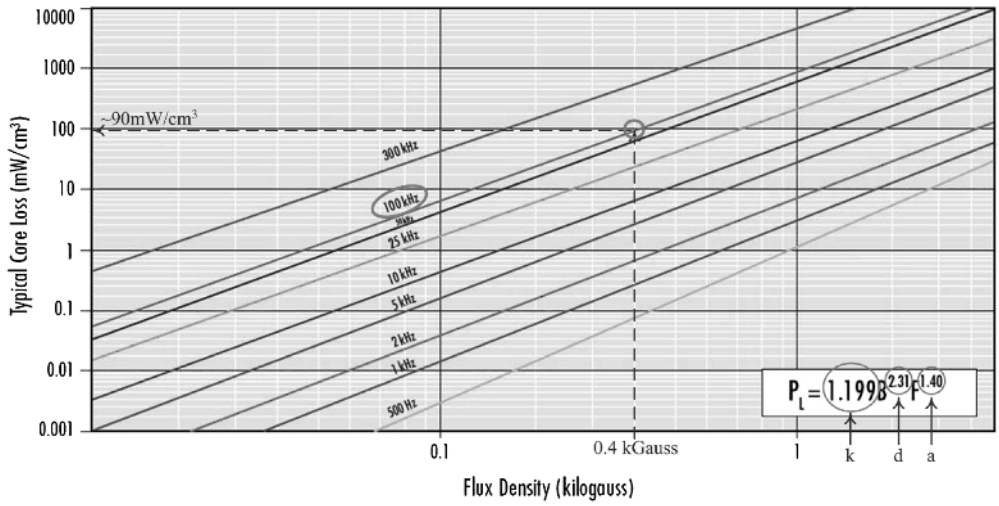

high thermal conductivity of these materials, the transformer power density and power processing capacity can be increased. In these transformers, if a large leakage inductance is required, in some applications, the leakage energy can be increased in an efficient way by shaping a large winding area out of the core.

1.3.7 Ultracapacitors

An ultracapacitor, also known as a double-layer capacitor, is an electrochemical device, which, like a battery, is capable of energy storage. The difference between the two devices is that batteries store charges chemically, whereas ultracapacitors store them electrostatically by polarizing an electrolytic solution. The charge separation takes place at the electrode–electrolyte interface. An ultracapacitor can be charged and discharged hundreds of thousands, or even millions, of times and can release energy much faster than a battery because no slow chemical reactions are involved. The amount of energy stored by an ultracapacitor is considerably much larger than that stored by a regular capacitor because its porous carbon electrodes have a very large surface area and the charge separation created by a thin dielectric separator is very small (currently, around 10 angstroms). An ultracapacitor can be seen as a high-energy version of a standard capacitor.

By 2010, ultracapacitors of 5000 Farads had already been manufactured. Energy densities of 30 Wh/Kg were reached in the same year. However, most of the ultracapacitors are available in the range 3–5 Wh/Kg, compared with a range of 30–40 Wh/Kg for a lead acid battery; per energy unit, ultracapacitors are still more expensive than batteries. For example, the Maxwell Technology MC ultracapacitors present a voltage of 2.7 V and one million cycles over 10-year lifetime. LS Ultracapacitors produces devices for 2.8 V (series LSUC 2.8 V) with capacitances in the range of 100 F (with an ESR of 11 mΩ) to 3000 F (with an ESR of 0.36 mΩ), or for 2.5 V (series LSHC 2.5 V) with a range of capacitances between 220 F (with an ESR of 18 mΩ) and 5400 F (with an ESR of 0.5 mΩ).

Ultracapacitors have many advantages compared to batteries. They have long life with little degradation over the time. They use no corrosive electrolytes or toxic materials, giving better safety. These

characteristics make them environmentally friendly. Ultracapacitors can be charged quickly, and present a very low ESR, thus diminishing charging and discharging energy loss, and they have a high specific power (power per weight unit). They work well at temperature extremes where the performance of batteries is hampered. However, being capacitor-type devices, the voltage of ultracapacitors varies with the energy stored, requiring electronic switching devices for charging and discharging. Their self-discharge rate is quite high. This is why the circuit model of an ultracapacitor includes, in addition to a capacitance, an inductance and a series resistance, as well as a parallel resistance for expressing the self-discharging energy loss. A single ultracapacitor cell has a low voltage, so, for practical applications, series of devices are necessary, which require voltage balancing mechanisms.

Due to their ecological advantages, ultracapacitors are today being used more and more. As they provide fast bursts of energy, ultracapacitors can be used in applications requiring short power pulses. They are much used in modern hybrid or fuel cell battery-based vehicles: they provide acceleration and energy in hill climbing, and serve as storage when recovering braking energy. When used in conjunction with a battery in a car, the ultracapacitor provides peak power, extends the life of the battery, allows for downsizing of the battery, diminishes the replacement and maintenance costs, and improves the fuel efficiency, particularly in urban driving conditions, by recuperating the breaking energy. Even if DC-DC converters are necessary in a system using both a battery and ultracapacitors, the increase in price is offset by these advantages in the modern world's quest for alternative sources of energy. Ultracapacitors are also used in home solar cell energy systems due to their fast charging capability. The use of ultracapacitors in power grids for providing energy during power outages is foreseen.

1.4 Basic Steady-State Analysis of Duty Cycle Controlled Converters with Constant Switching Frequency

1.4.1 Input-to-output voltage ratio for basic DC-DC converters

We saw in Section 1.2 that, to keep the output voltage of the converters constant despite variations in the input voltage and/or load, we had to adjust the relative ratio between the durations of the two switching stages: that in which the energy was transferred from the input to inductor, and that when the transfer was from the inductor to load. For the converters considered in Section 1.2, this was accomplished by changing the duty cycle value and operating with a constant switching frequency, as, let us remember, the durations of the two topologies are $T_{on} = DT_s$ and $T_{off} = (1 - D)T_s$.

Consider now that V_{in} and R are constant. Of course, in such a case, D is also kept constant, it is calculated to realize a certain required V_{out} for a given V_{in} (we remember that in the case of a buck converter, $V_{out} = DV_{in}$). Let us analyze the operation process of a converter in such a case when V_{in}, R, and, consequently, D meet their "nominal" values. The start-up process is assumed here to be finished, that is, the converter operates in a "regular" switching cycle. For convenience only, we denote the starting time of the considered cycle as zero.

For exemplification, we return to the buck-boost converter (Figure 1.43a) and, as we are still in the introductory chapter, we shall neglect the parasitic resistance of the elements. When the transistor is in the "on-state" (Figure 1.43b):

$$v_L = V_{in}$$

i.e.

$$L\frac{di_L}{dt} = V_{in},$$

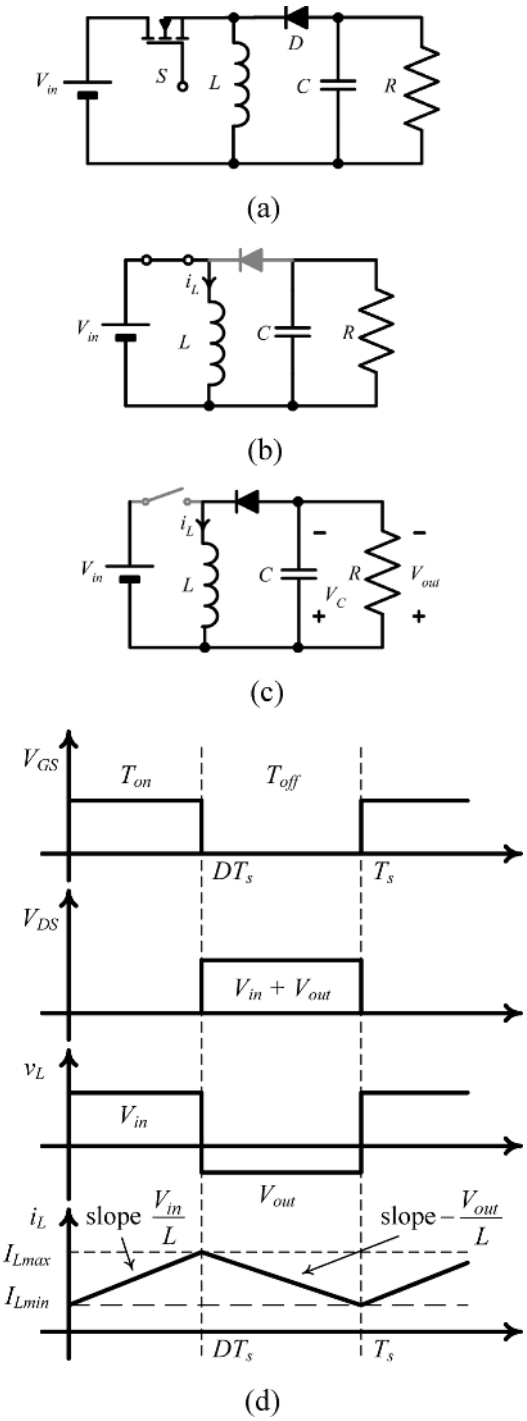

Figure 1.43 *Steady-state analysis of a buck-boost converter: (a) general structure; (b)* T_{on}*-stage; (c)* T_{off} *-stage; (d) switching diagram.*

giving:[3]

$$i_L(t) = I_{L\,min} + \frac{V_{in}}{L}t$$

where I_{Lmin} denotes the value of the inductor current at the beginning of this topological stage in the considered cycle.

The energy transfer to the inductor's magnetic field ends at $t = DT_s$, when the inductor is maximally charged, that is, the inductor current reaches its maximal value, I_{Lmax}.

Obviously, in this stage, v_{DS} of the transistor is ideally zero and the voltage across the diode, in absolute value, is $V_{in} + V_{out}$.

When the transistor is in the "off-state" (Figure 1.43c):

$$v_L + V_{out} = 0, \text{i.e. } v_L = L\frac{di_L}{dt} = -V_{out},$$

giving:

$$i_L(t) = I_{L\,\max} - \frac{V_{out}}{L}(t - DT_s)$$

that is, the inductor discharges, transferring its field energy to the load, and i_L decreases. As there is no change in the operating parameters (V_{in}, R, D), it is normal that the inductor current in the following cycle will start at the same value, I_{Lmin}, as in the present cycle, that is, i_L decreases until reaching I_{Lmin} at the end of the stage:

$$I_{L\,\min} = i_L(T_s) = I_{L\,\max} - \frac{V_{out}}{L}(T_s - DT_s) = I_{L\,\max} - \frac{V_{out}}{L}(1 - D)T_s$$

From Figure 1.43c, one can find that, in this topology, v_{DS} of the transistor is $v_{DS} = V_{in} + V_{out}$.

The main waveforms of the converter v_{GS}, v_{DS}, v_L, and i_L for the analyzed cycle are given in Figure 1.43d. This diagram is called a *switching diagram*.

When the converter parameters (V_{in}, R, D) are at their nominal values, the main waveforms repeat themselves identically in every switching cycle. We call such a cycle as "steady-state cycle." Such a

[3] The following references will be used throughout the book:

Once the orientation of a current through an inductor, i_L, has been chosen, we shall define the voltage across it, v_L, with the $+\ -$ polarity in the same direction with the arrow denoting the current's orientation. For this reference, $v_L = L\frac{di_L}{dt}$. If the inductor current is increasing, meaning that the inductor is in a charging process, $\frac{di_L}{dt} > 0$ and v_L will have a positive value. If the inductor current is decreasing, meaning that the inductor is discharging, $\frac{di_L}{dt} < 0$ and v_L will be negative (i.e., its actual polarity is opposed to that we considered). When writing KVL in a loop containing the inductor, we shall use the defined polarity of the inductor voltage, without asking the question if the inductor is in a charging or discharging phase.

Once the polarity of the voltage across a capacitor, v_C, has been chosen, we shall define the direction of the current, i_C, from the plus terminal to the minus terminal. For this reference, $i_C = C\frac{dv_C}{dt}$. If the capacitor is in a charging process, $\frac{dv_C}{dt} > 0$ and i_C will have a positive value. If the capacitor is in a discharging phase, $\frac{dv_C}{dt} < 0$ and i_C will have a negative value, i.e., it actually flows from the negative to positive terminal. When writing KCL in a node at which a capacitor is incident, we shall always use the defined orientation of the capacitor current, without minding if the capacitor is charging or discharging.

As known from circuit theory, the inductor current and capacitor voltage do not change orientation at a switching instant.

definition can be misleading, because we know from circuit theory that, for DC circuits in a steady state, an inductor is a short-circuit and a capacitor is an open-circuit. However, in power electronics, the definition has another meaning: it refers to the similarity of the converter waveforms in "steady-state" cycles, when no disturbances appear. Looking to the inductor current waveform, we see that in a steady-state cycle the inductor goes through a charging and discharging process, its current returning to the initial value at the end of the switching cycle. The steady-state inductor current has a periodicity of T_s. (We shall see in Chapter 4 an exception where the periodicity of the steady-state inductor current is larger than the switching period.) So, we see that within a so-called "steady-state cycle," we have "transient" phenomena. However, from now on in the book, *when speaking about transient cycles we shall refer to the operation of the converter when changes in input and/or load appear, leading to changes in the duty cycle, and making the switching diagrams for two transient cycles look different one from the other*. We shall use capital D when referring to a steady-state cycle and d for a transient cycle. However, as i_L, v_L, i_C, and v_C are variable, even in a steady-state cycle, we shall use lower case characters for them.

According to the above equations:

$$\int_0^{T_s} v_L(t)dt = \int_0^{T_s} L\frac{di_L}{dt}dt = \int_{i_L(0)}^{i_L(T_s)} Ldi_L = L[i_L(T_s) - i_L(0)] = 0$$

that is, *the integral of the inductor voltage over a steady-state cycle is zero*, showing that, by neglecting the losses on the parasitic resistances, all the energy accumulated in the magnetic field of the inductor was transferred to the load (a similar conclusion can be reached for the capacitor current).

This is a general result, applicable to any converter, as the energy transfer principle is the same. Based on it, if we develop the integral of v_L over each topological stage, we obtain:

$$\int_0^{T_s} v_L(t)dt = \int_0^{DT_s} v_L(t)dt + \int_{DT_s}^{T_s} v_L(t)dt = V_{in}DT_s + (-V_{out})(T_s - DT_s) = 0$$

The equation:

$$V_{in}DT_s + (-V_{out})(1 - D)T_s = 0$$

represents a volt-second balance for the inductor. It could be written directly according to the switching diagram of $v_L(t)$ based on the "area" interpretation of an integral (the two areas $V_{in}DT_s$ and $V_{out}(T_s - DT_s)$ have to be equal in order to have a zero value for the integral of v_L over this cycle).

From this equation, for the buck-boost converter:

$$V_{out} = \frac{D}{1 - D}V_{in}$$

By defining with $M = \dfrac{V_{out}}{V_{in}}$ the DC input-to-output voltage gain (also called the *DC voltage conversion ratio* or *DC voltage gain*), and writing for the buck and boost converters similar volt-second balances on their inductors (this is left as an exercise for the readers), Table 1.7 is obtained.

Note that the minus for the DC gain of the buck-boost converter in Table 1.7 is not a mistake compared with the previous result. We noted from the beginning that the output voltage had an opposite polarity to that of V_{in} (due to the fact that the inductor current could not change direction at the switching

Table 1.7 *DC conversion ratio of basic converters*

Converter	Buck	Boost	Buck-boost
M	D	$\frac{1}{1-D}$	$-\frac{D}{1-D}$

moment DT_s), and we wrote the equations accordingly. In Table 1.7 we considered that V_{in} and V_{out} had the same polarity for all the converters. The buck and boost converters do not change the polarity of the output voltage compared with the input voltage, but the buck-boost converter does. The minus in the formula of the DC gain for the buck-boost converter shows this change in the polarity of V_{out}.

From Table 1.7, as $0 < D < 1$, we see that, as expected, the buck converter can only step-down the input voltage, the boost converter can only step it up, and the buck-boost converter will step-down V_{in} if $D < 0.5$ and step-up V_{in} if $D > 0.5$.

Therefore, the DC conversion ratio of converters can be obtained by using the method called *volt-second balance on inductor(s)*. By duality, one can also use an equivalent method based on the property of the capacitor current to have a zero integral over a steady-state switching cycle.

1.4.2 Continuous and discontinuous conduction operation modes

In the previous switching diagram (Figure 1.43d) notice that $i_L(t)$ never falls to zero during a switching cycle. We call such an operation *continuous conduction mode* (CCM).

However, it is possible that the inductor releases all its energy to the load before the end of the T_{off} stage. This can happen if L has a small value, or if the stage is long (i.e., T_s is large, which means a small switching frequency, f_s), or if R is large (i.e., a low load current). In such a case, $i_L(t)$ drops to zero at some time during the second topological stage (Figure 1.44a). We can see this also graphically, if, for example, we decrease L in the diagram of $i_L(t)$ in Figure 1.43d, by increasing the slope of i_L. As, in a steady-state cycle, the initial and final values of the inductor current are the same, it implies that $i_L(t)$ starts from a zero value. From a topological point of view, it means that the converter goes cyclically through three switching stages in each cycle: in the first one, similar to a CCM operation, the transistor is on and diode off; in the second stage, the transistor is off and diode on; and, in the additional third stage, saying that $i_L = 0$ means that the diode is off (as well as the transistor) (Figure 1.44b–d). Of course, such an operation leads to a different DC voltage conversion ratio. We shall see in the next chapter that the dynamic behavior of a converter is also changed in this type of operation. The operation described in Figure 1.44 is called *discontinuous conduction mode* (DCM). As DCM can be reached by lowering the load current, it is also called "light operation mode;" the CCM is then called "heavy operation mode." It is clear that DCM can appear in a similar way in buck or boost converters. By designing a corresponding value for L, we can decide if the converter operates in either CCM or DCM. We shall see that each type of operation has its usefulness and, of course, also its own disadvantages.

1.4.3 Design of the elements of the basic converters

The design of the power stage of a basic converter is simple. The transistor and the diode are chosen according with their voltage and current ratings.

The capacitor is designed to limit the output voltage ripple. If we look, for example, to the first topological stage of a buck-boost converter (Figure 1.43b), in which the capacitor has to "keep a constant" output voltage, we can write:

$$v_C + RC\frac{dv_C}{dt} = 0$$

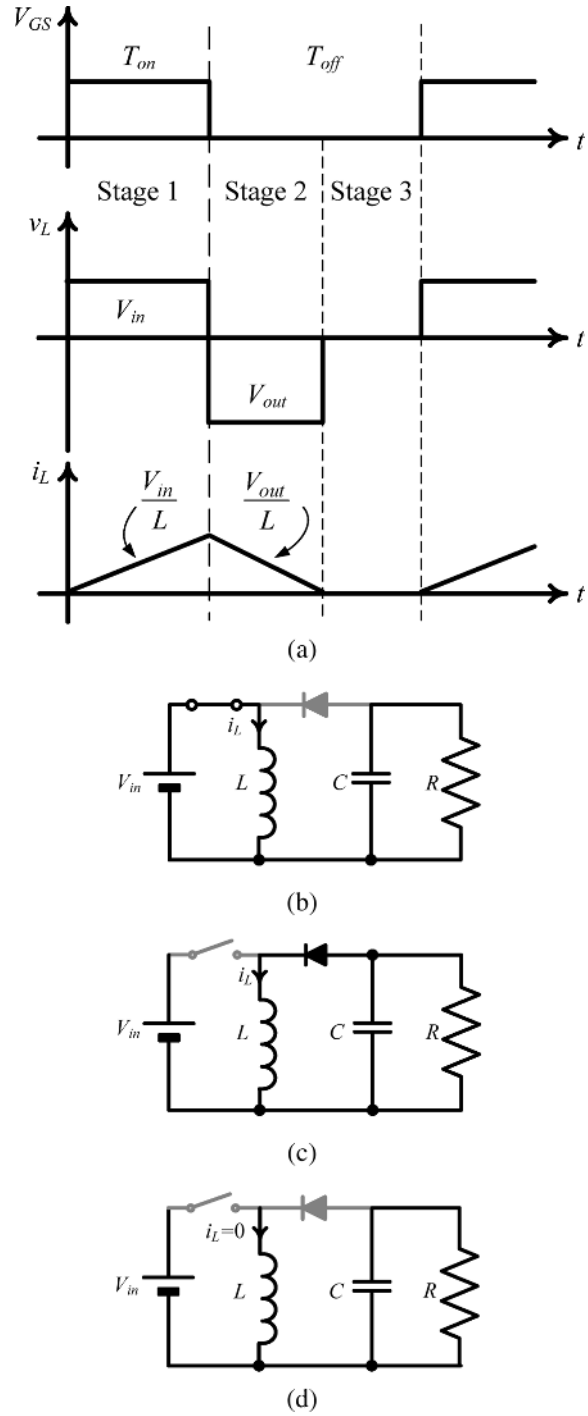

Figure 1.44 *(a) Inductor current waveform for a discontinuous conduction mode (DCM) operation; (b)–(d) equivalent switching stages of a buck-boost converter operating in DCM.*

implying:

$$v_C(t) = V_{C\max} e^{\frac{-t}{RC}}$$

V_{Cmax} is the value at the beginning of a new steady-state cycle, as C was charged by the inductor current during the off-stage and reached its maximum value V_{Cmax} at the end of the previous steady-state cycle. During the on-stage, C is discharged on the load (as C has not an infinite value, we can expect that the output voltage cannot be kept 100% constant, as ideally we would like, but that some changes, called *ripple*, will appear in it), reaching its minimum value, V_{Cmin}, at DT_s:

$$V_{C\min} = V_{C\max} e^{-\frac{DT_s}{RC}}$$

The change in v_C (and therefore in the load voltage) will be:

$$\Delta V_C = V_{C\max} - V_{C\min} = V_{C\max}\left(1 - e^{\frac{-DT_s}{RC}}\right)$$

Practically, as required by industry, this ripple has to be less than 1% of the load voltage to consider the output voltage as being "constant" over a cycle:

$$\frac{\Delta V_C}{V_{C\max}} = 1 - e^{\frac{-DT_s}{RC}} < 0.01$$

This inequality allows the value of C to be chosen for a certain nominal load R, and a converter designed to operate with a certain f_s at the required D (D was designed from the customer requirements of nominal V_{in} and desired V_{out}, according to Table 1.7).

Practically, an approximate but easier-to-use formula is preferred. From the same figure as above, $C\frac{dv_{out}}{dt} = -\frac{V_{out}}{R}$ (taking into account that $V_{out} = v_C$ if we neglect the series resistance of the capacitor) and introducing the first-order approximation $\frac{dv_{out}}{dt} = \frac{\Delta V_{out}}{\Delta t}$, with Δt being the duration of the interval in which the drop of the capacitor voltage took place, that is, the duration of the on-stage, $(0 - DT_s) = -DT_s$ (as the maximum value was reached at the instant 0, and the minimum value at the instant DT_s):

$$C\frac{\Delta V_{out}}{DT_S} = \frac{V_{out}}{R}$$

With the standard requirement that $\frac{\Delta V_{out}}{V_{out}} < 0.01$, we get:

$$C > \frac{100DT_s}{R}$$

which is equivalent to the exact design formula in which the exponential is replaced by the first two linear terms of its series expansion.

The constraints for designing the inductor value are less rigid. Generally, we used to design L such that the ripple in the inductor current is around 10–15% of the average value of this current. As such a requirement is more important for a boost converter, where the inductor current is identical to the input current

drawn by the converter from the supply, let us exemplify the design for this type of DC-DC converter; it will be left to readers to design L for buck and buck-boost converters.

According to Figure 1.7b, in the on-stage of the boost converter of duration DT_s, the inductor is charged, the current increasing from I_{Lmin} to I_{Lmax}:

$$\Delta I_L = I_{L\max} - I_{L\min} = \frac{V_{in} D T_s}{L}$$

Neglecting the losses, that is, assuming 100% efficiency, we can write:

$$V_{in} I_{in} = V_{out} I_{out}$$

where, for a boost converter, $V_{out} = \dfrac{V_{in}}{1-D}$, giving the average value of the input current as:

$$I_{L,av} = I_{in} = \frac{I_{out}}{1-D} = \frac{V_{out}}{R(1-D)} = \frac{V_{in}}{R(1-D)^2}$$

From the condition $\Delta I_L = (10-15)\% I_{L,av}$, we get that the value of L has to be:

$$L = \frac{V_{in} D T_s}{(10-15)\% I_{L,av}} = \frac{D[(1-D)^2] R T_s}{0.1 - 0.15}$$

1.4.4 Controller for duty cycle control (PWM)

Up to now, we have spoken only about the power stage of the converter, that is, the part through which the flux of energy is circulating from source to load. We said that by varying the duty cycle we can control the output voltage. Let us now focus attention on the control circuit.

Firstly, let us see how the nominal value of the duty cycle (D) is determined by the control circuit. Given in principle only in Figure 1.45 is the main block of the control circuit (later in the book we shall see its actual electronic implementation). This block is an electronic comparator. It has two inputs. At one of the inputs, a sawtooth signal of maximum value V_M and switching period T_s is applied. The operating switching frequency of the converter is dictated by an electronic clock (oscillator), which gives the frequency f_s of the sawtooth signal. Consider for a moment that, at the other input, a DC signal of value V_{ctr} is applied. The block operates as a comparator: when the sawtooth signal is lower than the DC signal, the output is a signal of high value. When the DC signal is lower than the sawtooth signal, the output is a signal of low value, say zero. Therefore, the output of this block, denoted as $d(t)$, is a pulse waveform of frequency f_s. But this is exactly the type of a signal to be applied to drive a transistor (i.e., v_{GS} for MOSFETs, or the signal to be applied to the gate of an IGBT). Therefore, the duration for which the signal $d(t)$ is high represents DT_s. From the similarity of triangles, we have:

$$\frac{DT_S}{T_S} = \frac{V_{ctr}}{V_M}$$

that is:

$$D = \frac{V_{ctr}}{V_M}$$

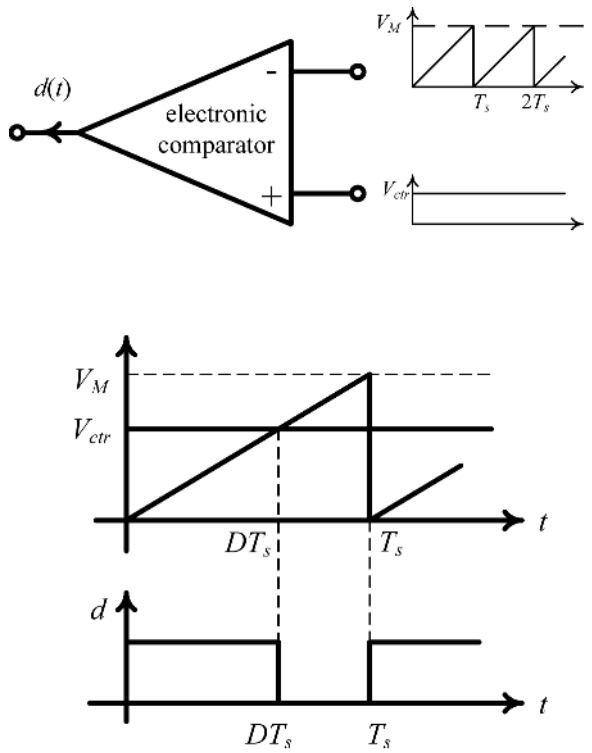

Figure 1.45 *The principle of operation of the main block of the control circuit.*

Thus, the circuit designer will choose his value for V_{ctr} and use V_M given by the manufacturer such that the nominal duty cycle calculated according to Table 1.7 is provided.

In reality, at the second input of the electronic comparator, there is applied a signal v_{ctr}, which is the output of a controller with the transfer function A(s). The closed-loop control is given in Figure 1.46a, still only in principle. It is the same for any basic converter, a buck converter was shown in the figure only for exemplification. The actual load voltage, V_{out}, is measured and compared with the reference voltage, E_{ref}. When a disturbance appears, an error $\varepsilon = E_{ref} - V_{out}$ is generated. This signal is passed through a controller with the transfer function $A(s)$. Usually, the controller is of either a PI (lead) or PID (lead-lag) type, as we shall see much later. In the case of a PI controller, the error, ε, is amplified and integrated (we know from control theory that a controller of the P type generates a steady-state error, this is why we always have to add an integration function. If we want to improve the dynamic response, that is, to have a shorter transient period, we add a derivative function. However, this one can create noise that has to be tackled by an appropriate design of the controller parameters. People in industry used to call the PI controller a "type II controller" and the PID controller a "type III controller").

In steady state, the output voltage has the required value, E_{ref}. Then, the error, ε, is zero and the value of v_{ctr} is a DC signal, V_{ctr}, as in the case discussed previously. If the error is negative, v_{ctr} is a DC value, V_{ctr_new}, lower than the previous value, V_{ctr} (Figure 1.46b). And if the error is positive, the new value, $V_{ctr\_new'}$, will be higher. For exemplification, consider that the disturbance is an increase in the input voltage, V_{in}. As a result, in the first moment, V_{out} has the tendency to increase. If, for nominal V_{in} and R (steady-state conditions), the error was zero and $v_{ctr} = V_{ctr}$, when the actual V_{out} increases over the required value, E_{ref}, the error becomes negative. The electronic comparator continues to work as always, giving a high output signal when the sawtooth waveform is lower than the new DC signal, V_{ctr_new}, and a low output signal (zero) when the new DC signal is under the sawtooth waveform. As a result, the width of the resulting pulse was changed from DT_s to dT_s. The new $d(t)$, with the same frequency, f_s, as previously but with the new width of the pulse, dT_s, is driving the transistor. As in our example $dT_s < DT_s$, the duration of the on-topological stage is shortened, the inductor, L, has less time to be charged, that is, less energy is transferred to it, and V_{out} starts decreasing. The process repeats itself for a few switching cycles until the actual value of V_{out} comes back to the required load voltage and v_{ctr} again becomes equal to the nominal value V_{ctr}, the converter returning to its steady-state operation. Obviously, if the disturbance was due to a decrease of the input voltage, the DC signal in the electronic comparator would have been raised, giving wider pulses, that is, increasing the duration of the on-switching stage. For changes in the load the result is similar (if the load current decreases, the control mechanism is similar to the case when the input voltage increases). The electronic comparator is called a PWM (*pulse-width modulator*) due to its role of adjusting the pulse width. It is implemented by a simple integrated circuit (IC) chip.

In many converters, to improve the transient response, an additional inner current feedback loop is added to the outer voltage feedback loop presented in Figure 1.46a. The inner loop is a fast one and the outer loop is a slow one. In Chapter 2, when modeling a DC-DC converter, we will have to find, in addition to the input-voltage-to-load-voltage and duty-cycle-to-load-voltage transfer functions, the input-voltage- and duty-cycle-to-inductor-current transfer functions to be able to design the controllers of the outer and inner feedback loops.

There are different ICs for implementing a PWM controller, each one serving a different purpose. For example, if we want only a voltage-mode control (based on a voltage feedback loop), we can choose the popular IC TL494, which also has overcurrent protection. If we want current-mode control (based on an inner current feedback loop in addition to the output voltage feedback loop), we can choose the chip UC3842.

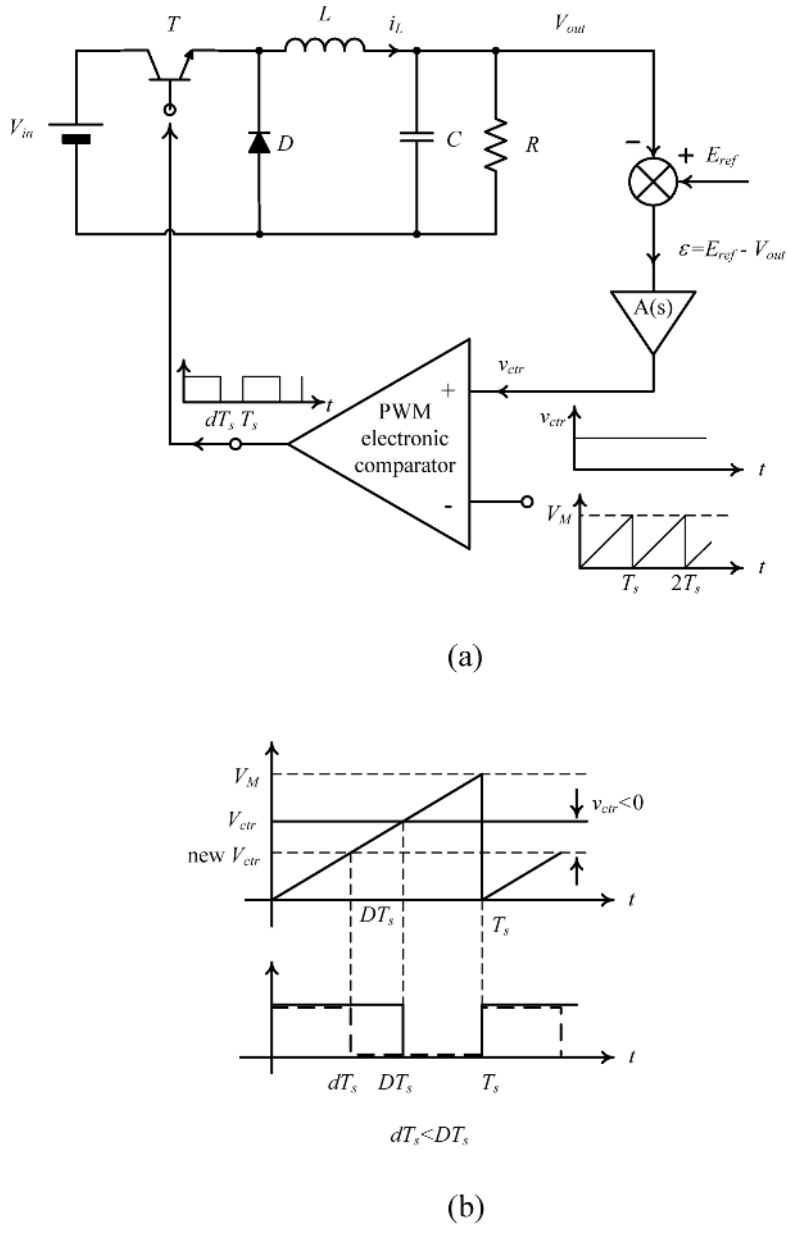

Figure 1.46 *(a) Closed-loop duty-cycle-controlled DC-DC basic converter; (b) principle of PWM.*

1.4.5 Conversion efficiency, hard-switching and soft-switching

In Section 1.3, the losses in switches, capacitors, inductors and transformers were discussed. We saw that the conduction losses are due to the energy loss in the on-state resistances of the switching devices of the MOSFET type, or in the parasitic resistances of the passive elements and wires. For switching devices like diodes and IGBT, the conduction losses are due to the forward voltage drop. To reduce these losses, the solid-state devices industry is permanently striving to produce better elements. A good converter layout would reduce the wire length and parasitic resistances of the connections. We saw in the preceding section that the nominal value of the parasitic resistance of a switch, r_{DSon}, is proportional to more than the square of the voltage rating of the switch. By using new techniques, such as a three-level topology, it is possible to halve the required voltage rating, implying a reduction in the on-state resistance by more than four times. However, this advantage is partially mitigated either by an increase in the complexity due to the need to use more devices or an increase in the current flowing through the switch. Three-level topology is discussed in Volume III.

The switching losses are due to the non-ideal characteristics of any switch. As we saw in the preceding section, the commutation from on-state to off-state, as well as from off-state to on-state, takes a finite, even very small time. During this commutation time, neither the voltage across the switch nor the current through it are zero. A switch, particularly of the MOSFET type, has a parallel output capacitance. If this is charged before the switch is turned on, at turn-on the energy accumulated in the capacitance is dissipated in the parasitic resistance, being an undesired loss. A minor carrier-based switch, like an IGBT, presents a tail current, which becomes upsetting when the switch is turned off.

In Figure 1.47a we consider a switch, S, in three consecutive states: on – off – on. Of course, when the switch is turned on, its voltage is ideally zero, and when the switch is off, is submitted to the voltage V_{off_state}. In a general way, let us denote the voltage across a switch by V_S and the current flowing through it by I_S. We saw (Figures 1.27 and 1.36) that when the switch commutes from the on-state to the off-state, the current does not drop instantaneously to zero and the voltage does not reach instantaneously its off-state value. In reality, this commutation process takes a finite time, t_f. Similarly, when the switch is turned on, during the commutation time, t_r, the current increases to the on-state value and the voltage decreases from the off-state to the on-state value. Therefore, for a very short period, either t_f or t_r, there is a loss of power as calculated in Section 1.3.5.1. It is obvious that if the converter operates at high switching frequencies, these repetitive small losses would bring down the efficiency. This process, accompanied by a switching loss, is called *hard-switching*. The current and voltage waveforms of the device, as can be seen in Figure 1.47a, are square waves: the commutation time, t_f or t_r, is hundreds or even thousands of time smaller than the durations T_{on}, T_{off}. This is why the duty cycle controlled hard-switching converters are also called *square-wave converters* (for simplicity, Figure 1.47a was drawn for the case of a MOSFET in a converter without inductor, but the concept remains the same for any other switch, see Figure 1.27 or Figure 1.33). The study of hard-switching converters will constitute the subject of Chapter 3. These converters, with duty cycle control, were largely used till the 1990s. They are still used in many applications, despite their lower efficiency due to the switching losses, which are however diminished in modern devices. We shall assign one chapter to their study for an additional reason: they constitute the theoretical basis for explaining and developing the modern converters.

What can we do in order to eliminate the switching losses? We saw that the switching losses were due to the fact that neither the current through nor the voltage across the switching device were zero during the commutation time. If we were able to make at least one of them zero during the commutation of the switch, obviously the energy loss would be zero. What if, for example, at some time before turning off the switch, we change the trajectory of I_S to a sinusoidal waveform? A sinusoid decays to zero naturally. How can we create such a sinusoid in our converter? Suppose that the switch is in the on-state and, at a very short time before the instant when we drive it off, we insert a resonant block,

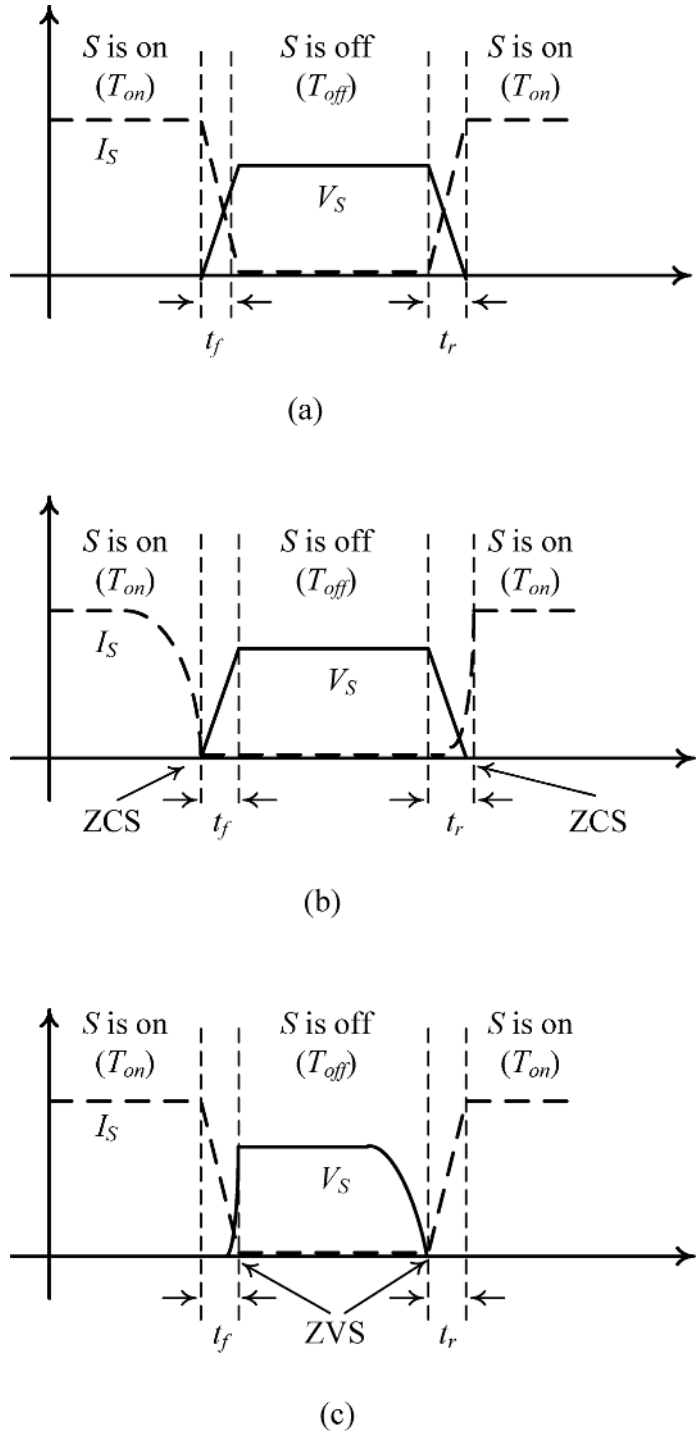

Figure 1.47 *(a) Hard-switching; (b) soft-switching: zero-current-switching (ZCS); (c) soft-switching: zero-voltage-switching (ZVS).*

L_r-C_r, in series with the switch. As we know, such a circuit would be described by a second-order differential equation, its solution being a sinusoidal current. Therefore, if the resonant period, T_r, of the resonant circuit is very small, i.e.,

$$f_r = \frac{1}{2\pi\sqrt{L_r\, C_r}} \gg f_s$$

the linear characteristic of I_S is transformed into a sinusoidal profile for the last moments of the on-topology (Figure 1.47b). Then, by driving the switching device off when this current reaches the value zero, the voltage on the switch will increase during the commutation process but, as the current was already brought to zero, the power loss will be zero. Similarly, when turning on the switch again, it is sufficient to have an inductor in series with it; as the inductor current cannot jump at the transition instant, it means that I_S, which is now equal with an inductor current, will remain zero during most of the commutation time, giving again an almost zero power loss. Such an operation, in which the current through the switch is zero during the commutation time, is called *zero-current-switching* (ZCS).

Similarly, if we place a capacitor in parallel with the switch, as the capacitor voltage cannot jump at a transient instant, when turning off the switch the voltage across it, equal now with a capacitor voltage, would remain zero during most of the commutation time (Figure 1.47c). Even if the current drops only gradually to zero, during the commutation time the power loss would be almost zero (towards the end of the commutation time, when the voltage rises, the current is already small). If we place the resonant block L_r-C_r with C_r in parallel with the switch at a certain time during the interval T_{off}, the linear DC voltage V_S would be transformed into a sinusoid. If we drive on the switch when the sinusoidal voltage across it drops naturally to zero, the power loss becomes zero. Such an operation, in which the voltage across the switch is zero during the commutation time, is called *zero-voltage-switching* (ZVS).

This technique of realizing ZCS and ZVS by inserting a resonant circuit was introduced in 1984 in quasi-resonant converters (QRCs). As the resonant elements L_r and C_r have very small values (to assure a small T_r, as seen previously), the additional conduction losses in their parasitic resistances were completely offset by the reduction in the switching losses. As the turn-off and turn-on processes had to be done at specific instants when either the current or the voltage across the switch was reaching zero, these converters could not be controlled by varying the duty cycle (in duty cycle controlled converters the switch is turned off at an instant dictated by the PWM, with no relation to the value of the current at that moment). We shall see in Volume III that the control of QRCs is based on varying the switching frequency.

However, ZCS and ZVS were already present in the natural operation of the so-called resonant converters, a class of converter available before 1984, which were used concomitantly with the hard-switching PWM converters. A later section of this chapter and a good part of Volume III is dedicated to the presentation of these switching frequency-controlled converters. Their use was largely spread in the decades before the end of 1980s, the interest in them is renewed nowadays due to their intrinsic operation with zero switching loss.

To realize ZCS and/or ZVS in duty cycle controlled converters, research in the 1990s came up with new solutions, creating the modern *soft-switching* converters. By using, in addition to the basic resonant block L_r-C_r, another switch (in a structure called an active snubber) or more passive elements and diodes (in a structure called a passive snubber), ZCS and/or ZVS can be created in PWM-controlled converters. It is important to note that, at turn-on, ZVS is preferable to ZCS, particularly for switches like MOSFETs, which present an output parallel capacitance. By bringing the voltage across the switch to zero before driving on the switch, the accumulated energy in the parasitic capacitance field would be ideally zero at the turn-on instant, such that no energy waste would appear. ZCS at turn-on is simpler to be realized: for example, a buck-boost converter operating in DCM would present a natural

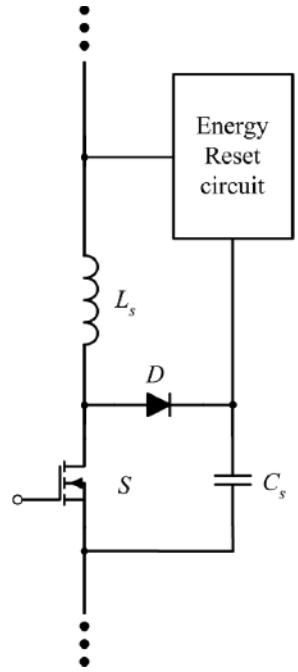

Figure 1.48 *Typical structure of a passive snubber.*

ZCS turn-on, due to the series connection of the inductor and transistor in the on-stage. As the current through the inductor was zero in the last switching stage of the previous cycle, it will increase slowly from zero at the beginning of a new cycle, with a slope limited by the inductor value. ZCS is preferable at turn-off, particularly for minority-carrier transistors like IGBTs, because ZCS would cancel their tail current, as the current was already brought to zero before the turn-off instant. The diode of a buck-boost converter operating in DCM would naturally turn off with ZCS, as it is connected in series with the inductor in the second switching stage. When the inductor current drops to zero, the diode will turn off naturally. ZVS is easier to be realized at turn-off; for example, as any MOSFET has a parallel capacitance, ZVS turn-off is produced naturally for them. Therefore, if we use MOSFETs, we prefer to have ZVS to eliminate capacitive turn-on losses, and if we use IGBTs we prefer to have ZCS to eliminate the effects of the turn-off tail current. Soft-switching converters feature a very high efficiency and a simple control. As the switching trajectories in soft-switching converters are modified into sinusoidal current or voltage waveforms, there are no large *di*/*dt* and *dv*/*dt*, implying a reduction of the electromagnetic interference (EMI), as compared with the EMI generated by hard-switching square-wave converters. The research on soft-switching converters has reached maturity in the first decade of the twenty-first century. We shall study them in detail in Volume III.

In terms of the component count, the passive snubber is the simplest one, as it does not necessitate an extra switch with its associated gate drive circuit. A typical structure of a passive snubber is shown in Figure 1.48. The role of the inductor L_s in series with the switch is to assure ZCS at turn-on. In the turn-on process, L_s absorbs energy and C_s is discharged by an *Energy reset circuit* (the purpose of a reset circuit is to bring the energy stored in a reactive element to zero.) The role of the capacitor C_s in parallel with the switch is to assure ZVS at turn-off. In the turn-off process, the energy stored in L_s is transferred to C_s. In the past, the energy reset circuit consisted of resistors only. Such a snubber was the simplest one but it

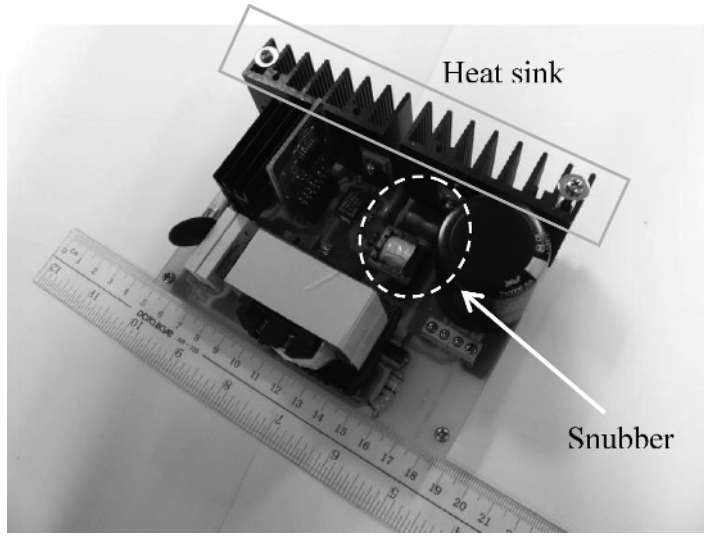

Figure 1.49 *A boost converter with snubber.*

introduces an energy loss. Today, dissipative snubbers are still used in low-cost applications, where the loss of efficiency is mitigated by the saving in the component count. Modern loss-less energy reset circuits are formed by reactive components that constitute an energy tank for re-circulating the energy in the resetting process to other parts of the converter. Figure 1.49 is the photo of a 1 kW boost converter which uses a passive loss-less snubber.

The study of the passive loss-less snubbers and more effective and efficient active snubbers will constitute the subject of a major part of Volume III.

1.5 Introduction to Switched-Capacitor (SC) Converters

Emphasized in Section 1.2 was the essential role that inductors play in power electronics circuits: transfer of energy from line to load in a controlled manner. However, the magnetic elements (inductors or transformers) have a large size. Even if operated at a high frequency, the inductor remains a bulky element. Those inductors amenable for an IC implementation have a value too small to be considered in power electronics. Even with the advent of newer, thin, monolithic (chip) inductors that are no longer bulky, in a more useful range of values, there are many applications where magnetic elements are undesirable; for example, the power supply of a pacemaker. And, as inductors in a practical range of values cannot be realized in integrated circuit technology, they prevent a converter from being realized in a single integrated chip. The quality factor, Q, of inductors decreases with the reduction in their size. Due to these features of inductors, we would prefer to have converters without magnetic devices. In applications where we need a DC-DC isolation between supply and load, we have to use transformers. But in many cases such isolation is not required, so it is possible to ask the question whether we can replace the inductors by capacitors for controllably transferring the energy. The first answer seems to be negative: the energy accumulated in the magnetic field of an inductor in a charging mode increases slowly, due to the slow, controllable increase in the current (di_L/dt); therefore, by changing the duty cycle, we can easily control this process. On the other hand, the capacitors charge quickly, reaching saturation, rendering it difficult to control their charging process.

The process is slower only if the capacitor is charged by a current source but other shortcomings limit the use of this method, as we will see in Volume II. And, it is known from circuit theory that 50% of the energy will be lost when the energy is transferred from a capacitor charged at voltage V to an uncharged capacitor;[4] therefore, such an energy transfer is highly ineffective.

Despite the above seemingly insurmountable difficulties, the idea of having a power supply with capacitors and switches only was too appealing to researchers not to strive for it. A switched-capacitor (SC) power supply would have a small size, low weight, high power density, as the printed circuit board (PCB), component height and cost of capacitors are much smaller than those of inductors and transformers. A switched-capacitor circuit would be the ideal power supply for portable electronic equipment where no DC-DC isolation is required. Without magnetic elements, the electromagnetic interference due to the magnetic field can be avoided. A SC power supply operating at such a high switching frequency that the capacitors could be built in IC technology, allowing for a chip realization of the entire electronic regulator, can even be imagined.

Let us try to imagine a step-down DC-DC converter formed by only switches and capacitors.

Consider (Figure 1.50a) that we connect n capacitors of equal value, $C_1 = C_2 = \ldots = C_n = C$, in series and that we charge them from a source of value V. After a very short time, depending on the value of the parasitic resistances in the charging circuit, each capacitor will be charged at almost the voltage V/n. Now move the capacitors to a parallel connection with a resistor, R (Figure 1.50b): if the discharging time is very small, by assuming zero losses it results that the voltage on the load is almost the same as that of the capacitors, that is, approximately we can say that the load voltage is V/n. Of course, such an electronic circuit is still far away from a power converter, first of all for the simple reason that, when charging the capacitors, the load remains at zero voltage (we remember that we must keep a constant output voltage).

To remedy this inconvenient, we can use two groups of capacitors, of equal value C: C_1, C_2, $\ldots$, C_n, and C'_1, C'_2, $\ldots$, C'_n (Figure 1.51). For half of a cycle, $T_s/2$, the first group of capacitors, C_1, C_2, $\ldots$, C_n, is in the charging process from the source V, while the second group of capacitors, C'_1, C'_2, $\ldots$, C'_n (charged in the previous half cycle), is in the discharging phase on the load R (Figure 1.51a and b). Their role is exchanged in the second half of the cycle (Figure 1.51c and d). In such a way, the load is all the time supplied at a voltage a little lower than V/n. However, we do not yet have a power supply: if V increases or decreases, the load voltage, V/n, will follow it.

How can we assure that the load voltage remains constant, even if V or R change? In other words, how can we introduce an element of control in this charging–discharging process? Up to now, we charged the capacitors for a "sufficient" time for them to reach V/n, that is, we charged them at saturation (theoretically, this value is reached only after an infinite time but, practically, the almost saturation voltage value is obtained in a short time, as the equivalent resistance in the charging circuit is formed by small value parasitic resistances in series). But what if we decide to control this process, such as to charge the capacitors only up to a fraction of V/n, say to a value V_x decided by us (Figure 1.52), that is, we charge them for the time t_{ch}, obviously less than $T_s/2$. The capacitor voltage charging characteristic in a typical resistor–capacitor circuit is given in the figure by the solid line. Now consider that a change, for example a drop, in the supply voltage occurs: V dropped to V_{new}. The charging characteristic will move to the dotted line. If we want to keep V_x constant, we can simply do it by increasing the charging time to t_{ch_new}. Obviously, if V increases we have to decrease the charging time. If we want to have enough

[4] Consider a capacitor C_1 charged at the voltage V, and another capacitor C_2, which is uncharged ($C_1 = C_2 = C$). Their total energy will be $C_1V^2/2 + 0 = C\,V^2/2$ and their total charge, q, will be $C_1V + 0 = CV$. After connecting them in parallel through a switch, as the total charge has to remain constant (according to the law of conservation of charge), it means that each capacitor will have the charge $q_1 = q_2 = CV/2$, implying that each capacitor will be charged at $V/2$. Therefore, the total energy accumulated in the electric field of the two capacitors will be: $C_1\,(V/2)^2/2 + C_2\,(V/2)^2/2 = CV^2/4$, meaning that half of the energy was dissipated in the switching process.

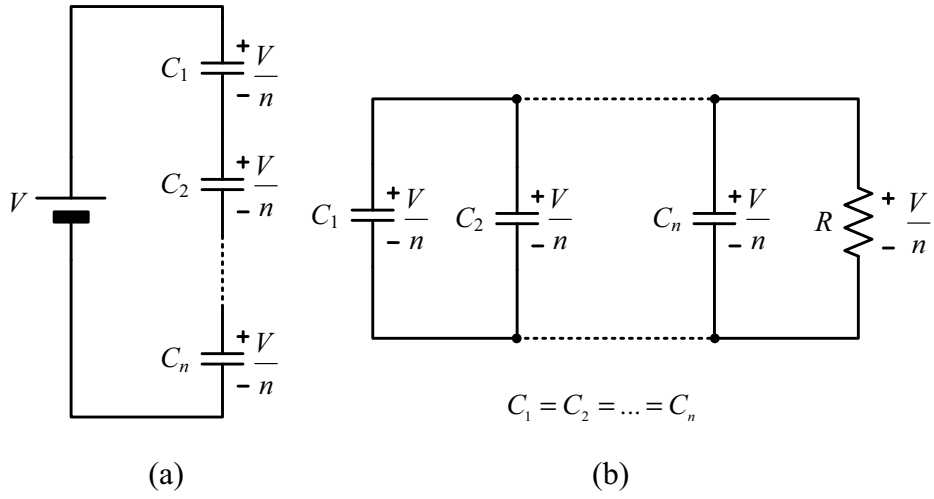

Figure 1.50 *(a) Series charging and (b) parallel discharging of* n *equal capacitors.*

regulation of the output voltage for large changes in the supply voltage, it is better to choose the designed point (t_{ch}, V_x) as much as possible in the middle of the linear part of the capacitor charging characteristic: for changes of V, we will have thus enough room for moving t_{ch} to the right or left, without entering the saturation region and without reaching $T_s/2$. Similarly, t_{ch} is controlled to obtain a constant load voltage if the load current increases or decreases (in such a case, V_x is increased or decreased for facing the changing load). In other words, we created a duty cycle given by the ratio t_{ch}/T_s. For nominal (steady-state) values of V and R, this will be the nominal duty ratio D. The operation of the circuit is shown in Figure 1.53. In the first half-cycle, capacitors C_1, C_2, . . . , C_n are charged for the time t_{ch} up to V_x, and then disconnected from the supply until the end of the half-cycle. During this time, C'_1, C'_2, . . . , C'_n, charged in the previous cycle to V_x, are discharged to the load, giving the output voltage V'_x ($V'_x < V_x$). In the second half-cycle, the role of the two groups of capacitors is interchanged. The charging time is controlled for getting a constant V'_x despite variations in V or R.

To exemplify the operation of the proposed step-down converter, consider the circuit in Figure 1.54a that is designed for stepping down a supply voltage of 12 V to a load voltage of 5 V. The circuit goes through four topological stages within a switching cycle (Figure 1.54b–e). The switching diagram of the switching waveforms of the converter in a steady-state cycle (driving signals d_{S1}-d_{S4} of the four transistors S_1–S_4, voltages V_{C1}–V_{C4} across the four capacitors, and the load voltage V_R) is shown in Figure 1.54f. The power stage is formed by two groups of capacitors C_1, C_2, and C_3, C_4 of equal value C, $r_{C1} \sim r_{C4}$ being their DC resistances, four transistors, S_1–S_4, $r_{S1} \sim r_{S4}$ being their on-resistances, and six diodes D_1–D_6. In the first topological stage, of duration t_{ch}, S_1 and S_4 are turned on, S_2 and S_3 are turned off (Figure 1.54b, in which the on-resistances of the switches in conduction and the DC resistances of the capacitors are specified; in SC converters, these resistances cannot be neglected, otherwise the charging process of the capacitors would seem instantaneous, representing an inadmissible approximation). Consequently, C_1 and C_2 are charged in series from the line voltage, with a very small time constant, as $r_{ch} = r_{S1} + r_{C1} + r_{C2}$, D_2 is turned on by the charging current, D_3 and D_1 are reverse-biased by V_{C1} and V_{C2}, respectively. The voltages on C_1 and C_2 increase from a minimal value, V_{Cmin} (which is different from zero as we are in a steady-state cycle and not in the first transient cycle of the start-up process), reaching the maximum value, V_{Cmax}, at the end of this topological stage. During this time, D_5 is reverse-biased by V_{C3}, V_{C4}, and C_3 and C_4 (charged at V_{Cmax},

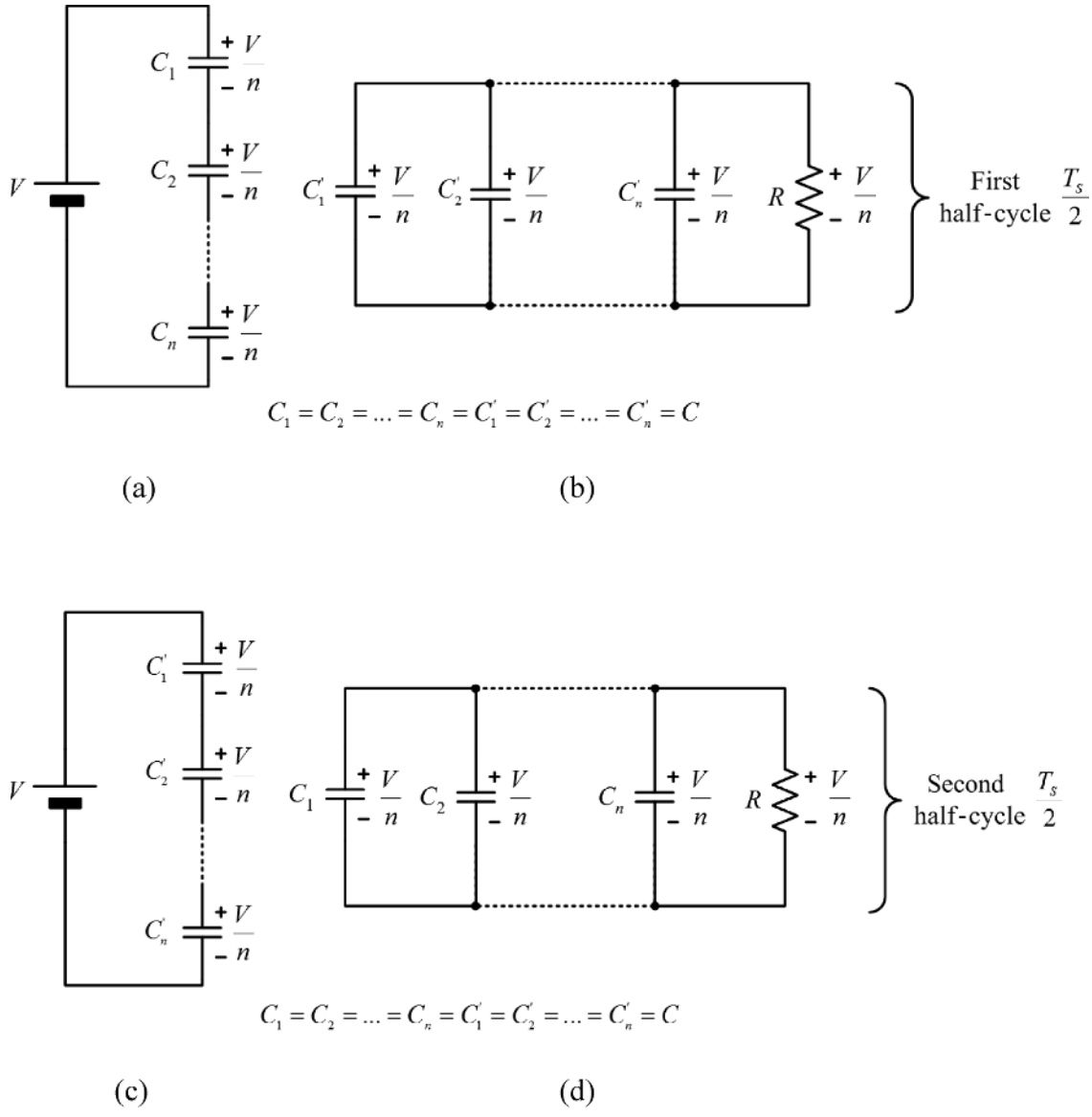

Figure 1.51 *(a) Series charging of the first group of capacitors in the first half-cycle; (b) parallel discharging on the load of the second group of capacitors in the first half-cycle; (c) series charging of the second group of capacitors in the second half-cycle; (d) parallel discharging of the first group of capacitors on the load in the second half-cycle.*

which was their voltage at the end of the previous cycle) discharge in parallel to the load, with a relatively large time constant, as the load R is present in the discharging circuit (normally $R \gg r_C, r_S$).

The operation in the first stage is interrupted by the control circuit (of PWM type): according to the value of the duty cycle, S_1 is turned off (Figure 1.54c). In the second topological stage, the charging of C_1 and C_2 is interrupted. They remain charged at the maximum voltage, V_{Cmax}. C_3 and C_4 continue their discharging

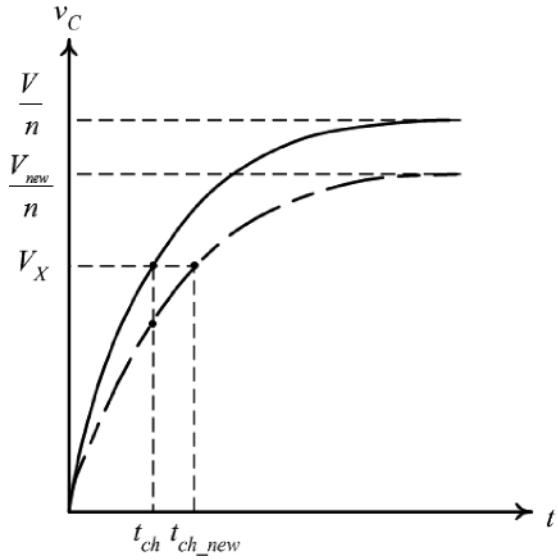

Figure 1.52 *Charging capacitor voltage characteristic in a typical capacitor–resistor circuit.*

on the load, their voltage reaching the minimum value, V_{Cmin}, at the end of this stage ($T_s/2$). During the first half-cycle, the load voltage, V_R, is dictated by that of the discharging capacitors in parallel, C_3 and C_4, being a little lower than V_{C3} (V_{C4}) due to the conduction losses in the discharging circuit. In the third switching topology, S_3 and S_2 are turned on, S_1 and S_4 are turned off (Figure 1.54d). Consequently, C_3 and C_4 are charged in series from the supply up to V_{Cmax}, and C_1 and C_2, which were charged at their maximum voltage in the previous half-cycle, are now discharged in parallel to the load. According to the PWM, S_3 is turned off after time t_{ch} (Figure 1.54e), C_3 and C_4 remain charged at their maximum voltage, ready to supply the load in the next cycle, and C_1, C_2 continue their discharging in parallel to the load. They will reach the minimum voltage, V_{Cmin}, at the end of the cycle, T_s. During the second half-cycle, the load voltage is determined by the voltages V_{C1}, V_{C2}, being a little lower than them due to the conduction losses in the discharging circuit. From Figure 1.54f, we can notice that the load voltage suffers from jumps at each half-cycle, as the supply of the load is changed from capacitors that finished their discharging stage to capacitors that just start their discharging phase. Such ripples in the output voltage can be kept under the desired limit by a corresponding design of C and T_s, and can be further reduced by adding a parallel capacitor to the load. However, some ripple in the load voltage is needed, as, without it, the capacitors will no longer be cyclically charged and discharged, that is, no energy will be transferred, which is equivalent to an infinite load value.

It is left to the reader to conceive a similar step-up DC-DC converter.

The study of SC power electronics raises many questions about the DC voltage gain, efficiency, voltage ripple, regulation, and an optimal design. As the capacitor charging current has a large di/dt that can create EMI, means for diminishing EMI have to be found. A question like what would be the best structure for the SC circuit, which can use the minimum number of switches and capacitors to realize a certain DC gain, results in many possible circuits. What will be the best method of control of these circuits? How can the line and load regulation range be enlarged? Is it possible to have soft-switching (or something similar) in these circuits? And, can soft-switching help the efficiency of the SC converters? Which factors affect the efficiency of charging and discharging of the capacitors in SC converters? How can the efficiency of the energy conversion through a switched-capacitor converter be improved? Is it possible to realize DC-AC or

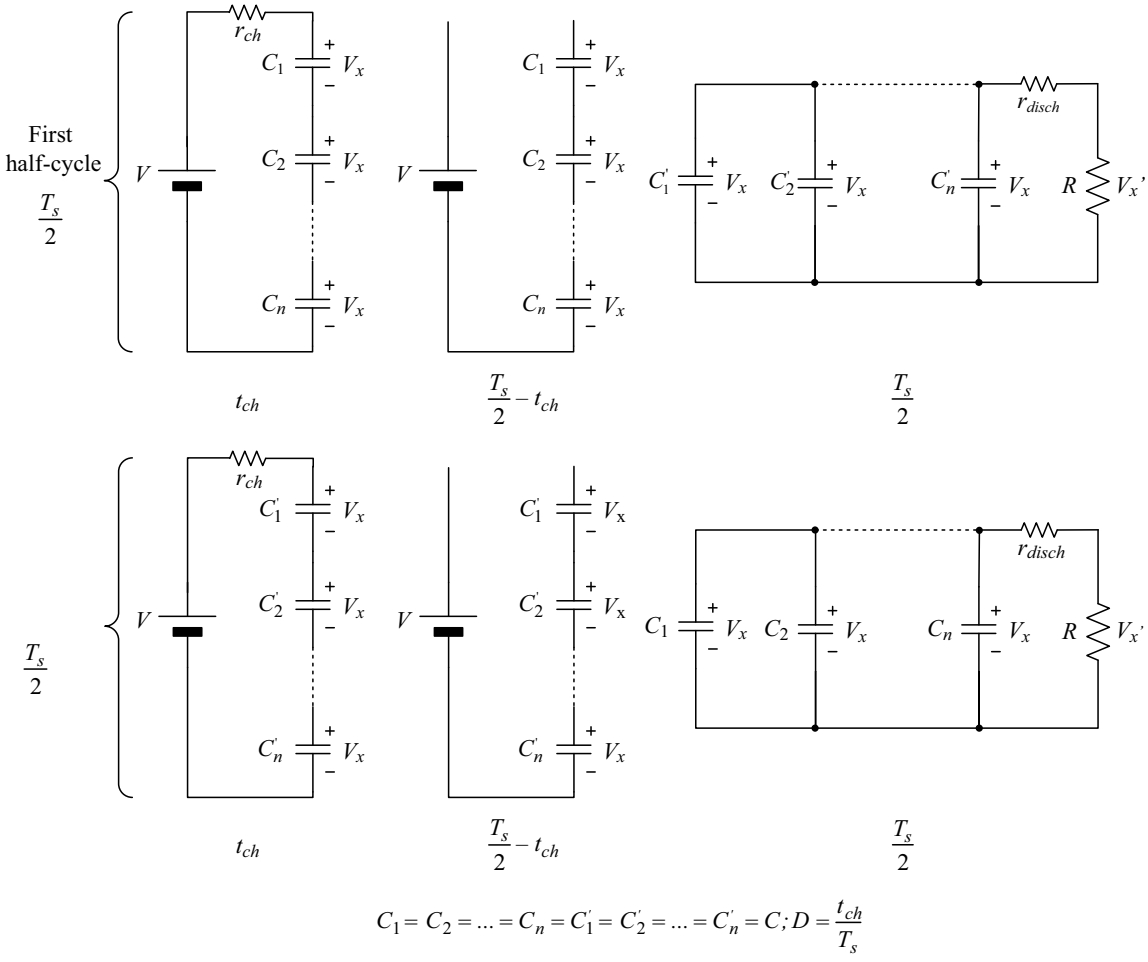

Figure 1.53 *Principle of a controlled cyclical operation of a SC converter (r_{ch} = equivalent DC resistance in the charging circuit of the capacitors; r_{disch} = equivalent DC parasitic resistance in the discharging circuit of the capacitors to the load).*

AC-DC switched-capacitor converters? For which power level are the SC converters suitable? To all this long series of questions, we shall look for answers in Volume II.

1.6 Frequency-Controlled Converters

1.6.1 Resonant converters

We saw that in duty cycle controlled hard-switching converters, the DC supply voltage was transformed into a square waveform during the switching operation and then rectified back to a DC voltage. In resonant converters, the DC supply voltage is firstly converted into a square waveform. Then, the square waveform is converted into a near sinusoidal waveform by a resonant tank circuit. Finally, the sinusoidal waveform is

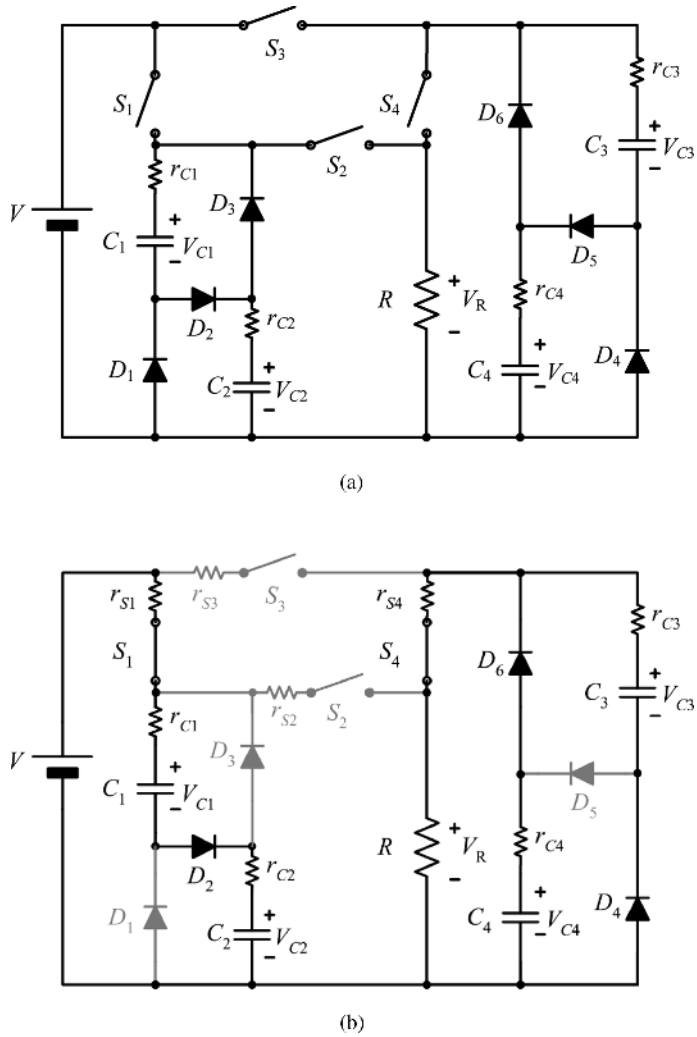

Figure 1.54 *(a) SC step-down 12 to 5 V DC-DC converter; (b)–(e) topological stages; (f) switching diagram.*

rectified to a DC voltage. The principal advantage is the property of a sinusoid of going naturally through the zero value, thus creating the possibility of realizing the switching action under a zero current or a zero voltage condition. Therefore, in resonant converters, soft-switching can be obtained naturally, without the need for additional snubbers. This allows a high-frequency operation without the concern of switching losses and electromagnetic radiation. And since the parasitic inductances and capacitances (like the leakage inductance of a transformer or the output parallel capacitance of a switch) can be included in the resonant process, they are no longer a burden that requires special care but become useful. However, as we shall see immediately, resonant converters have their drawbacks. Due to the character of their voltage and current waveforms, the resonant converters are also called *sinusoidal-wave converters*. Different resonant tank circuits give different types of resonant converters.

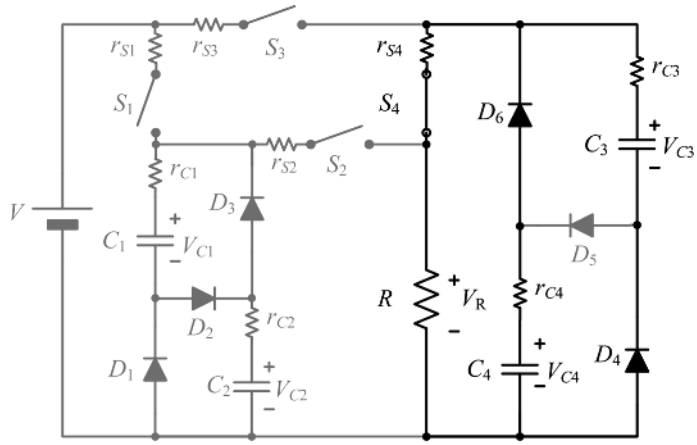

(c)

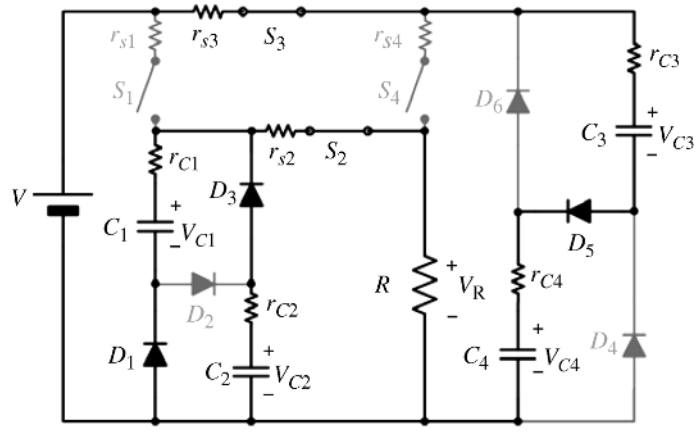

(d)

Figure 1.54 (*Continued*)

To exemplify the switching operation of a resonant power supply, consider the series-loaded resonant converter shown in Figure 1.55a. The capacitors C_1 and C_2, of a large, equal value, are used to provide a stable DC voltage, $V_{in}/2$, as the input to the resonant tank circuit when either one of the switches, S_1 or S_2, is in the on-state. S_1 and S_2 are used to convert the DC input voltage into an AC square waveform, v_{AB}. The parallel capacitors C_{S1} and C_{S2} include the drain-source capacitances of the switches S_1 and S_2, respectively. Diodes D_{S1} and D_{S2} are the anti-parallel diodes of S_1 and S_2, respectively. The resonant tank is formed by an L_r-C_r circuit in series with the reflected load. A high-frequency transformer is used to get the desired DC input-to-output voltage ratio. A rectifier formed by a bridge of four diodes, D_1–D_4, and an output capacitor, C, realizes the conversion of the sinusoidal waveform on the secondary side of the transformer into a DC load voltage. In practical converters, an inductor L is inserted at the input for smoothing the input current. In the following analysis, we will not take L into account because it does not affect the explanation of the operation of the converter.

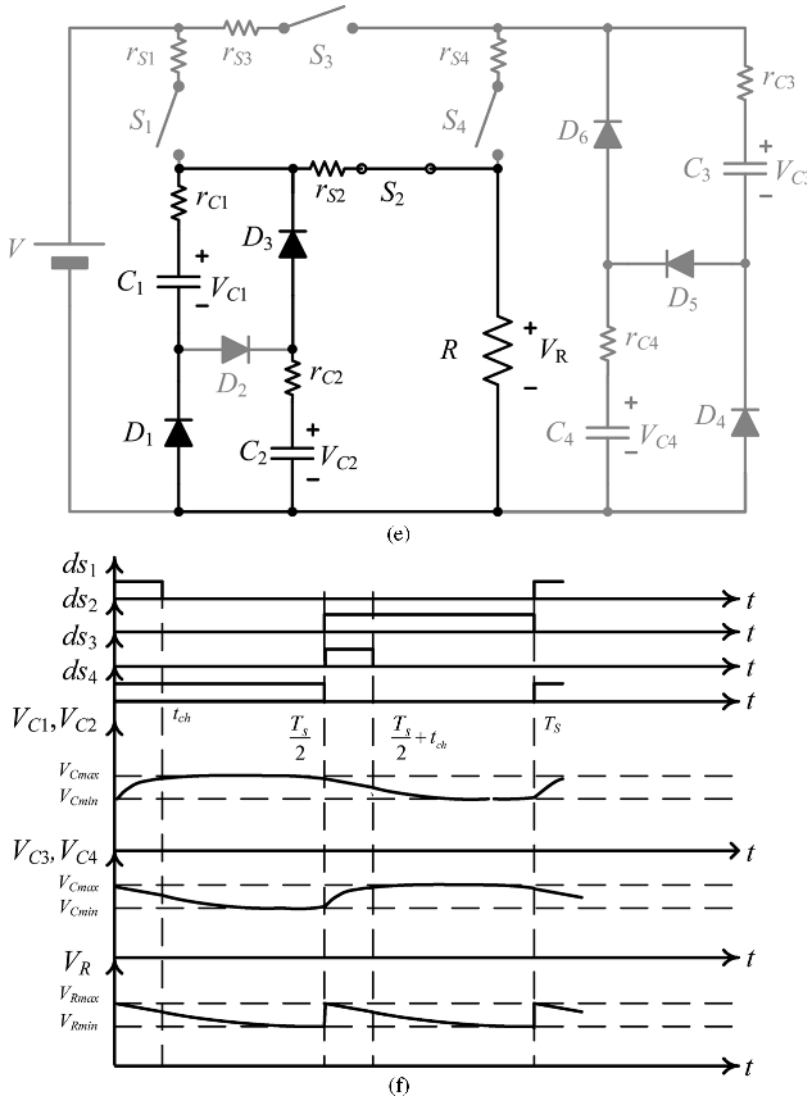

Figure 1.54 (*Continued*)

The duty cycles of the switches S_1 and S_2 are equal and slightly less than 0.5 (Figure 1.55b). Let us explain the operation of the converter in a typical steady-state cycle, starting at a moment denoted as t_0. Consider that S_2 is conducting before t_0. The voltage across C_{S2} will then be zero and the voltage across C_{S1} will be V_{in}. The rectifier diodes D_2 and D_3 conduct, and D_1 and D_4 are off (Figure 1.56a). The voltage v_{AB} is given by $v_{AB} = -V_{in}/2$ (giving $i_L < 0$). At t_0, S_2 is turned off. The current will be diverted from S_2 through C_{S2}, charging it. As Kirchhoff's voltage law has to be fulfilled at any moment, it means that the total voltage across capacitors C_{S1} and C_{S2} has to remain V_{in}. Consequently, the primary current i_L will divide into two currents of value $i_L/2$ (by assuming that the two switches have identical parallel capacitances), charging slowly (depending on the values of the capacitance and reflected load current) C_{S2} from zero to V_{in} and

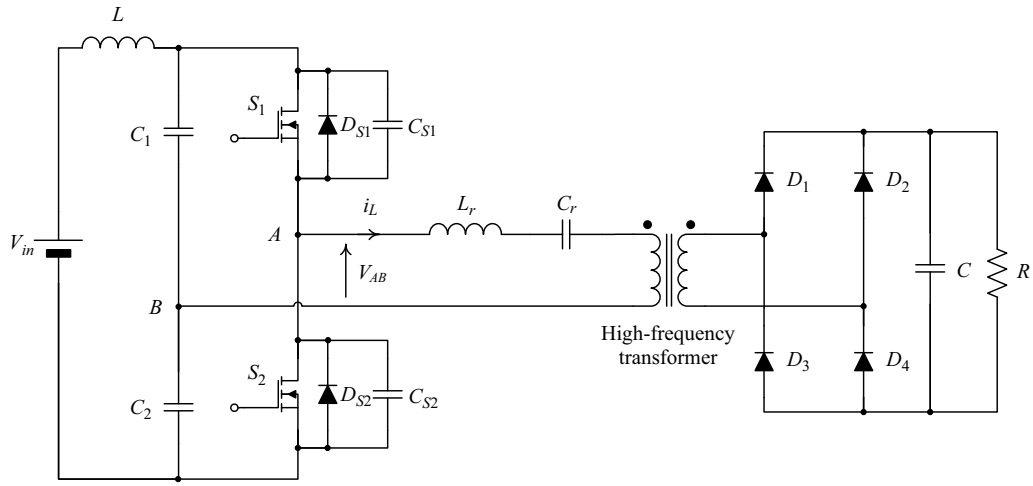

(a)

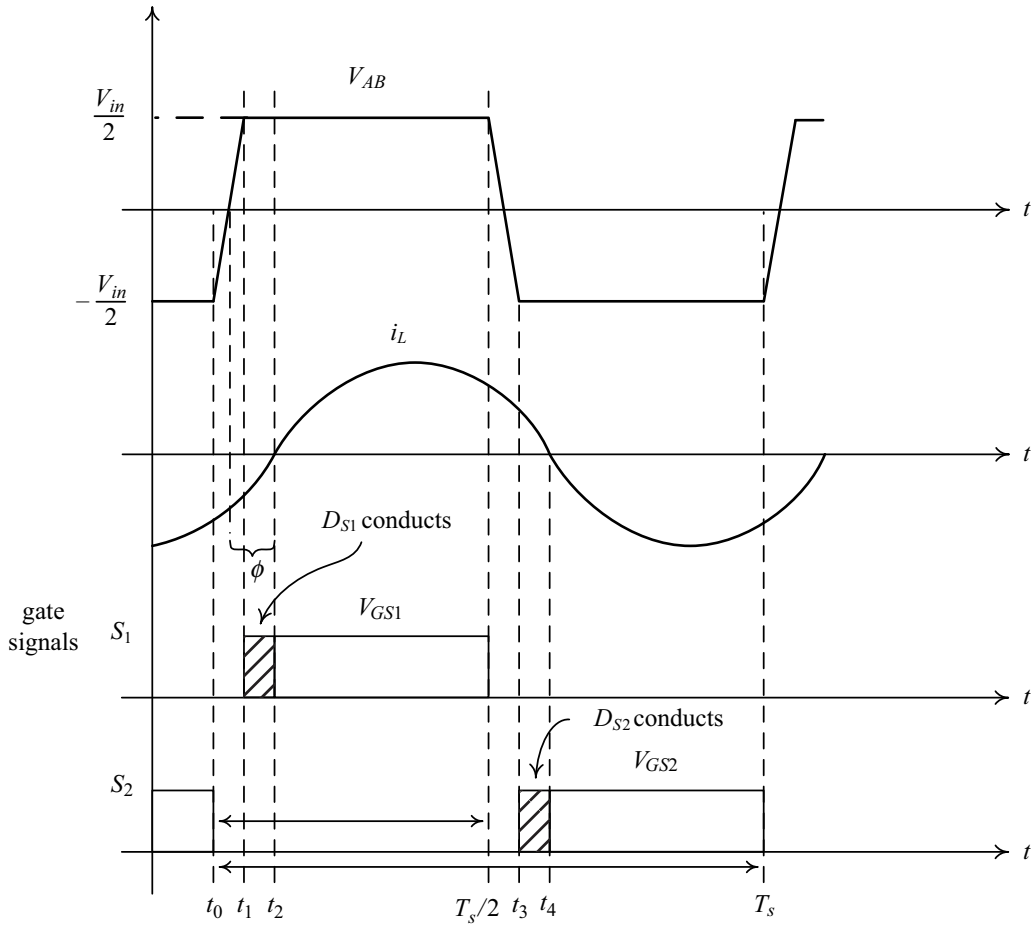

(b)

Figure 1.55 *Series-loaded resonant converter: (a) power stage circuit; (b) main steady-state waveforms.*

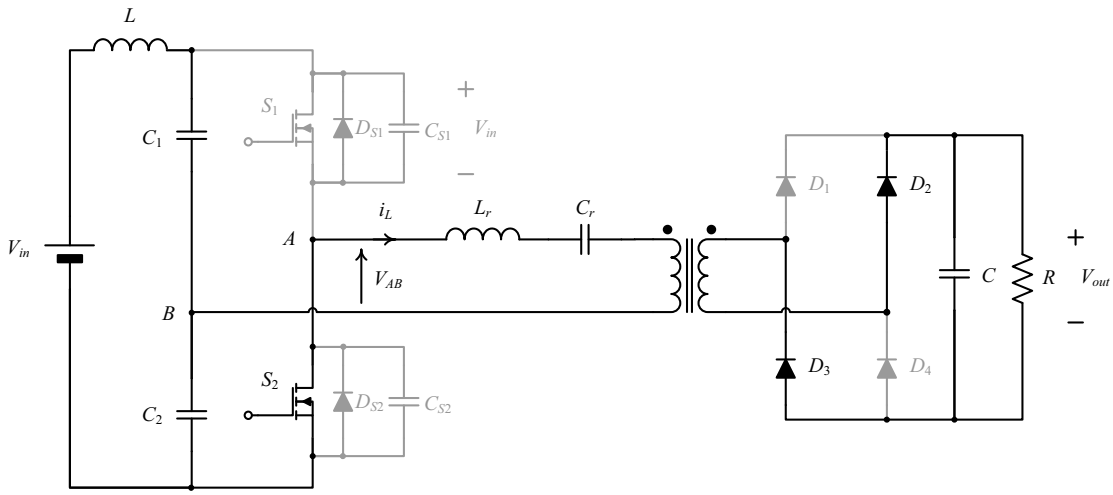

(a)

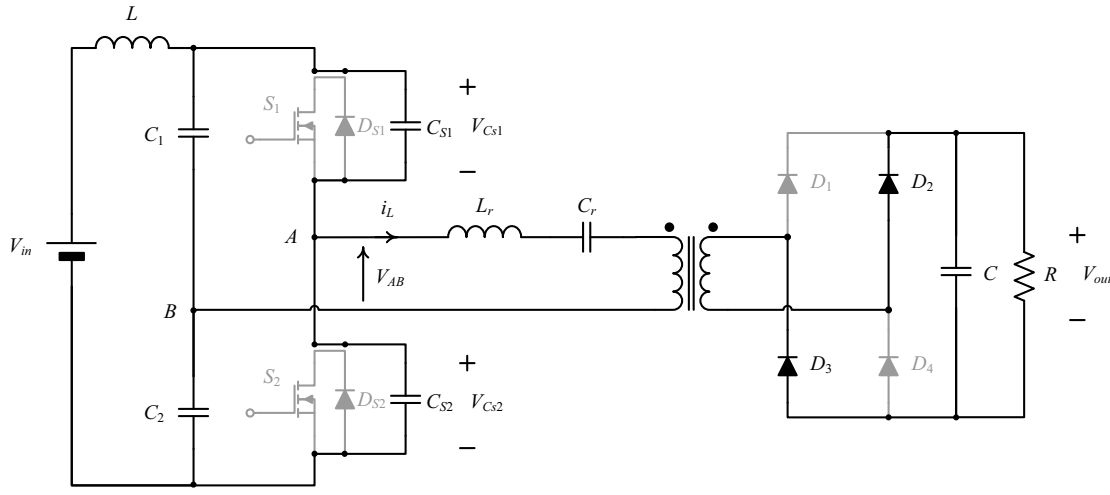

(b)

Figure 1.56 *Switching stages of the series-loaded resonant converter: (a) before* t_0*; (b)* $[t_0, t_1]$*; (c)* $[t_1, t_2]$*; (d)* $[t_2, T_s/2]$*; (e)* $[T_s/2, t_3]$*; (f)* $[t_3, t_4]$*.*

discharging C_{S1} from V_{in} to zero (Figure 1.56b). Therefore, the presence of the parallel capacitance assures the zero voltage (ZVS) turn-off of S_2. During the interval $[t_0, t_1]$, following the charging and discharging process of C_{S2} and C_{S1}, respectively, the voltage, $v_{AB,}$ given by $v_{AB} = -V_{in}/2 + v_{CS2}(t)$ is increasing from $-V_{in}/2$ to $V_{in}/2$. As i_L is still negative, D_2 and D_3 still conduct, and D_1 and D_4 are off. When C_{S1} is completely discharged, at t_1, the antiparallel diode of S_1, D_{S1}, starts conducting naturally, taking all the current i_L. The voltage across C_{S2} remains V_{in}. The voltage v_{AB} becomes equal to $V_{in}/2$ (Figure 1.56c). The rectifier

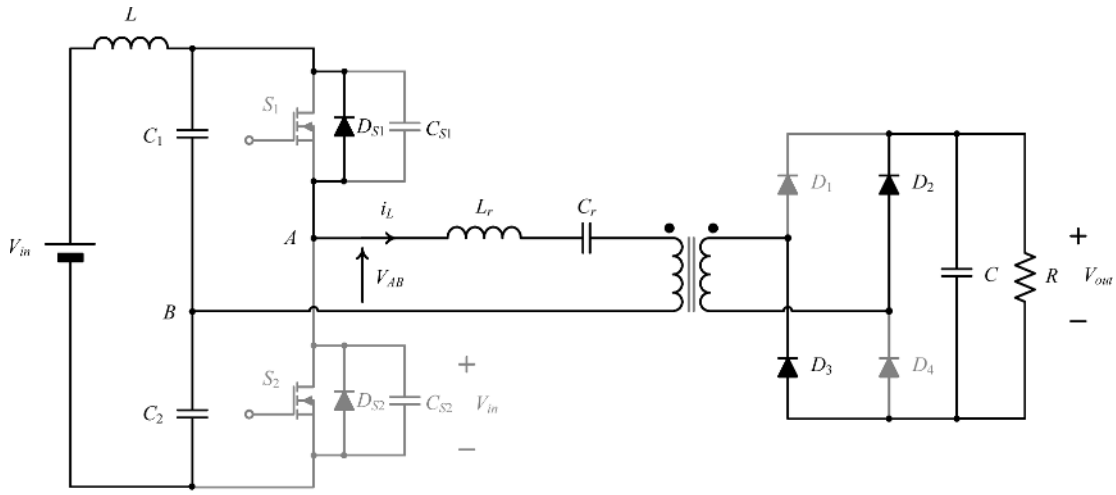

(c)

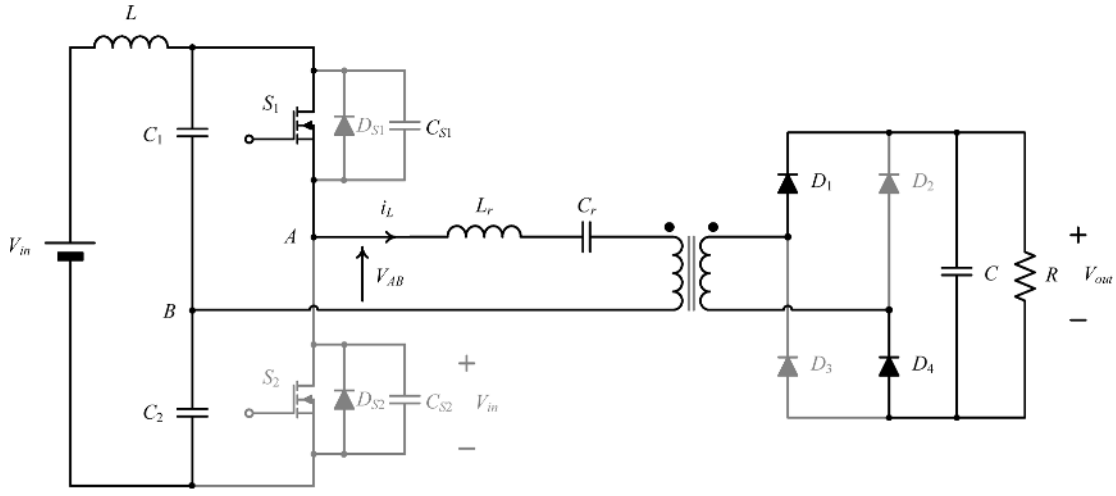

(d)

Figure 1.56 (*Continued*)

diodes, D_1–D_4, keep their states. After t_1, during the conduction interval of D_{S1}, the gate signal for turning on S_1 is applied. We saw in Section 1.3 that the turn-off process of a switch is not instantaneous. This means that, practically, at t_0, S_2 may not have finished its turn-off process. If S_1 is turned on exactly at the instant t_1, it would be possible that S_1 and S_2 conduct concomitantly, thus short-circuiting the supply source and causing a huge input current pulse (called *shoot-through* of the switches). To avoid shoot-through, a "*dead time*" is inserted between the instants of turning off S_2 and turning on S_1. When the

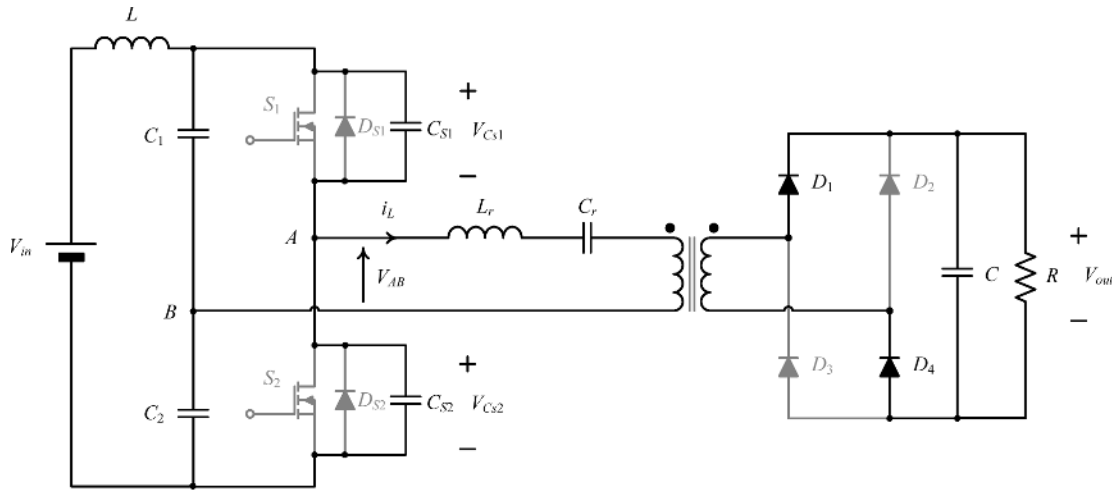

(e)

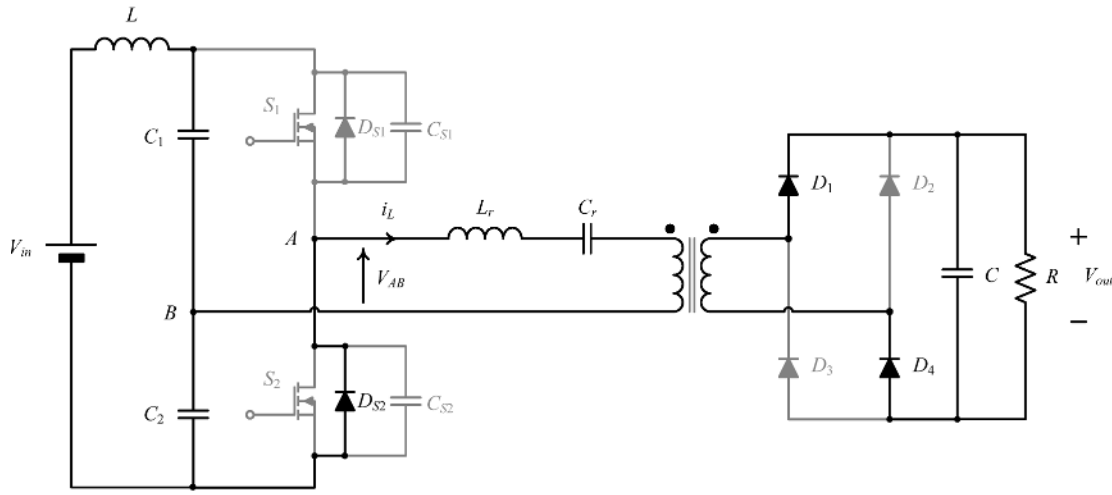

(f)

Figure 1.56 (*Continued*)

primary current, i_L, reaches zero, at t_2, D_{S1} stops conducting and S_1 takes over the current, i_L, which changes its direction (Figure 1.56d). Therefore, by discharging C_{S1}, the zero voltage turn-on of S_1 is realised. During the interval $[t_2, T_s/2]$, $v_{AB} = V_{in}/2$, i_L is given by:

$$i_L(t) = \frac{\frac{V_{in}}{2} - v_{Cr}(t_2)}{\omega_r L_r} e^{-\frac{R'}{2L_r}t} \sin \omega_r t$$

where

$$\omega_r = \sqrt{\frac{1}{L_r C_r} - \frac{R'^2}{4L_r^2}}$$

and R' is the reflected load resistance R to the primary side.

As i_L becomes positive at t_2, D_2 and D_3 turn off and D_1 and D_4 start conducting. One can see that the sinusoidal current, i_L, reaches a peak that can be many times larger than the nominal input current. As i_L flows through the on-state resistance of the switch and through the parasitic resistances in the circuit, such a sinusoidal waveform attracts considerable conduction loss. This is one of the main disadvantages of resonant converters.

At $T_s/2$, S_1 is turned off with ZVS due to the presence of C_{S1}: the current i_L charges C_{S1} from zero to V_{in} and discharges C_{S2} from V_{in} to zero, preparing the later zero voltage turn-on of S_2 (Figure 1.56e). Following these capacitors charging and discharging, respectively, v_{AB} decreases from $V_{in}/2$ to $-V_{in}/2$. D_1–D_4 keep their states. When C_{S2} is completely discharged, at t_3, D_{S2} starts conducting naturally. The voltage v_{AB} becomes equal to $-V_{in}/2$ (Figure 1.56f). D_1–D_4 keep their states. The current i_L continues its sinusoid from the previous time intervals. Immediately after t_3, a turn-on signal is applied to switch S_2. Again, practically, a dead time must be applied between the instants when S_1 is turned off and S_2 is turned on. When i_L reaches zero, at t_4, D_{S2} stops conducting. The current, i_L, now in the opposite direction, is taken over by S_2, arriving again to the topological stage of Figure 1.56a. The equation of i_L is similar to the previous formula given for the interval $[t_2, t_4]$, only that it has a negative sign. The converter will operate in this stage until the end of the cycle, T_s, when a similar new cycle begins.

In the above described converter, it is essential that i_L does not finish its negative part of the sinusoid before a new cycle begins (otherwise, when turning off S_2, i_L would be positive and D_{S1} would not start conducting at t_1). Similarly, i_L must still be positive when turning off S_1 at $T_s/2$ (otherwise, D_{S2} will not start conducting at t_3). This means that the current, i_L, has to lag the voltage, v_{AB}. The equivalent AC model of the converter is given in Figure 1.57. For $I_L(j\omega_s)$ lagging $V_{AB}(j\omega_s)$, we need the load angle

$$\theta = \tan^{-1} \frac{\omega_s L_r - \dfrac{1}{\omega_s C_r}}{R'}$$

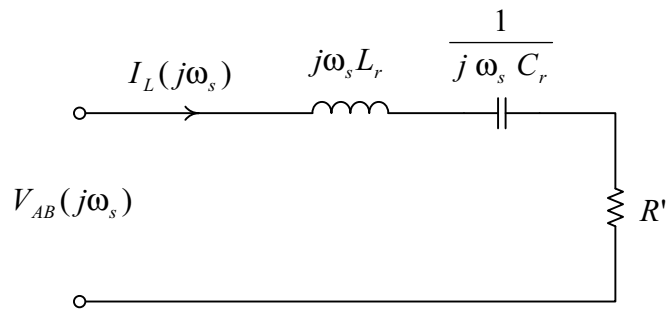

Figure 1.57 *Equivalent circuit of a series-loaded resonant converter with* R′ *representing the reflected load to the primary-side.*

to be positive. Thus,

$$\omega_s > \frac{1}{\sqrt{L_r C_r}}.$$

In other words, the switching frequency ω_s has to be higher than the resonant frequency. Such an operation is called "above resonance operation." As the current i_L lags the voltage v_{AB}, this type of operation is also called "lagging power factor mode." The advantages of the above resonance operation are clear: ZVS turn-on and turn-off of the switches, and an operation at a high switching frequency, implying a smaller size of the transformer and reactive elements. The method is suitable for resonant converters using MOSFETs; therefore, is less useful for converters with high supply voltage, V_{in}, for which no MOSFETs are available (we saw that the switch has to withstand the input voltage when it is in the off-state). Another type of operation is "the below resonance" or "leading power factor mode," in which the switching frequency is lower than the resonance frequency, and i_L leads voltage v_{AB}. In such an operation, the switches are turned on and off with ZCS, giving other advantages and disadvantages, and other applications to such a resonant converter.

It is possible to use resonant tanks other than the series one we saw above, such as a parallel one, in which the resonant capacitor is connected in parallel with the load, or a series-parallel tank of type LCC, in which one capacitor is in series with the inductor and another capacitor is in parallel with the load, or a series-parallel tank of type LLC, in which there are two inductors in series with a capacitor, one of them being in parallel with the load. Each one of the converters obtained with these different tanks has its advantages and its applications, as we shall see in Volume III.

As in resonant converters there is no interruption of the energy flow from supply to load, no duty cycle can be defined and no possibility for regulating the output voltage is available based on controlling the conducting time of a certain switch. In order to control the flow of energy going from supply to load, we have to control the average value of the instantaneous power, $v_{AB}\, i_L$. From Figure 1.55b we can see that, in a designed converter, we can achieve this only by extending or compressing the waveforms of v_{AB} and i_L, that is, by extending or shortening T_s. Therefore, to regulate the output voltage of the resonant converters, a *switching frequency - control* is required. An example of an integrated circuit for a frequency controller for resonant converters is STMicroelectronics' L6598. It can change the switching frequency from 240 to 60 kHz for a variation of the power from 25 to 150 W.

The disadvantage of frequency control is the implied difficulty of designing the filter of the converter. When choosing the circuit elements for filters, we have to know the operating frequency of the converter, because each reactive element has a specific frequency response. In addition, if we choose a magnetic element by considering the lowest possible operating frequency, that element will be oversized for all other frequencies in the controlling range. If we choose the magnetic element by using the highest possible operating frequency for a desired line and load regulation, that element might become saturated at the lower frequencies of the controlling range. Practically, when designing an inductor operating in a frequency-controlled converter, we have to choose a core material suitable for the designed controlling frequency range by using the datasheet provided by the manufacturer. We shall choose the magnetic material which has the highest performance factor for the required frequency range. The performance factor is frequency-dependent, so even if the design is optimized at a particular frequency, the performance will change for the other frequencies in the considered range.

1.6.2 Quasi-resonant converters (QRC)

We saw that duty cycle controlled converters have the advantage of a simple and robust PWM control. Depending on the type of converter, the voltages and currents the switches have to withstand are either the

values of the input or output voltage, respectively the values of the input or output current (e.g., in the case of the buck converter, the switches have to withstand the input voltage and output current; for the boost converter the switches have to withstand the output voltage and input current; the worst case being the buck-boost converter where the sum of the input and output voltage appears across the switch in the off-state). No extra voltage or current stresses appear for the above basic converters. The main disadvantage of these converters is their hard-switching. The resonant converters possess a natural soft-switching. However, their frequency control necessitates a more complicated design of the magnetic elements. And, in the resonant process, the waveforms of the voltages and currents in the converter reach sinusoidal peaks, which cause large stresses on the switches, requiring their overdesign. The ideal converter would combine the advantages of the PWM and resonant converters, and eliminate their drawbacks.

In the quest for such a converter, in 1984 a quasi-resonant converter (QRC) was proposed. It developed some ideas originated from patents and conference papers from the period 1971–1983. The starting point was to use a simple hard-switching converter, like those we have already met (buck, boost, or buck-boost), and insert, near the switch, a resonant block formed by two very small reactive elements, L_r and C_r, its resonant period, T_r, being much smaller than T_s:

$$T_r = 2\pi\sqrt{L_r C_r} \ll T_s$$

The series resistances of L_r and C_r are negligible due to the use of small value elements; therefore, the additional conduction losses will not be important.

The resonant circuit can be inserted with the inductor in series with the switch (Figure 1.58a and b) or with the capacitor in parallel to the switch (Figure 1.59a and b). We will see that the structures represented in Figure 1.58 create a ZCS condition. Remember that a MOSFET presents an intrinsic, built-in antiparallel diode. Therefore, a MOSFET will allow a bidirectional flow of current. If we want to have a unidirectional flow, we can insert a diode in series with the switch – we used to say then that the switch is operated in a "half-wave mode." Remember that the body diode presents recovery problems. Practically, if we want a bidirectional flow (an operation called "full-wave mode"), we use an additional diode in parallel with the MOSFET. As we already know, the presence of a series inductor will slow the rise of the current when we turn on the switch. The resonant process taking place in the L_r–C_r circuit will create a sinusoidal current; when the sinusoid reaches a zero value, we turn off the switch with ZCS.

The structures represented in Figure 1.59 are used to create a ZVS condition. As we remember, the presence of a parallel capacitor will slow the rise of the voltage across the switch when this is turned off. The sinusoidal waveform of the capacitor voltage created in the resonant circuit will pass naturally through zero. At that moment, the antiparallel diode of the switch will start conducting, creating a zero voltage condition for turning on the switch. The antiparallel diode of the switch will allow only the positive half-cycle of the sinusoidal resonant capacitor voltage, as this voltage is clamped to zero by the diode during the negative half-cycle. In such a case, it is said that the bidirectional switch with the resonant circuit is operated in a half-wave mode. If a unidirectional switch is used, the voltage across C_r can oscillate in both positive and negative half-cycles, giving a full-wave mode operation.

In resonant converters, the resonant circuit was present all the time in the energy flow, leading to a large circulation of energy. The resonant block was an integral part of the power conversion circuit. Unlike the resonant converters, in quasi-resonant converters the resonant circuit is used only when needed to obtain ZCS or ZVS. In other words, the resonant block in quasi-resonant converters is attached to the switch and used only to create the zero-switching (ZCS or ZVS) condition – this is why the structures in Figures 1.58 and 1.59 are also called "resonant switches."

To understand the operation of a quasi-resonant converter, consider the case when a resonant circuit is inserted in a buck converter, with the inductor in series with the switch, as in Figure 1.58a. A unidirectional

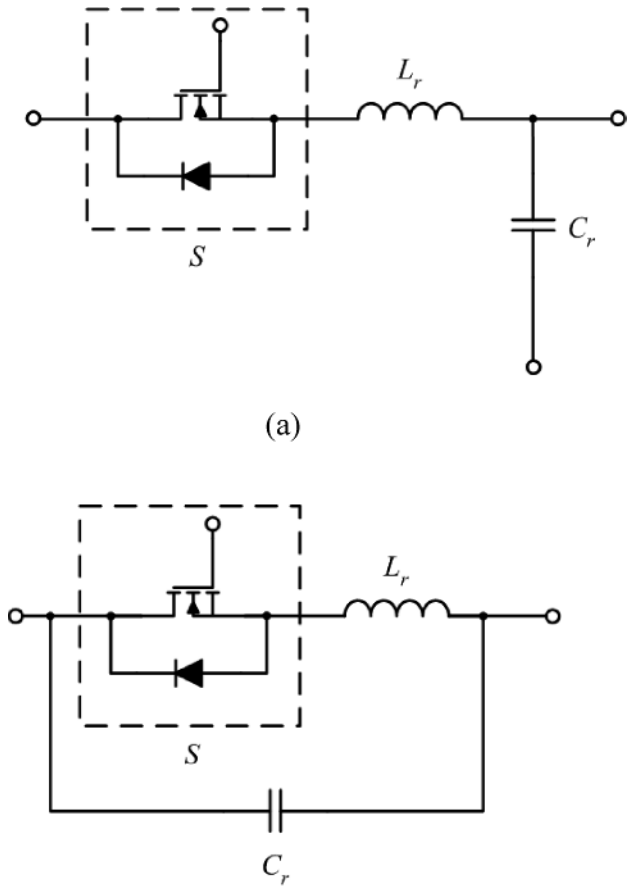

Figure 1.58 *Switch-resonant circuit structures for creating a ZCS condition.*

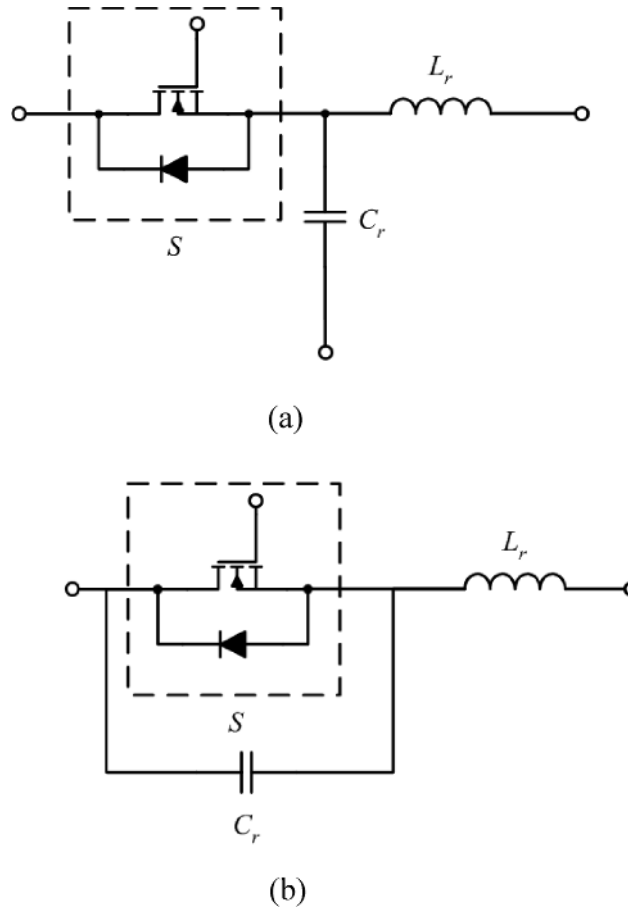

Figure 1.59 *Switch-resonant circuit structures for creating a ZVS condition.*

flow of energy is obtained by adding a series diode, D_s. The ZCS quasi-resonant buck converter in a half-wave mode operation is obtained (Figure 1.60a). As we saw in Figure 1.10, the output filter L–C with the load resistor R can be seen, in a first approximation, as a current sink, I_{out} (Figure 1.60b). We shall use this equivalent circuit here during the analytical analysis to reduce the number of reactive elements from four to two, thus having to solve only differential equations of order two. The accuracy will not be affected, as L_r and C_r have much smaller values. As $T_r \ll T_s$, i_{Lr} and v_{Cr} can make full sinusoids within a switching cycle, during which I_{out} can be considered approximately constant.

In a steady-state cycle, the converter will go through several switching stages (topologies). A switching diagram containing the main steady-state waveforms (the driving signal of the switch, resonant inductor current i_{Lr} and resonant capacitor voltage v_{Cr}) is given in Figure 1.61a. The equivalent circuits for each switching stage are given in Figure 1.61b–e. When we analyze a circuit, we always have to begin from its state in the last switching topology before starting a new switching cycle. Then, at the end of the analysis of the operation in the steady-state cycle, if our supposition was correct, we should arrive at the initial state. In our case, as the circuit is a buck converter, we know that its last switching stage is the freewheeling one (Figure 1.61b): S is turned off and the load current, I_{out}, freewheels through diode D. Obviously, in this stage, $i_{Lr}(t) = 0$, $v_{Cr}(t) = 0$.

A new steady-state switching cycle starts at t_0 by turning on switch S. Due to the presence of L_r, the switch current, i_{Lr}, rises slowly, giving the ZCS character for the switch turn-on. From Figure 1.61c we obtain:

$$V_{in} = L_r \frac{di_{Lr}}{dt}$$

with the solution:

$$i_{Lr} = \frac{V_{in}}{L_r} t$$

where, for simplicity, t_0 was taken as zero.

The slope of the rising switch current is limited by L_r. As long as i_{Lr} is smaller than I_{out}, the diode D conducts, its current being given by $i_D(t) = I_{out} - i_{Lr}$. As a result:

$$v_{Cr}(t) = 0$$

When $i_{Lr}(t)$ reaches the value of I_{out}, say at the instant t_1, the current through the diode drops to zero and the diode turns off naturally, that is, with ZCS, as $i_D(t_{1-}) = i_D(t_{1+}) = 0$. The converter enters the second switching stage, shown in Figure 1.61d. As diode D is now off, the current will flow through capacitor C_r. Kirchhoff's equations in the circuit of Figure 1.61d give:

$$\begin{cases} V_{in} = L_r \dfrac{di_{Lr}}{dt} + v_{Cr} \\ i_{Lr} - I_{out} = C_r \dfrac{dv_{Cr}}{dt} \end{cases}$$

By differentiating these equations:

$$\begin{cases} 0 = L_r \dfrac{d^2 i_{Lr}}{dt^2} + \dfrac{dv_{Cr}}{dt} \\ \dfrac{di_{Lr}}{dt} = C_r \dfrac{d^2 v_{Cr}}{dt^2} \end{cases}$$

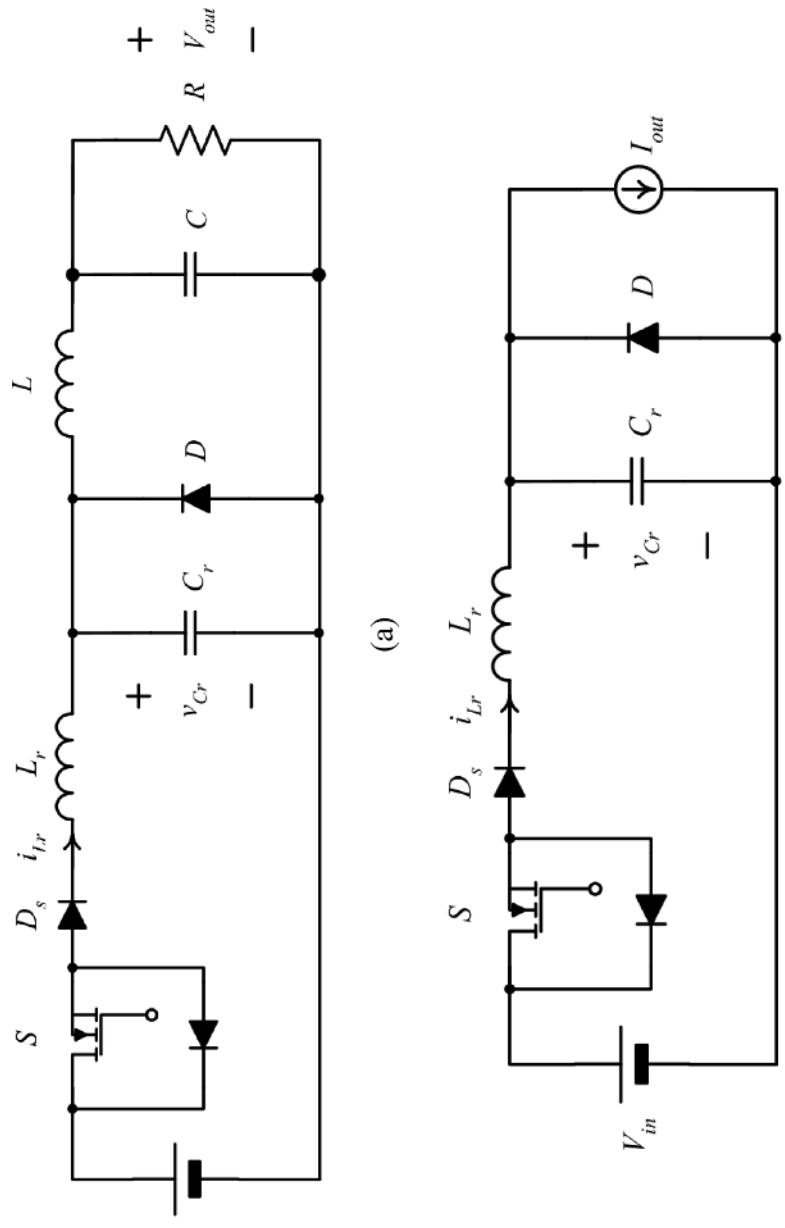

Figure 1.60 *(a) ZCS QRC buck converter in half-mode operation; (b) its approximate simplified structure.*

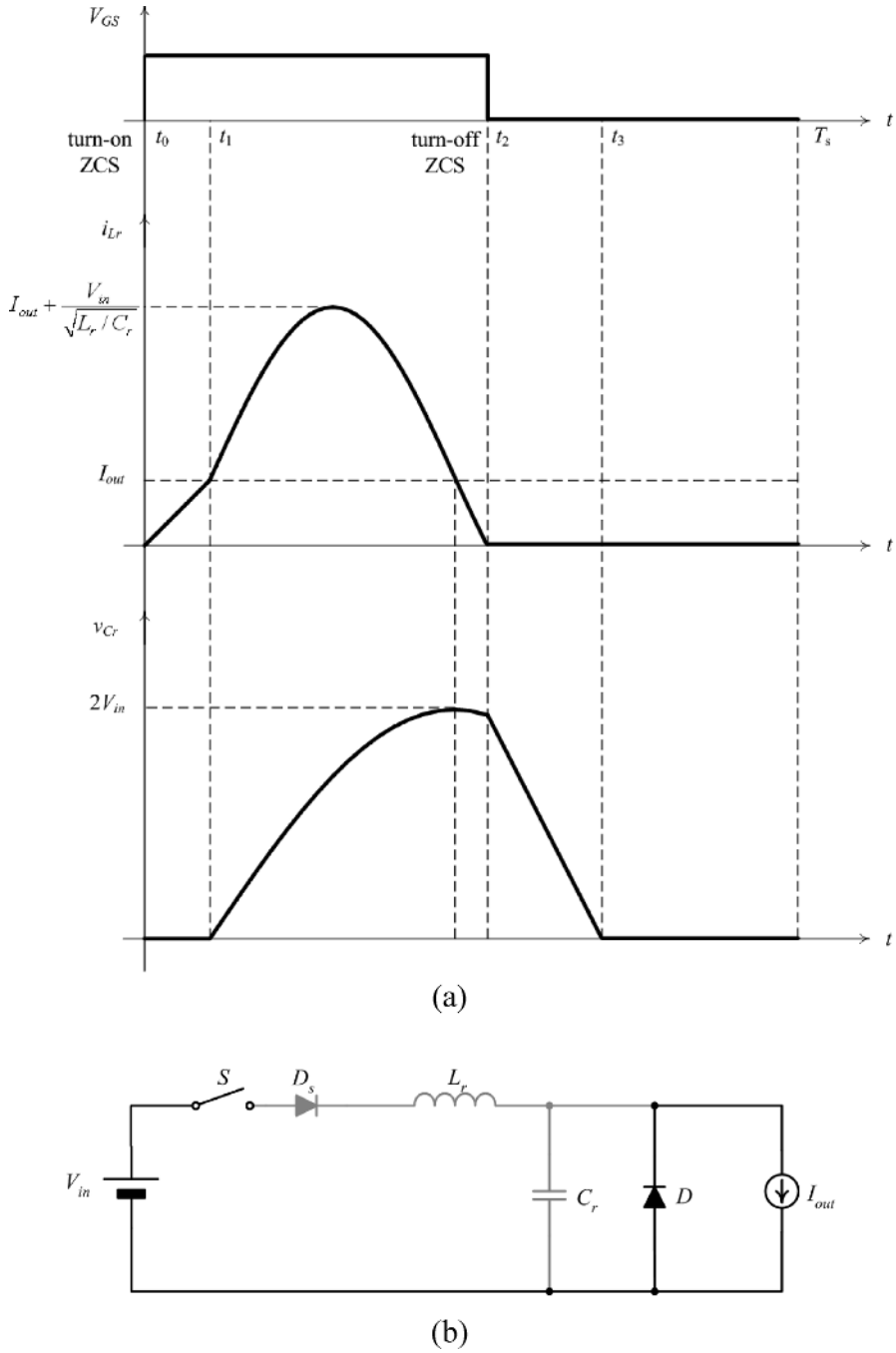

Figure 1.61 *(a) Switching diagram and (b)–(e) switching stages of a QRC ZCS buck converter in half-wave mode operation for the time intervals: (b) < t_0; (c) [t_0, t_1]; (d) [t_1, t_2]; (e) [t_2, t_3].*

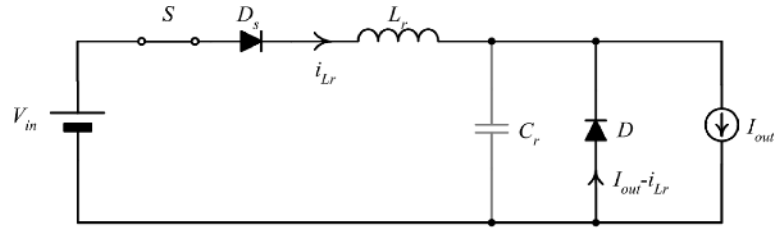

(c)

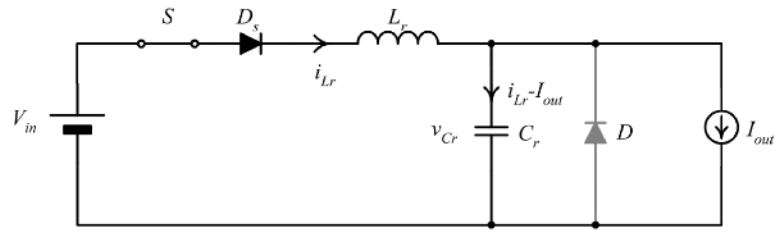

(d)

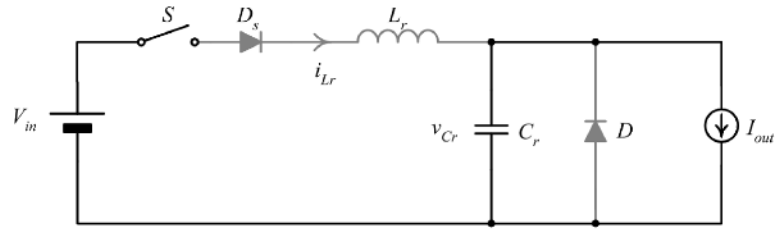

(e)

Figure 1.61 (*Continued*)

and introducing di_{Lr}/dt and dv_{Cr}/dt in the preceding equations, we get:

$$\begin{cases} V_{in} = L_r C_r \dfrac{d^2 v_{Cr}}{dt^2} + v_{Cr} \\ i_{Lr} - I_{out} = C_r \left(-L_r \dfrac{d^2 i_{Lr}}{dt^2} \right) \end{cases}$$

or

$$\begin{cases} \dfrac{d^2 v_{Cr}}{dt^2} + \dfrac{1}{L_r C_r} v_{Cr} = \dfrac{1}{L_r C_r} V_{in} \\ \dfrac{d^2 i_{Lr}}{dt^2} + \dfrac{1}{L_r C_r} i_{Lr} = \dfrac{1}{L_r C_r} I_{out} \end{cases}$$

with the initial conditions:

$$i_{Lr}(t_1) = I_{out}, v_{Cr}(t_1) = 0$$

the solution of these equations being:

$$\begin{cases} i_{Lr}(t) = I_{out} + \dfrac{V_{in}}{\sqrt{\dfrac{L_r}{C_r}}} \sin \dfrac{1}{\sqrt{L_r C_r}} (t - t_1) \\ v_{Cr}(t) = V_{in} \left[1 - \cos \dfrac{1}{\sqrt{L_r C_r}} (t - t_1) \right] \end{cases}$$

We can notice that the resonant current, i_{Lr} (which, let us not forget, is also the current flowing through the switch) has a sinusoidal peak of the value

$$\frac{V_{in}}{\sqrt{\dfrac{L_r}{C_r}}},$$

that is, while in a hard-switching buck converter the switch had to withstand the input current, in a quasi-resonant ZCS buck converter it has to conduct a current the maximum value of which is given by the output current in addition to a component that depends on the value of the input voltage. For large values of the input voltage, this peak can reach much higher values than the nominal input current. The resonant capacitor voltage, v_{Cr}, can reach two times the input voltage. As C_r is placed in parallel to the output diode D, it means that D has to withstand a voltage which is twice the value that a diode in a hard-switching buck converter has to withstand.

We see in Figure 1.61a that the sinusoidal resonant inductor current reaches zero at the instant t_2. If we want to turn off the switch S with ZCS, then we have to take the action exactly at this moment. This means that the interruption of the power flow from the supply to load cannot be done according to an instant "dictated" by a control circuit of the PWM type, as was the case for hard-switching converters. In quasi-resonant converters, S has to be switched off when a sensor indicates that the resonant inductor current has reached the value zero. Therefore, control of the "duty cycle" type is not possible in quasi-resonant converters.

By turning off S at t_2, the converter enters the third switching stage, described in Figure 1.61e. In this figure:

$$C_r \frac{dv_{Cr}}{dt} + I_{out} = 0$$

giving:

$$v_{Cr}(t) = v_{Cr}(t_2) - \frac{I_{out}}{C_r}(t - t_2)$$

that is, the resonant capacitor discharges linearly to the load.

When $v_{Cr}(t)$ reaches zero, diode D, which is in parallel to C_r, starts conducting with ZVS because

$$v_D(t_{2-}) = v_D(t_{2+}) = 0.$$

The converter enters the typical buck freewheeling switching stage shown in Figure 1.61b.

If we did not add diode D_s to the converter, the resonant inductor current would continue to flow in the second switching stage through the antiparallel diode of the switch, in the opposite direction, until ending its negative half-sinusoid and reaching zero again. We could turn off the switch at any moment during the

negative part of the sinusoid, realizing both ZCS (no current in transistor before turning it off) and ZVS (as its body diode was conducting). We will see in Volume III what the practical implications are of each mode of operation, half-wave (with D_s) and full-wave (without D_s).

Just looking at the diagram of i_{Lr} (i.e., the current through S) (Figure 1.61a), we can notice easily the ZCS at turn-on and turn-off of the switch:

$$i_{Lr}(t_{0-}) = i_{Lr}(t_{0+}) = 0,$$

that is, i_{Lr} starts increasing slowly after t_0;

$$i_{Lr}(t_{2-}) = i_{Lr}(t_{2+}) = 0,$$

that is, i_{Lr} reached zero before t_2.

We saw that no duty cycle control was possible in a quasi-resonant converter. As the resonant capacitor is in parallel to the output circuit, it means that the output voltage of the converter is proportional to the average voltage on the resonant capacitor. Therefore, to regulate the output voltage we can adjust the average of v_{Cr}. We see in Figure 1.61a that one way to accomplish this is by changing T_s. Therefore, as we controlled the resonant converters, we also have to use a switching frequency control for the quasi-resonant converters, with the detriments implied by such a type of control, as discussed before. Add to this disadvantage the problem of the high sinusoidal peaks, which affect the stresses on the switch and output diode, requiring their overdesign, which was leading to larger conduction losses, and we understand why quasi-resonant converters did not make their way in practical applications.

However, the quasi-resonant converter signified an important milestone in the development of modern converters. After discussing in detail the ZCS and ZVS quasi-resonant converters, we shall see in Volume III that the next chronological step was to solve the two main drawbacks of quasi-resonant converters: frequency control and sinusoidal peaks. The solution of the first problem was quite simple. We wanted to create something similar to the duty cycle. How could we achieve it? As the main switch had to turn off at the instant when a zero-switching condition was appearing, we had to add one more externally-controlled switch and use it to allow and interrupt the flux of energy from supply to load as desired. Thus, the relative duration between the instants of turning on the two switches became the new controlling quantity, allowing a PWM control. By adding one or more diodes or passive elements to the auxiliary switch, snubbers, as discussed in Section 1.4, were then proposed. The modern soft-switching PWM converters were thus born. Operating with a simple and robust PWM control, with soft-switching allowing for a very high switching frequency, these converters, with theoretical zero switching losses and conduction losses only slightly higher than those in hard-switching converters, spread quickly in industry. As the soft-switching PWM converters represent a large proportion of the DC-DC converters which have been used starting the 1990s, a large part of Volume III will be dedicated to their study. However, as the modern soft-switching PWM converters are basically hard-switching converters with passive or active snubbers, the understanding of their operation and their design is based on a deep knowledge of classical hard-switching converters. This is why, in Chapter 3 of this volume, all the hard-switching DC-DC converters receive considerable attention.

1.7 Overview on AC-DC Rectifiers and DC-AC Inverters

1.7.1 Rectifiers

In our daily life, we can only find single-phase or three-phase AC power out of the socket. Examples of single-phase AC mains supplies are: 220 V or 230 V, 50 Hz in Europe or Asia; 240 V, 50 Hz in Australia;

and 110 V or 120 V, 60 Hz in America. However, the operating voltage inside equipment is usually a low-voltage DC. For example, the operating voltages inside a desktop computer are 1.7 V, 3.3 V, 5 V, 12 V, and so on. Thus, it is necessary to use an AC-DC rectifier that can convert the AC power from the socket into a DC power for the application. Converting an AC voltage, v_s, into a DC voltage, V_{dc}, can be implemented by using a simple diode-bridge circuit and a capacitor, as shown in Figure 1.62a. Diodes D_1 and D_3 and operated complementarily with diodes D_2 and D_4. In the positive half-cycle of v_s (Figure 1.62b), D_1 and D_3 will conduct when $v_s > V_{dc}$. The output capacitor will be charged by the AC mains. The output voltage will follow the supply voltage. In the negative half cycle of v_s, as shown in Figure 1.62c, D_2 and D_4 will conduct when $-v_s > V_{dc}$. Again, the output capacitor will be charged by the AC mains and the output voltage will follow the supply voltage. The peak value of V_{dc}, $V_{dc,pk}$, is then equal to the peak value of v_s. That is:

$$V_{dc,pk} = \sqrt{2}\, V_{s,rms}$$

where $V_{s,rms}$ is the root-mean-square value of v_s.

When the value of the supply voltage starts to decrease and its value is smaller than V_{dc}, the diodes will stop conducting. The capacitor will supply energy to the load. Figure 1.63 shows the waveforms of v_s and V_{dc}.

If the supply voltage is 220 V, the peak value of the DC voltage obtained is equal to 311 V. Such a high voltage can be used in some applications like compact fluorescent lamps and electronic ballasts. However, many household applications require a low voltage supply, for example, 15 V for a battery charger. How can the 311 V be converted into 15 V? Instead of transforming the voltage on the DC side, the simplest way would be to use a transformer to firstly step down the 220 V AC voltage into a 10.6 V AC voltage as shown in Figure 1.64. Then, the low-voltage AC supply is rectified by a diode-bridge circuit. Thus, the DC voltage is equal to $\sqrt{2} \times 10.6 = 15$ V. Practically, the transformer will give a voltage higher than 10.6 V to compensate for the voltage drops of the diodes. However, there are drawbacks associated with the low-frequency transformer used for supplying the low voltage. For a transformer operated at 50 or 60 Hz, its physical size would be too large and its weight too heavy for today's applications, which require small size and light weight. Moreover, in practice, the conversion efficiency of low-frequency transformers is low.

In addition to the above disadvantage due to the transformer, the above simple circuit has another drawback. The current drawn from the AC supply is pulsating. As illustrated in Figure 1.63 and Figure 1.62b, D_1 and D_3 only conduct for a short interval in a line cycle when $v_s > V_{dc}$. Similarly, as shown in Figure 1.62c, D_2 and D_4 also conduct for a short interval in a line cycle when $-v_s > V_{dc}$. From an energy point of view, the energy required by the load will be transferred from the AC supply to the load during the two time intervals in a line cycle. The larger the value of the output capacitor, C, for getting a high quality DC voltage, the shorter the durations of the two time intervals and the higher the magnitude of the supply current pulses. What are the side effects of high current pulses?

Firstly, for the same output power, the size of the cable connecting the AC supply and the application is larger than necessary, because it requires using a cable that can carry such a high current pulse. Apart from low utilization, the cable loss is also increased.

Secondly, supply current pulses create fluctuation in the supplied voltage to the applications. As illustrated in Figure 1.65, the applications are connected in parallel to the same supply. The unavoidable leakage inductance of the distribution transformer of the mains supply and the stray inductance of the transmission cable appear as a source impedance, Z_s, between the AC supply and the applications. A highly pulsating supply current is rich in harmonics. In Figure 1.66 we can see that, if the input current, i_o, of one application contains harmonics, the supply current, i_s, will also contain harmonics. As the terminal voltage, $V'_s(s)$, is given by:

$$V'_s(s) = V_s(s) - I_s(s)Z_s$$

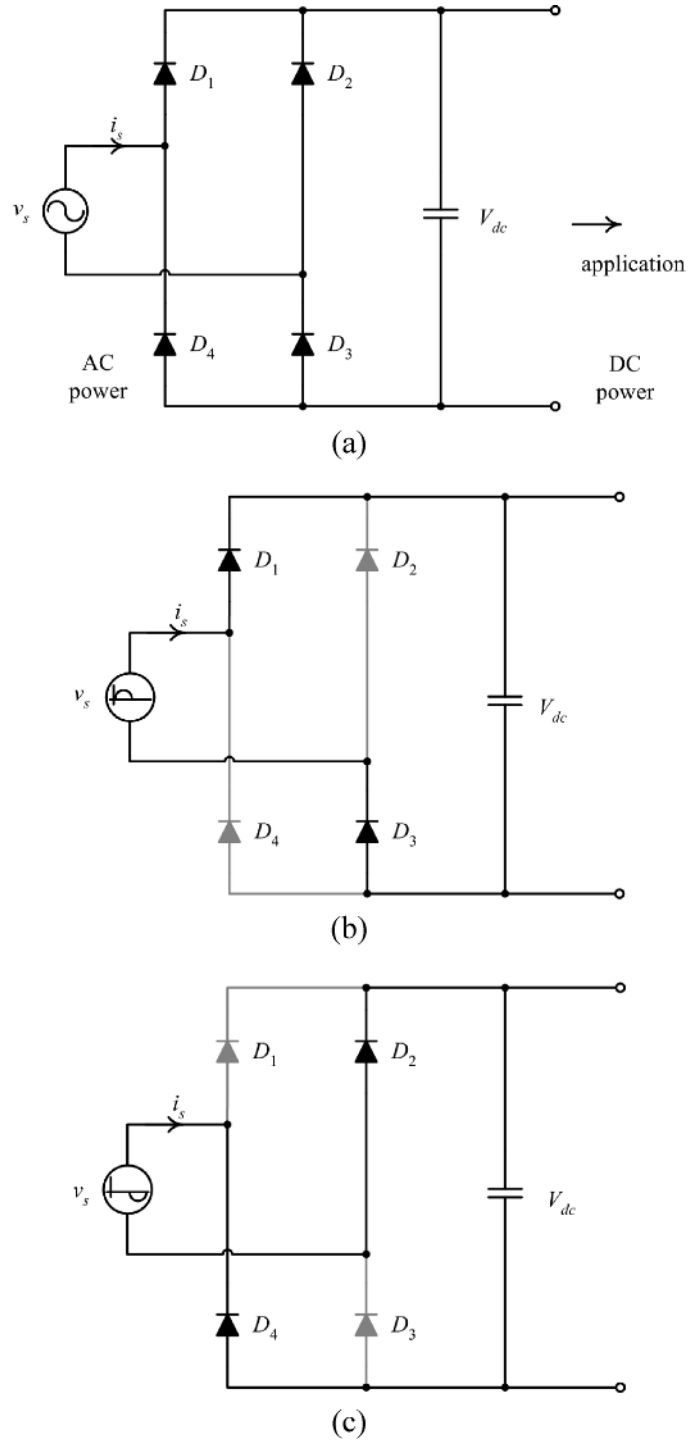

Figure 1.62 *(a) A simple rectifier using a diode-bridge circuit with an output capacitor; (b) operation of the circuit when* $v_s > V_{DC}$*; (c) operation of the circuit when* $-v_s > V_{DC}$*.*

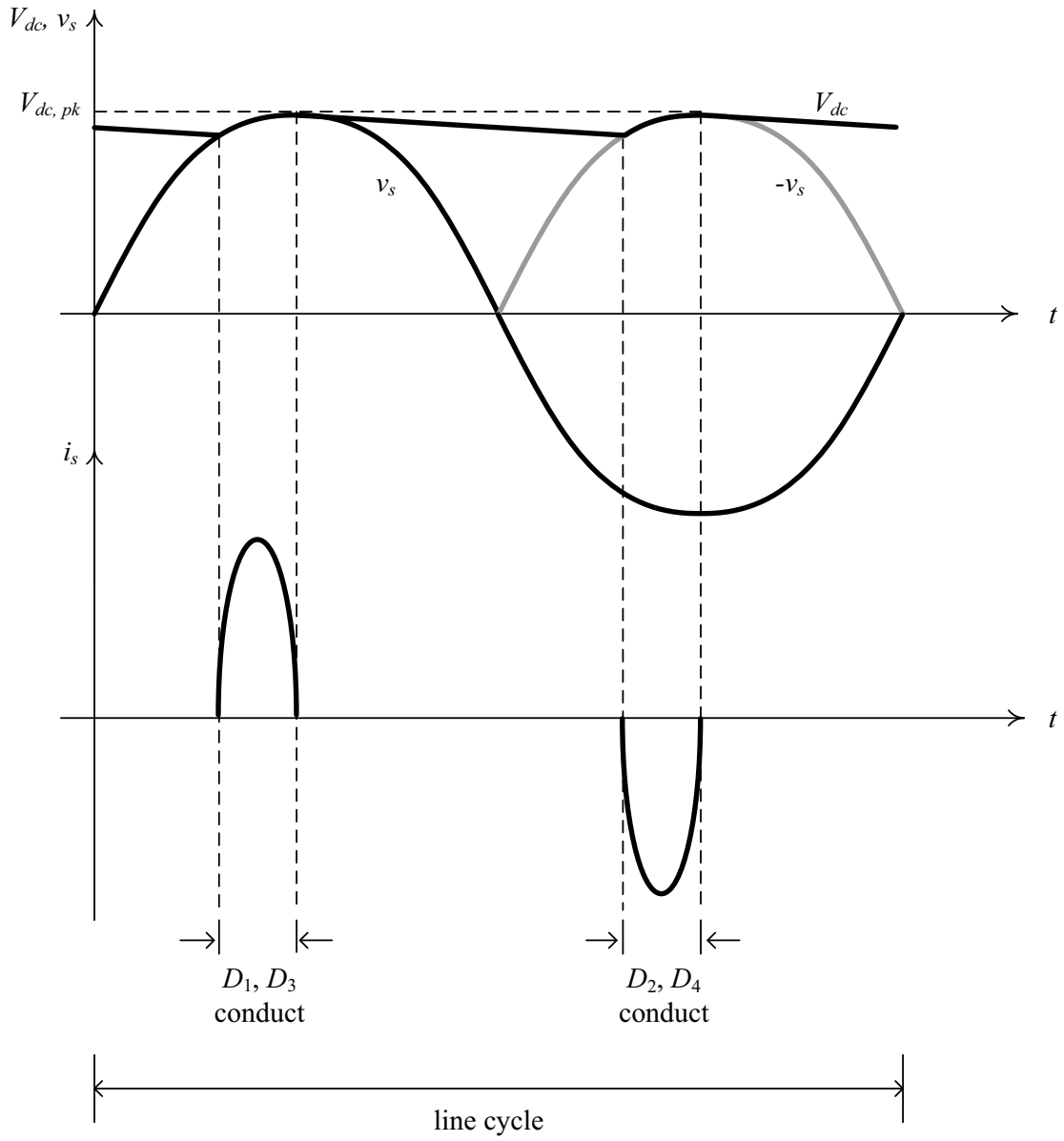

Figure 1.63 *Voltage and current waveforms of the diode-bridge-capacitor rectifier.*

(variables in capital letters denote Laplace transformed variables) the supply current harmonics will create harmonics in the terminal voltage, v_s', which is shared by all the applications. This means that the input current fluctuations of one application will affect other applications. This is considered to be a kind of interference through conductors, namely conducted electromagnetic interference.

Thirdly, the current pulses also introduce radiation due to the $L\,di/dt$ effect, where L is the stray inductance of the network. Thus, if the current pulse is fast changing, it will cause an increase in the radiated electromagnetic interference.

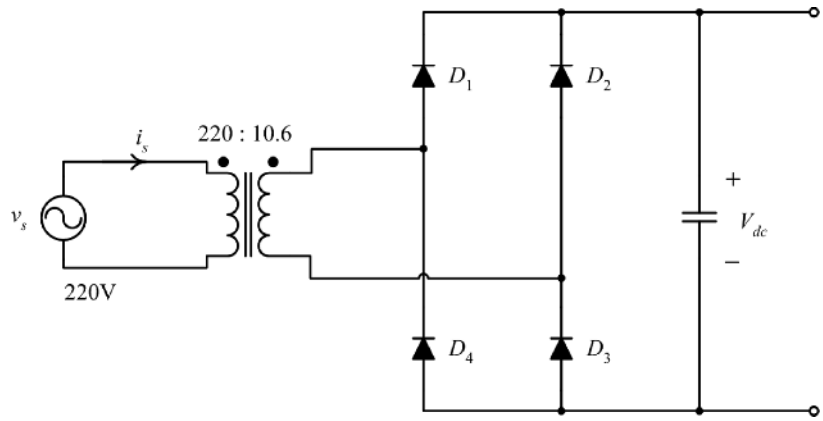

Figure 1.64 *A simple rectifier with an AC transformer.*

Due to the above undesired effects, many countries have developed their own National Electromagnetic Compatibility standards for limiting the harmonics content (in percentage of the amplitude of the fundamental component) in the current drawn by different equipment. Products entering into a country have to comply with the standards of that country. For example, Table 1.8 shows the IEC standard IEC-61000-3-2 Limits for harmonic current emissions for equipment with input current less than 16 A.

Then, what would be the ideal waveform of the supply current? Let us do a quantitative analysis. Assume that the supply voltage is a perfect sinusoid:

$$v_s(t) = V_m \sin \omega t$$

where V_m is the peak value of v_s and $\omega = 2\pi f$ is the angular frequency of the line frequency f.

Assume that we can express the supply current by the following Fourier series; this is valid because the supply current is typically a periodic waveform:

$$i_s(t) = I_{m1}\sin(\omega t - \theta_1) + \sum_{n=2}^{\infty} I_{mn} \sin(n\omega t - \theta_n)$$

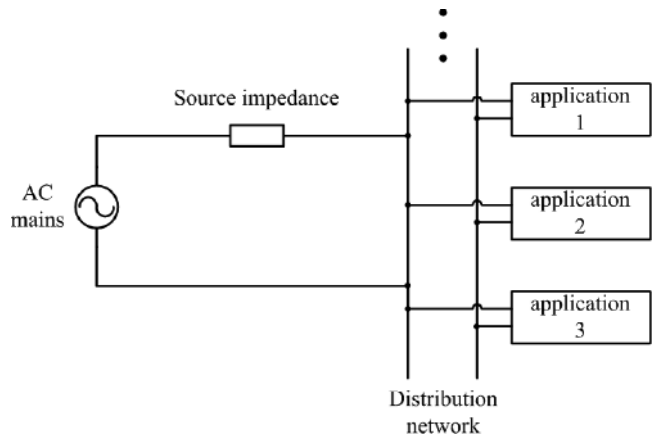

Figure 1.65 *Parallel connections of applications to the mains supply.*

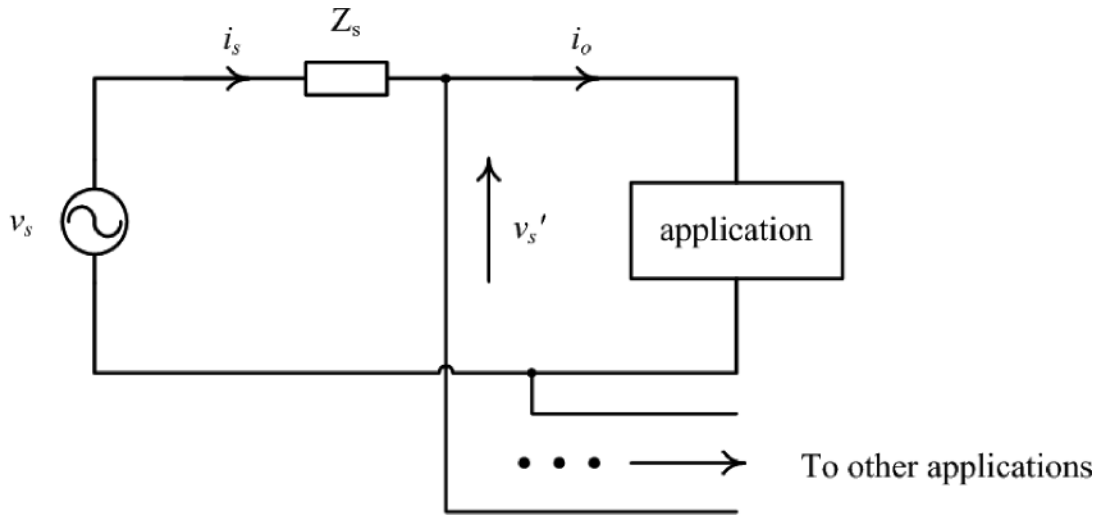

Figure 1.66 *Explanation of the cause of conducted electromagnetic interference.*

where I_{mn} and θ_n are the peak value and phase angle of the n-th harmonic of the supply current, and I_{m1} and θ_1 are the peak value and phase angle of the fundamental component of the supply current.

The root-mean-square values of v_s, $V_{s,rms}$, and i_s, $I_{s,rms}$, are equal to:

$$V_{s,rms} = \frac{V_m}{\sqrt{2}}$$

$$I_{s,rms} = \frac{1}{\sqrt{2}}\sqrt{\sum_{n=1}^{\infty} I_{mn}^2}$$

The average power, P, transferred from the supply mains to the application can be obtained by averaging the product of v_s and i_s over a line cycle. Thus:

$$P = \frac{1}{T}\int_0^T v_s(t) i_s(t) dt$$
$$= V_{s,rms}\, I_{m1,rms} \cos\theta_1$$

Table 1.8 *IEC-61000-3-2 Limits for harmonic current emissions (input current ≤ 16 A)*

(a) Class C equipment, like lighting equipment						
Harmonic	2	3	5	7	9	$11 \leq n \leq 39$
IEC limit (%)	2	30 λ*	10	7	5	3
(b) Class D equipment – equipment having a pronounced effect on the electrical supply system, of a power up to 600 W, like personal computers or television receivers						
Harmonic	3	5	7	9	11	$13 \leq n \leq 39$ (n – odd)
IEC limit (%)	2.3	1.14	0.77	0.4	0.33	0.15 (15/n)

*λ is the circuit power factor.

where

$$I_{m1,rms} = \frac{1}{\sqrt{2}} I_{m1}$$

is the root-mean-square value of the fundamental component of i_s, T being the period of the line cycle ($1/f$).

The transferred power can then be expressed as:

$$P = V_{s,rms}\, I_{s,rms}\, K_d\, K_p$$

where

$$K_d = \frac{I_{m1,rms}}{I_{s,rms}}$$

is called the *distortion factor* and

$$K_p = \cos\, \theta_1$$

is called the *displacement factor*.

The distortion factor is the ratio between the root-mean-square value of the fundamental component of the supply current to the root-mean-square value of the supply current. It is a measure showing the quality of the waveshape of the supply current. The higher its value, the closer is the waveshape of the supply current to a sinusoidal waveform. The maximum value of K_d is unity.

The displacement factor is a factor showing the displacement (phase difference) between the fundamental component of the supply current and the mains voltage. The maximum value of K_p is unity, implying that the fundamental component of the supply current would be in phase with the supply mains voltage.

The *input power factor* K_{PF} of the application is:

$$\begin{aligned} K_{PF} &= \frac{\text{Active Power}}{\text{Apparent Power}} \\ &= \frac{V_{s,rms}\, I_{s,rms}\, K_d\, K_p}{V_{s,rms}\, I_{s,rms}} \\ &= K_d K_p \end{aligned}$$

For a given power, the root-mean-square supply current, $I_{s,rms}$, is minimum if K_{PF} is equal to unity, requiring $K_d = 1$ and $K_p = 1$. In such a case, the supply cable would be optimally utilized. Therefore, the ideal supply current waveform is sinusoidal and in phase with the supply voltage. An application drawing such a current would introduce no harmonics, and therefore no interference to other applications sharing the same supply.

How then can one increase the input power factor of the circuit shown in Figure 1.62? The question can be interpreted in another way by considering the waveshape of the supply current shown in Figure 1.63. The input power factor will be increased if the duration of the input current pulses is increased. The easiest way would be to use an input inductor, acting as a filter, to change the waveform (Figure 1.67) However, this solution is less practical: as such an inductor would have to attenuate a wide frequency range of harmonics, its required value and physical size would be too large.

Back to the root cause of the low-power factor in the rectifier shown in Figure 1.62; if the conduction intervals of the diodes could be increased, the distortion factor K_d would be improved. A practical solution which is widely used in low-power applications, such as compact fluorescent lamps, is shown in

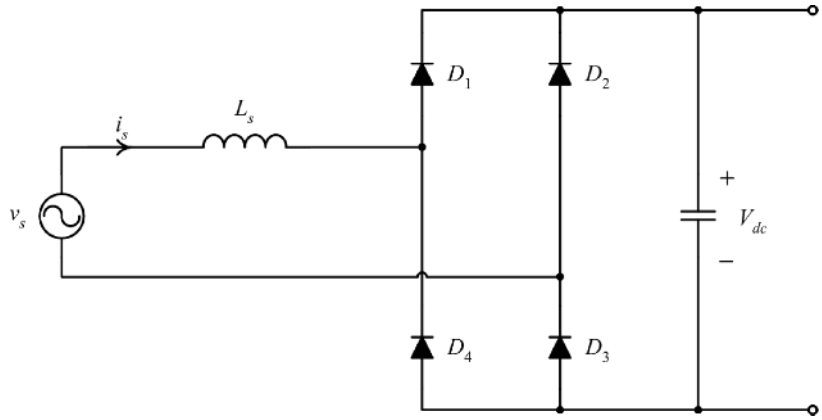

Figure 1.67 *A possible solution for improving the input current waveform of a rectifier.*

Figure 1.68a. The output capacitor is replaced by a diode–capacitor network, in which C_1 and C_2 are of the same value. Denote the voltage across each capacitor by V_C. The capacitors C_1 and C_2 are charged in series by the supply mains through D_6. The maximum voltage across them is V_m (i.e., the peak value of v_s). Thus, each one can be charged up to the maximum voltage $V_m/2$. They are discharged in parallel to the load through D_5 and D_7. At the beginning of a line cycle, $V_C = V_m/2$. However, the mains voltage has a smaller value than that of V_C. The diodes D_1–D_4 do not conduct. The two capacitors discharge to the load through the diodes D_5 and D_7 (Figure 1.68b). During this time, the load voltage is equal to the capacitor voltage $V_m/2$. The circuit operates in this configuration until the angle ωt becomes $\omega t = 30^\circ$ (i.e., $\pi/6$), when the value of the sinusoidal source voltage reaches $V_m/2$. Obviously, no current is drawn from the mains during this period of operation. Practically, the operation of this configuration ends a little earlier, before ωt reaches 30°. It is because the capacitors C_1 and C_2 in reality do not have infinite values but finite ones, so the voltage across them cannot remain constant during the discharging process. When the mains voltage reaches V_C, diodes D_5 and D_7 stop conducting. Diodes D_1 and D_3 start conducting. The load voltage V_{dc} follows the mains voltage (Figure 1.68c). As the voltage on C_1 and C_2 in series is higher than the mains voltage, D_6 does not conduct. When the mains voltage reaches a value equal to that across C_1 and C_2 in series, D_6 starts conducting (Figure 1.68d). The energy of the mains continues to supply the application such that V_{dc} follows the mains voltage and, simultaneously, charges both C_1 and C_2 up to $V_m/2$ (these capacitors were discharged to the load in the first configuration during the angle interval 0–30°, so their voltage decreased then under $V_m/2$). During this time, the input current presents a high peak due to the charging process of the capacitors. Immediately after the sinusoidal mains voltage decreases below the value of the voltage on C_1 and C_2 in series, D_6 turns off, that is, the circuit returns to the operation described in Figure 1.68c. The circuit continues its operation in this configuration until ωt reaches 150° (i.e., $5\pi/6$), when the mains voltage becomes lower than $V_m/2$. Then, the circuit operates again as in the configuration shown in Figure 1.68b. The process repeats for the negative half-cycle of the mains, the role of D_1 and D_3 being played now by D_2, D_4. The waveforms of the input current, i_s, and load voltage, V_{dc}, are shown in Figure 1.68e.

The effect of using the diode–capacitor network was to increase the equivalent conduction intervals of diodes D_1–D_4. As shown in Figure 1.68e, a current is drawn from the supply mains from 30 to 150°, and then from 210 to 330°. No current is drawn from the supply mains from 0 to 30°, 150 to 210° and 330 to 360°. The circuit can effectively increase the conduction angle. This circuit is called a "valley-fill" power factor corrector (PFC). As capacitors C_1 and C_2 have to provide energy to the load for some time intervals,

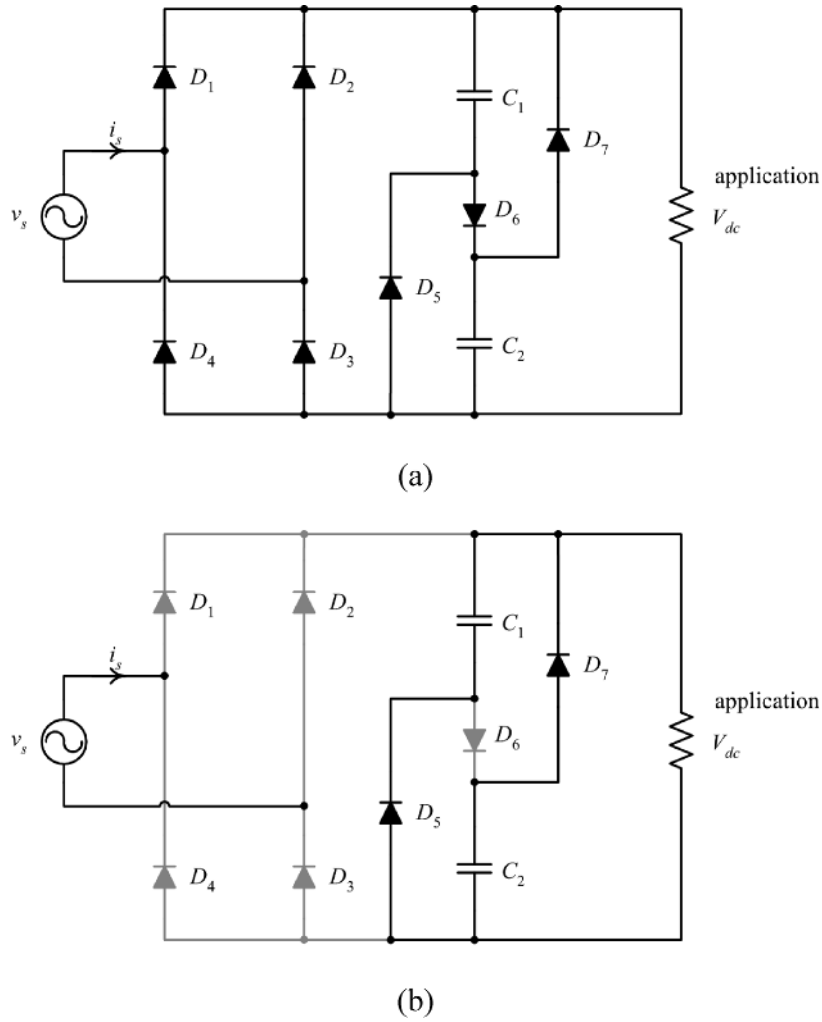

Figure 1.68 *Valley-fill power factor corrector (PFC): (a) circuit; (b) equivalent configuration for angle* ωt *[0°, 30°] and [150°, 180°]; (c) equivalent configuration for angle* ωt *[30°, 150°], except the capacitors charging period; (d) equivalent configuration for the capacitor charging period within the angle* ωt *[30°, 150°]; (e) waveforms of the mains voltage,* v_s*, input current,* i_s*, and load voltage,* V_{dc}.

they should have large values that increase with the load power, making the use of the valley-fill PFC unsuitable for high-power applications. (In such power applications, electrolytic capacitors, which have a short lifetime, are normally used, so solutions like that of a valley-fill circuit requiring additional capacitors are not welcome.) We shall see in Volume V better solutions for high-power applications.

Since there is a large current pulse when C_1 and C_2 are being charged in the valley-fill power factor corrector, there are some methods of reducing the pulse magnitude. The most popular method is to connect a current-limiting resistor in series with D_6, so that the capacitor charging current, and thus the supply current peak, can be reduced. Although the waveform of the input current can be improved by the valley-fill PFC solution, the output voltage remains problematic, because it is not a true DC but a rectified AC

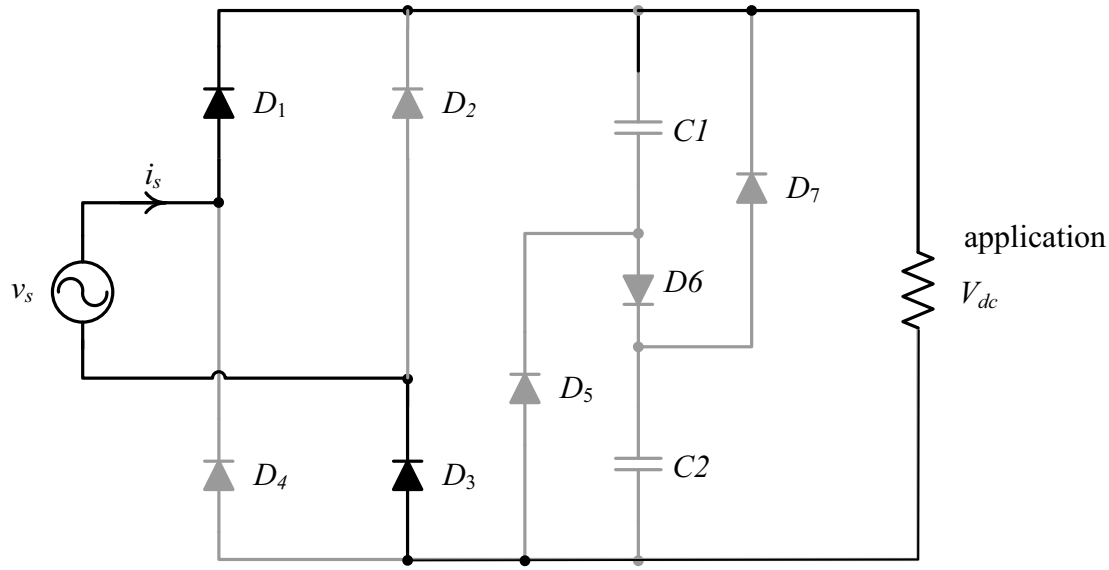

(c)

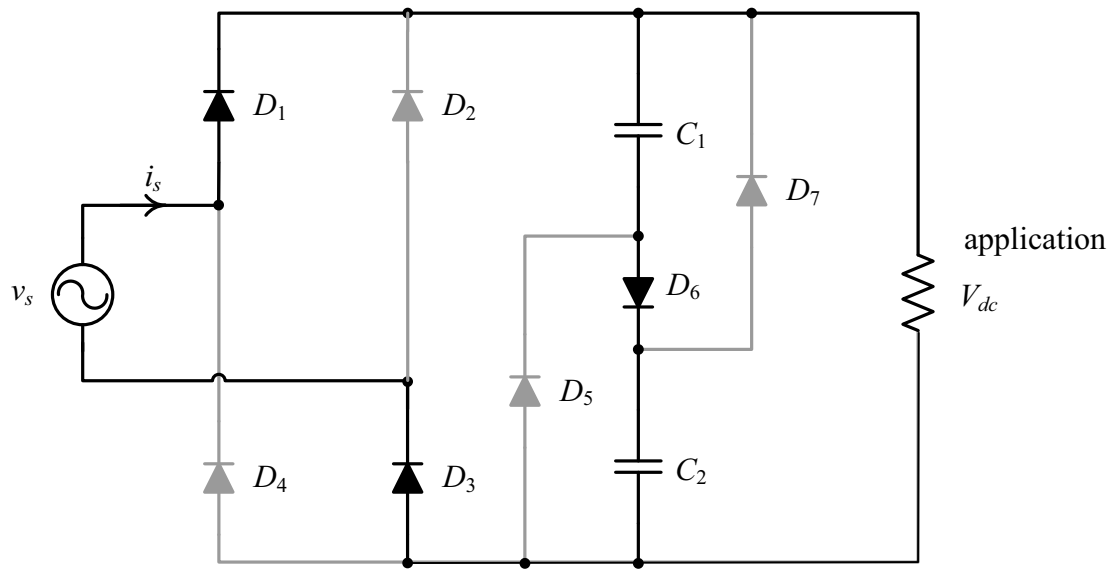

(d)

Figure 1.68 (*Continued*)

component superimposed onto a DC voltage. The magnitude of the voltage ripple is equal to one half of the peak voltage of the supply mains voltage, that is, $V_m/2$. Thus, unless the quality of the output voltage is unimportant, the DC load cannot be directly connected to the output of a valley-fill PFC. We would have to insert a DC-DC converter between the valley-fill PFC and load to tightly regulate the desired load voltage.

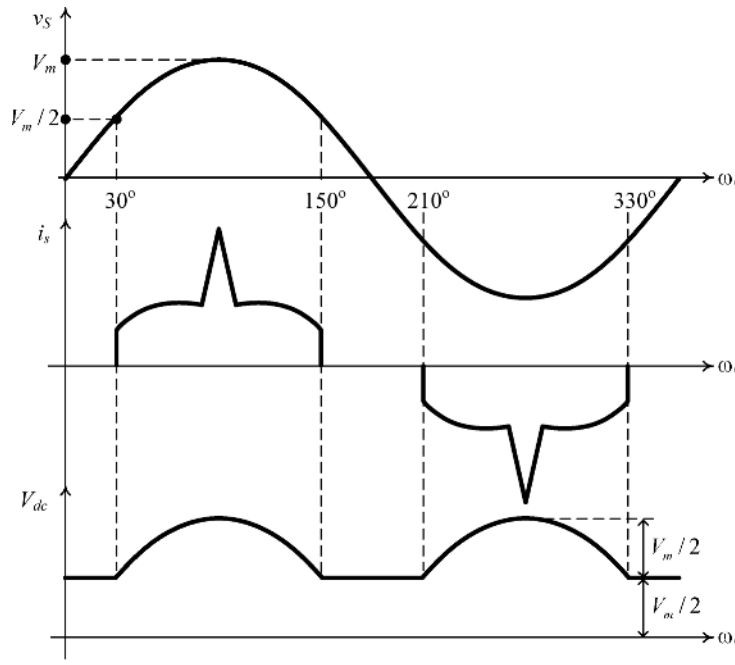

(e)

Figure 1.68 (*Continued*)

Let us revisit the requirements of an AC-DC converter. Firstly, its input current has to be sinusoidal. Secondly, the output voltage has to be tightly regulated. Then, the question is "how can a circuit draw a sinusoidal current from the supply mains?" Back to a simple AC-DC voltage conversion structure – a diode-bridge circuit. If we want to have a sinusoidal current drawn from the supply mains, the output current of the diode-bridge circuit has to be a rectified sinusoid. Denote v_{in} and i_{in} the output voltage and current of the diode-bridge circuit in the desired form of rectified sinusoids. Mathematically:

$$v_{in}(t) = V_m|\sin \omega t|$$

and

$$i_{in}(t) = I_m|\sin \omega t|$$

Then, the next question is "how can one process a rectified sinusoidal input voltage, draw a rectified sinusoidal current from the diode bridge, and give a tightly regulated DC voltage at the output?"

Recall that a DC-DC converter can process a variable non-negative input voltage and provide a constant DC output voltage. With a time-varying input voltage, the input current of the DC-DC converter can be shaped to be in phase with the input voltage. This means that we need to insert a DC-DC converter between the output of the diode-bridge rectifier and the load (Figure 1.69a). The desired waveforms v_{in} and i_{in} are shown in Figure 1.69b. Many DC-DC converter topologies have been proposed for use in AC-DC conversion. Nevertheless, no matter what the power processing method is, the ultimate goal is the same. To understand the principle, use here one of the basic DC-DC converters discussed in Section 1.2 to illustrate how

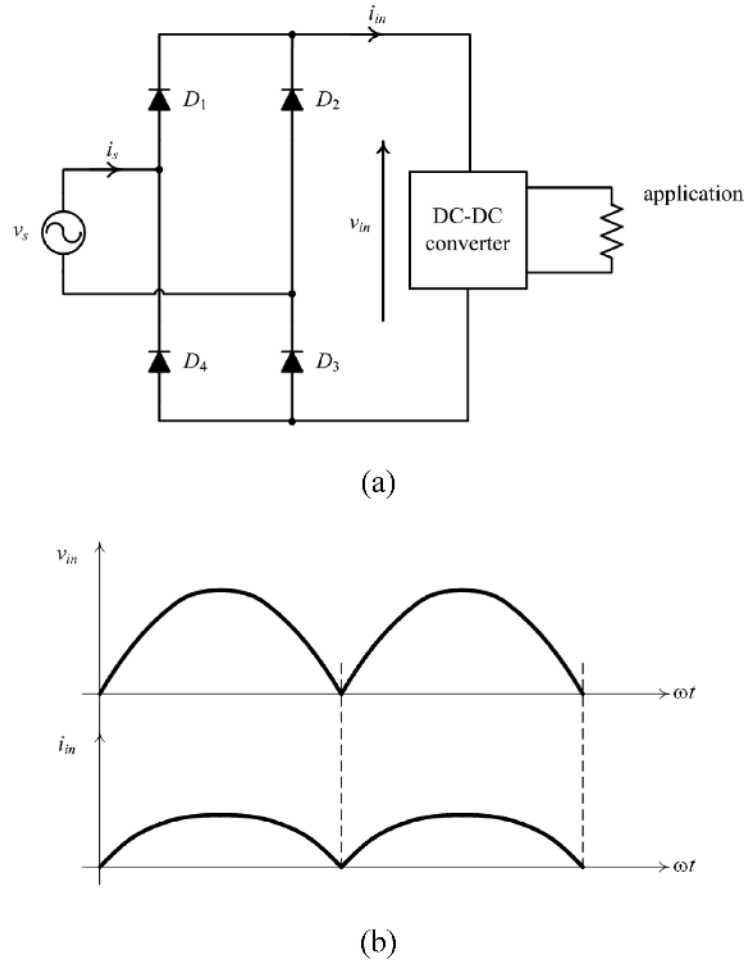

Figure 1.69 *Diode-bridge circuit followed by a DC-DC converter in AC-DC conversion: (a) circuit; (b) required voltage and current at the diode-bridge output.*

the AC-DC conversion is performed. Among the three basic DC-DC converters the boost converter has the main advantage that it can be designed to take a continuous input current, while the buck and buck-boost converters always take a pulsating input current. This is why a boost converter is used in the following discussion. However, it should be noted that the buck and buck-boost converters can also achieve the required objective.

The block diagram of the AC-DC converter using a boost DC-DC converter is shown in Figure 1.70. It is necessary to (a) shape the input current, i_{in}, as a rectified sinusoid in phase with v_{in}, and (b) regulate the output voltage, V_{out}. The controller senses and scales down the input voltage, v_{in}, and multiplies it with an error signal, v_{ctr}, from the output voltage error controller. The resulting signal is passed through a voltage/current converter V/I to generate a signal that serves as the reference current, i_{ref}. Similar to the control circuit seen in Section 1.4 for DC-DC converters, the output voltage error controller is typically a PI controller, which amplifies and integrates the error, ε, between the actual output, V_{out}, and V_{ref}. It has the transfer function $A(s)$. The scale-down resistive networks have

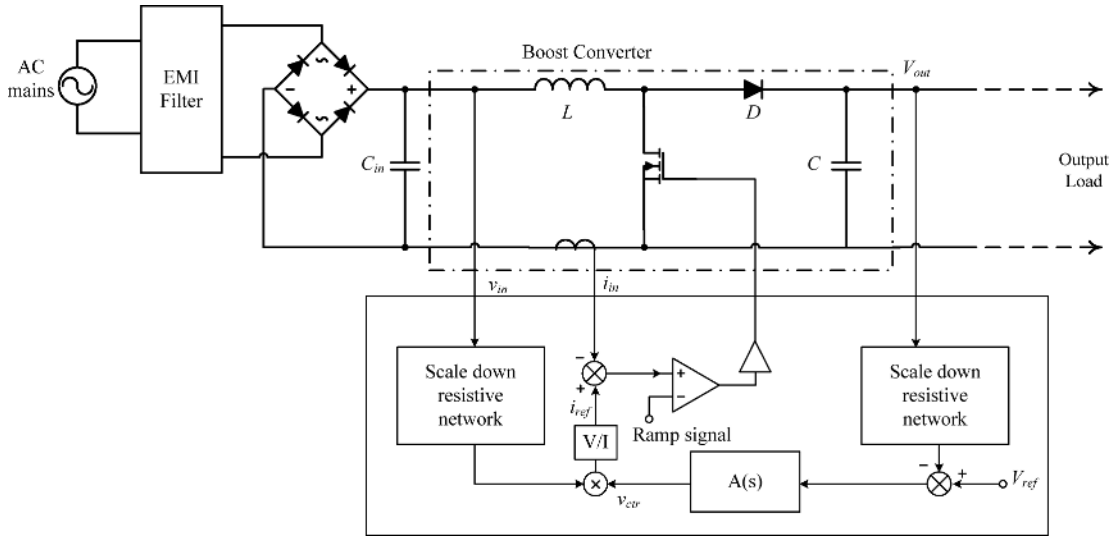

Figure 1.70 *Circuit diagram of an AC-DC converter with boost-type DC-DC converter.*

the purpose of reducing the power stage voltages v_{in} and V_{out} to smaller values suited for the control circuit. As in DC-DC converters, v_{ctr} is relatively constant in steady state. If V_{out} is lower than V_{ref}, v_{ctr} will increase. Then, i_{ref} will increase. Conversely, if V_{out} is higher than V_{ref}, v_{ctr} will decrease. Then, i_{ref} will decrease. The cutoff frequency of $A(s)$ is much lower than the line frequency, typically less than one-tenth of the line frequency, in order to avoid the line frequency signal from getting into ("jamming") the control loop.

The input current, i_{in}, is then shaped to follow i_{ref}, that is, as a rectified sinusoidal waveform in phase with v_{in}. The control method is based on comparing i_{in} and i_{ref}. If i_{in} is smaller than i_{ref}, the MOSFET will be turned on. If i_{in} is larger than i_{ref}, the MOSFET will be turned off. Practically, a stabilizing ramp is added in the comparator for ensuring the system stability when the duty cycle of the MOSFET is larger than 0.5. (Details on the stability issue of the current-mode control will be discussed in Volume IV). With such a control method, the input current becomes a low-frequency waveform that follows the rectified input voltage, on which a high-frequency current ripple is superposed. The high-frequency ripple is due to the switching action in the boost converter: remember that in DC-DC converters the inductor is charged and discharged in each cycle of period T_s, thus creating a ripple of frequency, f_s, in the inductor current, which is also the input current. To attenuate the high-frequency current ripple that can interfere with the supply mains, a high-frequency, propylene or ceramic capacitor, C_{in}, is used to provide a low impedance path for the high-frequency current ripple. The value of this capacitor has to be small, such that at low frequency its impedance to be very large. As a result, it will not distort the fundamental component of the current, preventing it from flowing through C_{in}. At high frequencies, even if C_{in} has a small value, ωC_{in} is large, that is, the impedance of C_{in} takes a small value, creating a path for the high frequencies, which are thus eliminated from the input current. With the supply current in phase with the supply mains voltage, the AC-DC converter shown in Figure 1.70 is also named a *power factor pre-regulator* or *power factor corrector*, because it is sometimes connected in front of another power converter in order to keep the line current sinusoidal. In Volume V, we shall discuss different power factor correctors and control methods for the power factor corrector.

1.7.2 Inverters

One of the emerging trends in the electricity industry is a shift from large centralized to small distributed energy resources (DERs) located at the point of consumption. DERs have many advantages over traditional energy technologies, including improved asset utilization, better power quality, and enhanced power system reliability and capacity. The eco-energy sources, like solar cells and fuel cells, generate DC power. Thus, a grid-connected inverter is usually needed to convert the DC power into AC power, which is then fed into the electricity grid. Some standards, like IEEE-1547, have imposed performance requirements on inverters interconnecting with electric power systems. Even when the eco-energy source is not fed into the electricity grid but has to supply a local load, an AC voltage is still needed for many applications. So, we have to see how we can invert a DC voltage into an AC one.

A DC-AC converter, called an *inverter*, is used to produce, ideally, a pure sinusoidal waveform from a DC source. As shown in Figure 1.71, the ideal output voltage, v_{out}, is a sinusoid with the magnitude V_m and angular frequency $\omega = 2\pi/T$. Mathematically:

$$v_{out}(t) = V_m \sin \omega t$$

Let us start from the basic concept of generating an AC voltage from a DC voltage. Figure 1.72 shows a simple configuration having two DC sources. Each source provides a voltage V_{in}. There are two MOSFETs, S_1 and S_2, connected in totem-pair. They are operating in antiphase. That is, when S_1 is on, S_2 is off, and vice versa. The output load is connected across the mid node between S_1 and S_2, and the mid node between the two DC sources. The magnitude of the output load voltage, v_{out}, is dependent on the states of S_1 and S_2. When S_1 is on and S_2 is off, v_{out} is equal to V_{in}. When S_1 is off and S_2 is on, v_{out} is equal to $-V_{in}$.

Figure 1.73 shows the waveform of v_{out}, which is a square waveform – the simplest AC output waveform. However, the waveform obtained is far from the ideal sinusoid. How then can one get a sinusoidal waveform from the square waveform? The direct way is to use an output low-pass filter to attenuate the high-frequency harmonics. However, a square waveform is rich in low-frequency harmonics. Figure 1.74 shows the frequency spectrum of the square waveform. The magnitude of the n-th harmonic, $v_{out,n}$, is:

$$v_{out,n} = \frac{1}{n} v_{out,1}$$

where $v_{out,1}$ is the magnitude of the fundamental component.

To obtain only the fundamental harmonic at the load, the output filter should have a low cutoff frequency. Then, the value and physical size of the components used in the filter would be very large.

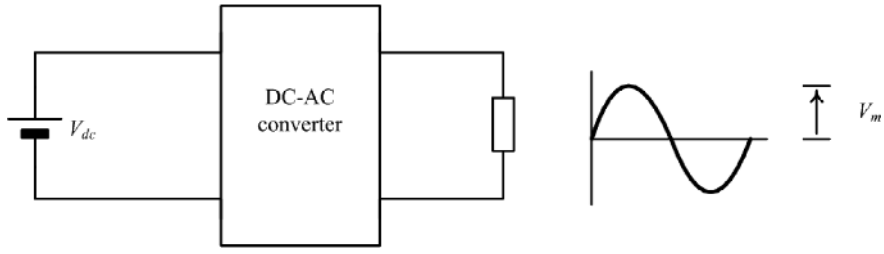

Figure 1.71 *Ideal inverter function.*

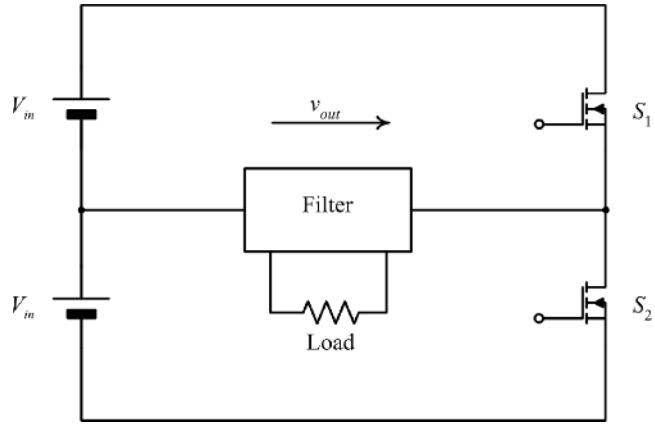

Figure 1.72 *Simple inverter circuit with two DC sources.*

How can the inverter circuit be modified such that the required value of the filter to be reduced? Consider the basic operation of a converter and compare its output with the ideal output waveform. Figure 1.75 shows the positive half-cycle of the ideal output voltage waveform, $v_{out,ideal}$. Consider a generic time instant, t_1. The value of the ideal output voltage waveform $v(t_1)$ is:

$$v_{out,ideal}(t_1) = V_m \sin \omega t_1$$

However, when S_1 is on, corresponding to the positive half-cycle considered in Figure 1.75, the actual output voltage is V_{in}. How can one convert V_{in} into $v_{out,ideal}(t_1)$? If we refer to Section 1.2, we can simply make use of the concept of DC-DC conversion, a buck type for example, for converting a DC voltage into another DC voltage of different value. As illustrated in Figure 1.75, if we switch S_1 (S_2 remains off) at a high frequency and the duty cycle of S_1 at t_1 is $d(t_1)$, the average value of v_{out} at t_1 is:

$$v_{out,avg}(t_1) = d(t_1)V_{in}$$

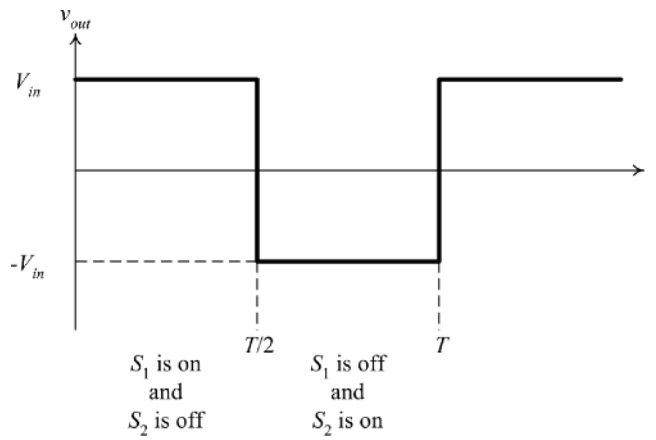

Figure 1.73 *Output waveform of the circuit shown in Figure 1.72 without filter.*

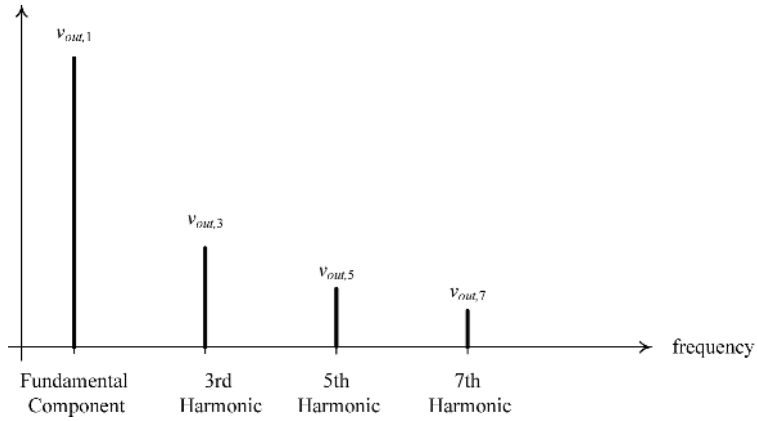

Figure 1.74 *Harmonic spectrum of the waveform shown in Figure 1.73.*

The duty cycle $d(t_1)$ must be controlled to make $v_{out,avg}(t_1) = v_{out,ideal}(t_1)$. Thus:

$$d(t_1) = \frac{v_{out,ideal}(t_1)}{V_{in}} = \frac{V_m}{V_{in}} \sin \omega t_1$$

It can be seen from the above equation that the duty cycle is time-varying, in other words it is "*modulated.*" The maximum value of the duty cycle depends on the ratio between the peak value of the ideal output voltage, V_m, and the DC voltage. This ratio is also called "modulation index," and is denoted by *M:*

$$M = \frac{V_m}{V_{in}}$$

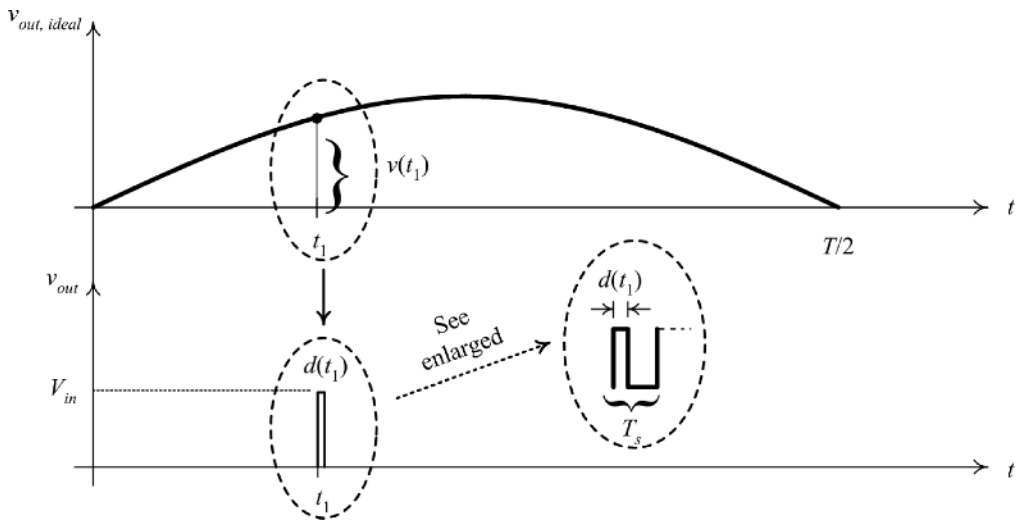

Figure 1.75 *Ideal output voltage waveform and the actual output voltage waveform.*

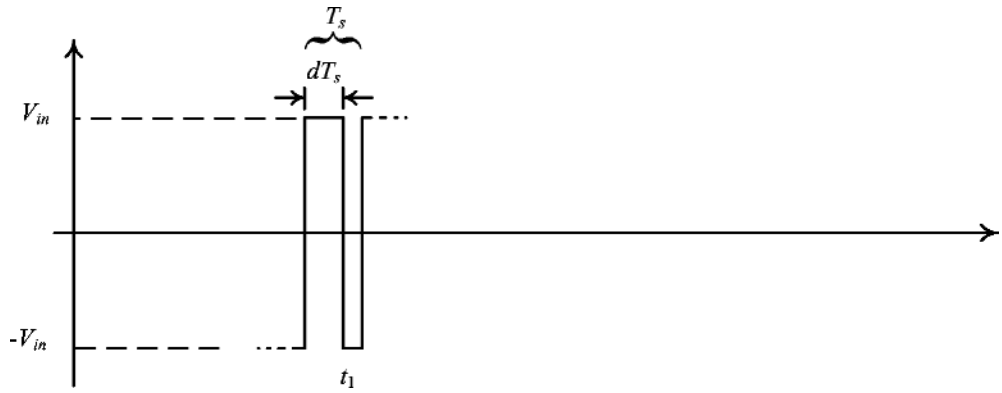

Figure 1.76 *Bipolar switching waveform.*

With the above technique, v_{out} will consist of the fundamental frequency (50/60 Hz) and switching harmonics. Depending on the power level of the inverter and characteristics of the switches, the switching frequency of S_1 and S_2 can be 100 times or even 1000 times higher than the fundamental frequency of the output. The frequencies of the switching harmonics are much higher than the fundamental frequency; they can be attenuated by a low-pass filter with a cutoff frequency lower than the switching frequency. As the cutoff frequency is still high, the physical size and value of the filter can be reduced in comparison with the filter needed for eliminating the harmonics from the AC square wave of Figure 1.73.

As the original value of v_{out} (without modulation – Figure 1.72) was either zero or V_{in} in the positive half-cycle, and either zero or $-V_{in}$ in the negative half-cycle, the modulation method described above is called *unipolar pulse width modulation* technique. The duty cycle of the switches starts from zero at the zero crossing point of v_{out} (remember that $v_{out}(t) = V_m \sin \omega t$) reaching its maximum value at the peak of the sinusoidal waveform, that is, at 90°.

There also exists another modulation technique, named the *bipolar pulse width modulation* technique. In the latter case, the value of v_{out} is switched between V_{in} and $-V_{in}$. The waveform is shown in Figure 1.76. At t_1, switch S_1 has the duty cycle $d(t_1)$, while switch S_2 has the duty cycle $[1 - d(t_1)]$. Thus, the average value of v_{out} is:

$$\begin{aligned} v_{out,avg}(t_1) &= d(t_1)V_{in} + (1 - d(t_1))(-V_{in}) \\ &= (2d(t_1) - 1)V_{in} \end{aligned}$$

Again, the duty cycle $d(t_1)$ is controlled to make $v_{out,avg}(t_1) = v_{out,ideal}(t_1)$, implying:

$$d(t_1) = \frac{1}{2}\left(1 + \frac{V_m}{V_{in}} \sin \omega t_1\right)$$

From the above equation it can be seen that the duty cycle of S_1 and S_2 is 0.5 at the zero crossing points of v_{out}.

The ideal output waveform with a unipolar modulation technique is obtained with a low switching loss, because only one switch can be turned on at any time, and presents a low total harmonic distortion, as we shall see in a detailed analysis in Volume V. However, the pulses near the zero voltage region (i.e., near the zero crossing points of v_{out}) are practically too narrow for the switching devices to respond and they will disappear in the actual output: the voltage $v_{out}(t) = V_m \sin \omega t$ has small values around $\omega t = 0, \pi, \ldots$, and

so on. There d has very small values and, practically, the actual switch does not have enough time to switch on and then, quickly, off. Pulse dropping also happens around the peak of the modulating signal. The advantage of the bipolar pulse width modulation is that the duty ratio of the pulses near the zero voltage regions is about 0.5. The output waveform distortion is low in this region. Nevertheless, the switching loss in bipolar pulse width modulation is higher than in unipolar pulse width modulation, as two switches are needed at any time. Apart from the above two modulation techniques, many other modulation techniques have been proposed for reducing the total harmonic distortion. These will be discussed in detail in Volume V.

For certain applications, it is necessary to generate a high-frequency sinusoid. An example is the electronic ballast for a fluorescent lamp. The efficacy (lumen per watt) at a high-frequency operation (above 20 kHz) is higher than that at the line-frequency operation by more than 10%. Moreover, the physical size and weight of the electronic ballast can be highly reduced with a high-frequency operation. Is it possible to use the above described pulse width modulation technique to generate a high-frequency sinusoid? Let us consider an example. If a 20 kHz AC sinusoidal waveform is required, by using the above pulse width modulation technique, a switching frequency at least 100 times higher than the output waveform frequency is needed. The required switching frequency would be then equal to $100 \times 20\,\text{kHz} = 2\,\text{MHz}$. As the switches are in hard-switching, the switching loss would be too large at such a high switching frequency. Therefore, we have to find another method to generate a high-frequency AC voltage waveform from a given DC voltage.

To generate a high-frequency sinusoid, it is possible to make use of the resonant technique, as in the resonant converters discussed in Section 1.6. A typical circuit of the electronic ballast is shown in Figure 1.77. It consists of two MOSFETs, which are operated in antiphase. The duty cycles of the switches S_1 and S_2 are equal and slightly less than 0.5. A capacitor of large value, C, is added. The DC voltage across it can be considered constant during a switching cycle. Its role is to prevent a DC component of the current flowing through the lamp. This is why C is called a DC blocking capacitor. The current flowing through the lamp will only contain an AC component. In steady state, as no DC current can flow through C, C is submitted to the voltage V_{dc} when S_1 is in the on-state and S_2 in the off-state, that is, for approximately half of the cycle, and to a zero voltage when S_1 is off and S_2 is on, that is, for approximate the other half of the cycle. The value of C is large. As the switching frequency of S_1 and S_2 is high, in order to obtain a high frequency AC voltage across the lamp, the period of a switching cycle is small. Consequently, in a steady-state cycle, the voltage on C does not vary too much. We can assume that the voltage across it is equal to the constant average value $V_{dc}/2$. Let us firstly explain the operation of the inverter when the fluorescent lamp is off. In this situation, the lamp behaves like an open circuit of infinite resistance. If the switching frequency of S_1 and S_2 is close to the resonant frequency of the resonant circuit formed by L_r and C_r, the voltage across the lamp is theoretically infinite. This can ignite the lamp with a high voltage.

After the lamp has been ignited, it behaves like a resistor. To analyze the operation of the circuit in a typical steady-state cycle, consider that at a moment t_0, S_2 is conducting (Figure 1.77b). The voltage across the parasitic capacitance of the switch C_{S2} is then zero and the voltage across C_{S1} is V_{dc}. The voltage v_{AB} is given by $v_{AB} = -V_{dc}/2$. At t_0, S_2 is turned off. The resonant inductor current, i_{Lr}, will divide into two currents of value $i_{Lr}/2$ (as it is assumed that $C_{S1} = C_{S2}$), slowly charging (depending on the values of the capacitance and load current) C_{S2} from zero to V_{dc} and discharging C_{S1} from V_{dc} to zero (Figure 1.77c). Therefore, the presence of the parallel capacitance assures the zero voltage (ZVS) turn-off of S_2. During the interval $[t_0, t_1]$, following the charging and discharging processes of C_{S2} and C_{S1}, respectively, the voltage v_{AB}, given by $v_{AB} = -V_{dc}/2 + v_{CS2}(t)$, is increasing from $-V_{dc}/2$ to $V_{dc}/2$. When C_{S1} is completely discharged at t_1, the antiparallel diode of S_1, D_1, starts conducting naturally. The voltage v_{AB} becomes equal to $v_{AB} = V_{dc}/2$ (Figure 1.77d). After t_1, during the conduction interval of D_1, the gate signal for turning on S_1 is applied. Like in a resonant converter, S_1 is turned on here with zero voltage. When i_{Lr} reaches zero,

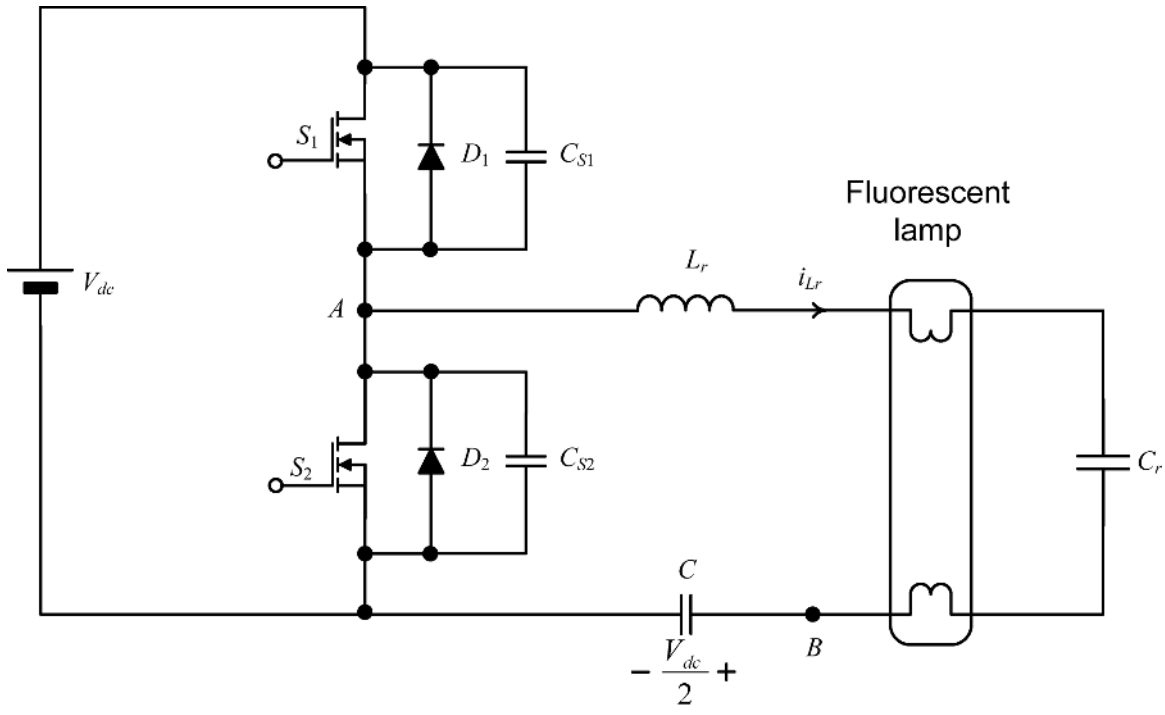

(a)

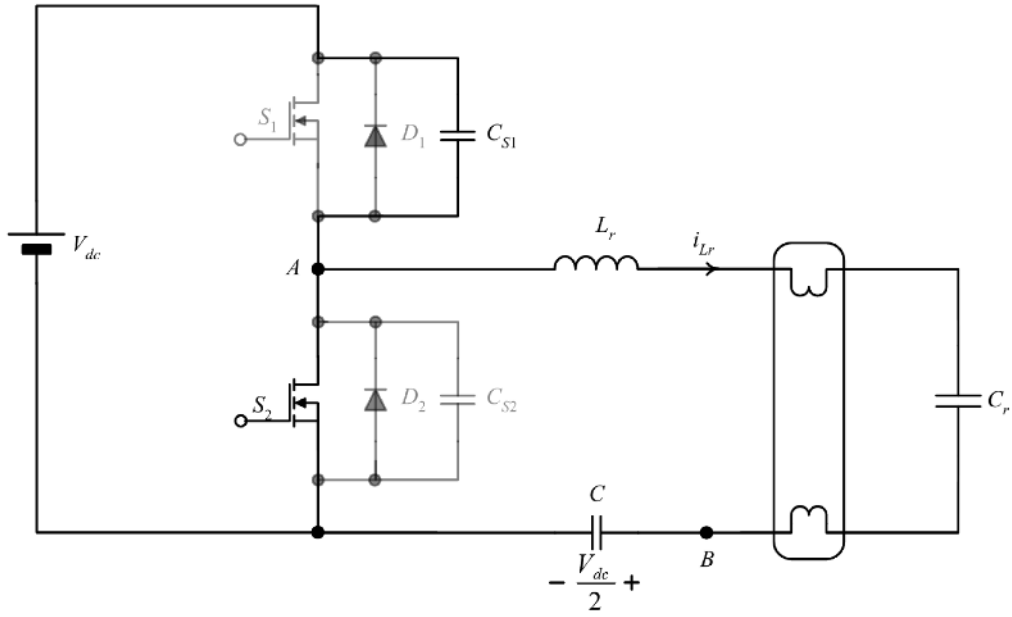

(b)

Figure 1.77 *An electronic ballast: (a) circuit schematic; (b) before* t_0*; (c)* $[t_0, t_1]$*; (d)* $[t_1, t_2]$*; (e) from* t_2*.*

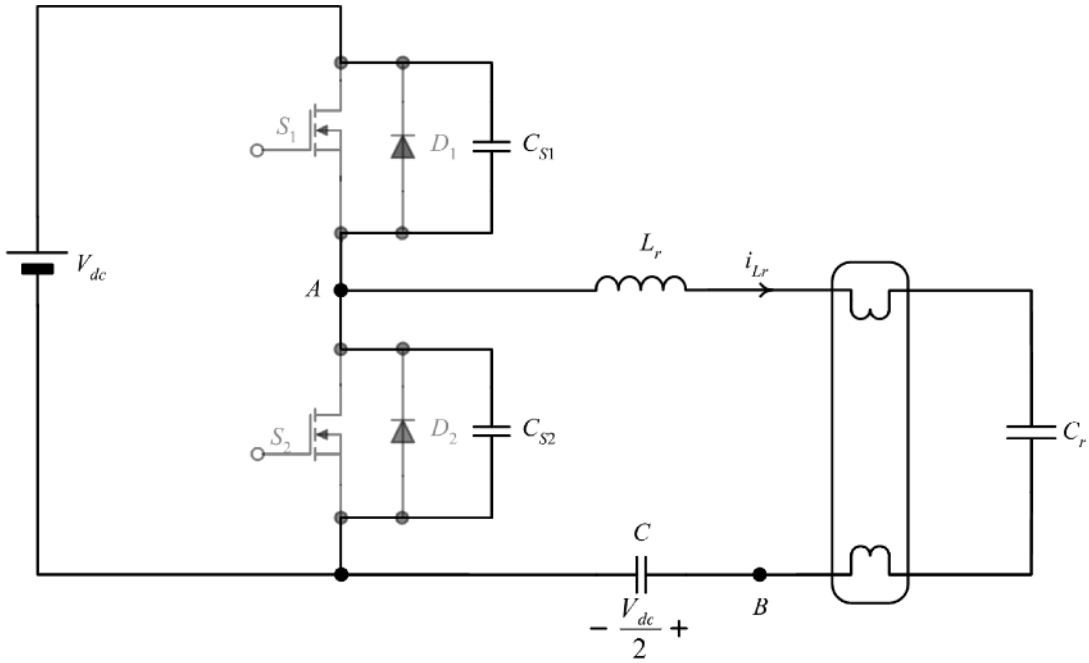

(c)

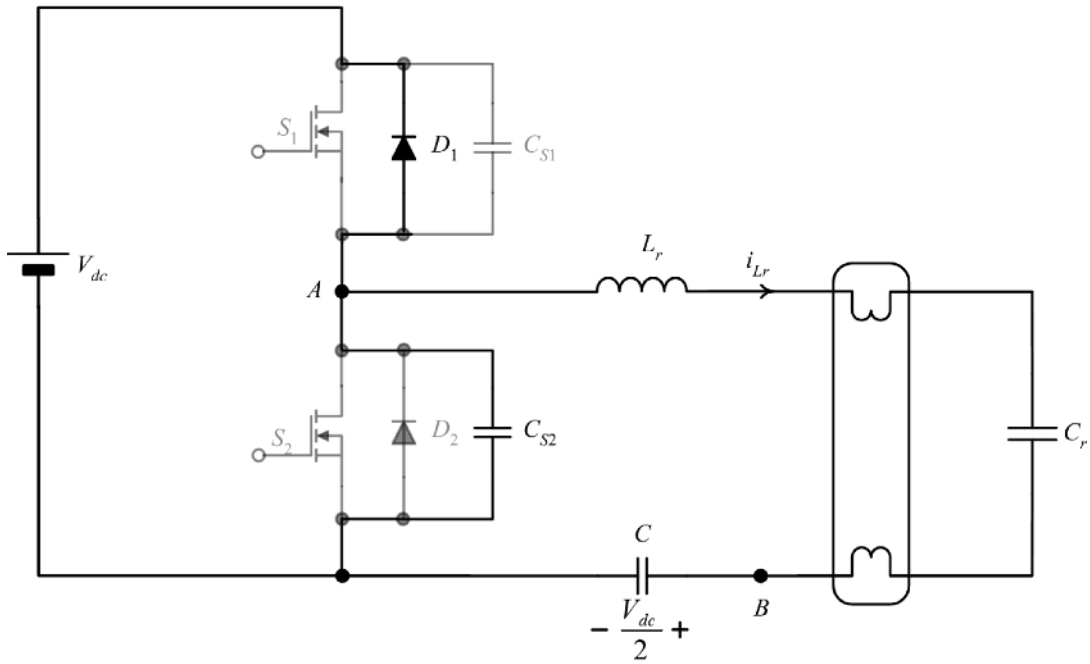

(d)

Figure 1.77 (*Continued*)

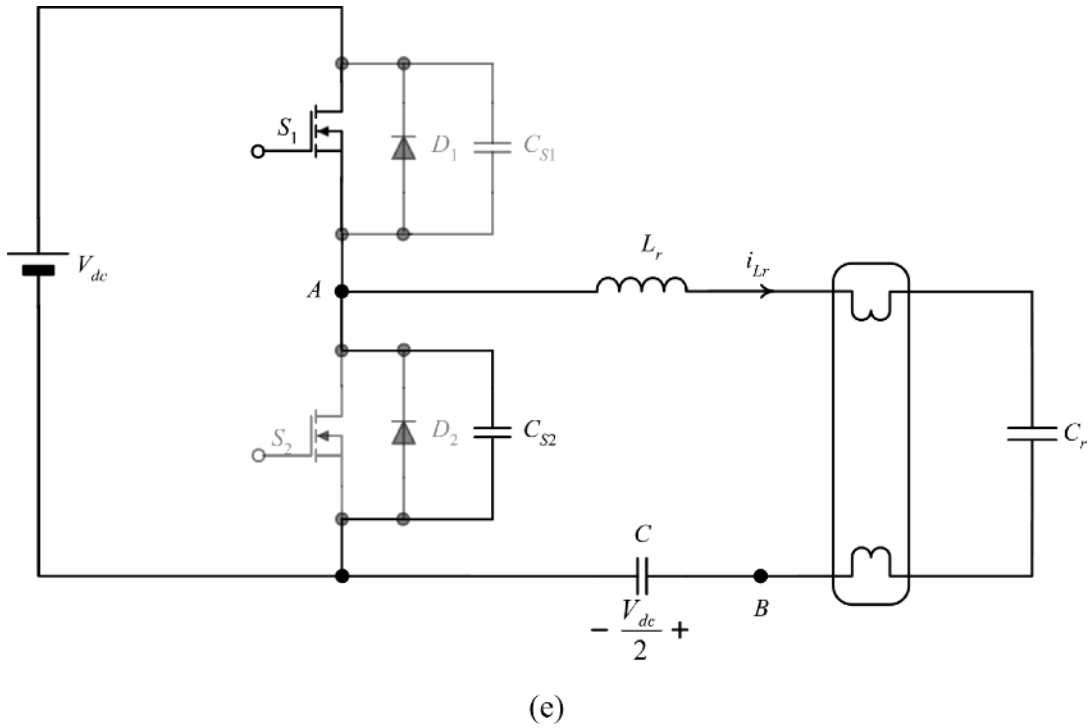

(e)

Figure 1.77 (*Continued*)

at t_2, D_1 stops conducting and S_1 takes over the current i_{Lr}, which changed its direction (Figure 1.77e). The operation is similar for turning off S_1 and turning on S_2. Figure 1.78 shows the waveforms of voltage v_{AB} and inductor current i_{Lr}.

The equivalent circuits of the topological stages shown in Figure 1.77b–e are *RLC* networks. By solving the second-order differential equations governing each one of these circuits, we can find the sinusoidal expression of i_{Lr}. Its frequency is the switching frequency of S_1 and S_2, f_s. We saw previously that the ignited lamp has a resistive character; therefore, the voltage across it will also be a sinusoid of frequency f_s. It is up to us to choose this frequency as high as is needed to get a good efficacy of the fluorescent lamp.

We can understand now the difference between the pulse width modulation technique and resonant technique in generating the AC voltage. In the PWM technique, the frequency of the output voltage is much lower than the switching frequency. In the resonant one, the frequency of the output voltage is the same as the switching frequency. Thus, the former technique generates a low-frequency output, while the latter one generates a high-frequency output.

The practical applications requiring a DC-to-AC inversion are various, comprising requirements like low frequency – high-power output, high frequency – low-power output, low power – high-voltage output, and many more. Each one of these cases has to be treated in a different manner, resulting in different topologies of inverters. A good part of Volume V will be dedicated to their study.

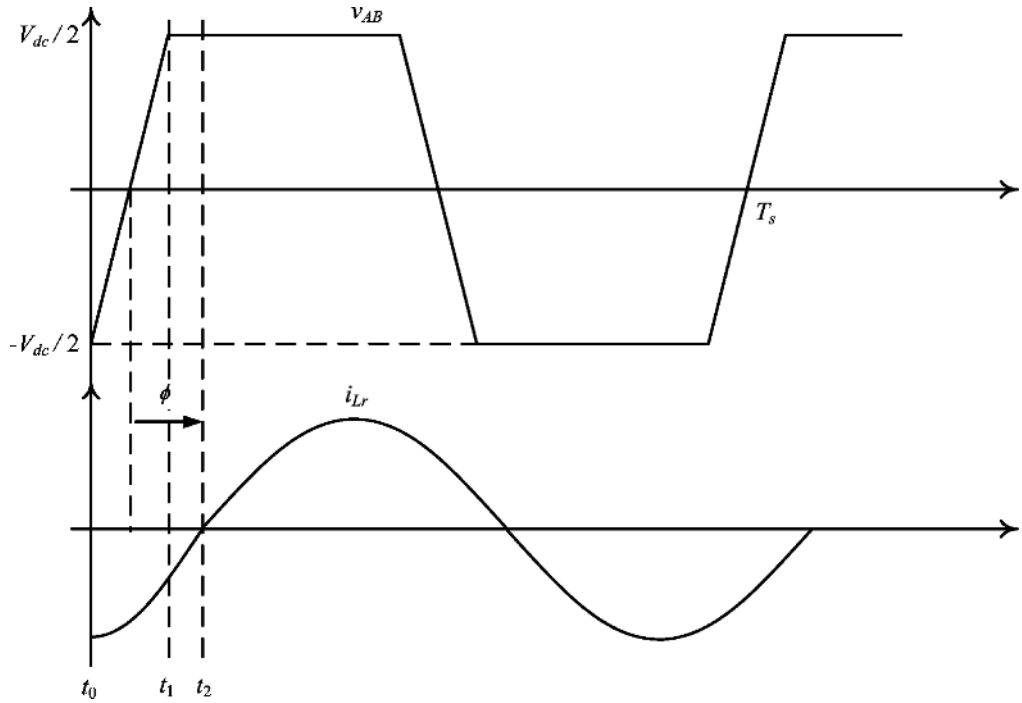

Figure 1.78 *Waveforms of the voltage between nodes "A" and "B" and inductor current, i_{Lr} for the electronic ballast.*

1.8 Case Studies

1.8.1 Case study 1

Keith, a fresh engineer, was asked by his supervisor to design a buck converter. The specification of the converter is given in Table 1.9. The converter is operated in continuous conduction mode. After two weeks, Keith came up with a design, which is shown in Figure 1.79. Unfortunately, the circuit could not operate properly.

a. Discuss why the design does not operate properly.
b. Modify the circuit structure so that it can meet the specification.
c. Derive the expressions for the peak value of I_{in} and the output voltage ripple, respectively, in terms of the duty cycle D of the MOSFET, V_{in}, I_{out}, V_{out}, L, C, and f_s.
d. What have to be the minimum values of the output capacitor C and output inductor L?

Table 1.9 *Specification of the buck converter*

Input voltage, V_{in}	9–12 V	Output power	2.5–5 W
Output voltage, V_{out}	5 V	Output voltage ripple	1%
Switching frequency, f_s	100 kHz		

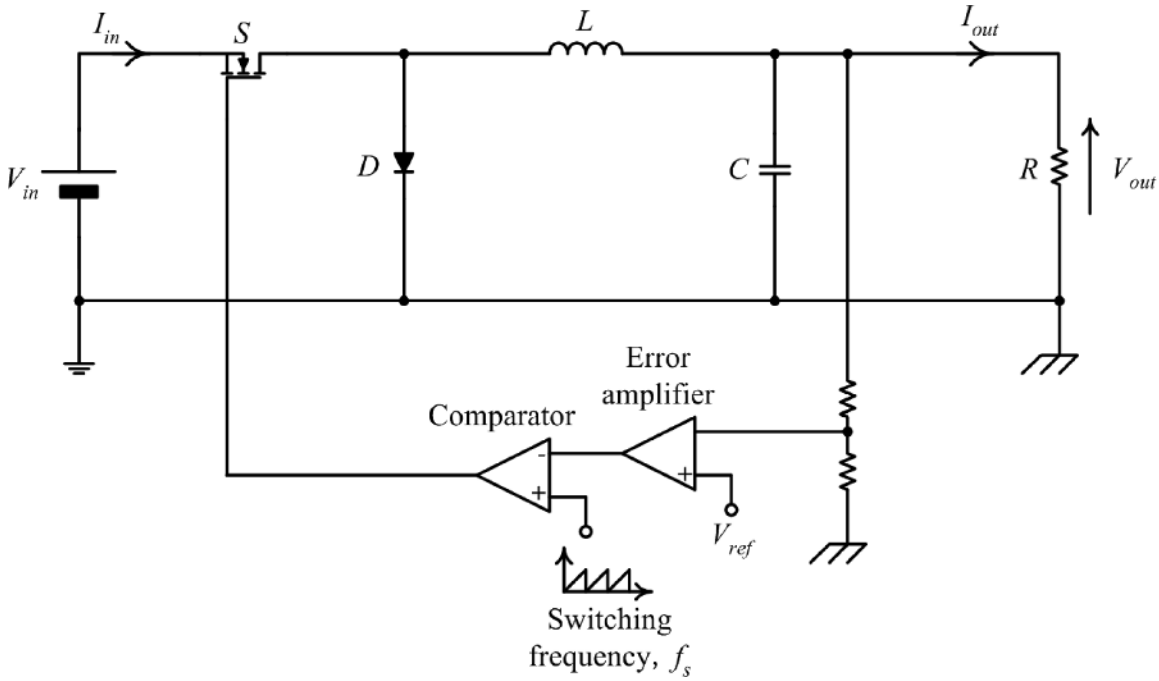

Figure 1.79 *Schematic diagram of Keith's circuit.*

Answer

a. The circuit does not operate properly for the following reasons:
   1. The MOSFET is wrongly connected. As illustrated in Figure 1.80, the supply voltage is short-circuited by the body diode of the MOSFET S and the freewheeling diode D. As shown in Figure 1.81, the connections of the drain and source of the MOSFET, and the anode and cathode terminals of the freewheeling diode, should be swapped.
   2. The inverting and noninverting inputs of the comparator should be swapped. In the Keith's circuit, the duty cycle of the MOSFET would be reduced if the output voltage, V_{out}, was smaller than the output voltage reference, V_{ref}, which is obviously wrong.
   3. The circuit also requires a floating gate drive, because when the MOSFET is in the on-state, the freewheeling diode voltage, V_D, is equal to V_{in} (assuming that the MOSFET has a zero on-state resistance). Thus, in order to keep the state of the MOSFET, the gate voltage would have to be $12\,\text{V} + 4.5\,\text{V}$ (plateau voltage) $= 16.5\,\text{V}$. It would be necessary to derive 16.5 V from the input voltage 12 V! Such a technical challenge can be solved by using a bootstrap capacitor circuit as presented in Figure 1.30.

b. Figure 1.81 shows a recommended structure for the buck converter. Readers may have other suggestions.

c. Figure 1.82 shows the waveforms of the gate signal, v_g, output voltage, v_{out}, inductor current, i_L, and capacitor current, i_C. During the interval DT_s, i_L is charged, that is, i_L increases from its minimum to its maximum value. During the period $(1 - D)T_s$, when the MOSFET S is off, i_L decreases from its maximum value to the minimum value. Denote by ΔI the ripple of the inductor current during a steady-state

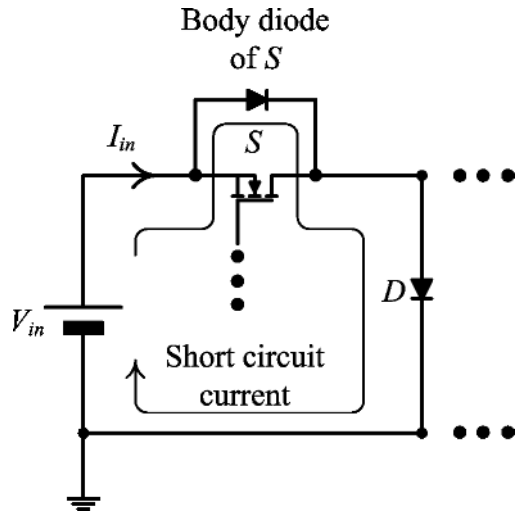

Figure 1.80 *Short-circuit current path formed by the body diode of* S *and freewheeling diode* D *in the proposed circuit of Figure 1.79.*

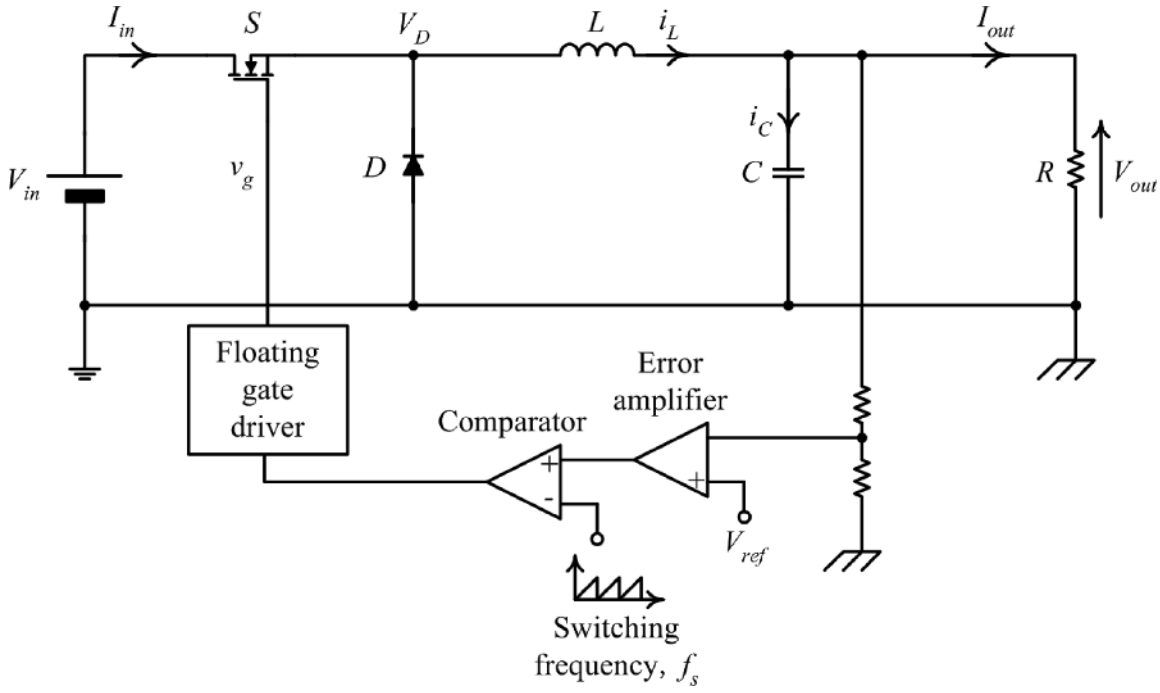

Figure 1.81 *Modification of the circuit given in Figure 1.79.*

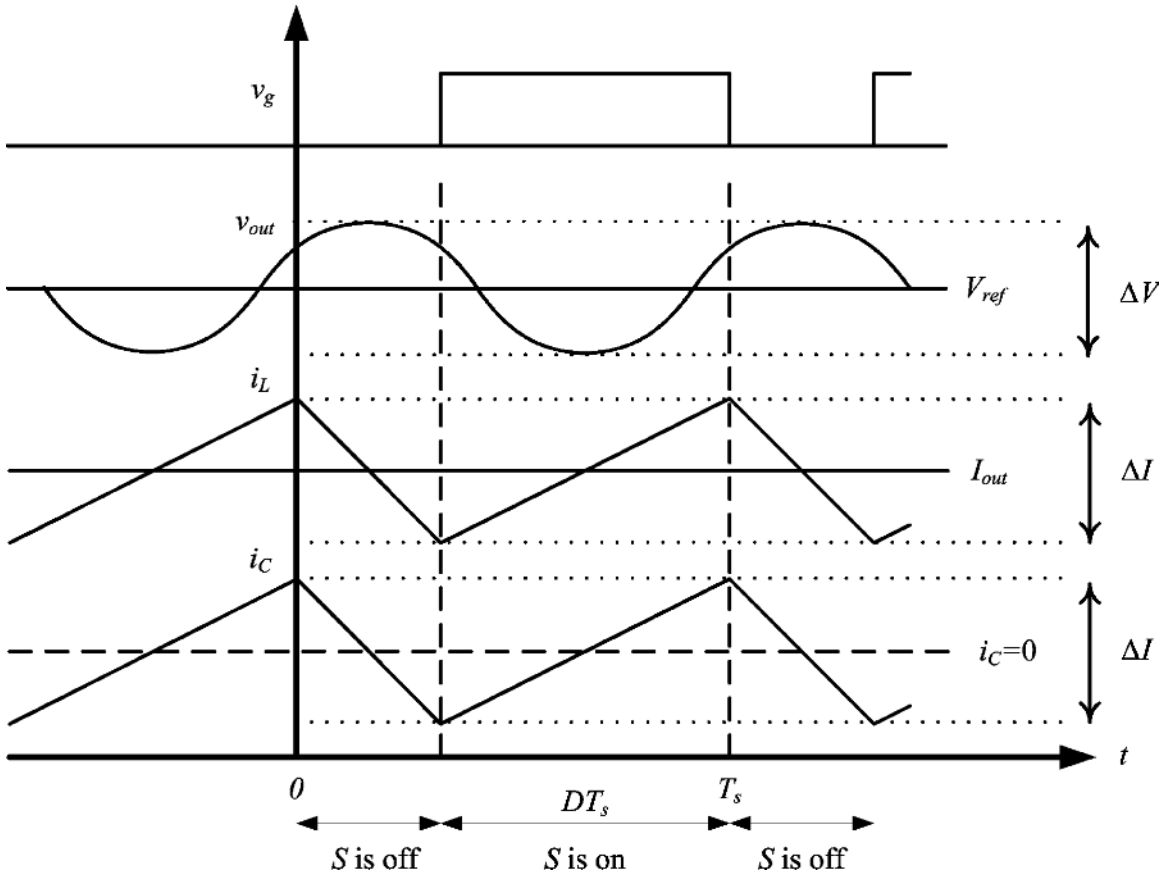

Figure 1.82 *Main waveforms of the buck converter.*

cycle, that is, the difference between the maximum and minimum values of i_L:

$$V_{out} = L\frac{\Delta I}{(1-D)T_s}$$

giving

$$\Delta I = \frac{V_{out}(1-D)T_s}{L}$$

The peak value of the input current I_{in} is equal to the peak value of the inductor current i_L, $I_{L,peak}$. In steady state, the average inductor current is equal to the output current I_{out} because the average capacitor current is zero. Thus, the peak value of I_{in}, $I_{in,peak}$ is:

$$\begin{aligned} I_{in,peak} &= I_{L,peak} = I_{out} + \frac{\Delta I}{2} \\ &= \frac{V_{out}}{R} + \frac{1}{2}\frac{V_{out}(1-D)T_s}{L} \end{aligned}$$

For calculating the output voltage ripple, it is assumed that all of the inductor current ripple goes to the output capacitor. This is valid because the output capacitor provides a low impedance path for the inductor current ripple. As no DC current can flow through C, it means that the current i_C is formed by the AC part (the ripple) of i_L. ΔI of the inductor current ripple indicates also the capacitor current ripple.

During the interval [0, DT_s], with 0 denoting the instant when S is turned on in the considered steady-space cycle, i_C can be described by the equation:

$$i_C(t) = \frac{\Delta I}{DT_s}t - \frac{\Delta I}{2}$$

with

$$i_C(0) = -\frac{\Delta I}{2}, \text{ indicating the minimum value of } i_C$$

$$i_C\left(\frac{DT_s}{2}\right) = 0, \text{ indicating the first zero-crossing of } i_C$$

$$i_C(DT_s) = \frac{\Delta I}{2}, \text{ indicating the maximum value of } i_C$$

With a simple integration, one obtains the equation of v_C:

$$v_C(t) = v_C(0) + \frac{1}{C}\left(\frac{\Delta I}{2DT_s}t^2 - \frac{\Delta I}{2}t\right),$$

with

$$v_C\left(\frac{DT_s}{2}\right) = v_C(0) - \frac{\Delta I}{8C}DT_s,$$

indicating the minimum value of v_C (as the differential of v_C, i_C is zero at $DT_s/2$ and the second derivative of v_C is positive) and:

$$v_C(DT_s) = v_C(0)$$

During the interval [DT_s, T_s], i_C can be described by the equation:

$$i_C(t) = \frac{\Delta I}{2} - \frac{\Delta I}{(1-D)T_s}(t - DT_s),$$

with

$$i_C\left[DT_s + \frac{(1-D)T_s}{2}\right] = 0, \text{ indicating the second zero crossing of } i_C$$

$$i_C(T_s) = -\frac{\Delta I}{2}, \text{ indicating the minimal value of } i_C$$

giving the equation of v_C:

$$v_C(t) = v_C(0) + \frac{1}{C}\left[-\frac{\Delta I}{2(1-D)T_s}(t - DT_s)^2 + \frac{\Delta I}{2}(t - DT_s)\right],$$

with

$$v_C\left[DT_s + \frac{(1-D)T_s}{2}\right] = v_C(0) + \frac{\Delta I}{8C}(1-D)T_s,$$

indicating the maximum value of v_C and:

$$v_C(T_s) = v_C(DT_s) = v_C(0)$$

By neglecting the equivalent series resistance of C, it results that the analytical expressions of v_{out} are identical to those of v_C for the two switching stages (note that here we denote with v_C and v_{out} the AC components, not the instantaneous values of the respective voltages). Accordingly, v_{out} was drawn in Figure 1.82 (note that the waveform is not a sinusoid, but its form is due to the quantity t^2 in its expressions). The output voltage ripple, ΔV, can be calculated as the difference between the maximum and minimum values of v_C as:

$$\Delta V = \frac{\Delta I}{8C}T_s$$

From Figure 1.82, we can also notice that, at the beginning of the on-stage, i_C is negative, showing that the capacitor is discharging to the load. During this period, the source (V_{in}) energy is transferred to the inductor and load. After half of the DT_s interval, i_C becomes positive, showing that the source energy is used to charge C, in addition to charging L and giving energy to the load. In the first half of the off-interval, i_C is positive, showing that the inductor energy is used for charging the capacitor, in addition to supplying the load. In the second half of the off-topology, i_C becomes negative, showing that L and C are both discharging on the load.

The time interval between two zero crossings of i_C is $T_s/2$. Based on Figure 1.82, the average value of the capacitor current when $i_C > 0$, $I_{C,avg,ch}$ is:

$$I_{C,avg,ch} = \frac{1}{2}\frac{T_s}{2}\frac{\Delta I}{2}\frac{1}{T_s/2} = \frac{\Delta I}{4}$$

giving another way of calculating the output voltage ripple, ΔV, as the integral of $I_{C,avg,ch}$ over $T_s/2$:

$$\Delta V = \frac{T_s}{2}\frac{1}{C}I_{C,avg,ch} = \frac{V_{out}(1-D)}{8LC}{T_s}^2$$

d. The value of the inductor, L, is chosen such that the current through the inductor never drops to zero, that is, the converter operates in CCM, according to the problem's requirement. We need $i_{Lmin} > 0$, or, according to Figure 1.82:

$$\frac{\Delta I}{2} < I_{out}$$

$$\frac{1}{2}\frac{V_{out}(1-D)T_s}{L} < I_{out}$$

$$L > \frac{R}{2}T_s(1-D)$$

Table 1.10 *Calculated minimal values of the inductor and capacitor for case study 1*

Output power (W)	Load resistance (Ω)	V_{in} (V)	D	Minimum value of L (μH)	Minimum value of C (μF)
2.5	10	9	0.5556	22.22	25
		12	0.4167	**29.17**	25
5	5	9	0.5556	11.11	50
		12	0.4167	14.58	**50**

Therefore, the above equation gives the minimum value of the inductor that can ensure continuous conduction mode operation. The boundary condition between CCM and DCM is reached in the case where the decreasing inductor current reaches zero exactly at the end of the switching cycle. The value of L for an operation at the boundary condition is obtained by changing the above inequality to an equality.

The value of the output capacitor, C, is chosen such that the percentage of the output voltage ripple from V_{out} (i.e., the "percentage output voltage ripple") is less than 1%, as required in the problem's specification:

$$\frac{\Delta V}{V_{out}} = \frac{(1-D)}{8LC} T_s^2 < 0.01$$

$$C > \frac{(1-D)}{8(0.01)L} T_s^2$$

The above equation gives the minimum value of the output capacitor.

The minimum duty cycle, $D_{\min}$, is calculated at the input voltage of 12 V:

$$D_{\min} = \frac{5}{12} = 0.4167$$

The maximum duty cycle, $D_{\max}$, is calculated at the input voltage of 9 V:

$$D_{\max} = \frac{5}{9} = 0.5556$$

As a result, for the converter operating in CCM with the load power from 2.5 to 5 W and output voltage ripple less than 1%, the required minimum values of the inductor and output capacitor are calculated as in Table 1.10.

Based on the above results, the minimum required values of L and C are 29.17 μH and 50 μF, respectively, so that, for the entire load variation range, the converter will be operating in continuous conduction mode and its output voltage ripple will be less than 1%.

1.8.2 Case study 2

Figure 1.83 shows the circuit diagram of a bidirectional DC-DC converter used in the electrical system of a car. The car's battery gives the DC voltage, V_{dc}, of 12 V. To this DC rail there are connected several loads. One of the purposes of the battery is to give energy for the ignition of the motor. At ignition, the motor takes a very large current (200–300 A), which would require a very large battery. As the ignition moment is brief in the operation of a car, such a solution is not justified. Another possibility is to use an auxiliary source of

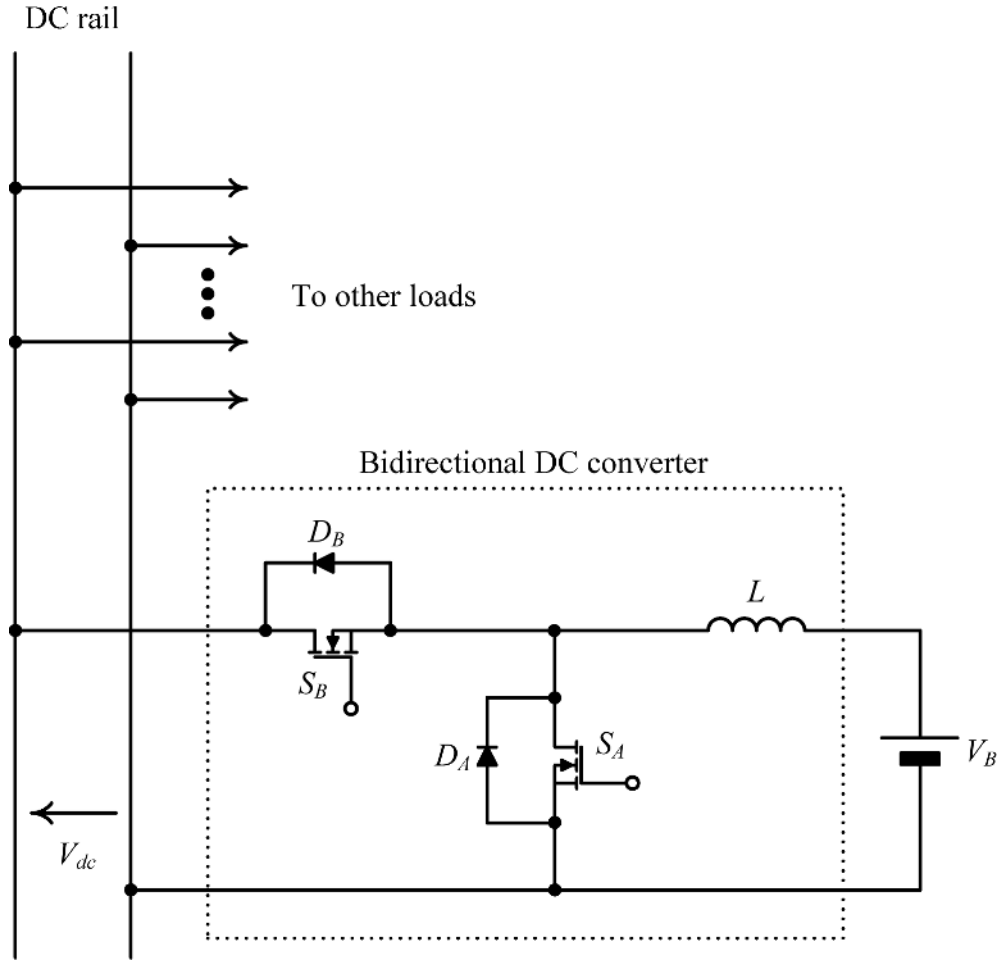

Figure 1.83 *Bidirectional DC-DC converter used in the electrical system of a car.*

energy (like a small battery or an ultracapacitor); its voltage is denoted in Figure 1.83 by V_B. The auxiliary source is connected to the DC rail by a bidirectional converter. The converter has two modes of operation: charging mode and discharging mode. At ignition, the source V_B provides energy to the DC rail. The converter operates in the discharging mode, its structure being that of a boost converter (regard the figure from the right to the left): V_B is the converter's input voltage now. The converter provides a voltage larger than V_B. During normal operation of the car, the battery V_B is charged by the DC rail. The converter operates in the charging mode, its structure being that of a buck converter (its output voltage is V_B).

a. Describe the operation when the converter is in the charging mode.
b. Describe the operation when the converter is in the discharging mode.
c. If the switching period of the converter is T_s, determine the minimum value of L so that the inductor current is nonzero during the discharging mode.
d. Suggest a modification of the above circuit to realize soft-switching. Discuss the merits and drawbacks of such a modification.

Answers

a. When the converter is in the charging mode, it is operated as a buck converter. As shown in Figure 1.84a, S_A is inhibited or is operated in synchronization with diode D_A (called a synchronous rectifier). The charging current is controlled by the duty cycle of S_B.
b. When the converter is in the discharging mode, it is operated as a boost converter. As shown in Figure 1.84b, S_B is inhibited or is operated in synchronization with the diode D_B (called a synchronous rectifier). The charging current is controlled by the duty cycle of S_A.
c. When the converter is in the discharging mode, it goes through two switching stages. They are shown in Figure 1.85.

When the MOSFET S_A is on:

$$V_B = L\frac{\Delta I}{DT_s}$$

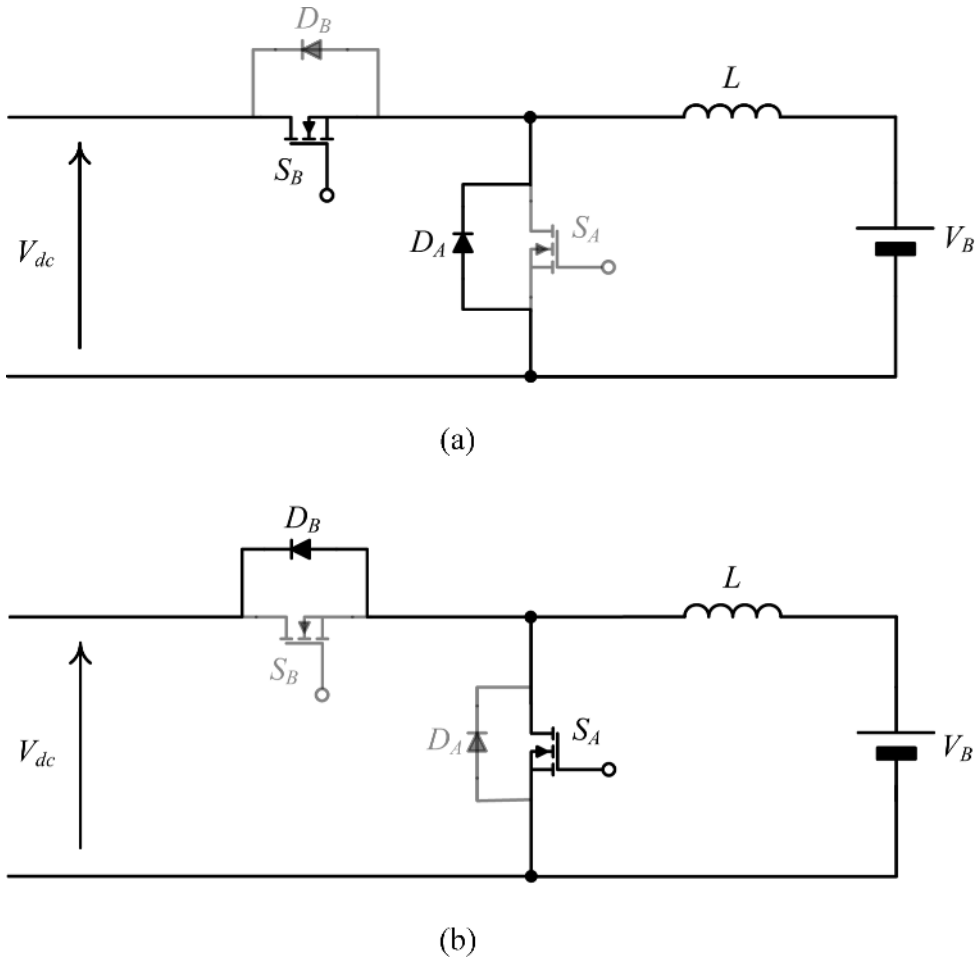

Figure 1.84 *Equivalent circuits of the bidirectional DC-DC converter: (a) charging mode; (b) discharging mode.*

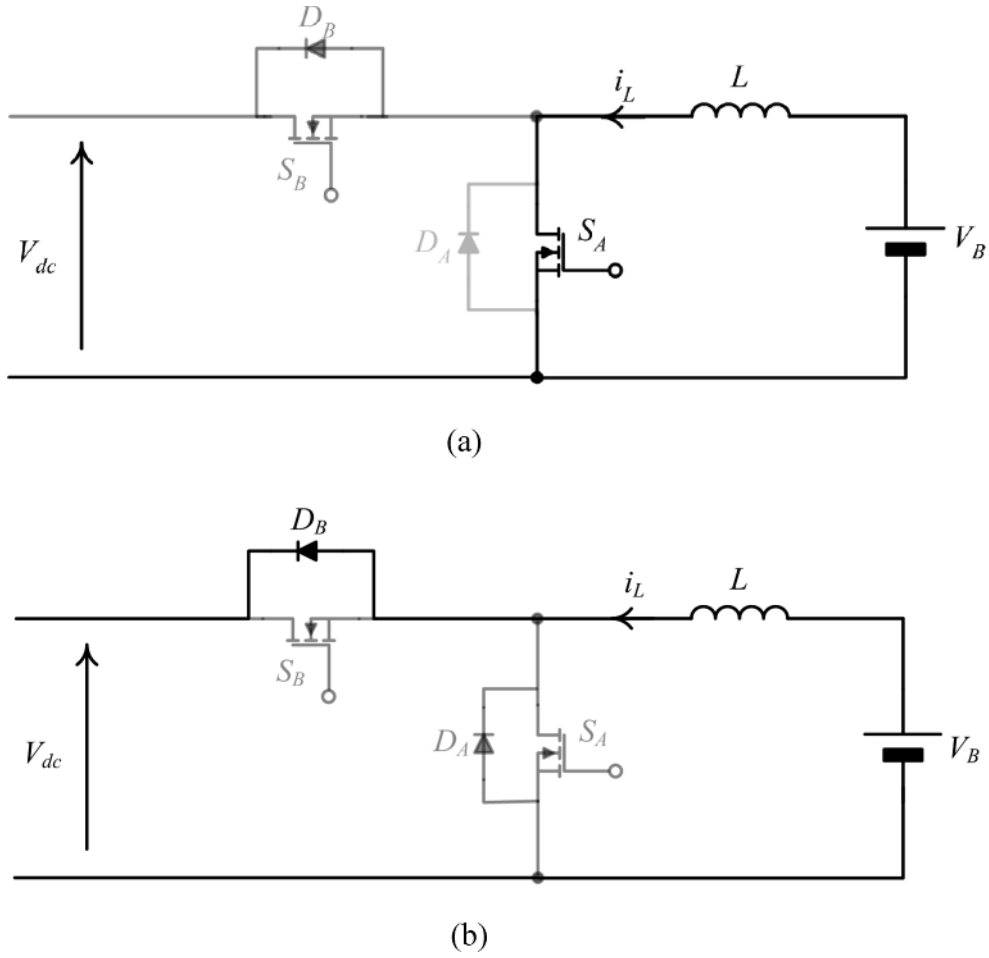

Figure 1.85 *Switching stages of the bidirectional DC-DC converter in the discharging mode: (a)* S_A *is on; (b)* S_A *is off.*

D being the duty cycle of S_A. It gives:

$$\Delta I = \frac{DV_B T_s}{L}$$

Figure 1.86 shows the gate signal v_g applied to MOSFET S_A and the inductor current waveform i_L.

To ensure that the inductor current never goes to zero, the average battery current, I_B, has to be larger than one half of the inductor ripple current, ΔI. That is:

$$I_B > \frac{\Delta I}{2}$$

$$> \frac{DV_B T_s}{2L}$$

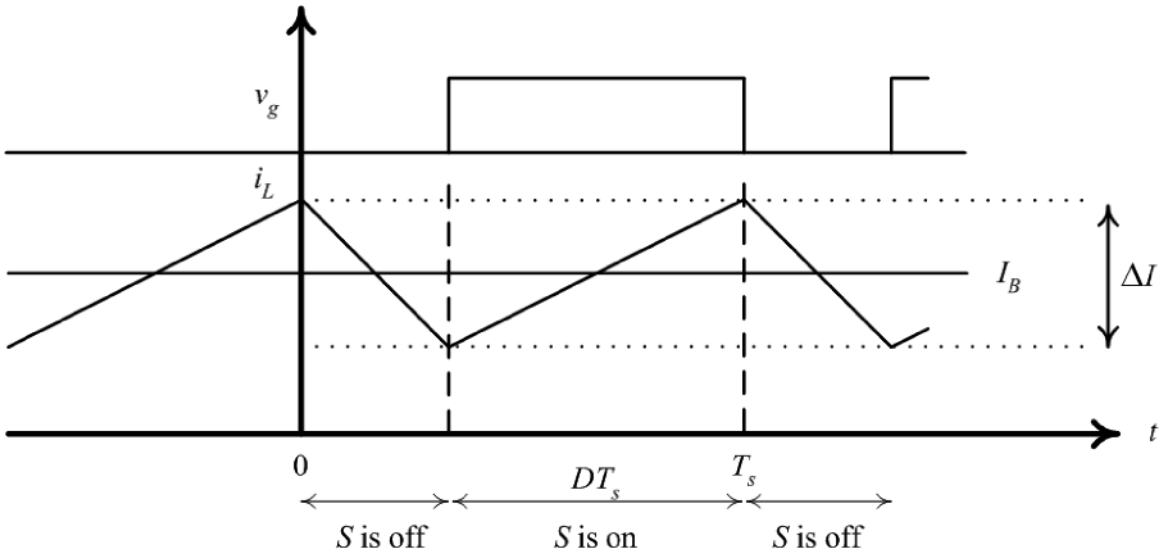

Figure 1.86 *Main waveforms of the bidirectional DC-DC converter of Figure 1.83 in the discharging mode.*

Assuming that the efficiency of the converter is 100%:

$$V_{dc}\, I_{dc} = V_B\, I_B$$

the output current, I_{dc}, is:

$$I_{dc} = (1 - D) I_B$$

implying

$$I_{dc} > \frac{D(1-D)V_B T_s}{2L}$$

$$L > \frac{D(1-D)V_B T_s}{2I_{dc}}$$

The above equation gives the minimum value of the inductor such that the converter is operating in the continuous conduction mode in the discharging mode.

d. As discussed in Section 1.6.2, one of the feasible ways of modifying the converter into a soft-switching one is to add an LC resonant tank to each switch (resonant switch). The main advantages are low switching losses and low electromagnetic interference. The main disadvantages are limited soft-switching range (as will be seen in Volume III), additional passive components, extra current/voltage stress on the switches, and variable frequency operation. We shall see in Volume III better ways to tackle the later problems, while keeping the advantages of zero voltage/current switching.

1.8.3 Case study 3

A company has to produce a new DC power supply. During the design process, the company charged one of its engineers to conduct an experiment to study the switching characteristics of the designed converter.

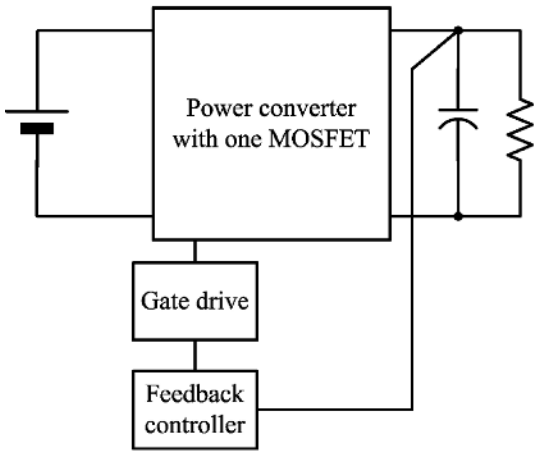

(a)

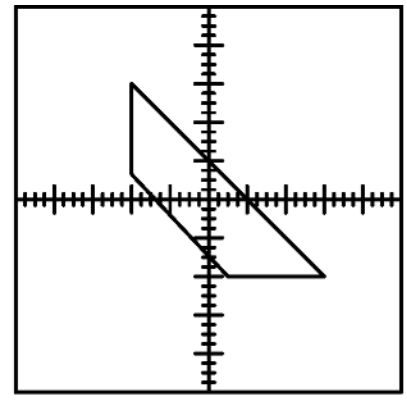

(b) Switch current (Ch Y): 2A/div;

Switch voltage (Ch X): 20V/div

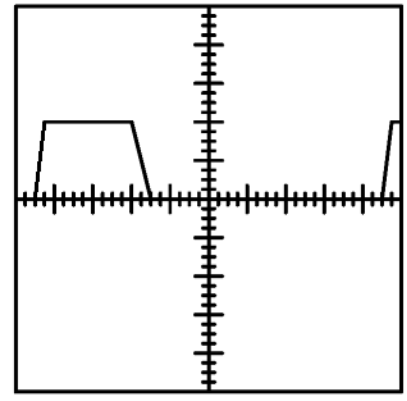

Switch current: 5A/div

Time base: 2μs/div (0.5μs/subdiv)

(c)

Figure 1.87 *Experiment conducted on a power converter containing one MOSFET: (a) converter scheme; (b) X-Y plot of the switch voltage and current; (c) oscillogram of the switch current.*

The general scheme of the converter, which contains one MOSFET, is presented in Figure 1.87a. The engineer is particularly interested in studying the duration of the transient times of the switch and finding the value of the switching loss. If the switching loss is too large, he may consider adding a soft-switching snubber, and repeating the experiment to verify again the switching loss with the new switching trajectories. Figure 1.87b shows the experimental X-Y plot of the MOSFET voltage and current, and Figure 1.87c shows

the time waveform of the MOSFET current as obtained on an oscilloscope. For simplicity, the on-state resistance of the MOSFET is assumed to be zero.

a. Based on the experimental figures, the engineer had to determine:
   i. the turn-on and turn-off times of the MOSFET
   ii. the switching frequency of the MOSFET.
b. To sketch the time waveforms of the MOSFET voltage and current.
c. To calculate the switching loss of the MOSFET.
d. To find a method for reducing the turn-off time of the MOSFET.

Answers

a. To study this case, it is necessary to identify the operating conditions of the MOSFET by using its switching trajectories. Based on Figure 1.87b, the on/off states of the MOSFET are illustrated in Figure 1.88. The young engineer has to deal here with a trick he has not learnt at university: when taking the switching trajectories in the laboratory, he correctly arranged the traces in the center of the page to avoid running off of it. However, then, he should have found the actual axes from his understanding of the switch operation: when the switch is on, the voltage across it is approximately zero, and when the switch is off, the current through it is zero. According to this observation, he has to shift the axes to the bottom-left of the figure, as shown with dotted lines in Figure 1.88.
   i. Based on Figure 1.87c, the turn-on time (the time taken from the off-state to on-state) is given by one subdivision of time, which is equal to 0.5 μs (in the figure, one division, with 2 μs/div, has four subdivisions). The turn-off time (the time taken from the on-state to off-state) is given by two subdivisions, which is equal to 1 μs.

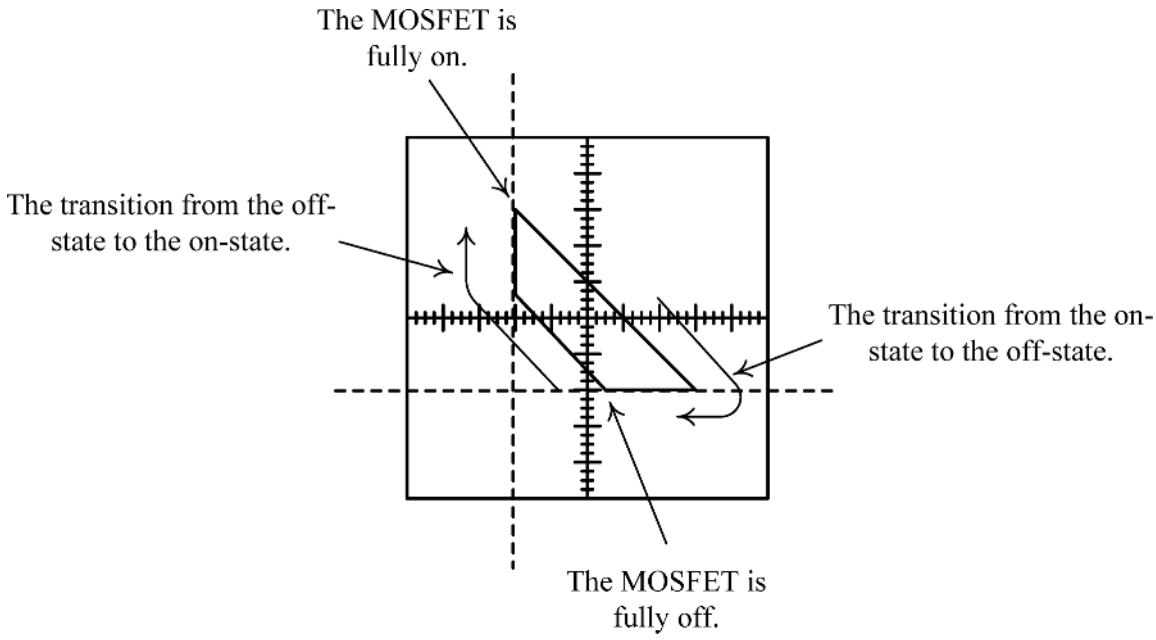

Figure 1.88 *Illustration of the states of the MOSFET in the circuit shown in Figure 1.87 (switch current (Ch Y): 2A/div; switch voltage (Ch X): 20 V/div).*

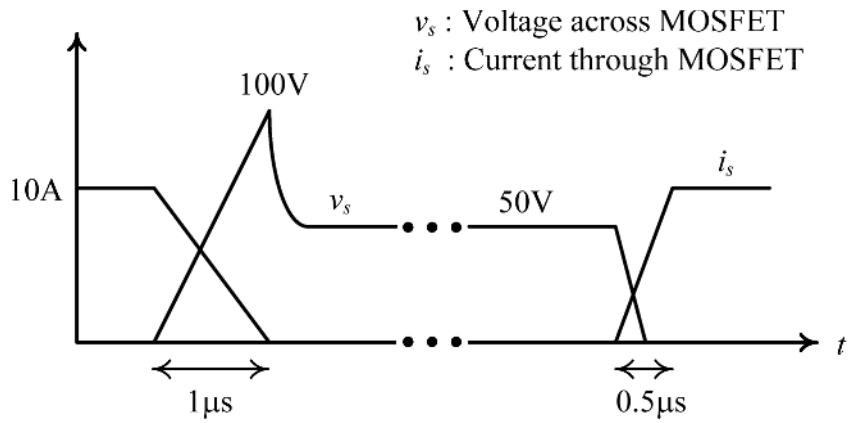

Figure 1.89 *Switching trajectories of the MOSFET in the converter shown in Figure 1.87.*

ii. Based on Figure 1.87c, the switching frequency of the MOSFET is 1/(9 divisions × 2 μs/div), which is equal to 55.56 kHz.

b. Figure 1.89 shows the time waveforms of the MOSFET voltage and current, which are derived by combining the waveforms taken from Figure 1.87b and c. Start from the point when the MOSFET is fully turned on. According to Figure 1.88 (the axes with dotted lines), its voltage is zero and its current is 10 A (five divisions of 2 A/div). When the switch turns off, its current decreases linearly to zero and its voltage increases to 100 V (five divisions of 20 V/div), and then decreases to the fully off-state voltage of 50 V (2.5 divisions). At turning on, the voltage decreases to zero and the current increases at 5 A (which is reached when the voltage dropped to zero), and then increases to 10 A for the fully on-state.

c. As discussed in Section 1.3.5.1, the turn-on power loss ($P_{sw(ON)}$) and turn-off power loss ($P_{sw(OFF)}$) of the MOSFET are given by:

$$P_{sw(ON)} = \frac{V_{off\_state} I_{on\_state}}{6} t_r f_s$$

$$P_{sw(OFF)} = \frac{V_{off\_state} I_{on\_state}}{6} t_f f_s$$

In calculating the turn-on loss, note that the voltage drops to zero after 0.25 μs. At that moment, the current is 5 A. When calculating the turn-off loss, note that during the transient time of 1 μs the current dropped from 10 A to zero and the voltage increased from zero to 100 V. Thus, the total power loss P_{loss} is equal to:

$$\begin{aligned} P_{loss} &= P_{sw(ON)} + P_{sw(OFF)} \\ &= \frac{1}{6}(50 \times 5 \times 0.25 \times 10^{-6} + 100 \times 10 \times 1 \times 10^{-6}) \times 55.56 \times 10^3 \\ &= 9.84\,\text{W} \end{aligned}$$

d. To reduce the turn-off time of the MOSFET, we must quickly extract the charge stored in the gate-source capacitance. A simple method is to use a PNP transistor (Figure 1.90). When its gate signal has a logic value: low, the transistor provides a short-circuit path for the gate-source capacitance to neutralize its stored charge. Such a circuit has an additional advantage of eliminating nuisance triggering of

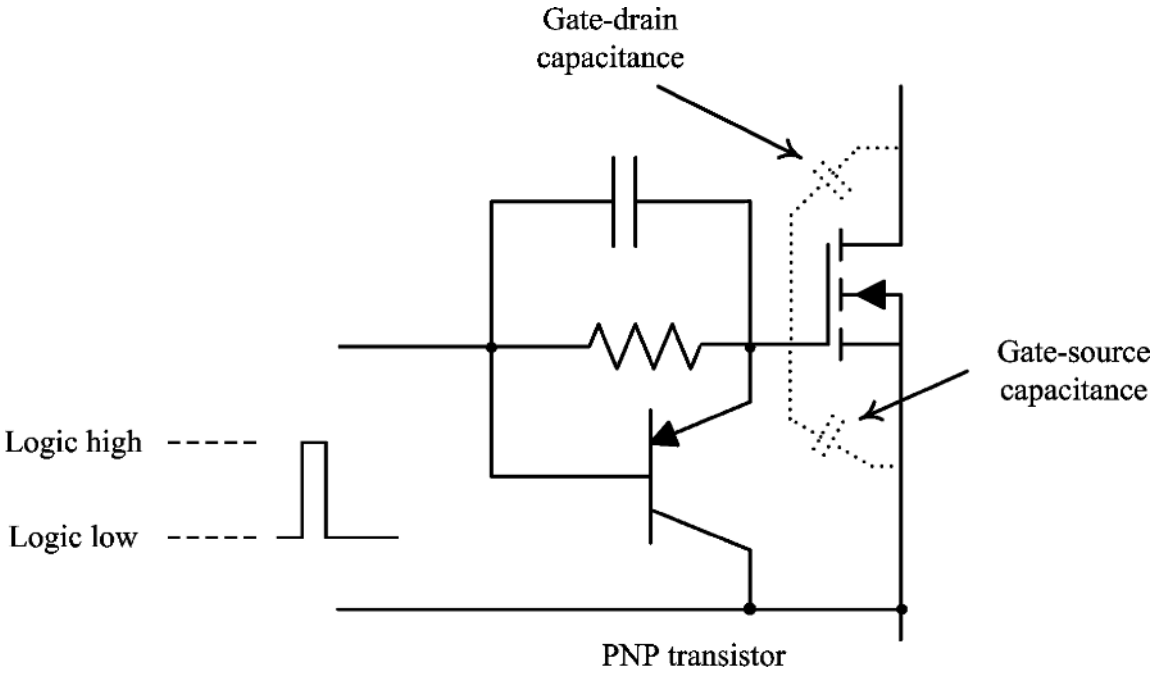

Figure 1.90 *Method of reducing the turn-off time of the MOSFET.*

the MOSFET: if the drain voltage of the MOSFET is changing quickly due to what happens in another part in the converter, a gate current would be generated through the gate-drain capacitance, partially turning on the MOSFET. The added PNP transistor will create a bypass to the source for such a gate-drain capacitance current and, as a result, the undesired current will not get into the gate. Another method of reducing the turn-off time is the use of a negative gate voltage in the off-state. However, this solution requires an additional circuit for generating the negative voltage.

1.9 Highlights of the Chapter

- Power electronics circuits are widely used in every practical area of our life.
- Power electronics convert energy, so their efficiency is of prime interest.
- Power electronics circuits operate in a switching mode. They must deliver a controllable output voltage despite variations in the supply voltage or load.
- The regulation function is realized by controlling the amount of energy transferred from the source to load per switching cycle: duty cycle (PWM) control and switching frequency control are the regulation means.
- The switching devices and passive elements are chosen to satisfy the maximum levels of voltages and currents that the devices have to withstand in their operation by adding a safety margin. For the same voltage and current ratings, choose the elements with less conduction and/or switching losses, and longer life expectancy.

- The energy losses are dissipated as heat, so a better efficiency means also a smaller cooling system.
- The DC-DC hard-switching converters are used for their simplicity and robustness. They also represent the basic topologies for the development of DC-DC soft-switching converters, AC-DC rectifiers, and DC-AC inverters.

Problems

1.1. Derive the formulas of the switching losses in devices.

(Hint: For converters without inductors, write the time functions of I_D and V_{DS} during t_{r2} and t_{f2} and calculate the average power.)

1.2. Calculate the switching loss of the switch Infineon SPP17N80C3 when the switch is used in a buck converter with the input voltage of 300 V and output current of 4 A. The switching frequency of the converter is 100 kHz. [A: $P_{SW(ON)} = 0.9$ W, $P_{SW(OFF)} = 0.36$ W.]

(Hint: use Figure 1.10 and Table 1.1, and neglect t_{r3} and t_{f3}.)

1.3. By applying the volt-second balance to the inductor in a boost converter, derive its DC conversion ratio.

(Hint: Refer to Table 1.7)

1.4. By applying the volt-second balance to the inductor in a buck converter, derive its DC conversion ratio.

1.5. Derive an ampere-second balance for a capacitor in a basic DC-DC converter.

(Hint: analogous to the development of the volt-second balance on an inductor.)

1.6. Use the ampere-second balance method to re-derive the DC voltage conversion ratio and DC current conversion ratio for the basic converters.

1.7. There is a boost converter (Figure 1.7) with input voltage $V_{in} = 48$ V and load resistance $R = 12\,\Omega$. The required average output voltage is 120 V. The value of the inductor, L, is 290 μH and of the capacitor, C, 330 μF. The converter is operated at the switching frequency of 100 kHz. Calculate (a) the duty cycle of the switch, (b) the average input current.

[Answers: (a) 0.6, (b) 25 A.]

1.8. For the same problem as above, calculate (a) the inductor current ripple, (b) the minimum and maximum values of the inductor current.

[Answers: (a) 0.993 A, (b) 24.503 A, 25.497 A.]

1.9. For a boost converter with $V_{in} = 48$ V and $V_{out} = 120$ V, $L = 290$ μH and $f_s = 100$ kHz, determine the value of R for which the boost converter will enter DCM.

(Hint: at the boundary between CCM and DCM, the average input current is half of the maximum inductor current.)

[Answer: 603.6 Ω.]

1.10. For a boost converter with $V_{in} = 48$ V and $V_{out} = 120$ V, $f_s = 100$ kHz, and the output power varying from 120 W to 1.2 kW, design the minimum required value of the inductor such that the converter is operating in CCM within the power range.

[Answer: 57.6 μH.]

1.11. For the boost converter with $V_{in} = 48$ V and $V_{out} = 120$ V, $f_s = 100$ kHz, and $R = 12\,\Omega$, design the values of the inductor and capacitor for 1% output voltage ripple and 15% input current ripple.

[Answers: 76.8 μH, 50 μF.]

1.12. There is a buck-boost converter (Figure 1.6) with input voltage $V_{in} = 48$ V and load resistance $R = 120\,\Omega$. The required average output voltage is 120 V. The value of the inductor, L, is 1000 μH and of

the capacitor, C, 10 μF. The converter is operated at the switching frequency of 100 kHz. Calculate (a) the duty cycle of the switch, (b) the average input current.

[Answers: (a) 0.714, (b) 2.5 A.]

1.13. For the same problem as above, calculate (a) the inductor current ripple, (b) the minimum and maximum values of the inductor current.

[Answers: (a) 0.343 A, (b) 3.33 A, 3.67 A.]

1.14. For the buck-boost converter with $V_{in} = 48$ V and $V_{out} = 120$ V, $L = 1000$ μH and $f_s = 100$ kHz, determine the value of R for which the buck-boost converter will enter DCM.

[Answer: 2450 Ω.]

1.15. For the buck-boost converter with $V_{in} = 48$ V and $V_{out} = 120$ V, $f_s = 100$ kHz, and the output power varying from 12 to 120 W, design the minimum required value of the inductor such that the converter is operating in CCM within the power range.

[Answer: 489.6 μH.]

1.16. There is a buck converter (Figure 1.8) with input voltage $V_{in} = 48$ V and load resistance $R = 4.8$ Ω. The required average output voltage is 24 V. The value of the inductor, L, is 400 μH and of the capacitor, C, 330 μF. The converter is operated at the switching frequency of 100 kHz. Calculate (a) the duty cycle of the switch, (b) the average input current.

[Answers: (a) 0.5, (b) 2.5 A.]

1.17. For the same problem as above, calculate (a) the inductor current ripple, (b) the minimum and maximum values of the inductor current.

[Answers: (a) 0.3 A, (b) 4.85 A, 5.15 A.]

1.18. For the buck converter with $V_{in} = 48$ V and $V_{out} = 24$ V, $L = 400$ μH and $f_s = 100$ kHz, determine the value of R for which the buck converter will enter DCM.

(Hint: at the boundary between CCM and DCM, the average output current is half of the maximum inductor current.)

[Answer: 160 Ω.]

1.19. For the buck converter with $V_{in} = 48$ V and $V_{out} = 24$ V, $f_s = 100$ kHz, and the output power varying from 12 W to 120 W, design the minimum required value of the inductor such that the converter is operating in CCM within the power range.

[Answer: 120 μH.]

1.20. By using two capacitors per group, as in the circuit in Figure 1.54, is it possible to step-down the voltage from 12 V to 6 V? Why not?

1.21. In the same circuit, is it possible to step-down to 5.7 V? Why not?

(Hint: think to the regulation problem.)

1.22. Draw a similar circuit with that in Figure 1.54 for stepping down 12 V to: (a) 4 V and (b) 3.3 V. Is there any difference in the two circuits? What about their regulation capacity for changes in the supply voltage of +/−10%?

1.23. Find a design formula for C and T_s for realizing a certain required ripple in the output voltage for the circuit shown in Figure 1.54 (for a given value of R).

1.24. Show a SC circuit in principle for stepping-up the supply voltage.

1.25. Draw a SC DC-DC converter for stepping-up the voltage from 5 to 9 V.

1.26. Draw a SC DC-DC converter for stepping-up the voltage from (a) 5 to 12 V, (b) 6 to 12 V. Is there any difference in the two circuits? What about their regulation capacity?

1.27. Consider a boost quasi-resonant ZCS converter and explain its cyclically switching operation. Draw the switching diagram and topological stages.

(Hint: use the equivalent scheme of a hard-switching boost converter – Figure 1.9. Before starting a new steady-state cycle, the boost converter was in the off-topology; therefore, its output diode was on and the voltage on the resonant capacitor was V_{out}. When turning on the switch, the current in the output diode is I_{in}-$i_{Lr}(t)$, until this current reaches zero, the diode remains in the on-state, clamping the resonant capacitor voltage at V_{out}. Only when the output diode turns off, does the resonant capacitor start the resonance process with the resonant inductor.)

1.28. The supply voltage v_s and input current i_{in} of an AC-DC converter are expressed as:

$$v_s(t) = 311 \sin 2\pi(50)t$$

$$i_{in}(t) = 10\cos[2\pi(50)t - 20^\circ] + 1\sin[2\pi(150)t + 30^\circ] + 0.5\sin[2\pi(250)t + 40^\circ]$$

Determine:

a. the root-mean-square values of v_s and i_{in} [Answers: 220 V, 7.11 A].
b. the input power of the converter [Answer: 532 W].
c. the displacement and distortion factors of i_{in} [Answers: 0.342, 0.995].
d. the power factor [Answer: 0.340].

Bibliography

ABB Power Electronics to power the NASA Arc-heated Scramjet Test Facility. ABB Press Release (June 25, 2003).

Akagi, H. (1998) The state-of-the-art of power electronics in Japan. *IEEE Transactions on Power Electronics*, **13** (2), 345–356.

Ames, B. (2009) Power electronics drive next-generation vehicles, Military @ Aerospace Electronics Web Exclusive, http://www.nampet.org/resources/new_4.htm.

Amon, E.A., Schacher, A.A., and Brekken, T.K.A. (2009) A novel maximum power point tracking algorithm for ocean wave energy devices. Proc. IEEE Energy Conversion Congress and Exposition (ECCE'09), San Jose, CA, September 2009, pp. 2635–2641.

Blake, C. (2009) Power technology roadmap trends 2008–2013. Proc. Applied Power Electronics Conf. (APEC), Washington, DC (Plenary session communication).

Bose, B.K. (1980) Power electronics – an emerging technology. *IEEE Transactions* on *Industrial* Electronics, **36** (3), 403–413.

Bose, B.K. (2010) Global warming. Energy, environmental pollution, and the impact of power electronics. *IEEE Industrial* Electronics *Magazine*, **4** (1), 6–17.

British Standards Institution, Electromagnetic compatibility (EMC) – Part 3-2: Limits – Limits for harmonic current emissions (equipment input current up to and including 16 A per phase), BS EN 61000-3-2 Ed.2:2001 IEC 61000-3-2 Ed.2:2000.

Buchanan, E.E. and Miller, E.J. (1975) Resonant switching power conversion technique. Proc. IEEE Power Electronics Specialists Conf., pp. 188–193.

Bush, S. (2009) Fujitsu reveals GaN transistor for power supplies. *ElectronicsWeekly.com*, http://www.electronicsweekly.com/Articles/2009/07/02/46422 (accessed November 30, 2009).

Buso, S., Spiazzi, G., Faccio, F., and Michelis, S. (2009) Comparison of DC-DC converter topologies for future SLHC experiments. Proc. IEEE Energy Conversion Congress and Exposition (ECCE'09), San Jose, CA, September 2009, pp. 1775–1782.

CETS (Commission on Engineering and Technical Systems) (1997) Energy-Efficient Technologies for the Dismounted Soldier, The National Academies Press, Washington, DC, http://books.nap.edu.

Chen, J. and Ioinovici, A. (1996) Switching-mode DC-DC converter with switched capacitor based resonant circuit. *IEEE Transactions* on *Circuits* and *Systems – Part* I, **43** (11), 933–938.

Cheong, S.V., Chung, H., and Ioinovici, A. (1992) Development of power electronics based on switched-capacitor circuits. Proc. International Symposium on Circuits and Systems (ISCAS '92), San Diego, CA, May 1992, pp. 1907–1911.

Cheong, S.V., Chung, H., and Ioinovici, A. (1994) Inductorless DC-to-DC converter with high power density. *IEEE Transactions* on *Power* Electronics, **41** (22), 208–215.

Chung, H. and Yan, W.T. (2010) Method and apparatus for suppressing noise caused by parasitic inductance and/or resistance in an electronic circuit or system. US Patent Application Serial No. 12/435,954.

Ciprian, R. and Lehman, B. (2009) Modeling effects of relative humidity, moisture, and extreme environmental conditions on power electronic performance. Proc. IEEE Energy Conversion Congress and Exposition (ECCE'09), San Jose, CA, September 2009, pp. 1052–1059.

Datta, M., Senjyu, T., Yona, A. *et al.* (2009) Smoothing output power variations of isolated utility connected multiple PV systems by coordinated control. *Journal of* Power *Electronics*, **9** (2), 320–333.

Nano-Device Laboratory, GaN transistor technology: problems of self-heating, traps and flicker noise, University of California, Riverside, http://ndl.ee.ucr.edu/GaN-devices.htm (accessed May 7, 2012).

GaN transistor bets silicon (2008) http://www.photonics.com/Content/ReadArticle.aspx?ArticleID=33765 (accessed November 30, 2009).

Han, S.K. and Youn, M.J. (2007) High-performance and low-cost single-switch current-fed energy recovery circuit for AC plasma display panel. *IEEE Transactions* on *Power Electronics*, **22** (4), 1089–1097.

Han, S.K., Moon, G.W., and Youn, M.J. (2007) Cost-effective zero-voltage and zero-current switching current-fed energy recovery display driver for AC plasma display panel. *IEEE Transactions* on *Power* Electronics, **22** (4), 1081–1088.

Hashimoto, T., Shiraishi, M., Akiyama, N. *et al.* (2009) System in package (SiP) with reduced parasitic inductance for future voltage regulator. *IEEE Transactions* on *Power Electronics*, **24** (6), 1547–1553.

Huang, M.H., Fan, P.C., and Chen, K.H. (2009) Low-ripple and dual-phase charge pump circuit regulated by switched-capacitor-based bandgap reference. *IEEE Transactions* on *Power Electronics*, **24** (5), 1161–1172.

Ikeda, N., Kaya, S., Li, J. *et al.* (2008) High power AlGaN/GaN HFET with a high breakdown voltage of over 1.8kV on 4 inch Si substrates and the suppression of current collapse. Proc. of the 20th Int. Symp. on Power Semiconductor Devices & ICs, May 2008, Orlando, FL, pp. 287–290.

Ioinovici, A. (2001) Switched-capacitor power electronics circuits. *IEEE Circuits* and *Systems Magazine*, **1** (3), 37–42.

Kankam, M.D. and Elbuluk, M.E. (Nov. 2001) A survey of power electronics applications in aerospace technologies. NASA Report, TM-2001-211298, http://gltrs.grc.nasa.gov/GLTRS.

Khan, M.A., Kuznia, J.N., Bhattarai, A.R., and Olson, D.T. (1993) Metal semiconductor field effect transistor based on single crystal GaN. *Applied Physics Letters*, **62**, 1786.

Kim, J.H., Lim, J.G., Chung, S.K., and Song, Y.J. (2009) DSP-based digital controller for multi-phase synchronous buck converters. *Journal of* Power *Electronics*, **9** (3), 410–417.

Kim, C.H., Park, H.S., Kim, C.E. *et al.* (2009) Individual charge equalization converter with parallel primary winding of transformer for series connected lithium-ion battery strings in an HEV. *Journal of* Power *Electronics*, **9** (3), 472–480.

Kwon, J.M. and Kwon, B.H. (2009) High step-up active-clamp converter with input-current doubler and output-voltage doubler for fuel cell power systems. *IEEE Transactions* on *Power Electronics*, **24** (1), 108–115.

Lam, E., Bell, R., and Ashley, D. (2003) Revolutionary advances in distributed power systems. Proc. Applied Power Electronics Conf. (APEC), Miami Beach, FL, Vol. 1, pp. 30–36.

Lee, J.P., Min, B.D., Kim, T.J. *et al.* (2009) Design and control of novel topology for photovoltaic DC/DC converter with high efficiency under wide load ranges. *Journal of* Power *Electronics*, **9** (2), 300–307.

Lidow, A. and Sheridan, G. (2003) Defining the future for microprocessor power delivery. Proc. Applied Power Electronics Conf. (APEC), Miami Beach, FL, vol. 1, pp. 3–9.

Liserre, M., Sauter, T., and Hung, J.Y. (2010) Future energy systems. Integrating renewable energy sources into the smart power grid through industrial electronics. *IEEE Industrial* Electronics *Magazine*, **4** (1), 18–37.

Liu, K.H. and Lee, F.C. (1984) Resonant switches – a unified approach to improved performances of switching converters. Proc. of the International Telecommunication Energy Conf., New Orleans, LA, November 1984, pp. 344–351.

Liu, K.H., Oruganti, R., and Lee, F.C. (1985) Resonant switches – topologies and characteristics. Proc. IEEE Power Electronics Specialists Conf., Toulouse, France, June 1985, pp. 62–67.

Ma, G., Qu, W., Yu, G. *et al.* (2009) A zero-voltage-switching bidirectional DC-DC converter with state analysis and soft-switching-oriented design consideration. *IEEE Transactions* on *Industrial Electronics*, **56** (6), 2174–2184.

Mak, O.C., Wong, Y.C., and Ioinovici, A. (1995) Step-up DC power supply based on a switched-capacitor circuit. *IEEE Transactions* on *Power Electronics*, **42** (1), 90–97.

McDonald, T. (April, 2009) GaN based power technology stimulates revolution in conversion electronics. www .bodospower.com.

Meehan, A., Gao, H., and Lewandowski, Z. (2009) Energy harvest with microbial fuel cell and power management system. Proc. IEEE Energy Conversion Congress and Exposition (ECCE'09), San Jose, CA, September 2009, pp. 3558–3563.

Moschytz, G.S. (2010) From printed circuit boards to systems-on-a-chip. *IEEE Circuits* and *Systems Magazine*, **10** (2), 19–29.

Murata Products (2010) PDF Catalog Inductors, http://www.murata.com/products/inductor/catalog/index.html (accessed April 25, 2012).

Ng, V.W., Seeman, M.D., and Sanders, S.R. (2009) Minimum PCB footprint point-of-load DC-DC converter realized with Switched-Capacitor architecture. IEEE Energy Conversion Congress and Exposition (ECCE'09), San Jose, CA, September 2009, pp. 1575–1581.

Orikawa, K. and Itoh, J.I. (2010) A comparison of the series – parallel compensation type DC-DC converters using both a fuel cell and a battery. Proc. IEEE Energy Conversion Congress and Exposition (ECCE '10), Atlanta, GA, September 2010, pp. 1414–1421.

Palma, L. and Enjeti, P.N. (2009) A modular fuel cell, modular DC-DC converter concept for high performance and enhanced reliability. *IEEE Transactions* on *Power Electronics*, **24** (6), 1437–1443.

Park, J.H., Cho, B.H., Lee, J.K., and Whang, K.W. (2009) Performance evaluation of 2-dimensional light source using mercury-free flat fluorescent lamps for LCD backlight applications. *Journal of* Power *Electronics*, **9** (2), 164–172.

Pavlovsky, M., Tsuruta, T., and Kawamura, A. (2009) Fully bi-directional DC-DC converter for EV power train with power density of 40kW/l. Proc. IEEE Energy Conversion Congress and Exposition (ECCE'09), San Jose, CA, September 2009, pp. 1768–1774.

Perreault, D.J., Hu, J., Rivas, J.M. *et al.* (2009) Opportunities and challenges in very high frequency power conversion. Proc. Applied Power Electronics Conf. and Expo. (APEC), Washington, DC, pp. 1–14.

Peter, P. and Agarwal, V. (2010) PV fed boost type switched capacitor power supply for a nano satellite. Proc. IEEE Energy Conversion Congress and Exposition (ECCE '10), Atlanta, GA, September 2010, pp. 3241–3246.

Podlesak, T.F., Stewart, A.G., and Tuttle, J.E. (1998) Matrix converters for hybrid vehicle applications, SAE International, http://www.sae.org/technical/papers/981901.

Silicon Carbide Inverter Demonstrates Higher Power Output, *Power Electronics Technology* (Feb 1, 2006) http://power-electronics.com/news/silicon-carbide-inverter.

NASA (2009) Power Management and Storage. SBIR, Topic S3 Spacecraft and Platform Subsystems, http://sbir .gsfc.nasa.gov/SBIR/sbirsttr2009/solicitation.

Qin, Y.X., Chung, H., Lin, D.Y., and Hui, S.Y.R. (2008) Current source ballast for high power lighting emitting diodes without electrolytic capacitor. Proc. 34th IEEE Annual Conference on Industrial Electronics, November 2008, pp. 1968–1973.

Renesas Electronics Corporation (2010) Renesas Power MOSFETs, IGBTs, Triacs, and Thyristors, http:// documentation.renesas.com/eng/products/transistor/rej13g0003_pmfe.pdf (accessed December 2010).

Richelli, A., Colalongo, L., Tonoli, S., and Kovacs-Vajna, Z.M. (2009) A 0.2–1.2 V DC/DC boost converter for power harvesting applications. *IEEE Transactions* on *Power Electronics*, **24** (6), 1541–1546.

Savage, N. (2009) Building an on-chip high-voltage transmission grid is one way researchers think they could distribute power better. *IEEE Spectrum*, **46** (12), 15.

Schwarz, F. (Nov. 1971) Load insensitive electrical device, US Patent 3,621,362.

Schwarz, F.C. (1975) An improved method of resonant current pulse modulation for power converters. Proc. IEEE Power Electronics Specialists Conf., pp. 194–204.

Shen, Z.J., Okada, D.N., Lin, F., Anderson, S., and Cheng, X. (2006) Lateral power MOSFET for megahertz-frequency, high-density dc/dc converters. *IEEE Trans. on* Power *Electronics*, **21** (1), 11–17.

Stanford, E. (2004) Power technology roadmap for microprocessor voltage regulators, http://www.apec-conf.org/2004/APEC04_SP1-1_Intel.pdf (accessed October 2009).

TDK USA Corp., TDK Inductor Products, http://www.tdk.com/inductors.php (accessed April 25, 2012).

Villalva, M.G., Gazoli, J.R., and Filho, E.R. (2009) Comprehensive approach to modeling and simulation of photovoltaic arrays. *IEEE Transactions* on *Power Electronics*, **24** (5), 1198–1208.

Vinciarelli, P. (Nov. 1983) Forward converter switching at zero current, US Patent 4,415,959.

Waffler, S. and Kolar, J.W. (2009) A novel low-loss modulation strategy for high-power bidirectional buck + boost converters. *IEEE Transactions* on *Power Electronics*, **24** (6), 1589–1599.

Walters, K., Rectifier reverse switching performance. MicroNote Series 302, Microsemi Corp. (www.microsemi.com/micnotes/302.pdf; accessed October 2009).

Wang, H., Vladan Stankovic, A., Nerone, L., and Kachmarik, D. (2009) A novel discrete dimming ballast for linear fluorescent lamps. *IEEE Transactions* on *Power Electronics*, **24** (6), 1453–1461.

Wang, Y., de Haan, S.W.H., and Ferreira, J.A. (2010) Design of low-profile nanocrystalline transformer in high current phase-shifted DC-DC converter. IEEE Energy Conversion Congress and Exposition (ECCE'10), Atlanta, GA, September 2010, pp. 2177–2181.

Witulski, A.F. (1995) Introduction to modeling of transformers and coupled inductors. *IEEE Transactions* on *Power Electronics*, **10** (3), 349–357.

Yi, K.H., Choi, S.W., and Moon, G.W. (2009) Comparative study of a single sustaining driver (SSD) with single- and dual-energy recovery circuits for plasma display panels (PDPs). *IEEE Transactions on Power Electronics*, **24** (2), 540–547.

Zhao, Q., Tao, F., and Lee, F.C. (2001) A front-end DC/DC converter for network server applications. Proc. IEEE Power Electronics Specialists Conference, Vancouver, BC, Canada, pp. 1535–1539.

Zhu, G. and Ioinovici, A. (1997) Steady-state characteristics of switched-capacitor electronic converters. *Journal of* Circuits *Systems and Computers*, **7** (2), 69–91.